Université de Montréal

Numerical modelling of the impact of climate change on the morphology of Saint-Lawrence tributaries

par
Patrick Michiel Verhaar

Département de géographie
Faculté des arts et des sciences

Thèse présentée à la Faculté des études supérieures
en vue de l'obtention du grade de Philosophiæ Doctor (Ph.D.)
en géographie

Février, 2010

Université de Montréal
Faculté des études supérieures

Cette thèse intitulée:

Numerical modelling of the impact of climate change on the morphology of Saint-Lawrence tributaries

présentée par:

Patrick Michiel Verhaar

a été évaluée par un jury composé des personnes suivantes:

Jeffrey Cardille
président-rapporteur

Pascale M. Biron
directrice de recherche

André G. Roy
membre du jury

André St-Hilaire
examinateur externe

Antonia Cattaneo
représentante du doyen de la FES

Thèse acceptée le: 22 janvier 2010

RÉSUMÉ

Cette thèse examine les impacts sur la morphologie des tributaires du fleuve Saint-Laurent des changements dans leur débit et leur niveau de base engendrés par les changements climatiques prévus pour la période 2010–2099. Les tributaires sélectionnés (rivières Batiscan, Richelieu, Saint-Maurice, Saint-François et Yamachiche) ont été choisis en raison de leurs différences de taille, de débit et de contexte morphologique. Non seulement ces tributaires subissent-ils un régime hydrologique modifié en raison des changements climatiques, mais leur niveau de base (niveau d'eau du fleuve Saint-Laurent) sera aussi affecté. Le modèle morphodynamique en une dimension (1D) SEDROUT, à l'origine développé pour des rivières graveleuses en mode d'aggradation, a été adapté pour le contexte spécifique des tributaires des basses-terres du Saint-Laurent afin de simuler des rivières sablonneuses avec un débit quotidien variable et des fluctuations du niveau d'eau à l'aval. Un module pour simuler le partage des sédiments autour d'îles a aussi été ajouté au modèle. Le modèle ainsi amélioré (SEDROUT4-M), qui a été testé à l'aide de simulations à petite échelle et avec les conditions actuelles d'écoulement et de transport de sédiments dans quatre tributaires du fleuve Saint-Laurent, peut maintenant simuler une gamme de problèmes morphodynamiques de rivières. Les changements d'élévation du lit et d'apport en sédiments au fleuve Saint-Laurent pour la période 2010–2099 ont été simulés avec SEDROUT4-M pour les rivières Batiscan, Richelieu et Saint-François pour toutes les combinaisons de sept régimes hydrologiques (conditions actuelles et celles prédites par trois modèles de climat globaux (MCG) et deux scénarios de gaz à effet de serre) et de trois scénarios de changements du niveau de base du fleuve Saint-Laurent (aucun changement, baisse graduelle, baisse abrupte). Les impacts sur l'apport de sédiments et l'élévation du lit diffèrent entre les MCG et semblent reliés au statut des cours d'eau (selon qu'ils soient en état d'aggradation, de dégradation ou d'équilibre), ce qui illustre l'importance d'examiner plusieurs rivières avec différents modèles climatiques afin d'établir des tendances dans les effets des changements climatiques. Malgré le fait que le débit journalier moyen et le débit annuel moyen demeurent près de leur valeur actuelle dans les trois scénarios de MCG, des changements importants dans les taux de transport de sédiments simulés pour chaque tributaire sont observés. Ceci est dû à l'impact important de fortes crues plus fréquentes dans un climat futur de même qu'à l'arrivée plus hâtive de la crue printanière, ce qui résulte en une variabilité accrue dans les taux de transport en charge de fond. Certaines complications avec l'approche de modélisation en 1D pour représenter la géométrie complexe des rivières Saint-Maurice et Saint-François suggèrent qu'une approche bi-dimensionnelle (2D) devrait être sérieusement considérée afin de simuler de façon plus exacte la répartition des débits aux bifurcations autour des îles. La rivière Saint-François est utilisée comme étude de cas pour le modèle 2D H2D2, qui performe bien d'un point de vue hydraulique, mais qui requiert des ajustements pour être en mesure de pleinement simuler les ajustements morphologiques des cours d'eau.

Mots clés : modèle mophodynamique, fleuve Saint-Laurent, changements climatiques, transport de sédiments en charge de fond, niveau de base, risque d'inondation, débit efficace, période de récurrence, débit demi-charge.

ABSTRACT

This thesis investigates the impacts of climate-induced changes in discharge and base level on the morphology of Saint-Lawrence River tributaries for the period 2010–2099. The selected tributaries (Batiscan, Richelieu, Saint-Maurice, Saint-François and Yamachiche rivers) were chosen because of their differences in size, flow regime and morphological setting. Not only will these tributaries experience an altered hydrological regime as a consequence of climate change, but their base level (Saint-Lawrence River water level) will also change. A one-dimensional (1D) morphodynamic model (SEDROUT), originally developed for aggrading gravel-bed rivers, was adapted for the specific context of the Saint-Lawrence lowland tributaries in order to simulate sand-bed rivers with variable daily discharge and downstream water level fluctuations. A module to deal with sediment routing in channels with islands was also added to the model. The enhanced model (SEDROUT4-M), which was tested with small-scale simulations and present-day conditions in four tributaries of the Saint-Lawrence River, can now simulate a very wide range of river morphodynamic problems. Changes in bed elevation and bed-material delivery to the Saint-Lawrence River over the 2010–2099 period were simulated with SEDROUT4-M for the Batiscan, Richelieu and Saint-François rivers for all combinations of seven tributary hydrological regimes (present-day and those predicted using three global climate models (GCM) and two greenhouse gas emission scenarios) and three scenarios of how the base level provided by the Saint-Lawrence River will alter (no change, gradual decrease, step decrease). The effects on mean annual sediment delivery and bed elevation differ between GCM and seem to be related to whether the river is currently aggrading, degrading or in equilibrium, which highlights the importance of investigating several rivers using several climate models in order to determine trends in climate change impacts. Despite the fact that mean daily discharge and mean annual maximum discharge remain close to their current values in the three GCM scenarios for daily discharge, marked changes occur in the mean annual sediment transport rates in each simulated tributary. This is due to the important effect of more frequent large individual flood events under future climate as well as a shift of peak annual discharge from the spring towards the winter, which results in increased variability of bed-material transport rates. Some complications with the 1D modelling approach to capture the complex geometry of the Saint-Maurice and Saint-François rivers suggest that the use of a two-dimensional (2D) approach should be seriously considered to accurately simulate the discharge distribution at bifurcations around islands. The Saint-François River is used as a test case for the 2D model H2D2, which performs well from a hydraulics point of view but which needs to be adapted to fully simulate morphological adjustments in the channel.

Keywords: morphodynamic model, Saint-Lawrence River, climate change, bed-material transport, base level, flood risk, effective discharge, recurrence interval, half-load discharge.

CONTENTS

LIST OF TABLES

LIST OF FIGURES

LIST OF APPENDICES

NOTATION

α	coefficient Ackers and White [1973] equals 10	-
β_τ	direction of shear stress relative to longitudinal direction	rad
β_{si}	direction of sediment transport relative to longitudinal direction	rad
λ	bed porosity	-
ν	kinematic viscosity of water	m^2/s
ϕ	grain size class $D = 2^{-\phi}$	-
ψ	τ/τ_{ri}	-
ρ	density of water	kg/m^3
ρ_s	density of sediments	kg/m^3
τ	bed shear stress	Pa
τ_{ri}	reference shear stress of size fraction i	Pa
τ_{rs50}	shear stress of D_{s50}	Pa
θ_i	non dimensional shear stress (Shields number) for size fraction i	-
$_{1}, _{2}, _{3}$	subscripts for branches, $_1$ = upstream, $_2$ and $_3$ = bifurcates	
A_i	coefficient	-
B	channel width	m
b	power of the sediment transport equation $q_s \sim au^b$	-
C	coefficient	-
c	power of nodal point relationship	-
c_i	weighting factor for mixing bedload with substrate	-

d	exponent	-
D_a	particle size that begins to move under the same conditions as uniform material	m
D_i	grain size of fraction i	m
D_{16}	subsurface particle size for which 16% of the sediment sample is finer	m
D_{50}	subsurface particle size for which 50% of the sediment sample is finer	m
D_{84}	subsurface particle size for which 84% of the sediment sample is finer	m
D_{gri}	dimensionless particle size of the ith fraction	-
D_{s50}	median grain size of bed surface	m
D_{sm}	mean grain size of bed surface	m
e	transition exponent	-
E_i	proportion of volume material in the exchange layer	-
F_i	proportion of fraction i in surface size distribution	-
F_x, F_y	resulting momentum in longitudinal and lateral direction	kg·m/s
F_{gri}	mobility number of sediment	-
g	acceleration due to gravity	m/s^2
H	water depth	m
h	water surface elevation	m
h_{ds}	downstream water elevation	m
k	exponent	-
L_a	active layer thickness	m
L_{sub}	thickness of the first sublayer	m
n	Manning-Strickler value	$s/m^{1/3}$

p_i	proportion of volume material in bedload	-
Q	water discharge	m^3/s
q	specific discharge	m^2/s
Q_s	total sediment transport	m^3/s
q_x	longitudinal specific discharge	m^2/s
q_y	lateral specific discharge	m^2/s
q_{ib}	volumetric bed material transport per unit width of size i	m^2/s
Q_{si}	total sediment transport of size fracion i	m^3/s
$Q^{\star}_{si}$	dimensionless sediment transport rate of size fraction i	-
R	parameter to adjust the sediment transport ratio at a bifurcation	-
R_Q	is the ratio of water discharge at a bifurcation	-
R_{Qs}	is the ratio of sediment transport at a bifurcation	-
s	ratio of sediment to water density	-
t	time	s
U	mean velocity	m/s
u	longitudinal velocity	m/s
$u_{\star}$	shear velocity	m/s
v	lateral velocity	m/s
x	longitudinal distance	m
X_i	rate of sediment transport in terms of mass flow per unit flow rate for the ith fraction	g/g/s
y	lateral distance	m
z	bed elevation above reference datum	m

DEDICATION

Ter gedachtenis aan mijn geliefde peetoom Frans van Beek (1938–2009) en peettante Ria van Beek-Mensch (1940–2005). Die zich altijd zeer betrokken hebben getoond met mijn leven, die mij gesteund hebben om dit avontuur aan te gaan en die mij dit graag hadden zien afronden.

In memoriam of my beloved godfather Frans van Beek (1938–2009) and godmother Ria van Beek-Mensch (1940–2005). Who were always very involved with my life, who encouraged me to start this adventure and who would have liked to have seen me finish.

Ria:
’blijf lachen’
’keep laughing’

Frans:
’Zonder verleden geen toekomst’
’Without past no future’

ACKNOWLEDGEMENTS

This thesis was financially supported by an NSERC Strategic Grant and by the Canada Research Chair in Fluvial Dynamics (André Roy, Université de Montréal). I would like to thank them to have given me the opportunity to complete my thesis.

Jean Morin and Olivier Champoux, at Environment Canada are greatly thanked for their support and help in setting up the 2D model for the Saint-François River with H2D2, during two study-visits at their office in Québec City. Also many thanks to Yves Secretan at INRS-ETE, who provided assistance on the initial setup for the incorporation of bed material transport in H2D2 and from whom I learned a great deal about programming in complex software.

The collection of all the field data could not have been done with the great help of Claudine Boyer, who coordinated all the field campaigns. Environment Canada is greatly thanked for granting access to their survey boat and equipment – special thanks to Guy Morin for driving the boat and for his helping hand in collecting data in the field. Without the help of the following summer field assistants the collection of data and the treatments would not have been possible, thanks to: Geneviève Ali, Michele Grossman, Francis Gagnon, Jeremy Groves, Olivier Lalonde, and Samuel Turgeon.

The adaptation of SEDROUT was streamlined by the great help of Trevor Hoey, at University of Glasgow, who made me become familiar with the code and programming. Rob Ferguson, at Durham University, was a great help along with Trevor to set up the models for the tributaries and to help structuring the analysis. I would like to thank both, Trevor, but in particular Rob, for their contributions to the papers and for their critical and very useful comments.

The input from Ouranos and in particular of Diane Chaumont and Isabelle Chartier is highly appreciated. Their contribution to the papers and their help to respond to comments from reviewers was very useful.

Furthermore, I would like to thank André Roy and Laël Parrot, for their guidance and support throughout my doctorate. Their input and vision were of great value to this thesis. Also I'm grateful for the comments of the committee members: André Roy, André St-Hilaire, Jeffrey Cardille and Antonia Cattaneo. Last, but definitely not least, I could not have finished this thesis without the great help and support of my supervisor Pascale Biron. The comments, questions, discussions and support were highly appreciated and I'm very glad that her support was not limited to the professional side of fulfilling a thesis and included personal support, opportunism, encouragement and patience.

The personnel of the geography department is thanked for their help in sorting out administrative work for my inscription, study permits and teaching assistantships, merci beaucoup.

As with all large projects and especially with the realisation of a doctorate the personal support is also a necessity. Therefore I would like to thank the people close to me who had supported me throughout the project and were there from the beginning on. My parents, dank jullie wel pap en mam voor de motivatie, steun en aan moedigingen, for their encouragements, my brother en sister in law, ook jullie bedankt voor alles en ook voor de foto's van een vrolijk nichtje, ook Caitlin voor de mooie versieringen. My friends back in the Netherlands, for giving feedback, support and being jealous I lived in that lovely place called Montréal: David, Dirk, Frank, Michel and Simon.

Many thanks to my close friends that supported me, dragged me through rough times, and were available to listen to me. Thank you, Luis/Renée/Hernandez, I'll never forget our adventures in Pierrefonds et les autres 'côneries'.... and of course the introduction to the Latino life style (Rodriguez Sanchez). Viele danke, Matt und Katha for your time, support and comprehension in difficult times. There are some students from the department I would like to thank, for their help on little problems with computers, courses and programs, but also helping me to settle down in Montréal and learning French. First of all the students from the lab: merci beaucoup pour le bonne atmosphère, les discussions et explications Bruce, Géneviève Ali, Géneviève Marquis, Hélène, Jay, Julie, Katherine, Laurence, Mathieu, Michele, Olivier et Rachel. Second the students from the forth floor: Clement, Cristiane, Guillaume, Mélanie (pour assuré que je perde un bon bout de temps pendant mon doctorat et l'aide a apprentissage de français) et Rodolphe pour boire du café, de la bière (thirsty Tuesdays), etc. And also a great thanks to my roommates I had over the time for sharing food, friends and just being there: Crystal (best roommates ever!), Nathalie, Simon, Bianca, Ieva, Vidas, Ismaïl, Mélodie, Steve and Max; thanks for all guys!! And many more, but someone needs to know when to stop, once again all thanks for the support, help and distractions (which are also important to survive)!!

CHAPTER 1

INTRODUCTION

Climate change can affect large river systems through variations in discharge and water levels. The variation in discharge leads to changes in sediment transport capacity and has potential consequences for infrastructures, navigation and flood risk. As the water level of the mainstream is the base level for incoming streams, variation in water level will also have an impact on tributary streams. This research investigates the impacts of various climate change scenarios on five tributaries of the Saint-Lawrence River (Québec) through the use of a one-dimensional (1D) numerical morphological model. The project is novel in its focus on relatively short time scale ($\sim$ 100 years), as very little research has been undertaken to evaluate the possible impacts of short to medium term climate change on river morphology and sediments, despite their potential ecological and economical importance.

Rivers tend to search for equilibrium between external forcing (discharge and water level) and internal dimensions (width, depth, slope, sinuosity, etc.). Changes in discharge and downstream water level can have very large impacts on local river morphology, because of the non-linear character of morphological processes. Morphological response to changes in discharge and/or base level is largely dependent on local settings such as sediment type, bed slope, bank material, etc. Climate changes do not simply result in increasing or decreasing discharge, but they actually alter the shape of the hydrograph, for example with increased spring flow and lower summer discharge. Therefore, a direct derivation of the consequences for sediment transport cannot be made and numerical models need to be used. However, studies that link the effects of future changes in temperature and precipitation to hydrology and river morphology are very sparse [Gomez *et al.*, 2009].

A major issue when dealing with a numerical modelling approach is dealing with the uncertainty of predictions and models. The input for our morphodynamic model comes from prediction of greenhouse gas scenarios that drive global or regional climate models to predict changes in temperature and precipitation, which are then used in a hydrological model to obtain river discharges. These initial steps were carried out by the Ouranos research centre, a consortium on regional climatology and adaptation to climate change [www.ouranos.ca, Chaumont and Chartier, 2005]. Ouranos is the main source of North American regional climate simulations and, as such, it is recognized as a leading research centre in climate change in Canada that brings together 250 scientists and professionals from different disciplines. Ouranos is a partner in the NSERC Strategic grant that has funded this project. The discharge scenarios provided by Ouranos were used to force a morphodynamic model that transfers bed shear stress into sediment transport rates. The transformation from discharge to morphological changes is described in this thesis.

The overall objective of this study is to explore the morphological impacts on rivers of near-future climate change. The specific objectives are:

1. To modify and validate a one-dimensional morphodynamic model for the geomorphological context of selected tributaries of the Saint-Lawrence River;

2. To determine how climate-induced changes in near-future hydrology will affect the stability and sediment delivery of tributaries of the Saint-Lawrence River;

3. To determine variations in bed-material transport at the event scale in order to determine the impact of more frequent extreme events on rivers;

4. To explore the potential of two-dimensional (2D) long-term morphological simulations.

Chapter 2 provides the background information on key variables of the river system, climate change, morphological modelling as well as a description of the study area. A general review of these aspects is presented along with a discussion of the past and current knowledge of river adaptation to climate change and prediction/simulation of future climate change effects on precipitation, temperature, discharge and river morphology. The choices of models, study areas and sediment transport formula are justified.

Chapters 3, 4 and 5 correspond to articles that are published in or submitted to international scientific journals. As such, some repetition occurs to enable the individual publications to be read on their own. These chapters include a detailed methodology for the analysis done within each article. Chapter 3 describes the choice, modification and validation of the morphological model (SEDROUT) for the selected tributaries. Results of the simulations are presented in chapter 4 by focusing on yearly average and global trends in the comparison between scenarios, whereas chapter 5 examines more closely the event scale in order to address the role of extreme events in river response to climate changes.

Chapter 6 explains in more detail the problems faced with modelling some of the selected tributaries with a 1D model, namely the Saint-Maurice, Yamachiche and Saint-François rivers. The chapter also explores the use of two-dimensional modelling on one of the selected tributaries (Saint-François River). Because of complexities such as islands, two-dimensional modelling could help resolve the problems faced with the 1D model, despite the increased computational cost. Finally, chapter 7 provides a general conclusion and directions for future research on the impacts of climate change on river morphology.

The response of a river to changes in discharge and/or base level is complex. Most of the research focuses on one of the two aspects over short time scales or the combination of the two over very long temporal scales. The combination of discharge change and base level change on a near future scale has not been addressed before in geomorphological models. Furthermore, research on near future climate is typically limited to changes in discharge, ecological effects related to changes in habitat or flood risk assessment, based on usually only one climatic scenario. This project will investigate the effects of both a change in discharge and base level on the morphology of the tributaries and the main stream using various scenarios. Finally, there is a lack of research on climate change on mild slope, sand-bed rivers. Given that most of human settlements around the world are located in the low-land areas of the river system, morphological changes in these areas can have potentially large impacts.

Morphodynamic simulations with discharge scenarios obtained from two different green house gas scenarios and the use of different climatic models are a major strength of this study. Examining different tributaries within the same region also makes this research unique and enhances the potential for generalization of the results. Finally, the intermediate temporal scale ($\sim$100 years) combined with a fairly large spatial scale (around 15 km), also contribute to the originality of this research.

CHAPTER 2

BACKGROUND

2.1 The river system

Rivers are constantly trying to find an equilibrium state in which there is a balance between the water force and channel resistance [e.g. Schumm, 1977; Leopold and Bull, 1979]. Over intermediate time scales, rivers are in a near equilibrium state where the balance between stream power and sediment transport is almost achieved, which is characterized by a stable longitudinal profile; among others Schumm [1977] defined this as the graded state. This pseudo equilibrium state is one where the water slope and bed slope are constant over time although the elevation of the bed and water may change, i.e. aggradation or degradation may occur. Perturbations in water discharge or base level will interrupt this balance and the river system will adjust by finding a new balance between stream power and sediment transport (Figure 2.1). Aggradation or degradation of alluvial rivers is thus a result of the balance between sediment supply on one side and sediment transport capacity (or stream power) on the other side. However, this model is very general and the effects of the shape of the hydrograph or thresholds for sediment transport are not taken into account.

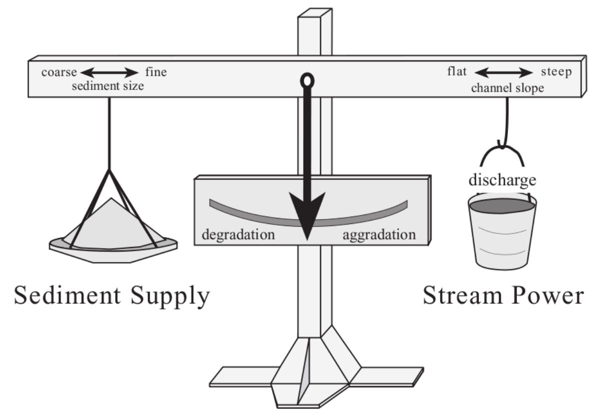

Figure 2.1: Balance model for aggradation or degradation of an alluvial river. [Blum and Törnqvist, 2000]

The river system possesses different types of equilibrium depending on the time scale of interest. As proposed and explained by Schumm [1977], this will vary from the smallest time scale with static equilibrium, meaning a constant bed elevation and continuous sediment transport rate along the river, to a large time scale dynamic metastable equilibrium with episodic erosion (Figure 2.2). Time scales in climate research are important, since climatic parameters like precipitation and temperature are highly dynamic at all time scales, ranging from hours up to more than 100 000 years [Vandenberghe, 1995]. The period of interest is critically important to determine the type of event that is important for landscape evolution [Bogaart and van Balen, 2000]. For example, at scales of hours to days, the dominating events are individual events, like thunderstorms; at scales of months to year, seasonal variations (e.g. snowmelt in the spring); at scales of decades, gradual climate change like global warming; from centuries to millennium, long-term climate oscillations; and at even larger time scales, transition and interglacial cycles. Together all these events shape the landscape and river channels.

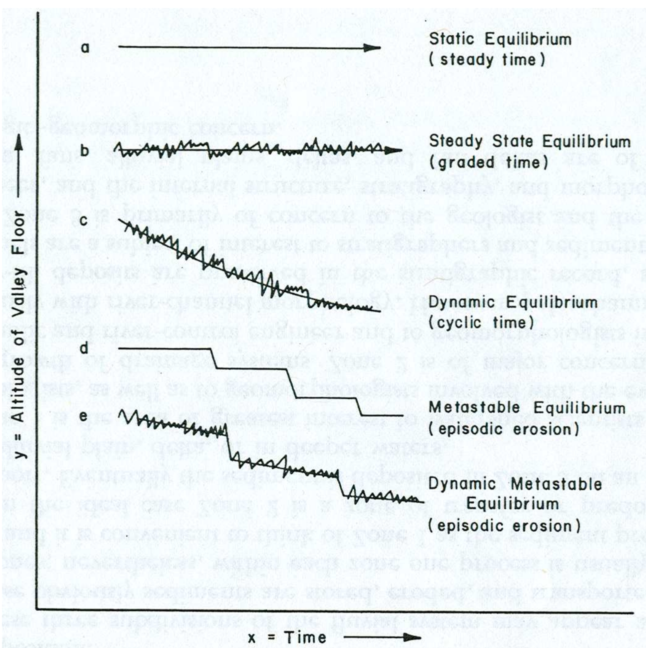

Figure 2.2: Types of equilibriums based on Schumm [1977].

A simplification or idealized representation of the river system can be very helpful to understand the important processes in river systems. Schumm [1977] divided the river system in three zones and identified the dominant process in each case. In upstream to downstream order these are: the production zone, the transfer zone and the deposition zone. Erosion, transport and deposition of sediments occur in all the three zones. However, sediments are generally coming from the upstream region and transported through the middle section and deposited in the downstream zone. In natural rivers, sediments are not transported to their depositional site at once. During their journey down the river they are stored temporarily in the system as colluvial, alluvial fan or fluvial deposits. These deposits are eroded later on and sediments are transported again.

The river system is considered a complex system [Leopold and Bull, 1979; Hey, 1986; Knighton, 1998; Phillips, 2003]. In order to be defined as complex, a system must have one or more of the following behaviours: non-linear, unpredictable, multiple equilibrium states, memory and multiple (temporal and spatial) scales. Typical examples of complex systems are: ecosystems, economies, transportation networks and neural systems [Parrott, 2002]. In the context of complex systems, unpredictability and non linearity refer to multiple equilibrium states that can exist within the system and for which one can therefore not predict the outcome directly. However, it does not imply that the evolution cannot be simulated; it is only impossible, or very hard, to postulate based on general assumptions what equilibrium state will be reached. Numerical models can still be used to evaluate different responses to input parameters, a practice that is often employed in geomorphology, by the evaluation of past events or comparison of different future changes (sensitivity analyses) [Coulthard and Macklin, 2001; Hulse *et al.*, 2009]. Conceptual models and numerical morphological models possess a complex non-linear behaviour which is not an artefact of the model, but which is observed in many geomorphic phenomena [Phillips, 2003].

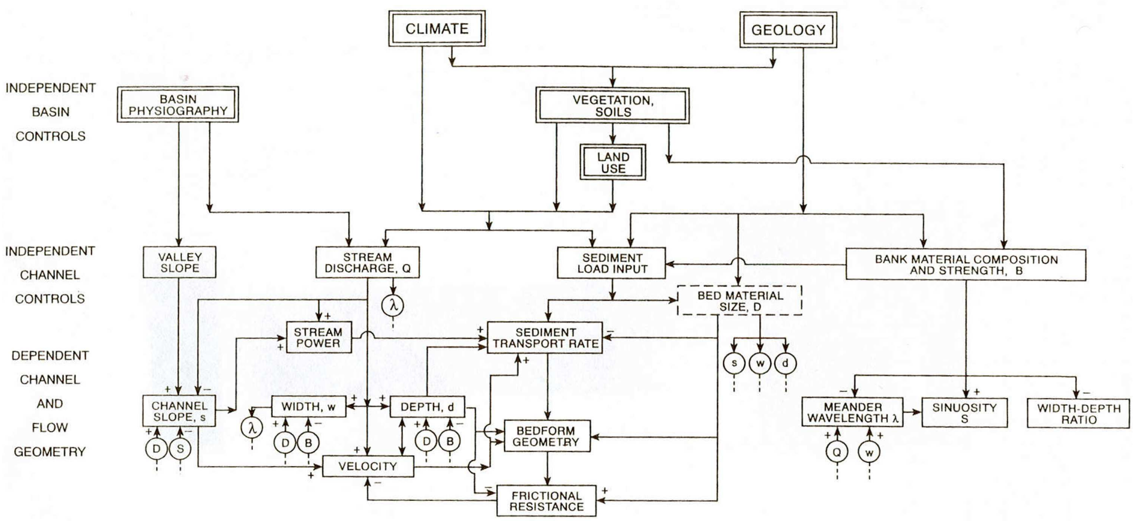

Figure 2.3: Overview of interrelationships in the fluvial system. Adapted from Knighton [1998].

Over the years several attempts have been made to incorporate all the inter-relationships within-river system to be able to predict river response to any change in external forcing or within the river system [e.g. Schumm, 1977; Hey, 1986; Knighton, 1998; Eaton *et al.*, 2004]. Figure 2.3 provides an overview of these relationships. Although this overview contains all the factors in play, it is difficult to see the impact of a specific change due to the large number of feedback loops. This is the unpredictable aspect as defined above. Ideally, a river system model should include all these inter-relationships, although it is virtually impossible to define all the boundary conditions.

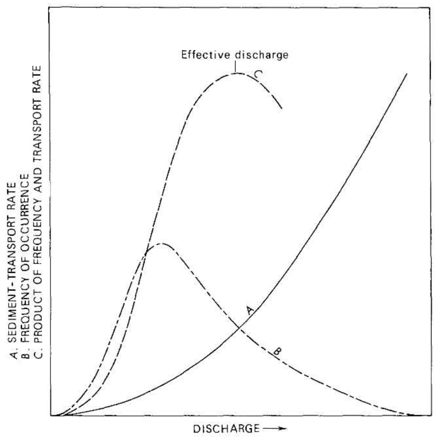

Figure 2.4: Relations between rate of transport, applied stress, and frequency of stress application. Adapted from Wolman and Miller [1960].

A common assumption in geomorphology is that the median magnitude floods are the most influential in long-term landscape evolution [Figure 2.4 Wolman and Miller, 1960]. Effective, dominant, channel forming or half-load discharge are the concepts that exist to determine the magnitude and recurrence interval of these floods [Wolman and Miller, 1960; Vogel *et al.*, 2003; Doyle *et al.*, 2007]. The dominant flood is often associated with bankfull discharge, which is generally true for stable rivers in an unconfined environment [Andrews, 1980; Van Den Berg, 1995]. The recurrence interval of the bankfull discharge varies among rivers from about 1 year to 32 years depending on their morphological state [Wolman and Miller, 1960; Andrews, 1980; Carling, 1988; Knighton, 1998; Barry *et al.*, 2008]. Long recurrence intervals are most likely found in degrading rivers where banks are high [Knighton, 1998]. The most common recurrence interval for bankfull discharge is about 1.5 years [Knighton, 1998, among others]. However, it is not always obvious to determine bankfull discharge as the bankfull stage of cross sections may not exhibit a clear limit between the channel and the bank.

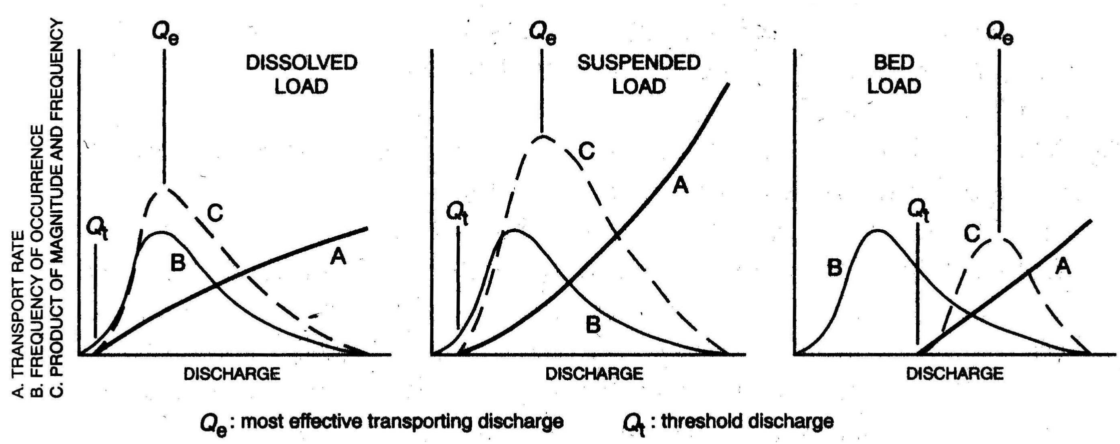

Figure 2.5: The effective discharge for dissolved load, suspended load and bedload. Adapted from Knighton [1998].

Wolman and Miller [1960] proposed to use a combination of discharge ranges and total volume transported to determine which discharge is transporting the largest volume. The method was first developed for suspended load in rivers where rating curves of suspended transport were available. However, the idea of effective or dominant discharge has been criticized when generalized towards bedload transport due to the large variability of the measurements [e.g. Andrews, 1980; Nash, 1994; Vogel *et al.*, 2003; Doyle and Shields, 2008]. In Figure 2.5 it can be seen that the magnitude of the effective discharge and hence the recurrence interval depends on the type of sediment transport [e.g. Knighton, 1998]. Channel dimensions are more related to bedload transport than suspended transport, therefore it seems more likely that the effective discharge is a relatively rare event. The effective discharge is found to vary greatly between rivers [Pickup and Warner, 1976; Ashmore and Day, 1988; Nash, 1994; Torizzo and Pitlick, 2004]. One of the difficulties with this concept is that it is very sensitive to how the discharge ranges are defined [Crowder and Knapp, 2005] and it relies on sediment rating curves which are mostly not well known for a given river. An alternative approach is the half-load discharge (value above and below which half the long-term sediment load is transported) which is a more robust measure of discharge [Vogel *et al.*, 2003]. This approach uses the cumulative sediment transport in a similar way to how the median diameter of grain size distribution is determined.

Alluvial rivers will respond to climate change through changes in discharge related to variation of precipitation and evaporation, which will consequently influence discharge magnitude, flood frequency and duration [Gibson, 2005; Molnar *et al.*, 2006], and base level [Schumm, 1977; Leopold and Bull, 1979; Tucker and Slingerland, 1997; Blum and Törnqvist, 2000]. Base level changes are often considered only in terms of sea level variation, especially in climate change and river basin research, but major rivers act as local base levels for their tributaries [Slingerland and Snow, 1988; Schumm, 1993; Church, 1995]. Both discharge and base level changes have different effects on the river morphology and the prediction of the river response for each variable taken individually is difficult as it depends on other factors such as the magnitude, duration and direction of the perturbation [Schumm, 1993; Van Heijst and Postma, 2001]. The assessment of the river response to both discharge and base level changes can only realistically be done by numerical modelling.

Base level, as defined by Powell [1875], is used to identify the elevation to which rivers or landscape will erode. Essentially this level is the sea level, although it is known that rivers will erode slightly below it [Schumm, 1993]. Base level is also defined as the local level to which rivers erode, for instance the water level in the main stream or in a lake, or the bed rock in degrading rivers. Therefore, the water level in the Saint-Lawrence River is the base level for all its tributaries. A base level change is often viewed as a perturbation that occurs in a short reach, which may affect the reaches upstream [e.g. Leopold and Bull, 1979; Begin *et al.*, 1981; Bonneau and Snow, 1992]. However, the upstream distance influenced by the base level change cannot easily be determined beforehand [Blum and Törnqvist, 2000]. Some studies show that the base level in the main stream is only affecting the tributaries locally [Leopold and Bull, 1979]. On the contrary, Slingerland and Snow [1988] simulated the response of a river network to a lowering of its base level. Flow in the tributaries was in the order of 10% of the discharge in the main stream. The response of the system was cyclic, with periods of erosion and sedimentation in the main stream, due to a change in the input of sediment in the main stream by erosion of the tributary. The type of response to a base level lowering also depends on the rate of base level change [Bonneau and Snow, 1992]. A slow rate will lead to a period of initial steepening of the channel followed by parallel erosion (Figure 2.6a). Continuous steepening occurs when the rate of change is higher than the response of the head waters. A slow rate of base level change allows the river to adjust its pattern and maintain its slope, whereas a higher rate leads to incision [Schumm, 1993]. The type of response is also highly dependent on local settings and controls. According to Schumm [1993] classification, base level controls are direction, magnitude, rate and duration; geological controls are lithology, structure and nature of valley alluvium, and geomorphic controls are inclination of exposed surface, valley morphology, river morphology and adjustability.

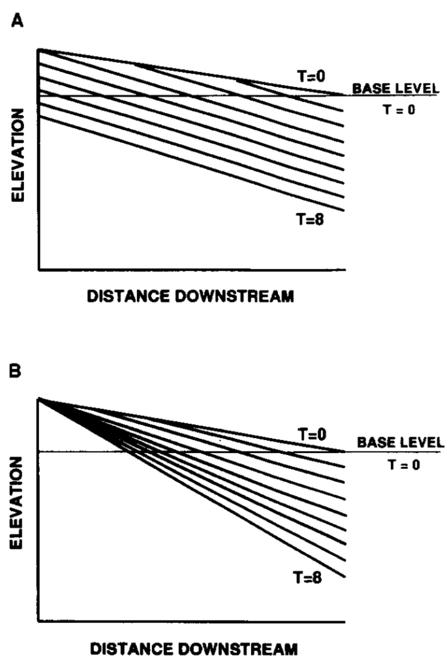

Figure 2.6: Extremes in profile adjustment to continuous base level lowering. Adapted from Bonneau and Snow [1992].

A river has several degrees of freedom to respond to changes in discharge and base level, namely bed elevation, channel width, channel depth, meander wave length, sinuosity, bed slope, width to depth ratio and bed composition [Knighton, 1998; Eaton and Church, 2004]. Schumm [1977] developed a simplified river model that described the direction of change for all these variables as a function of change in discharge and sediment transport rate. His river model, however, only gives a qualitative description of the expected changes. Schumm [1993] also argued that the main response of an unconfined sand-bed river to a change in base level is a change in river pattern [Simon and Hupp, 1986; Simon, 1989, 1992]. However, field studies such as Begin *et al.* [1981] show that this is not necessarily the case and that the river response can be more in terms of incision when a base level lowering occurs. Discrepancies in the type of response between rivers may also be related to sedimentology, as rivers with cohesive sediment will erode their banks [Schumm, 1993; Doyle and Harbor, 2003]. However, a case study in the Jordan River revealed that non-cohesive sediments also underwent incision as a primary response to base level lowering [Hassan and Klein, 2002], so other variables must intervene in river adjustment. For example, the slope of the continental shelf, in the case of sea level change, plays a role in the river response [Summerfield, 1985; Blum and Törnqvist, 2000]. When the slope of the continental shelf is steeper than the river channel slope, incision and increased sinuosity are the most likely responses. If the slope of the continental shelf is less steep, then aggradation or channel straightening will occur. When the slopes are the same, the river will maintain its sinuosity and there will be no change in sinuosity further upstream.

2.2 Climate change

2.2.1 Past climate change

Climate is an important factor on the evolution of landscape and rivers. It is known that climate gradually changes over time in cycles. Since the last glacial period the earth temperature rise caused the ice caps to melt and the sea level to rise by about 120 m over that period [IPCC, 2007]. Since the beginning of the Holocene, about 12 000 years ago, the Earth temperature and precipitation have been fairly constant relative to the glacier inter-glacier cycle [e.g. Antoine, 2003].

Resolving what happened in the past is often seen as a necessity for future predictions [Dearing *et al.*, 2006]. Unfortunately, records of past climate are influenced by human activity. Therefore, the reconstruction of climate can only be done when climate, human activities and earth processes, including their interactions are reproduced at all locations and scales [Dearing, 2006].

More recently changes in climate (precipitation and temperature) have been observed (for example, in ice cover) all over the world. Various records of ice cores and tree ring data indicate that greenhouse gas (GHG) concentrations and global temperature are rising due to human activity. The effect of changing GHG concentrations in the atmosphere varies around the globe and contributes to more extreme meteorological events, like hurricanes, heat waves, etc. [Goudie, 2006; Hansen *et al.*, 2006, and references herein]. The global trend is that the earth surface temperature is increaseing over the last decades.

Changes in climate over several decades have been recorded in some watersheds, for example the Waipaoa River in New Zealand [Gomez *et al.*, 2009]. The evaluation of river basin sediment transport as a consequence of these changes is complicated by the other changes within the river basin, such as forest clearing, hydraulic structures, etc. Recent climate changes have also been observed in Québec. Over a 44 year period from 1960 to 2003 the temperatures increased between 0.5°C and 1.2°C with a strong East-West gradient because of large water bodies in the East [Bourque and Simonet, 2008]. Other indicators such as the length of the frost-free season, growing degree-days and heating degree-days have changed over the last decades as well.

2.2.2 Future climate change

There is now a clear consensus that the global climate will continue to change in the near future, at least partly because of human activities [IPCC, 2007]. Human activities have greatly increased concentrations of greenhouse gases, such as carbon dioxide and methane. These elevated concentrations will result in higher mean temperature of the earth, however on a regional scale it will alter temperature (increase or decrease) and precipitation which inevitably also affects hydrological systems and river flows [Graham *et al.*, 2007; Minville *et al.*, 2008]. For the assessment of climate change on temperature and precipitation a good understanding of the global interactions of GHG concentrations with temperature and precipitation is necessary. Furthermore, an estimation of the future GHG emissions is required.

Over the last decades intensive research on both the emission rates and the interaction on global and regional scale have been carried out [IPCC, 2007]. The results of these exercises are surrounded by relatively large error margins, not only because of the difficulty of predicting future emission rates, but also due to the relatively poor understanding of the processes involved. Furthermore, predictions of temperature and precipitation are based on a cascade of modelling steps from GHG emission rates, through global or regional climate modelling.

Predictions on global climate modifications need to be translated to regional changes in order to foresee the effects within watersheds. Different methods for this translation are available, of which the perturbation or delta method is the most widely used [Graham *et al.*, 2007]. The perturbation method uses a reference period (mostly 1961-1990) for precipitation and temperature and calculate delta values for each season for one representative year in the future. These delta values are then applied to the reference time serie to produce estimates for the future period(s). Although other approaches such as downscaling or runoff routing are increasingly being used, each method has its own limitations [Rosberg and Andréasson, 2006; Graham *et al.*, 2007; Rydgren *et al.*, 2007; Quilbé *et al.*, 2008]. The advantage of the perturbation method is that it is simple, stable and robust and it represents very well changes in mean precipitation and temperature. However, individual events are captured less accurately than in the other available methods [Rosberg and Andréasson, 2006]. Based on direct comparison of downscaling with the delta method by Hay *et al.* [2000] it was concluded that due to uncertainties in GCM's ability to simulate current conditions, future impacts of both methods remain questionable.

Overall, it is expected that in Québec for the period 2010–2099 the mean temperature will increase, especially in the cold season [Bourque and Simonet, 2008]. For the winter and spring seasons, the precipitation would also increase. As a consequence, the discharge regime of rivers within the province of Québec should change [Chaumont and Chartier, 2005]. Although the mean annual discharge remains close to current values, the timing of spring floods will change drastically [Boyer *et al.*, 2009].

2.3 Climate change impact on rivers

Fluvial response to climate change has been a topic of study in fluvial geomorphology for many decades. Most of these studies look at historical changes in climate and try to match known climatic events with stratigraphic records, based on the principle that we can learn from the past about present and future climate-human-environment interactions [Blum and Törnqvist, 2000; Dearing, 2006]. Looking at long time scales (20 000 years), these periods are still relative short compared to an entire glacial and interglacial cycle of about 100 000 years. Over these long time scales sea level (base level) is linked with climate as sea level high stands are linked with warm periods, and lows in sea level are associated with cold periods.

A climate-induced change in discharge is almost always accompanied by a change in sediment transport [Schumm, 1977]. The effect of such a combined change is different in rivers with a sand bed than in gravel-bed rivers [Gaeuman *et al.*, 2005]. In Figure 2.7, it can be seen that the primary response for sand-bed rivers is an adjustment of the bed elevation, whereas gravel-bed rivers will adjust primarily through width. Observations from field data [Gibson, 2005] show that it is difficult to isolate the effect of climate change on rivers as it happens in a continuous changing landscape and changes in discharge and sediment transport occur concurrently [Schumm, 1993]. Bogaart and van Balen [2000] use a numerical model to investigate the effects of changes in water discharge and sediment supply. They compared the results of a simultaneous variation of the discharge and sediment supply, with a time lag between the maximum discharge and maximum sediment supply, and they found that the change itself is not as important as the phase-lag between them. The phase lag between discharge and sediment supply varies between different river basins, and therefore the response is different for each river.

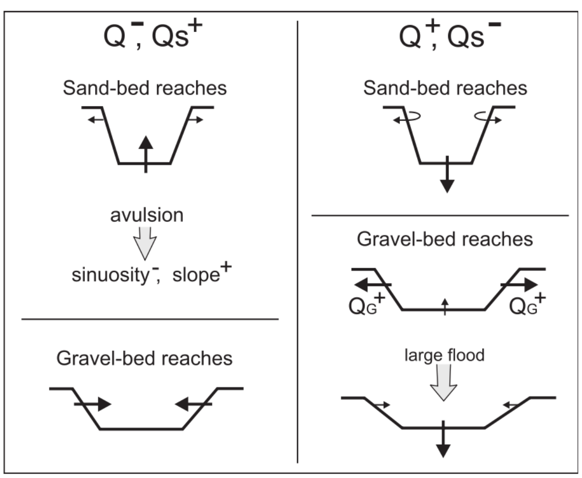

Figure 2.7: Primary river adjustment (bold arrows) in sand-bed and gravel-bed rivers to changes ($^+$: increase, $^-$: decrease) in discharge (Q) and sediment supply (Qs). On the left increased discharge or decrease sediment transport. Adapted from Gaeuman *et al.* [2005].

Climate-change related studies on rivers mostly focus on reproducing historical data [e.g. Blum and Törnqvist, 2000; Bogaart and van Balen, 2000; Hassan and Klein, 2002; Molnar *et al.*, 2006]. Because of the importance of the anticipated near-future climate changes, some simulations are increasingly being used to assess the impacts on discharges, water levels and economical (navigation, hydro-power or water resources) or ecological aspects (e.g. river habitats) [Morin and Côté, 2003; Gibson, 2005; Fowler *et al.*, 2007]. These studies mostly use a worst-case scenario approach.

Because of the complexity of river responses described above, even if a simplified approach is used, the type of response to a single climatic perturbation is often not clear. Field studies, laboratory experiments and models have been used to generalize river behaviour and analyse equilibrium states [Schumm, 1977; Rhodes, 1987; Howard, 1988; Bonneau and Snow, 1992; Van Heijst and Postma, 2001]. But despite all the efforts made to generalize findings, river responses are strongly related to local settings and therefore no general rule exists. Furthermore, the situation is complicated by the large number of degrees of freedom in a river system [Hey, 1986; Knighton, 1998] and the fact that response is dependent on the flow history [Rhodes, 1987; Phillips, 2003]. This complexity is illustrated by the study of Veldkamp and Tebbens [2001] which simulated climate and base level change for the river Meuse and found that preserved fluvial sedimentary records did not relate to neither climate change nor to sea-level change in the lower reaches of the river basin. Furthermore, the link between climate change and river response remains difficult to establish [Vandenberghe and Maddy, 2001; Bogaart *et al.*, 2003], at least in part because the uncertainty in the input variables for river response models includes uncertainty in both outputs of climate models and of hydrological models used to convert changes in temperature and precipitation into river discharge [Graham *et al.*, 2007].

2.3.1 Past impacts

There are several studies linking past impacts of climate change to river morphology [e.g. Blum and Törnqvist, 2000; Bogaart and van Balen, 2000; Knox, 2000; Vandenberghe and Maddy, 2001; Adel, 2002]. For example, Blum and Törnqvist [2000] were able to summarize the general history of climate change (precipitation and sea-level change) on the Mississippi River valley, over a series of glacial periods (Figure 2.8).

To better understand the relationship between climate and the stratigraphic record, physical and numerical modelling studies has been conducted [Tucker and Slingerland, 1997; Syvitski *et al.*, 1998; Veldkamp and Tebbens, 2001; Bonnet and Crave, 2003]. The advantage of these studies is that effects of discharge change or base level can be isolated. Bogaart and van Balen [2000] show that there is no link in the downstream part of the River Meuse with climate or base-level changes. However, Antoine [2003] revealed that some fluvial systems

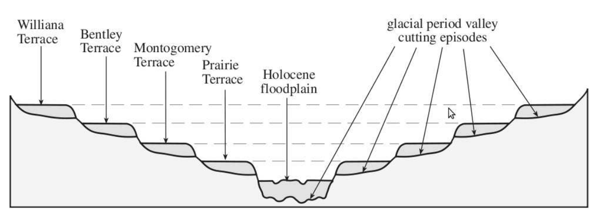

Figure 2.8: Mississippi valley terrace sequence from glacial periods. Adapted from Blum and Törnqvist [2000].

respond very quickly with respect to the time scale of climate change, in the order of 100 to 1000 years, to climatic variations of short duration. The major difficulty in this type of research is to match climate with sediment record, especially for long periods back in time due to the uncertainty in both climate parameters and in dating the sediment record.

2.3.2 Future impacts

The assessment of climate change impacts on river hydrology and morphology is essential for hydro-electricity, navigation, flood risk and ecology [Lane *et al.*, 2007, 2008]. Most research projects focus on the hydrology, although assessing morphologogical changes and thus sediment transport is essential as degradation and aggradation will alter the flood risk and flood frequency of rivers [Lane *et al.*, 2008]. A change in hydrological regime and base level has a direct effect on flood risk and an indirect one through morphological changes. Without morphological modeling, it is impossible to say what this influence is.

One of the major problems to predict future climate effects is the lack of data to verify the outcome of climate models, this applies to hydrological and morphological models. Although in some cases historical data are available for model calibration and validation, the validation of future output is impossible [Gomez *et al.*, 2009]. The underlying assumption is that the change in river hydrology can be directly predicted/simulated, whereas the morphological changes take more time to adapt to the new hydraulic conditions.

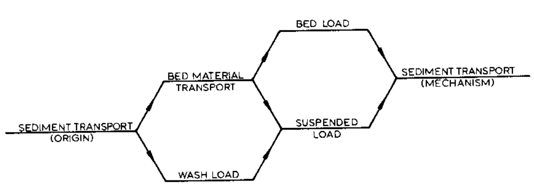

Figure 2.9: Sediment transport classification based origin and mechanism. Adapted from Jansen *et al.* [1979].

As stated before not only the magnitude, but the frequency and duration of floods and the timing with the base level determine the amount of sediment transported [Schumm, 1977]. Therefore, it is impossible to predict based on a change in maximum annual discharge or mean daily discharge how sediment transport will be affected. Morphological modelling of all these parameters can provide the answer to the combined effects of these changes.

2.4 Sediment transport

Water movement within a river causes sediment transport. Despite great efforts to mathematically describe this relationship between hydraulics and sediments [e.g. Einstein, 1950; Toffaleti, 1968; Ackers and White, 1973; Parker, 1990b; Komar, 1996; Tingsanchali and Supharatid, 1996; Batalla, 1997; Wilcock and Crowe, 2003; Barry *et al.*, 2004], there is no general sediment transport formula available. Data sets with water velocity and sediment transport rate show significant variations due to difficulties in measuring the exact transport rate, variations in sediment size, shape and density, and the variations in water movement including turbulence [Dietrich and Gallinati, 1991; McLean *et al.*, 1999; Wu *et al.*, 2000]. Sediment transport is classified based on its origin (bed material or wash load) or on its mechanism (bedload or suspended load) (Figure 2.9). Wash load is transported in suspension and is supply limited, whereas bed material can be transported as bedload as well as in suspension. For the choice of sediment transport formula, this classification is important as bedload formulae only need information about the bed material. Suspended load and total load can contain bed material as well as material that is not found on the river bed (e.g. bank material). For the transport of bed material in sand-bed rivers a total load formula is required as it is transported as bedload and in suspension.

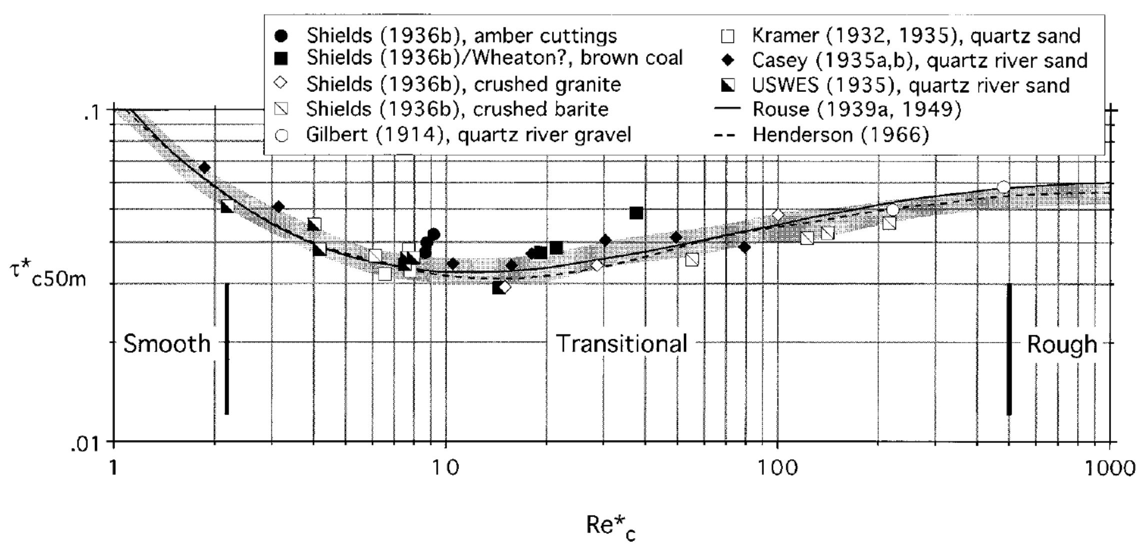

Figure 2.10: Shields diagram. Adapted from Buffington [1999].

One of the classic approaches in sediment transport studies is the assumption of critical shear stress as described by Shields [1936]. The water movement is represented by the shear stress on the sediment particles. Below a critical value there is no sediment transport. The critical shear stress value depends on the flow type and the sediment size (Figure 2.10). The flow type and sediment size are expressed in non-dimensional variables, the calculation of the critical shear stress in laminar and transitional flow is iterative, whereas for hydraulically rough flows Shields non-dimensional critical value is considered a constant (with values ranging between 0.030 and 0.073, Buffington and Montgomery [1997]). The definition of incipient motion, at which sediment transport is starting, is a matter of debate [Buffington, 1999]. The different definitions lead to variations in the critical shear stress value. Most methods for calculating sediment transport are based on a power function of the absolute difference between the applied shear stress and the critical one, with no transport for shear stress below the critical value.

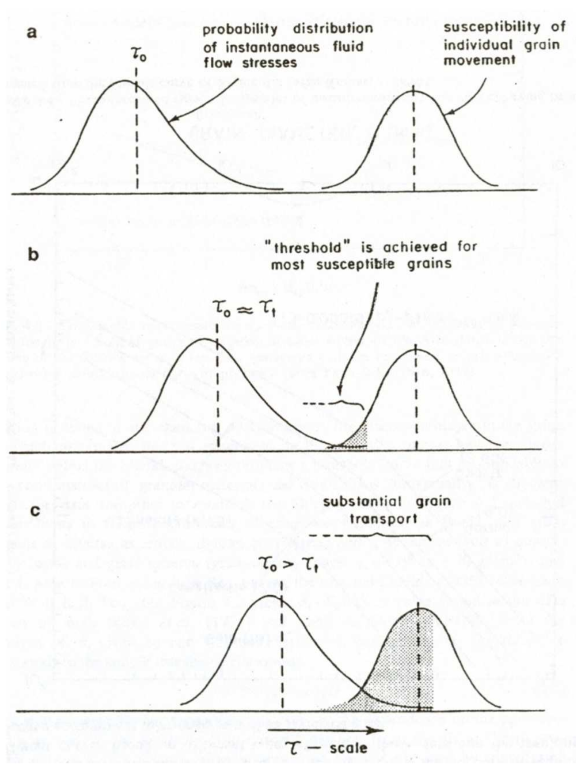

Figure 2.11: Schematic illustration of the probability of initial transport according to Grass [1970]. Adapted from Komar [1996].

Experiments on sediment transport have clearly shown that there is significant sediment transport below the critical shear stress. Within the literature two alternative approaches to the method by Shields [1936] can be found. First, there is a stochastic one which does not contain any critical value for the shear stress (Figure 2.11) [Einstein, 1950; Grass, 1970]. The second approach uses the same critical value as Shields, but it is relating sediment transport to the ratio of applied to critical shear stress, which allows for some sediment transport below the critical shear stress value [Komar, 1996].

Besides the discussion on what would be the appropriate mathematical approach for sediment transport, sediment heterogeneity is complicating the task of determining a proper formulation [Egiazaroff, 1965; Komar, 1996]. As shown in Figure 2.12, the actual transport rate is a function of the grain size distribution on the bed. The larger particles in a bed mixture are more exposed to the water flow than they would be within a bed of particles of the same size. At the same time, the smaller particles are sheltered by the bigger particles. This concept is called hiding and exposure [Egiazaroff, 1965; Ashida and Michiue, 1971; Parker *et al.*, 1982; Andrews, 1983; Proffitt and Sutherland, 1983; Wilcock and Crowe, 2003]. Some researchers [e.g. Parker *et al.*, 1982] believe that this will lead to equal mobility of the particles within the mixture, where all sizes of material move once a threshold shear stress is reached. This would give horizontal lines in Figure 2.12, as the different grain sizes start moving at the same time.

Different studies have compared the available sediment transport equations under different hydraulic conditions and sedimentological settings. Within the context of sand-bed and sand-gravel mixtures the formulae of Ackers and White [1973] and Wilcock and Crowe [2003] perform best according to the comparative work of Tingsanchali and Supharatid [1996]; Batalla [1997]; McLean *et al.* [1999] and Barry *et al.* [2004]. More detailed information on these sediment transport formulae is presented in Appendix II. The Wilcock and Crowe [2003] formula uses a similarity collapse over fractional transport rate, as successfully used for substrate-based empirical models [e.g. Ashida and Michiue, 1971; Parker *et al.*, 1982]. The similarity collapse has the following form:

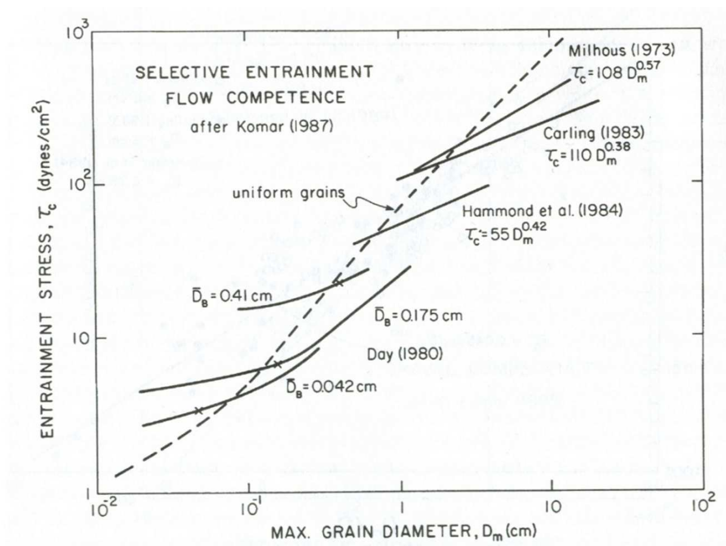

Figure 2.12: Flow stress versus grain size diameter. Adapted from Komar [1996].

$$Q^{\star}_{si} = f\left(\frac{\tau}{\tau_{ri}}\right) \tag{2.1}$$

where τ is the bed shear stress, τ_{ri} is the reference shear stress of size fraction i and $Q^{\star}_{si}$ is the dimensionless sediment transport rate of size fraction i defined by:

$$Q^{\star}_{si} = \frac{(s-1)gq_{ib}}{F_i u^3_{\star}} \tag{2.2}$$

where s is the ratio of sediment to water density, g is the acceleration due to gravity, q_{ib} is the volumetric bed material transport per unit width of size i, F_i is the proportion of fraction i in surface size distribution and $u_{\star}$ is the shear velocity.

The shear stress reference value τ_{ri} is scaled against that of the mixture by comparing the grain size diameter:

$$\frac{\tau_{ri}}{\tau_{rs50}} = \left(\frac{D_i}{D_{s50}}\right)^k \tag{2.3}$$

where τ_{rs50} is the shear stress of D_{s50}, D_i is the grain size of fraction i, D_{s50} is the median grain size of bed surface and k, the exponent, is defined as described in Appendix II.

The Ackers and White [1973] original formula was developed for uniform sediment, but later the coefficients were revised to allow for graded sediment transport [White and Day, 1982] and to correct for the over prediction of fine sediments and relative coarse sediments [Wallingford, 1990]. It is defined as:

$$Q^{\star}_{si} = C\left\{\frac{F_{gri}}{A_i} - 1\right\}^d \tag{2.4}$$

where F_{gri} is the mobility number of sediment in the ith fraction and C, A_i and d are empirical coefficients depending on the dimensionless particle size (D_{gri}).

$$Q^{\star}_{si} = \frac{X_i H}{sD_i}\left\{\frac{u_{\star}}{U}\right\}^e \tag{2.5}$$

where X_i is the rate of sediment transport in terms of mass flow per unit flow rate for the ith fraction, H is the water depth, U is the mean velocity, e is a transition exponent that is a function of the dimensionless particle size.

$$F_{gri} = \frac{u^e_{\star}}{\left[gD_i\,(s-1)\right]^{1/2}}\left\{\frac{U}{\sqrt{32}\log_{10}\left(\alpha H/D_i\right)}\right\}^{1-e} \tag{2.6}$$

with $\alpha = 10$ for turbulent flow. In equation 2.4 A_i is replaced with A'_i for the White and Day

[1982] settings and is calculated as follows:

$$A_i' = \left(0.4\frac{D_a}{\sqrt{D_{50}}}+0.6\right)A_i \tag{2.7}$$

$$D_a = D_{50}\left(1.62\left(\frac{D_{84}}{D_{16}}\right)^{0.5}\right)^{-0.55} \tag{2.8}$$

where D_a is the particle size that begins to move under the same conditions as uniform material and D_{16}, D_{50} and D_{84} represent the subsurface particle size for which respectively 16%, 50% and 84% of the sediment sample is finer. Finally the sediment transport rate can be calculated in terms of mass per unit flow rate (X_i):

$$Q_{si} = X_i Q \frac{\rho_s}{\rho} \tag{2.9}$$

where Q_{si} is the total sediment transport rate for fraction i, Q is the water discharge, ρ the density of water and ρ_s the density of sediments.

Graded sediment transport, i.e. transport over a range of size fractions, can be calculated from the uniform sediment transport formula for each fraction. For each fraction the contribution to the total sediment transport is given the same proportion as that fraction in the active layer (sediments available for transport). The underlying assumption here is that every fraction is at transport capacity and therefore the rate should be scaled to what is available in the river bed.

2.5 Numerical modelling

As mentioned above, in natural rivers, a change in discharge or sediment transport never comes alone. The combination of these two changes leads to uncertainty in the expected river response. A numerical model can be helpful to determine the river response and quantify this effect. Ideally, numerical models contain the same interactions and feedback loops as the system under study. To be efficient, a numerical model should not be more complex than necessary [Jansen *et al.*, 1979], and only the most important processes should be incorporated in the model.

Morphological development of river channels can be simulated by a variety of numerical models, ranging from one to three dimensions; uncoupled, semi-coupled and fully coupled models, etc. Well known and widely used models are: in 1D (CHARISMA, HEC-6 (or HEC-RAS), SEDROUT, GSTARS(1½D)), 2D (CCHE2D, RMA2D, MIKE21, DELFT2D) and 3D (TELEMAC, MIKE3 and DELFT3D). Description of these models can be found in the comparative work of Yang and Simões [1999]; Langendoen [2001]; Duc *et al*. [2004] and Papanicolaou *et al*. [2008]. One-dimensional models remain a common approach for simulation of reach-scale flow, morphodynamic and habitat problems, where the length is equal to several times the river channel width [Lane and Ferguson, 2005]. These models are also used in complex geometry and can even include meander migration [Abad and Garcia, 2006; Crosato, 2007]. However, 2D or 3D approaches, which require more data and computer processing time, have sometimes been used [Morin *et al*., 2000; Darby *et al*., 2002; Olsen, 2003; Kleinhans *et al*., 2008; Papanicolaou *et al*., 2008].

Discharge variation for numerical simulation of river morphology can be represented in different ways, i.e. daily or yearly discharges, representative floods, or catastrophic events. The assumption often made is that for each river a discharge exists that transports most of the sediments and corresponds to the river dimensions. This assumption goes back to the effective discharge concept of Wolman and Miller [1960], and as discussed above there is a lot of uncertainty about this discharge. For graded sediments in models and variation of discharge over time the range of all discharges should be combined within the model.

2.5.1 1D models

One dimensional models use depth and width averaged variable as water elevation, water velocity and sediment transport rate. This implicitly assumes that velocity and transport rates are equally distributed over the river width and depth [Ferguson, 2003], which is a valid assumption only for rivers with approximately rectangular cross-sections and minor variation in water surface width [Cui *et al*., 1996; Ferguson, 2003].

The basic governing equations for these models are the conservation of mass and momentum equations:

$$\frac{\partial h}{\partial t} + \frac{\partial q}{\partial x} = 0 \tag{2.10}$$

$$\frac{\partial u}{\partial t} + u\frac{\partial u}{\partial x} + g\frac{\partial h}{\partial x} = 0 \tag{2.11}$$

where h is the water surface, q is the specific discharge, t is the time, x is the longitudinal distance and u is the longitudinal velocity.

The Exner and Hirano equation is used for mass conservation:

$$-(1-\lambda)\frac{\partial z}{\partial t} = \frac{\partial Q_s}{\partial x} \tag{2.12}$$

where z is the bed elevation, λ the bed porosity and Q_s is the total sediment transport.

Complex geometries are difficult to capture within a 1D model. Tributary input of water discharge and sediment transport can be incorporated with relatively simple assumptions such as an "instantaneous" mixing of bedload at junctions [Hoey and Ferguson, 1994; Li *et al*., 2008]. The modelling of bifurcations or island(s) is more problematic, as sediment distribution is typically different from the water discharge distribution [e.g Wang *et al*., 1995; De Vriend *et al*., 2000]. The topography of the bifurcation is an important factor for the sediment distribution. As can be seen in Figure 2.13, the location of the channel downstream of the bifurcation or along an island is a factor which is not accounted for in a 1D model. The influence of the bifurcation topography on the grain size distribution is called the 'Bulle'-effect [Bulle, 1926; Riad, 1961; Miori *et al*., 2006].

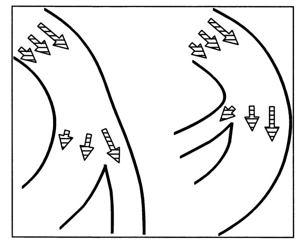

Figure 2.13: Sediment distribution at a bifurcation in a river bend highlighting the 'Bulle'-effect. Adapted from De Vriend *et al.* [2000].

The variation of sediment transport direction between different grain sizes complicates the modelling of bifurcations. At a bifurcation in or after a river bend, the channel on the inside will not only receive relatively less sediment transport, but the sediment will also be relatively fine compared to the main stream as the coarser particle tend to move to the deeper area on the outer side of the river bend [De Vriend *et al*., 2000; Frings and Kleinhans, 2008]. As illustrated in Figure 2.14, on a transverse slope the coarser particles will move towards the deeper area due to gravitational force [Engelund, 1974]. The lateral slope of the river bed upstream of a bifurcation influences the distribution of the grain sizes between the river branches.

To compensate for geometric inaccuracy in 1D models, a nodal point relationship based on the width of the river branches has been proposed by Wang *et al*. [1995]:

$$\frac{Q_{s2}}{Q_{s3}} = \frac{B_2}{B_3}\left(\frac{Q_2 B_3}{Q_3 B_2}\right)^c \tag{2.13}$$

where B the width of the channel, c is power, and $_2$ and $_3$ are subscripts for branches downstream of the bifurcation. The stability of the bifurcation depends on the choice of c. Wang *et al*. [1995] found that the bifurcation will be unstable for every value of $c < {}^{b}/_{3}$ and one of the branches will close. If $c > {}^{b}/_{3}$ the bifurcation is stable and both branches remain open. When $c = {}^{b}/_{3}$, the outcome is undetermined (Figure 2.15). Assuming that the sediment transport is proportional to the water velocity to the bth power, $q_s = au^b$. For all transport equations where $b > 3$ and where the friction formula is based on Chézy equation, it follows that $q_s \sim q^{b/3}$. For $c > {}^{b}/_{3}$ the closing of one channel, with $q_s \sim q^c$ at the upstream boundary, would lead to a much larger decrease in sediment input than the sediment capacity, resulting in erosion of that channel and an increase in discharge. In variable discharge simulations, the distribution of sediment transport varies and leads to a more oscillating behaviour of the river bottom, as the branches receive more or less sediment than the equilibrium rate [De Vriend *et al*., 2000].

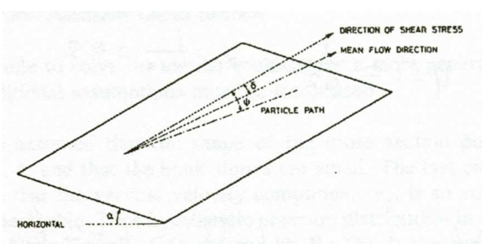

Figure 2.14: Motion of sediment particle on a transverse slope. Adapted from Engelund [1974]

Recently, Miori *et al*. [2006] proposed a 1D model that takes into account width change and variable discharge. They adopted a "quasi two-dimensional approach" from Bolla Pittaluga *et al*. [2003] (Figure 2.16). Even though their approach is close to a 2D model, they found that even in the case of ideal circumstances (constant discharge) there are several equilibrium stages and results are very sensitive to the initial conditions. Also, the bed topography at the bifurcation is not accounted for. Furthermore, the results of morphological modelling remain highly sensitive to the sediment transport formula [Havis *et al*., 1996; Tingsanchali and Supharatid, 1996; McLean *et al*., 1999]. All formulae have their advantages and disadvantages [Tingsanchali and Supharatid, 1996; Batalla, 1997; McLean *et al*., 1999; Barry *et al*., 2004] and ideally more than one formula should be tested.

Different methods exist to incorporate bank erosion within morphological models in one, two or three dimensions. Bank erosion is not only adding sediments to the system, it could also result in width adjustment of the channel, which is mostly neglected by 1D models [Piégay *et al*., 2005]. This is important in bank erosion caused by river incision, contrary to meander migration which is mostly a lateral shift where sediment input is compensated by sedimentation on the inner bank. The major drawbacks of process-based bank erosion

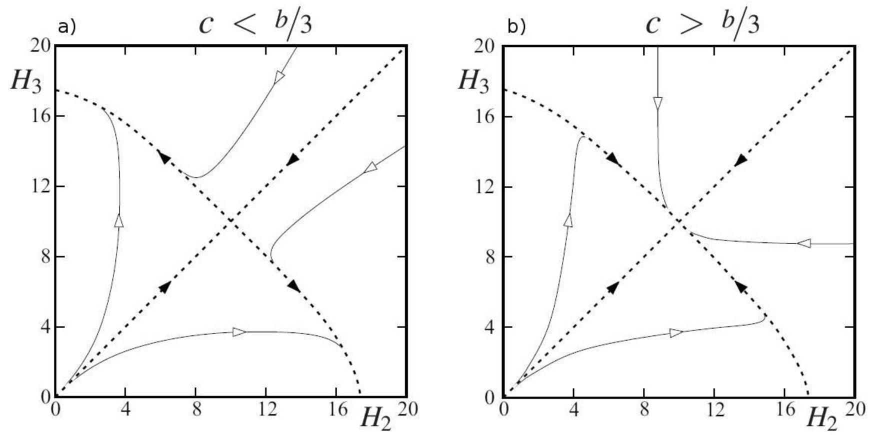

Figure 2.15: Stability of nodal point relationship in 1D models, a) unstable bifurcation b) stable bifurcation [Wang *et al.*, 1995]. With H_2 and H_3 representing the water depth in both bifurcates, c the power in the nodal point relationship and b the power of the sediment transport formula. Dotted lines indicate phase limits under stationary conditions, continuous lines give possible pathways of bifurcate depth development.

in morphological models are first, that they mainly rely on calibrated erosion rates rather than the character of the bank sediments, second, that they are often restricted to idealised or artificial geometries [Darby *et al.*, 2002; Piégay *et al.*, 2005]. Most 1D models use excess shear stress at the toe and excess bank height [Mosselman, 1998] that depend on a calibration parameter and their predictability is therefore low. However, at the event scale, 1D models without bank failure match fairly well observed bed elevation changes El kadi Abderrezzak and Paquier [2009]. For a fully integrated analysis the coupling of fluvial erosion, seepage and stability submodels is required [Darby *et al.*, 2007] and this would require a 2D approach [Piégay *et al.*, 2005].

Even if there are well-known advantages of 1D over 2D models in terms of data requirements and computational effort [Papanicolaou *et al.*, 2008], the above-mentioned limitations of 1D models for complex channels may lead us to believe that 2D models are more optimal for morphological simulations of overbank flow and sedimentation patterns in lakes. However, it remains unclear whether 2D models really provide a more accurate description of the morphology within channels. Most of the 2D models are not yet capable of simulating bank erosion [Darby *et al.*, 2007], and are therefore unable to predict changes in river pattern. Moreover, 2D models that use a calibrated bank retreat module, like Mike21C, cannot predict changes in river pattern either as the change in the model is not based on the actual resistance of the bank, but on past rates of erosion. If a physical model for bank erosion is available, re-gridding of the model is very complex in long-term simulations [e.g Olsen, 2003; Crosato, 2007]. A comparison of model performance by Rathburn and Wohl [2001] concluded that (pseudo) 2D modelling was not necessarily better in reproducing river morphology than a 1D model. However, in gravel-bed rivers, the shear stress is close to the critical shear stress and sediment transport is limited to a small section of the cross-section [Ferguson, 2003], therefore 1D modelling in these rivers is less suitable, unless an effective-width approach is used [Ferguson and Church, 2009]. For sand-bed rivers, on the other hand, as shear stress is mostly well above the critical shear stress over almost all the cross-section, 1D models can be considered representative of the natural processes [Lane and Ferguson, 2005].

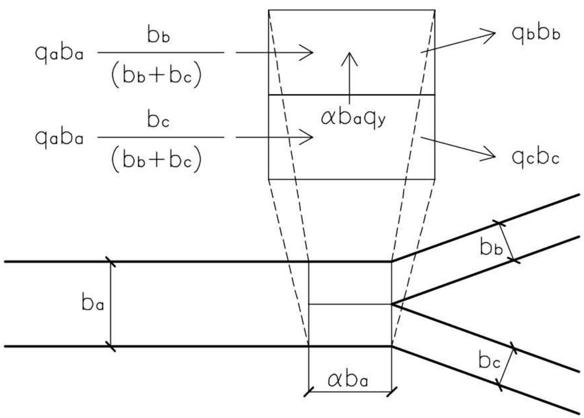

Figure 2.16: Scheme of nodal point relationship. Adapted from Miori *et al.* [2006].

One of the major challenges in modelling river morphology is to ensure the model results are representative of the river under study. Often the calibration and validation of the morphological model are conducted on the same data set. Cao *et al.* [2002] argued that the use of the term calibration and validation is actually misleading not only because of the small number of empirical data, but also due to the implicit assumption that a single set of unique parameters exists that leads to a satisfying accuracy of the numerical model. Moreover, in a model with several thousand nodes, like 2D and 3D models, proving that the model is accurate for all these points in virtually impossible. The difficulty of calibration and validation of morphological models therefore raises questions about the predictive capacity of these models [Phillips, 2003].

Despite these drawbacks 1D models have several advantages over 2D and 3D models. They have been successfully applied in a wide variety of fluvial and morphological simulations [Cui *et al.*, 1996; Ferguson *et al.*, 2001; Talbot and Lapointe, 2002; Kleinhans *et al.*, 2008; Ferguson and Church, 2009], that even include some very complex topographies. In this thesis, the 1D model SEDROUT, developed by Hoey and Ferguson [1994], will be used. This model was developed to simulate aggradation and downstream fining, and handles graded sediments and records bed stratigraphy. SEDROUT is based on the approach of Parker [1990b], ACRONYM 3, that routes sediment through a river section with a constant width. SEDROUT is generalized to allow long profiles and cross-section profiles of any shape. The grain size distribution is recorded for the transport, active layer, and four layers in the substrate. These four underlying layers not only keep track of the composition during aggradation, but they can also represent variation in erodability of the river bed under degradational conditions. The layer concept in SEDROUT uses sublayers with a thickness that is equal to the active layer.

In Figure 2.17, a definition diagram of SEDROUT is presented. SEDROUT uses a step-backwater algorithm to estimate the hydraulic conditions. Hydraulics are considered to be steady, however hydrographs can be incorporated within the model. The computation starts at the downstream end of the river section and proceeds upstream with the use of a step-backwater approach, with depth-averaged flow equations. At the downstream end the water level can be specified or equilibrium flow can be assumed. In the latter case, the model will extend until the downstream water level reaches equilibrium elevation. The working equations for the model are the conservation of mass equation 2.10 and momentum equation 2.11.

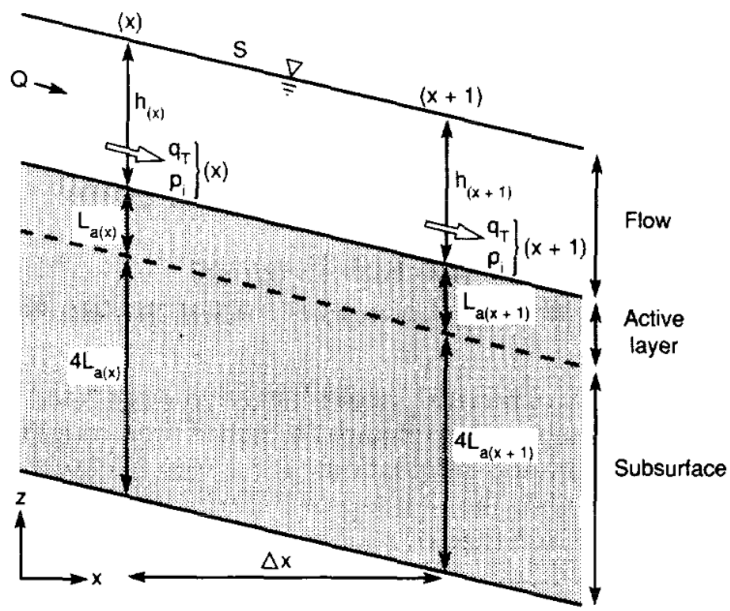

Figure 2.17: Definition diagram of SEDROUT [Hoey and Ferguson, 1994].

Two different friction equations are available in SEDROUT, namely Darcy-Weisbach friction factor and Manning-Strickler's n-value. Both are a function of the grain size within the active layer for gravel-bed rivers. The roughness values depend on bed forms and channel topography as well. In turn bed forms, especially dunes in sand-bed rivers, are a function of flow conditions and can change drastically between flow stages. To simplify morphodynamic simulation often a constant roughness value is chosen, which can be spatially variable, for floodplain vegetation for example.

The morphological computation is done after the hydraulics is calculated for the whole river reach, meaning that the model is fully uncoupled. In SEDROUT three different sediment transport formulae are available. Originally, the bedload transport algorithm of Parker [1990b] was the only one available but, subsequently, two other options were added: those of Einstein [1950] and Wilcock and Crowe [2003].

After calculation of sediment transport rates using one of the transport equations, the bed level and composition is updated using the Exner and Hirano equation for the mass conservation of sediment in total and for each particle size:

$$(1-\lambda)\frac{\partial L_a F_i}{\partial t} = -\frac{\partial\left(q_T p_i\right)}{\partial x} + E_i\left(\frac{\partial Q_s}{\partial x} + (1-\lambda)\frac{\partial L_a}{\partial t}\right) \tag{2.14}$$

$$E_i = c_i F_i + (1-c_i)\, p_i; \quad 0 \leq c_i \leq 1 \tag{2.15}$$

where L_a is the active layer thickness, F_i, p_i and E_i are the proportions of the volume material in the i-th size class in the active layer, the bedload and the exchange layer (between the active layer and the substrate) and c_i is a weighting factor allowing the bed-load material to be mixed with the substrate [Hoey and Ferguson, 1994; Toro-Escobar *et al.*, 1996]. The original option for the thickness of the active layer is a function of the grain size, which is suitable for gravel-bed rivers [Armanini, 1995]. A thickness as a function of the grain size makes the solution of the momentum equation an iterative process.

SEDROUT was first tested on the Allt Dubhaig River (Scotland) by Hoey and Ferguson [1994]. This small gravel bed river has strong downstream fining and a nearly constant width. The model predictions matched closely the observed downstream fining. Consequently, a sensitivity analysis of the model was conducted by Hoey and Ferguson [1997] with the same data set. The sand/gravel bed Vedder River, a tributary of the Fraser River in British Colombia (Canada), was successfully modelled with SEDROUT by Ferguson *et al.* [2001]. Good visual and quantitative agreement with the mean trend of gravel/sand accumulation along the river was found under aggrading conditions, towards a local base level. Extending the use of SEDROUT to gravel/sand mixtures suggests that Parker's equation for bedload transport can be applied to gravel-bed rivers with some sand. However, a modification of the equation to allow for differences in bed sorting is necessary to obtain satisfactory results. The aggradation and degradation response to artificial meander straightening in a gravel-bed river, the Sainte-

Marguerite River in Québec (Canada), was modelled by Talbot and Lapointe [2002] and matched field observations better than a theoretical model. More recently, Ferguson and Church [2009] simulated gravel transport and aggradation in the complex Fraser River with SEDROUT, using the concept of effective width. An overview of the dimensions of these rivers is given in Table 2.1. The rivers modelled using SEDROUT show its potential for long-term morphological simulations in a variety of river settings.

2.5.2 2D models

Two dimensional models can firstly be split in depth- and width-averaged models, the latter is mostly used in conceptual simulations or stratification studies in deep waters like lakes or seas. Depth-averaged are mostly used in complex geometry simulations such as bifurcations and meander bends. Different discretisation schemes can be used for capturing the topography of the studied river, such as finite difference, finite element or finite volume. Finite elements can be defined by curve linear grids or unstructured triangular grids. To deal with real topography and a range of flow stages a wetting and drying or movable boundary needs to be used [Leclerc *et al.*, 1990; Yang and Simões, 1999]. To allow for channel migration or bank erosion in finite element models it is necessary to re-grid the numerical mesh after each iteration [Mosselman, 1998; Crosato, 2007]. Although this is already possible, it requires calibration or fitted meander migration [Langendoen, 2001; Darby *et al.*, 2002, 2007].

Governing equations for 2D models are similar to those of 1D, but have an extra spatial component, the equation for mass conservation is:

$$\frac{\partial h}{\partial t} + \frac{\partial q_x}{\partial x} + \frac{\partial q_y}{\partial y} = 0 \tag{2.16}$$

where, q_x and q_y are the longitudinal and lateral discharge per unit width, respectively, and y is the lateral direction. The momentum conservation equations are:

$$\frac{\partial u}{\partial t} + u\frac{\partial u}{\partial x} + v\frac{\partial u}{\partial y} + g\frac{\partial h}{\partial x} = F_x \tag{2.17}$$

$$\frac{\partial v}{\partial t} + u\frac{\partial v}{\partial x} + v\frac{\partial v}{\partial y} + g\frac{\partial h}{\partial y} = F_y \tag{2.18}$$

		Allt-Dubhaig [Hoey and Ferguson, 1994]	Sainte-Marguerite River [Talbot and Lapointe, 2002]	Vedder River [Ferguson *et al.*, 2001]	Fraser River [Ferguson and Church, 2009]
Flood discharge	(m^3/s)	6–10	110	335	9000
Bankfull width	(m)	10–30	45	100–250	525
Bed slope	(-)	2.2×10^{-2}	2.34×10^{-3}	4.6×10^{-3}	$6–48\times10^{-5}$
Bed mean grain size	(mm)	95	70	50	0.4–42
Channel pattern		meandering	meandering	braiding	braiding
Type of bed change		aggradation	aggradation and degradation	aggradation	aggradation
Simulation length	(years)	>100	33	–	20
Modeled reach length	(km)	2.5	12	9	38

Table 2.1: Characteristics of the rivers previously simulated with SEDROUT

where F_x, F_y are the resulting momentum in respectively the longitudinal and lateral directions and v is the velocity in lateral direction.

Very shallow areas can be problematic for depth-averaged models as the shear stress tends to be over predicted when the Manning-Strickler formula is used [Li and Millar, 2007], which results in over estimation of bed-material transport. However hydraulics over complex river bed topography, as simulated by Li *et al.* [2008], give realistic spatial patterns of bed shear stress under various flow conditions.

2.5.3 3D models

Depth-averaged models assume a vertical logarithmic velocity profile, which is valid for uniform flow and to some extent for gradually varying open channel flow. In rivers with complex topography, for example around hydraulic structures, the flow and sediment motion are typically three dimensional. Since the 1980s different 3D models have been developed first with only sediment transport over a rigid riverbed, and later with added erosion and sedimentation [e.g. Olsen, 2003; Nagata *et al.*, 2005] (see Papanicolaou *et al.* [2008] and Lu and Wang [2009] for reviews). The advantage of 3D-flow field computation is that the sediment transport direction for both suspended load and bedload can be derived from the water velocity direction directly instead of using approximations for secondary flow. The 3D models are also used to investigate the theoretical understanding of certain processes, such as meander formation [Olsen, 2003]. However, the use of these 3D model is mainly restricted to flume studies, or short river reaches (< 5 km) and very short time scale (in the order of days) [Dargahi, 2004].

2.6 Saint-Lawrence River system

The Saint-Lawrence River is one of the world's largest river system, originating from Lake Ontario and flowing into the Atlantic Ocean. The Saint-Lawrence River itself has relatively low sediment transport rates, with most of the sediments coming from its tributaries. Five tributaries were selected for this research. Three of them are located on the north shore of the Saint-Lawrence River: the Batiscan River, Saint-Maurice River and Yamachiche River, and two on the south shore: the Richelieu and Saint-François River (Figure 2.18).

The tributaries are located in the Saint-Lawrence Lowlands, a low-lying area which was

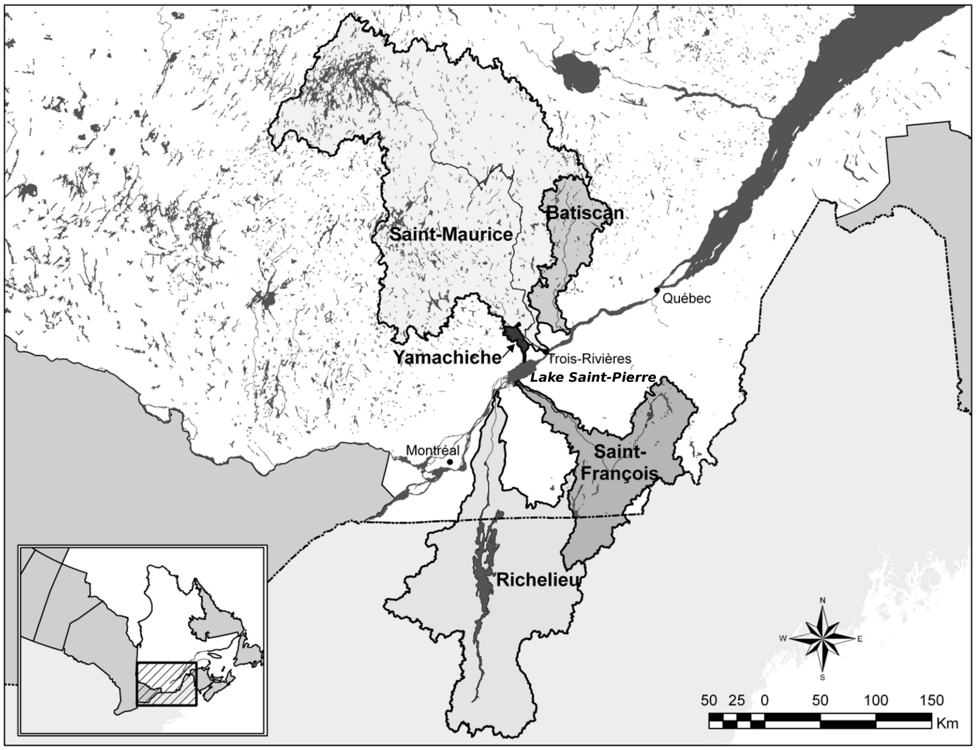

Figure 2.18: Location of the tributaries of the Saint-Lawrence River

submerged by the Champlain Sea after the last glaciation. The Lake Saint-Pierre is a remnant of the Lampsilis Lake (a vestige of the Champlain Sea) (Figure 2.18). Its level has been relatively stable in the last 3000 years, although human occupation and the Saint-Lawrence Seaway dredging have modified the hydrology and sediment input of the Saint-Lawrence River and of its tributaries [Rondeau *et al.*, 2000]. The donwstream parts ($\pm$ 15 km) of the tributaries are flowing trough fine sediments. Their bed consist of coarse sediment with size of medium sands (with some gravel) to fine sediments of the size of silt and clay.

These rivers were selected because of their breadth in discharge, size, hydrological regime and sedimentology, and also because they are located on both the north and south shore of the Saint-Lawrence River. The location on the north and south shore is important as the watersheds extend into different regions where climate change is not expected to have the same effects. The different sizes are important as they are representative of the whole range of tributaries found around the Saint-Lawrence River. Results from these rivers can therefore be used to generalize the effects to other tributaries nearby. The Yamachiche River, which is relatively unimportant for creating changes in the Saint-Lawrence River and Lake

Saint-Pierre because of its small size, is included because information on its past evolution is available [Bondue *et al.*, 2006], which could help validating the morphological model. In general, the tributaries are sand-bed rivers with some coarser fractions in it. The Saint-Maurice River contains more gravel and boulders in the upstream reach.

GCM	Country	Resolution (lat×long)	GHG-scenario
CSIRO-Mk2	Australia	3.2°×5.6°	A2 and B2
ECHAM4	Germany	2.8°×2.8°	A2 and B2
HadCM3	United Kingdom	2.25°×3.75°	A2b and B2b

Table 2.2: Global climate model and GHG-emission scenarios

The Saint-Lawrence River is of great economical value for Canada and it is part of the Saint-Lawrence Seaway, which connects the Great Lakes with the Atlantic Ocean. It passes several narrow sections, rapids and lakes. Because of this variety the Saint-Lawrence River contains different habitats that contribute to a diverse ecosystem. In the past, dredging for the Saint-Lawrence Seaway at the mouth of Lake Saint-Pierre resulted in a water level drop of 0.5 m within the lake. The Saint-François and Yamachiche rivers developed deltas at their mouth that propagated into Lake Saint-Pierre [Bondue, 2004]. This lake is very wide (10–12 km) and shallow (mean depth < 3 m) and is of great ecological value. It has been a UNESCO biosphere reserve since 2001 on account of its marginal habitats [Jacques, 1986; Morin and Côté, 2003; Hudon, 2004; Hudon and Carignan, 2008], as the most important habitats are located at the edge of land and water. The Saint-Lawrence Seaway navigation depths are critical in the lake, such that any decrease in water level or increase in sedimentation may have important economical consequences. More than half of the suspended sediment input from the south shore tributaries comes from three rivers: the Yamaska, Richelieu and Saint-François rivers [Rondeau *et al.*, 2000]. Because the lake is very shallow, an increase in sediment input could result in sedimentation and reduction of water surface area and perimeter.

Several studies have observed a change in winter and spring flow over the last century in eastern North America [e.g. Zhang *et al.*, 2001; Hodgkins and Dudley, 2006; Boyer *et al.*, in press]. It is expected that in the near future these changes will continue and alter the flow regime of the rivers within this area, for the Saint-Lawrence River itself [Croley, 2003] as well as for its tributaries [Chaumont and Chartier, 2005; Quilbé *et al.*, 2008]. In the near future, discharges and water levels within the Saint-Lawrence River and its tributaries are predicted to decrease [Croley, 2003]. Thus, the tributaries will not only experience a change in discharge, but also a lowering in their base level (Saint-Lawrence water level). These changes may lead to a change in sediment supply from the tributaries to the Saint-Lawrence River. Discharge scenarios were simulated by Ouranos for two different greenhouse gas emission scenarios, namely A2(b) and B2(b), according to the IPCC and reported in the Special Report on Emissions Scenarios (SRES). These scenarios represent two different families: the A2 scenario emphasizes economic development and the B2 scenario relates to sustainable development. The changes in rainfall, snowfall, minimum and maximum temperature were simulated with 3 different global climate models: CSIRO-Mk2; ECHAM4 and HadCM3 (Table 2.2).

Two-dimensional hydrodynamic modelling of the Saint-Lawrence River portion between Montréal and Trois-Rivières is already available (model H2D2 [Morin and Bouchard, 2001]). This model is mainly used to verify water elevations under different hydrological regimes, combinations of tributary inflow and management of upstream hydro-power dams. H2D2 can only simulate suspended sediments over a rigid topography, although currently it is being adapted to include sediment transport and variations in bed elevation and bed composition. Ideally in the near future, an integrated 2D model of the Saint-Lawrence River and its tributaries will be available. The work presented in this thesis is a first step towards this objective, as it will enable a better understanding of the sedimentary dynamics of the tributaries.

Paragraphe de liason A

The morphological effects of climate on the Saint-Lawrence River tributaries are investigated with the use of the SEDROUT one-dimensional morphodynamic model. SEDROUT needed to be adapted to the characteristics of the selected tributaries, such as: sediment type and the presence of islands. Furthermore, SEDROUT needed to be adapted to simulate variable discharge and downstream water level including a tidal effect and change over time. Note that within this thesis SEDROUT is the original version of the model, whereas SEDROUT4-M refers to the enhanced model. Chapter 3 describes the changes made to the code. A copy of the modified code (SEDROUT4-M) can be found in Appendix III, where some additional changes to the code, that are not presented in chapter 3, are also described. Besides the description of the modifications and justification to use SEDROUT4-M in this thesis, chapter 3 also verifies if these modifications are working correctly using simulations of theoretical situations. Validation of the hydraulics of the models for four tributaries of the Saint-Lawrence River is presented in the last part of chapter 3, namely for the Batiscan, Richelieu, Saint-Maurice and Saint-François rivers. The Yamachiche River was not validated because of critical flow occurring in the simulations of this river (see chapter 6 for details).

CHAPTER 3

A MODIFIED MORPHODYNAMIC MODEL FOR INVESTIGATING THE RESPONSE OF RIVERS TO SHORT-TERM CLIMATE CHANGE [1]

3.1 Introduction

Rivers are directly affected by climate change through changes in discharge consequent on precipitation and evaporation and through base level changes [Schumm, 1977; Leopold and Bull, 1979; Tucker and Slingerland, 1997; Blum and Törnqvist, 2000; Bogaart and van Balen, 2000]. Base level change is often considered only in terms of sea level variation, but major rivers act as local base levels for their tributaries.

In the Saint-Lawrence River system in eastern Canada, the effects of climate change on precipitation and snow melt are anticipated to lead to reduced discharges in the Saint-Lawrence River [Croley, 2003] and changed discharges in its tributaries over the next century [Chaumont and Chartier, 2005]. As discharge in the Saint-Lawrence River declines, its tributaries will experience reduced base levels, contrary to the global sea level situation (or rise). The effects on tributaries of a lowering of the mainstream water level have previously been recognized in a series of conceptual channel evolution models [e.g. Simon and Hupp, 1986; Simon, 1989, 1992] and in the context of flow regulation for a gravel-bed river [Church, 1995]. However, to our knowledge, no study has investigated the effect of a climate-induced change in discharge and lowering of base level over intermediate time (50–100 years) and spatial ($\sim$ 15 km) scales in sand-bed, lowland river reaches. Such conditions are of worldwide importance, being where most human settlements are located, such that morphological change has potentially significant impacts.

The consequences for the tributaries of near-simultaneous changes in hydrological regime and base level could include changes in any or all of sediment transport rate, bed elevation, bed composition, channel dimensions, and channel pattern. Many numerical models for channel change at reach scale have been developed by university researchers, consultancy firms, and government agencies [see reviews by Yang and Simões, 1999; Langendoen, 2001; Duc

[1] the basis of this chapter is published in GEOMORPHOLOGY, 2008 Vol.**101**(4)

et al., 2004; Lane and Ferguson, 2005]. These models vary in dimensionality (one-, two-, or three-dimensional) and generality (e.g., whether they are restricted to sand-bed or gravel-bed channels, can handle graded beds, or can simulate changes in width). In the context of the Saint-Lawrence tributaries, a model needs to handle graded beds (though mainly sandy), very low slopes, incision, and permanent islands. The spatial scale exceeds 10 km and the timescale is $\sim$ 100 years so only 1D and 2D models can realistically be envisaged. In this study, we use a 1D (i.e., width-averaged) model. This is partly for pragmatic reasons (lower requirement for field data for calibration and validation, simplicity, shorter computer processing time) and partly because of doubts over the utility of a 2D model.

The rivers we are modelling have very low stream power, resulting in low hydraulic attack on the banks. Although river banks could nevertheless be undermined and fail under gravity following bed degradation [Darby and Thorne, 1996], these rivers are unlikely to experience major bank retreat or planform change, which in any case are not yet handled well by 2D models [Langendoen, 2001; Darby *et al*., 2002].

Field studies of sand-bed rivers suggest that the primary response to downstream water level change is a change in bed elevation [Hassan and Klein, 2002; Gaeuman *et al*., 2005], which implies that the key requirement is accurate simulation of sediment transport rates. One-dimensional models can seriously underestimate bedload flux in gravel-bed rivers if flow and transport are concentrated in only part of the channel width [Ferguson, 2003; Li *et al*., 2008], but this bias is generally small in sand-bed rivers where shear stress is normally far above the threshold for motion. In one of the few comparative studies of transport models, Rathburn and Wohl [2001] found that a pseudo 2D model performed less well than a 1D model in a coarse-bed channel.

The 1D model used in this study is SEDROUT [Hoey and Ferguson, 1994]. This has much in common with the best-known 1D model, HEC-6 [U.S. Army Corps of Engineers, 1996], but was designed from the outset to handle graded sediment and to record bed stratigraphy during aggradation. As with other such models, SEDROUT solves the depth-averaged flow equations using a step-backwater method and a choice of friction equations; uses the calculated shear stresses at each cross section to compute bed-material transport using a choice of rate equations; then updates bed level and composition using the Exner and Hirano equations for overall and fractional sediment conservation. These conservation equations are, respectively,

$$-(1-\lambda)\frac{\partial z}{\partial t}=\frac{\partial Q_s}{\partial x} \tag{3.1}$$

where z is the bed elevation, x is the streamwise distance, λ is the bed porosity, Q_s is the total sediment transport, and t is the time; and

$$(1-\lambda)\frac{\partial L_a F_i}{\partial t}=-\frac{\partial\left(Q_s p_i\right)}{\partial x}+E_i\left(\frac{\partial Q_s}{\partial x}+(1-\lambda)\frac{\partial L_a}{\partial t}\right) \tag{3.2}$$

where L_a is the thickness of the active layer, and F_i, p_i, and E_i are the proportions of the volume of material in the ith size class in the active layer, the bedload, and the exchange layer between the active layer and the substrate. During incision, E_i is defined by the subsurface stratigraphy; and during aggradation it is often taken to be equal to F_i or to a weighted combination of F_i and p_i [Hoey and Ferguson, 1994; Toro-Escobar *et al.*, 1996].

SEDROUT was first applied to simulate rapid downstream fining of bed material by size-selective transport in a small gravel-bed river [Hoey and Ferguson, 1994]. SEDROUT has subsequently been shown to have applicability across a range of time- and space-scales [Hoey *et al.*, 2003], for example reproducing well the effect of artificial meander straightening in a gravel-bed river in Québec [Talbot and Lapointe, 2002] and changes in sediment flux and bed composition along a large gravel/sand tributary of Fraser River, Canada [Ferguson *et al.*, 2001].

This paper summarises modifications to SEDROUT4 (previous version) to increase its utility for investigating river response to short-term climate change scenarios and verifies these new features. The modifications include allowing variable steady discharge on a day-to-day basis; variable downstream water level (base level) at year-to-year, seasonal, and tidal timescales; inclusion of a transport equation specifically developed for fine-graded sediment; the ability to route water and sediment round midstream islands; and an improved treatment of how bed stratigraphy evolves during alternating erosion and deposition. Verification tests include simulation of measured present-day flow and transport variables in tributaries of the Saint-Lawrence River. The impact of climate change will be reported separately [Verhaar *et al.*, in press], by applying the modified model (SEDROUT4-M, current version) to these tributaries and simulate different discharge and water level scenarios.

3.2 Study areas

The four tributaries of the Saint-Lawrence River system studied here are all located between Montréal and Québec close to Lake Saint-Pierre. Two tributaries are on the north shore of the river (Saint-Maurice River and Batiscan River), and two are on the south shore (Richelieu River and Saint-François River) (www.geog.umontreal.ca/hydro/TributairesSt-Laurent/). The tributaries are located in the Saint-Lawrence Lowlands, a low-lying area which was submerged by the Champlain Sea after the last glaciations (Figure 3.1). The Lake Saint-Pierre is a remnant of the Lampsilis Lake (a vestige of the Champlain Sea). Its level has been relatively stable in the last 3000 years, although human occupation and the Saint-Lawrence Seaway dredging have modified the hydrology and sediment input of the Saint-Lawrence River and of its tributaries [Rondeau *et al.*, 2000]. All the tributaries have very mild slopes, and the river bed material ranges from fine silt and clay, to coarse sand and gravel, with even some boulders in the Saint-Maurice River. The length of the studied reaches upstream from the junction with the Saint-Lawrence River ranges from 14 to 17 km (Table 3.1). All of the tributaries are regulated to some extent by hydroelectric power dams. The river dimensions, discharge, and sedimentology are given in Table 3.1. In the Saint-François River and the Saint-Maurice River, permanent islands are present in their lower reaches.

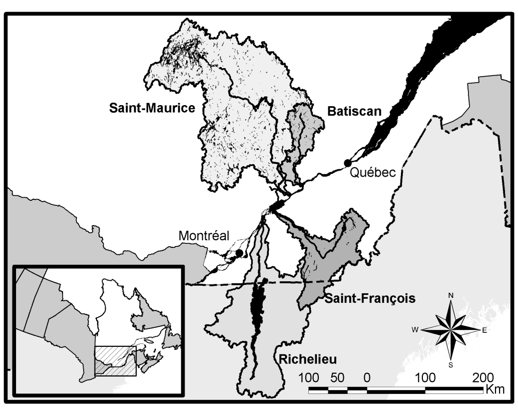

Figure 3.1: Geographical location of the tributaries of the Saint-Lawrence River.

Bed topography data were collected from a boat equipped with a sonar and GPS at different flow stages (bankfull and low flow) in 2004 or 2005. A second bed topography survey of all the tributaries was taken in 2006. Velocity measurements were taken with an ADCP (Acoustic Doppler Current Profiler). Bed composition was derived from bed samples taken with a grab bucket from the boat every three or four cross sections. Bedload sediment transport samples were taken at low and moderate discharge stages using a 76-mm Helley-Smith sampler (Table 3.2).

Name of river	Water surface bankfull width (m) mean (min-max)	Total length of studied reach (km)	Average discharge (m^3/s) (min-max)	Energy slope (-)	Sediment type upstream - downstream	Degree of regulation
Batiscan	167 (77–277)	17	99 (14–849)	6×10^{-5}	Clay to sand - silt to sand	Moderate
Richelieu	198 (89–278)	15	346 (40–1260)	5×10^{-5}	Silt to sand	High
Saint-François	233 (88–415)	15	208 (3–2520)	3×10^{-5}	Silt to gravel - silt to sand	High
Saint-Maurice	238 (70–507)	14	693 (76–5300)	1×10^{-5}	Silt to boulders - silt to cobbles	High

Table 3.1: Characteristics of the Saint-Lawrence and its tributaries

3.3 Additions and changes to the model

The modifications to the SEDROUT code can be divided into three groups. The first group contains changes required to deal with sand-bed rivers, as SEDROUT was originally designed for gravel-bed rivers. The next group covers the climate change adaptations, whereas the last group concerns specific changes for one or more of the tributaries studied here.

3.3.1 Sand-bed rivers

SEDROUT was developed using the bedload transport algorithm of Parker [1990b], but has subsequently had two alternatives added: those of Einstein [1950] and Wilcock and Crowe [2003]. Parker's equations are specifically for gravel, and the other two are based on experiments carried out with mixed gravel/sand beds. Ferguson *et al*. [2001] modified Parker's [1990b] bedload formula to permit calculation of transport rates in poorly sorted (including bimodal) mixed sand- and gravel-bed rivers. The bed sediments in the four tributaries range from silt to coarse sand with some gravel in the upstream reaches. As the sediment transport formulae available in SEDROUT have not been tested for this range of grain sizes, we implemented a bed-material transport formula which is more suitable for these particles sizes. A range of suitable formulae exist, including those of Toffaleti [1968] and Ackers and White [1973], which are total load formulas. As the reaches characterized by fine sediments in this study are short, we assumed that the fine suspended load is supply controlled (wash load) and is therefore not relevant in our simulations. All formulae have their advantages and

Name of tributary	Date	Discharge (m^3/s)	Width (m)	# with transport/total samples	Bedload (g/m/s)	Bedload (g/s)	Suspended load (mg/L)	Suspended load (g/s)	Total load (g/s)
Batiscan	2004-05-18	-	-	-	-	-	13.0	0	-
	2005-10-19	340	226	5/9	6.0	1357	15.9	5390	6747
Richelieu	2005-07-14	420	-	-	-	-	26.7	11 227	-
	2005-11-18	750	235	3/7	0.99	233	52.8	39 586	39 820
	2006-06-15	760	194	3/3	3.9	752	27.3	20 767	21 520
St-François	2004-05-18	-	-	-	-	-	92.6	0	-
	2005-10-12	250	280	0/9	None	None	11.9	2987	-
	2005-10-28	615	220	5/12	24.8	5454	-	-	-
	2006-06-14	-	-	-	-	-	138.2	0	-

Table 3.2: Overview of collected field data.

disadvantages, but using comparative work by Tingsanchali and Supharatid [1996]; Batalla [1997]; McLean *et al*. [1999] and Barry *et al*. [2004], we decided to implement the total load formula from Ackers and White [1973]. Since its initial development, two revised parameter settings for this formula have been proposed. We retain the option of using the original values [Ackers and White, 1973], or the revisions HR Wallingford [1990], or White and Day [1982] parameters. Each of these alternatives was applied to the Saint-François River using the measured bulk bed composition and a range of discharges including the ones at the time of our field measurements. The White and Day [1982] parameter setting, which explicitly allows for size-selective effects in entrainment, gave the best match with our field measurements (Figure 3.2). The field measurement is the average of 5 measurements at 3 different locations on a single cross section with a standard error in the same order of magnitude as the average value.

The active layer thickness L_a in SEDROUT was originally set to a user-specified multiple of D_{84} (diameter for which 84% by weight of the particles are smaller) [Parker, 1991; Hoey and Ferguson, 1994]. Scaling L_a on surface grain size is appropriate for gravel-bed rivers, but in sand-bed rivers a length scale such as dune amplitude is more relevant [e.g. Van Niekerk *et al*., 1992]. Here we have used a fixed value of 0.10 m as a minimum value as we did not observe any dunes in our reaches.

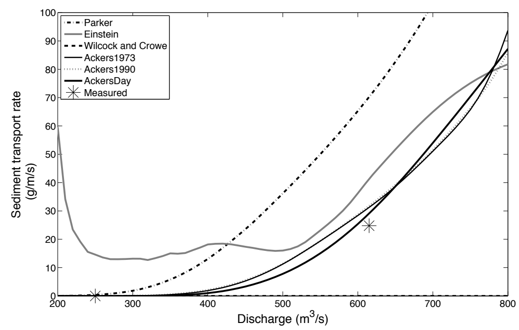

Figure 3.2: Comparison of the different transport formulae in SEDROUT on the Saint-François River under continuous increasing discharge. Note: the Wilcock and Crowe equation does not predict any sediment transport for this discharge range.

SEDROUT solves the discretised equations using explicit finite difference methods, with a time step that varies to satisfying the Courant-Friedrichs-Lewy (C-F-L) condition. Three conditions are used in SEDROUT to ensure numerical stability under a range of conditions, one from Park and Jain [1987] and two from Parker [1990a]. As is common in sediment routing models, one of the Parker [1990a] conditions is that the change in bed elevation during any one time step should be small compared to the transport layer thickness. This was originally computed using a C-F-L condition directly based on D_{84}. For sandy environments, this condition is based on the actual transport layer thickness in the model.

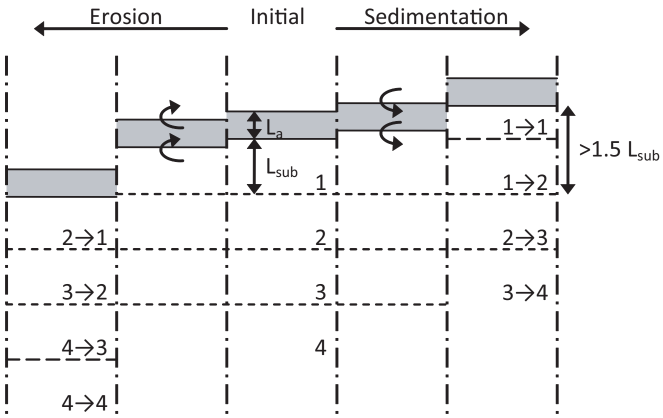

Figure 3.3: Revised concept of layers in SEDROUT: the centre represents the initial structure, where L_a is the active layer and L_{sub} are the sublayers; to the right: update in the case of sedimentation where arrows indicate the direction of deposited sediments. When the uppermost sublayer becomes > 1.5 times the original value, it is subdivided and the lowest layer is erased. To the left: update in the case of erosion; far left is the new definition when the uppermost sublayer is < 0.

SEDROUT and other models [e.g. Parker, 1991] have been developed for aggrading systems, and model treatment of aggradation has been thoroughly parameterised and validated [e.g. Toro-Escobar *et al.*, 1996]. Treatments of degradation have been developed and tested for conditions of static armour development [e.g. Willetts *et al.*, 1987; Parker and Sutherland, 1990]. Static armour development as a consequence of zero upstream sediment supply is a unique case that can be solved using simple assumptions of vertical sediment exchange. These assumptions may not apply in cases of less severe degradation, but suitable formulations for this case have yet to be fully tested. Simulations with variable discharge and downstream water levels over several years are likely to result in alternating aggradation and degradation. SEDROUT, like some other morphological models, allows for the possibility of vertical variation in the initial bed composition by defining several layers. Additional layers of the same thickness as the current active layer are defined during progressive aggradation, or layers are eroded during progressive degradation. Note that the thickness of all layers evolves in response to changes in the surface grain size distribution as a consequence of the definition of L_a. In conditions of alternating aggradation and degradation accompanied by surface fining and coarsening, we found that the original algorithm produced excessive mixing between sublayers as the bed surface moved up and down and the active layer thickness varied. To solve this problem, the algorithm was rewritten to use sublayers bounded at fixed elevations. Only the sublayer directly under the active layer has a variable thickness, filling the space between the lower boundary of the active layer and the top boundary of the second sublayer (which has a fixed elevation). This layer is divided into a new sublayer when its thickness exceeds 150% of the other sublayers. When this layer becomes ≤ 0, a new sublayer is defined under the lowest sublayer and the upper sublayer is erased (Figure 3.3). The lowland tributaries of the Saint-Lawrence River have very low slopes (Table 3.1). Using a step-backwater hydraulic scheme in such cases can be unstable, so we allow user specification of the tolerance value for convergence of the step-backwater calculations. A value of 0.1 mm is used in this study.

3.3.2 Climate change

SEDROUT was developed for generic situations where it was adequate to use a steady dominant discharge to represent the integrated effect of a spectrum of individual floods. Because bedload transport rates are non-linear functions of discharge, the effective discharge is displaced toward higher flows than the mean [e.g. Wolman and Miller, 1960]; simulating individual floods is better than using yearly averages [Molnar *et al.*, 2006]. We have therefore added the option of using a hydrograph file with a user-specified time step (for present purposes, discharge is held steady for one day at a time). Different series of daily discharges for the period 2010 to 2099 for each tributary [Chaumont and Chartier, 2005] were used, based on two greenhouse gas emission scenarios, A2 (economic growth) and B2 (local sustainable solutions). For three different horizons (2010–2039, 2040–2069, 2070–2099), the discharge scenarios were generated by applying the delta method (constant shift) to a historical sequence of precipitation and temperature (1961–1990) with the use of three different global climatic models. These new sequences of precipitation and temperature were used as an input for a hydrologic model to simulate daily discharges. The effects of river regulation on the discharge were considered negligible for the Batiscan River, but were taken into account for the Saint-Maurice simulation. For the Saint-François and Richelieu rivers, data on reservoirs were lacking and this effect could not be incorporated in the simulations. Although the mean annual discharges remain very similar to current values, individual floods change significantly under the different scenarios.

The water level in the Saint-Lawrence River is the base level for all the tributaries. We used a daily average water level based on recorded water levels for the period 1995–2005 at four different gauging stations. Successive days in which the water level was within a 25-mm range were combined to reduce file size. To simulate the effect of climate change, an extra module was added to the program to change the mean annual water level in the Saint-Lawrence River. Because of the lack of more detailed information on how the water levels in the Saint-Lawrence River will change over time, we considered two different scenarios: (i) a gradual change in water level that involves lowering the hydrograph each year by a pre-assigned value; and (ii) a step change at a certain point in time.

Discharges and water levels are read from separate files at the beginning of each day and held constant during the day. This quasisteady approach is often used in river engineering [Jansen *et al*., 1979] and allows longer time steps to be used, which is an advantage in long-term simulations. However, its use is restricted to short river reaches and slowly varying hydraulic regimes, both of which conditions apply here.

3.3.3 Tributaries

The Saint-François and Saint-Maurice rivers have islands in their downstream reaches. To simulate the hydraulics and sediment transport with SEDROUT4-M, these rivers were separated into discrete sections, each containing a single channel. Independent hydraulic computations are performed for each section. At each bifurcation, the water levels of the two sections are compared. If the difference between these water levels exceeds the specified tolerance for the hydraulic computation (0.1 mm), the discharge ratio is redefined and water levels are recalculated until the difference is smaller than the tolerance.

Sediment coming from upstream is portioned between the branches around an island using the discharge ratio between the channels. This ratio is used for all the size classes. This is the simplest relationship for sediment transport distribution at a bifurcation, but also the only option when modelling using a variable discharge [De Vriend *et al*., 2000]. Within each branch channel, the sediment transport rate is calculated at each cross section and sediment is routed normally.

The Batiscan and Saint-Maurice rivers join the Saint-Lawrence River below its tidal limit so their base levels oscillate. Over the period 2000–2005, the average tidal range for the Batiscan River is 0.80 m; and for the Saint-Maurice River it is 0.20 m. An extra module was added to SEDROUT4-M to update the downstream water level at a constant time interval in addition to the day-to-day variations in main stream flow. The assumptions made are a tidal period of 12 h, and therefore two total periods in one day to fit in with using a daily discharge update; and a water level depicted as a sine function, i.e., within the Saint-Lawrence River the tidal wave progresses upstream without deformation.

3.4 Assessment of SEDROUT performance

The island module, layer module, and tidal module available in SEDROUT4-M are initially checked for consistency using simulations of ideal small-scale situations and of the Batiscan tributary. Following this, the model is calibrated and validated to present-day conditions in all four tributaries. Finally, an example of a full simulation of one climate-change scenario is presented for the Richelieu River.

The initial topography data for the tributaries is based on our sonar surveys. The number of cross sections is equal to 80, 99, 96, and 104 for the Bastican, Richelieu, Saint-François, and Saint-Maurice rivers, respectively. The first two tributaries have a single channel; whereas, to incorporate the islands, the Saint-François River contains four channel sections and the Saint-Maurice River contains five. The initial bed composition in all cases is based on field measurements of surface bulk grain size distribution at each surveyed cross section.

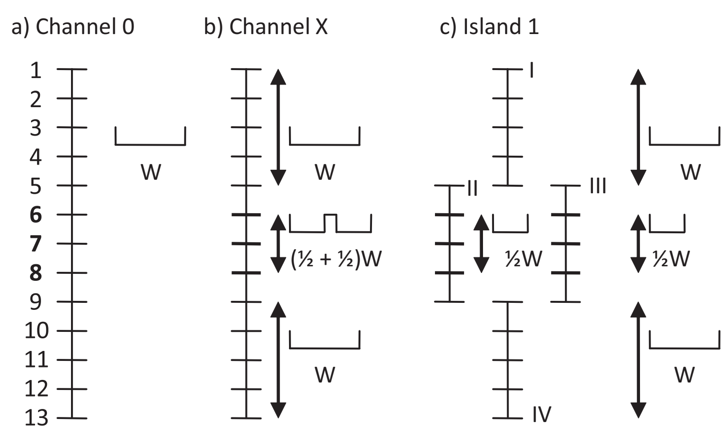

Figure 3.4: Explanation of the "Channel X" and island simulations used to test the island option in SEDROUT: a) "Channel 0" is used to generate an equilibrium starting condition for the test; b) "Channel X" has an island represented by the cross-sectional shape only; c) "Island 1" represents the actual island module. Bold numbers (6,7,8) indicate the position of the island.

3.4.1 Testing SEDROUT adjustments

In order to test the SEDROUT4-M version, small artificial channels with and without islands were developed. The first is a single channel, with 13 rectangular cross sections, each 100 m wide, with a horizontal initial bed, constant grain size distribution, and exposed to a constant discharge and downstream water level (Figure 3.4a, "Channel 0"). After the system reached equilibrium, two new models were generated using the bed topography and composition from this equilibrium channel. The first is called "Channel X" and has 13 cross sections, of which cross sections 6, 7, and 8 have the shape of two channels, each half the width of the original channel (Figure 3.4b). The other, called "Island 1," has four channel sections, each containing five cross sections, in which channel sections II and III have cross sections with half the width of "Channel 0," except for the upstream and downstream cross sections (Figure 3.4c). These two models ("Channel X" and "Island 1") were then run with the same discharge and downstream water level. By using two channels with the exact same topography around the island, the water and sediment distribution between the channels are each 50%. Furthermore, the bed topography, water levels, and grain size distributions are theoretically the same. In Figure 3.5, the water level and bed topography comparison between the two models reveals no differences, indicating that the island option in SEDROUT4-M is working correctly.

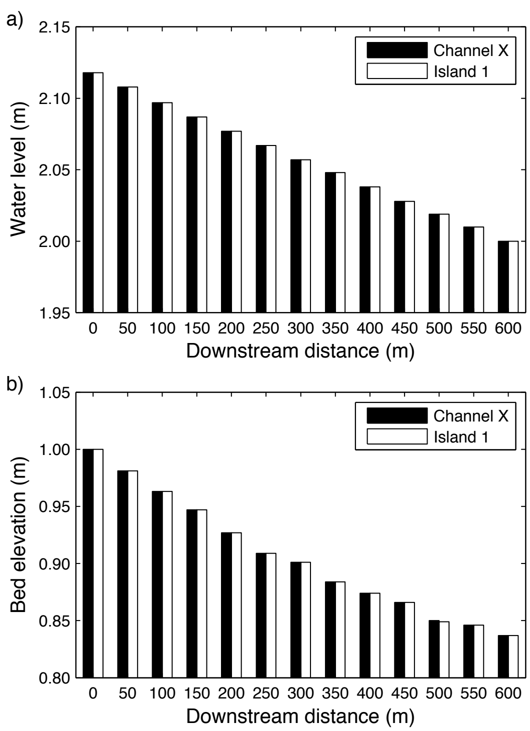

Figure 3.5: Comparison between "Channel X" and "Island 1" for a) water level and b) bed level.

The "Channel 0" was then used to evaluate the change made to the layer module. In Figure 3.6, percentages of a single fraction in the five layers are given over the test-run duration along with the bed elevation for the downstream cross section (13). In this test run, the discharge is variable over time to create a sequence of erosion and sedimentation, and the downstream water level is held constant. An active layer thickness of 0.025 m and a sublayer thickness of 0.050 m are used. The redefinition of the layers is seen to work correctly during both erosion and sedimentation. The layers are updated each time the bed elevation reaches a multiple of 0.050 m during erosion and every odd (larger than 1) multiple of 0.025 m during sedimentation. Figure 3.6 shows that grain size distribution of the sublayers remains constant during the first erosion period until t = 61 d. When sedimentation begins, the grain size distribution in the first sublayer starts to change toward the distribution of the active layer. The update of the sublayers works satisfactorily at t = 98 d and t = 133 d in the sedimentation phase as the active layer becomes thicker than 75 mm. In the second erosion phase, from t = 153 to 193 d, sediment is transferred from the first sublayer back to the active layer; and when the sublayer thickness reaches zero, the sublayers are successfully updated at t = 155, t = 164 and t = 175 d.

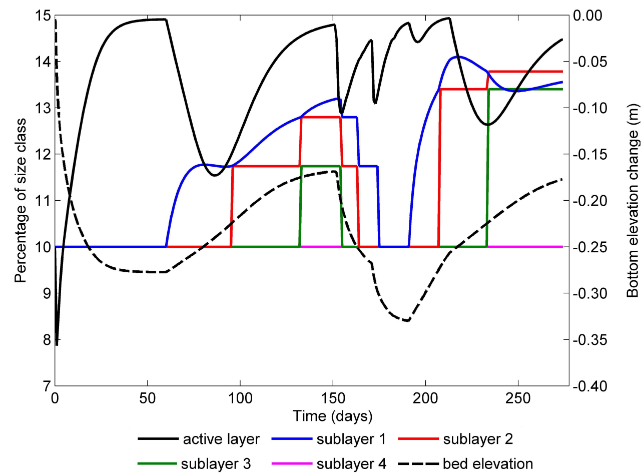

Figure 3.6: Variation in the percentage of the smallest grain size class (0.25–0.50 mm) in the new layer module in the active layer and in the four underlying sublayers, as well as in the bed elevation during the simulation at the downstream end of a small-scale model ("Channel 0", Figure 3.4a).

Three different simulations with a duration of one year were carried out for the Batiscan River to investigate the effect of the tide on the sediment transport calculations. The first simulation uses a constant water level, the second updates the tide level every hour and the third one updates the tide every half-hour. Figure 3.7 shows that adding a tide module has an effect on the bed elevation in the downstream end of the Batiscan River (in the downstream 5 km), but the interval of 1 h gives results very similar to those with the half-hour interval. Therefore, in the long-term simulations, the 1-h update of the tide will be used to keep the time step as large as possible without losing accuracy.

3.4.2 Calibration and validation

Calibration and validation of model hydraulics were done by adjusting the roughness parameter and by comparing the calculated water levels at given discharges with the measured ones. Previous applications of SEDROUT to gravel-bed rivers have used a logarithmic roughness law, but for the present sand-bed application we use Manning's n. Best-fit regression gave optimum values of n = 0.022, 0.037, 0.030, and 0.043 for the Batiscan, Richelieu, Saint-François, and Saint-Maurice rivers, respectively.

In addition to the calibration and validation of the model with water level data, we compared the simulated mean velocity at each cross section with our field measurements. The Ackers-White total load equation uses mean and shear velocity, so it is important that the simulated values correspond to the measured ones. Observed and simulated mean velocities are compared in Table 3.3. The ADCP data were collected during two successive days in each case (three days for the Batiscan River). The simulations are done for each day of measurement using the average discharge and downstream water level. For the Batiscan River, part of the difference between the measured and simulated velocities is from the tide effect. The measurements were taken over the day and include the tidal variation of the downstream water level; whereas the simulation of the velocities was done with a fixed downstream water level, resulting in higher relative difference. The Saint-François River has the highest relative error, which is partly from the presence of an island, where the discharge ratio between the two channels along the island is not simulated perfectly, resulting in over prediction in one channel and under prediction in the other. The overall agreement is very good, with an average absolute difference of 11%.

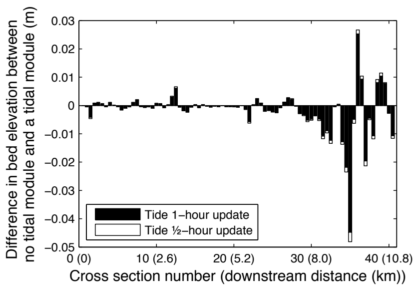

Figure 3.7: Effect of adding a tidal module on a test simulation of the Batiscan River. The y-axis represents the difference between no tide effect and having a water level update every hour (black bars) or every half-hour (white bars).

Name of tributary	Flow condition	ADCP (m/s)	SEDROUT (m/s)	Mean difference (m/s)	Mean absolute difference (m/s)	
Batiscan	Moderate	0.471	0.502	0.031	0.058	(12.3%)
Saint-François	Low	0.133	0.154	0.021	0.044	(33.0%)
	Moderate	0.428	0.457	0.029	0.036	(8.4%)
Saint-Maurice	Moderate	0.703	0.727	0.024	0.053	(7.5%)
Richelieu	Low	0.437	0.442	0.006	0.015	(3.4%)
	Moderate	0.649	0.658	0.009	0.015	(2.2%)

Table 3.3: Velocity comparison between field measurements with ADCP and simulations using SEDROUT

For the Saint-François River, the discharge ratio of the channels around the island is compared with our field data. At low flow (65 m^3/s), the measured discharge ratio with the ADCP was 29/71%, whereas the simulated ratio with SEDROUT4-M was 25/75%. At high flow (549 m^3/s), ADCP discharge ratio was 32/68% versus 30/70% in SEDROUT4-M. The discharge ratio is thus in good agreement with the measured ratio, with a difference of 4%

at low flow and only 2% at high flow, even though within the model there is no option to calibrate the discharge ratio between the two sections.

Morphological validation of any model of this type is difficult [Cao and Carling, 2002a]. Our sediment transport measurements show large variations in bedload transport rate, which is often the case when using Helley-Smith samplers [e.g. Gaudet *et al.*, 1994], partly because of temporary fluctuations of bedload transport [Cudden and Hoey, 2003]. The White and Day [1982] parameter setting indicates threshold transport values around 150, 450, and 330 m^3/s for the Batiscan River, Richelieu River, and Saint-François River, respectively. As can be seen in Table 3.3, these values are close to the discharge values during our bedload transport surveys. Therefore, the comparison of measured and simulated transport rates is further complicated here by the fact that field measurements were taken at flow conditions close to the threshold for motion.

3.4.3 Long-term simulation

Two long-term simulations with the Richelieu River model have been performed to test the capability of simulating a 90-year period with a variable discharge and changing downstream water level. The first is a reference scenario that is based on simulated discharges for the reference period 1961–1990 combined with current water levels in the Saint-Lawrence River, both held constant over the simulation period. The discharge for the second scenario is based on the A2 climate scenario predicted with the CSIRO-Mk2 model [Chaumont and Chartier, 2005]. The water level corresponds to a gradual decrease in the Saint-Lawrence River of 0.01 m/y.

Figure 3.8a shows the yearly sediment balance for the CSIRO A2 scenario with 0.01 m/y drop in water level. The sediment balance is the difference between sediment transport at the upstream boundary (in-going) and at the downstream boundary (out-going), with negative values indicating erosion. We expect to observe, from a continuous decrease in downstream water level, a general trend of lower bed levels over the simulation period, although transient aggradation may occur for parts of the time. The changes in discharge (higher mean annual discharge and increased variation) should lead to an increase in extreme erosion events. The combination of these two effects is apparent in Figure 3.8a that shows the cumulative sediment balance for both scenarios, suggesting consistency between long-term simulations with SEDROUT4-M and expectations, although full validation is required.

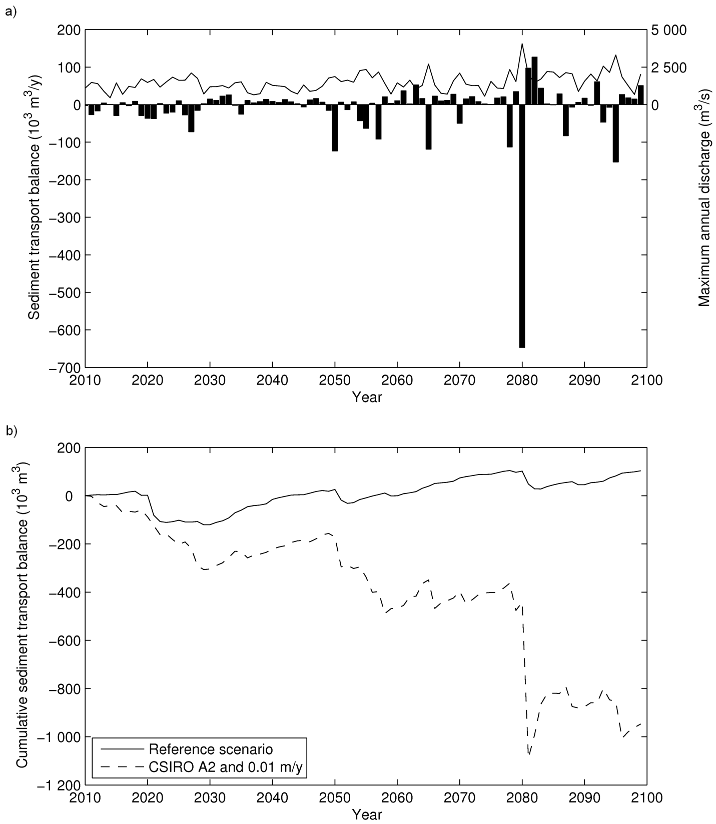

Figure 3.8: a) Long-term simulation of the Richelieu River, using CSIRO A2 discharge scenario and 0.01 m/y drop in downstream water level, showing yearly sediment transport balance (bars) and annual maximum discharge (line). The sediment transport balance values correspond to yearly transport at the upstream boundary minus that at the downstream boundary; b) Cumulative sediment transport balance for a reference scenario (1961–1990 discharge with no water level drop) and the CSIRO A2 climate scenario with a 0.01 m/y drop. Negative values indicate erosion, whereas positive values indicate deposition.

The stratigraphic record for two cross sections (mid-distance and at the downstream end of the study reach) is shown in Figure 3.9. The initial D_{50} is the same for all the layers, but different at each cross section. By 2100, the sequences of sedimentation and erosion have greatly modified the vertical grain size distribution, with coarser particles in the upper part of the profile (Figure 3.9).

3.5 Discussion

The 1D model SEDROUT has been extended and modified to allow simulations using climate-induced changes in discharge and downstream water levels. Simulations with an artificial channel show that SEDROUT4-M is capable of simulating moderately complex channels with islands. The new layer concept avoids artificial mixing between the sublayers during alternating sedimentation and erosion. A stratigraphic record can also be built during a long-term simulation, which is an advantage over some other 1D morphological models such as HEC-6. However, the choice of the thickness of the sublayers remains arbitrary. As the choice of the transport layer thickness influences the stratigraphic record and grain size distribution of the transport layer [Ribberink, 1987], this issue can create some difficulties when comparing results from different studies. A relatively thick transport layer will result in almost no change in grain size, whereas a relatively thin transport layer results in a quickly adapting grain size distribution and can cause artificial armouring of the bed [Hoey and Ferguson, 1997].

Calibration simulations were used to obtain the overall roughness for each tributary. However, the range of discharges and water levels available for calibration was small and the discharges were mostly low to moderate. This could lead to roughness values that are slightly low for high flow simulations, especially for the Batiscan River where Manning's n is only 0.022. Unfortunately, we have no data to verify this effect. On the other hand, the downstream reach of the Batiscan River is relatively straight and thus shows no indication that a higher roughness caused by the channel pattern would be required. Also, the cross-sectional shape in this case seems compatible with a low Manning's n indicated by the calibration. The value of Manning's n for the Saint-François River (0.030) is close to standard values for sand-bed rivers. Some of the inaccuracy in water levels could be from the fact that the model is not capable of dealing with the hysteresis effect in the stage-discharge curve, as the model is calibrated using a steady flow approach. For the Richelieu River, the relatively high Manning's n value (0.037) can be explained by its meanders in the downstream reach and the strong asymmetrical cross-sectional shapes in this reach. The Saint-Maurice River has the highest Manning's n (0.043) because of the presence of large bed material (cobbles and boulders) that we observed in our field surveys. Although the Manning's n values are different for each river, they are all more or less within the limits of 0.024 to 0.075 for the lower regime in sand-bed rivers [Barnes Jr., 1967].

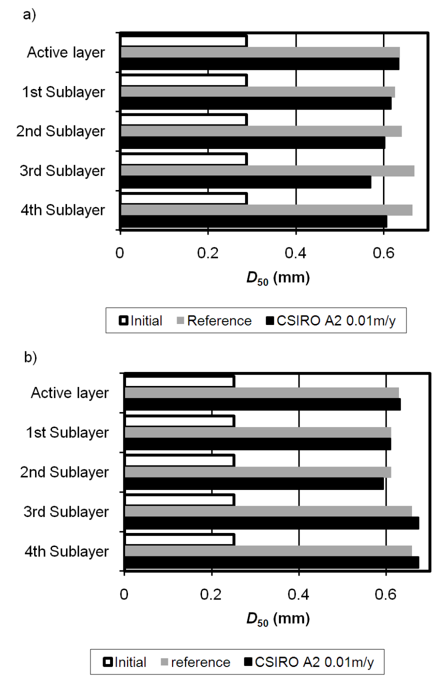

Figure 3.9: Grain size (D_{50}) of the layers at two cross sections in the Richelieu River for the reference scenario and the CSIRO A2 climate scenario with a 0.01 m/y drop: a) in the centre of the studied reach (at 4.6 km from the downstream limit) and b) at the downstream end.

The sediment transport rate is calculated from the mean cross section velocity in the 1D model. An essential part of the validation is therefore to verify that the model is capable of simulating these velocities accurately. As shown in Table 3.3, the simulated velocities are in good agreement with our field measurements. The positive mean difference indicates that for all rivers velocities are slightly overpredicted. The relative error is smaller for the high flow condition than for the low flow condition. As most of the morphological work is occurring during high flow, this relatively good agreement indicates an overall good performance of the 1D model.

The accuracy of sediment transport formulae is generally considered as poor [e.g. Van Rijn, 1984; Barry *et al*., 2004]. Calibration and validation are difficult because of sparse field data and error related to Helley-Smith sampling. The best test for accuracy of the transport rate predictions would be against inverse morphological estimates from resurveys of the rivers. Long-term simulation using these formulae should always be treated with caution. Nevertheless, trends and differences between future scenarios can be identified, even if the sediment transport formula is systematically over- or underpredicting actual transport rates.

3.6 Conclusion

The modification of the 1D morphodynamic model SEDROUT4-M allows for a wide range of river types to be simulated, from gravel-bed rivers in the original design to sand-gravel mixtures and sand-bed rivers, which are typically found in the downstream reaches of watersheds. Moderately complex rivers with islands or multiple channel deltas can also be simulated with this model. The extended layer concept, present in the original design, provides an opportunity to simulate the stratigraphy of the grain size distributions of the river bed.

Future research on the effect of the choice of transport layer thickness is needed, as the use of a variable thickness based on the discharge and grain size could give a better physical description of the sediment transport process and stratigraphic record. However, SEDROUT4-M is now also capable of simulating daily variations in discharge and downstream water levels over relatively long simulation periods (100 years). With the tidal module and the option to change downstream water level over time, the model can investigate the impacts of base level change on rivers based on different climatic scenarios. These are key elements of expected near-future climate changes in several watersheds across the world, which were tested here for the Saint-Lawrence River tributaries. The modified version of SEDROUT4-M is thus a valuable and powerful tool to investigate the effects of climate change on river systems, but the potential applications go well beyond climate-change scenarios as a very wide range of river morphodynamic problems can now be simulated.

Paragraphe de liason B

In chapter 3 the modifications to and the performance of SEDROUT4-M were described and tested, and the validation of the hydraulics was presented for the Batiscan, Richelieu, Saint-Maurice and Saint-François rivers, based on measured water elevations and velocities. The next two chapters (4 and 5) will present the results of morphological simulations over the period 2010 to 2099. Daily discharge time series are available from a hydrological model (HSAMI) that uses the temperature and precipitation time series from three different GCMs (CSIRO-Mk2, ECHAM4 and HadCM3) for two GHG-emission scenarios (A2(b) and B2(b)) as input conditions. After running the various scenarios it was felt that a general assessment of the results per horizon would be the appropriate first step. In chapter 4 the analysis focuses on the mean annual sediment transport rates for three future time periods and bed elevation by the end of 2099. Although hydraulic results were satisfactory for the reaches where water level and ADCP velocity data were available, it was felt that an assessment of the morphological performance would be helpful. Differences in bed topography between the two field campaigns, are compared to those of morphological simulations. The main purpose of chapter 4 is to analyse the effects of expected changes in discharge and base level due to climate change over the period 2010–2099. The analysis is done by comparing the outcome of hydrological simulations using different GCM series with a reference scenario that contains the simulated discharge for the reference period 1961–1990.

CHAPTER 4

EFFECTS OF DISCHARGE AND BASE LEVEL CHANGE DUE TO CLIMATE CHANGE ON BED ELEVATION AND YEARLY BED MATERIAL TRANSPORT OF SAINT-LAWRENCE TRIBUTARIES: A NUMERICAL MODELLING APPROACH [2]

4.1 Introduction

There is now a clear consensus that the global climate will continue to change in the near future, at least partly because of human activities [IPCC, 2007]. Regional-scale changes in mean temperature and precipitation will inevitably affect hydrological systems and river flows, and there have been many recent studies of how this may affect navigation, hydropower, flood risk, and river management [e.g. Pruski and Nearing, 2002; Nearing *et al.*, 2005; De Wit *et al.*, 2007; Fowler *et al.*, 2007; Lane *et al.*, 2007; Quilbé *et al.*, 2008]. It is well known from historical studies that climate change also has an indirect effect on bed-material transport and river morphology [e.g. Blum and Törnqvist, 2000; Knox, 2000], and Lane *et al.* [2007] noted that channel change can modulate the direct effect of climate change on flood risk, but attempts to predict how climate change will affect river channels are only just starting to appear [e.g. Gomez *et al.*, 2009]. Historical studies have not established clear and globally-applicable empirical relations between climate change and river response [Vandenberghe and Maddy, 2001; Bogaart *et al.*, 2003], but modelling provides an alternative approach [e.g. Tucker and Slingerland, 1997; Coulthard and Macklin, 2001; Veldkamp and Tebbens, 2001; Coulthard *et al.*, 2005; Gomez *et al.*, 2009]. When looking into the future there is uncertainty in climate scenarios, climate models, and hydrological models used to convert changes in temperature and precipitation into changes in river discharge [Graham *et al.*, 2007]. Moreover, river response depends on base level as well as hydrology [e.g. Blum and Törnqvist, 2000] and in some situations both of these are expected to change. Responses to base-level change can be complex and depend on the type and duration of change and type

[2] the basis of this chapter is accepted by EARTH SURFACE PROCESSES AND LANDFORMS, ON 2009-October-14, ESP-09-0229
entitled: Numerical modelling of climate change impacts on the Saint-Lawrence River tributaries

of river [Schumm, 1977; Begin *et al.*, 1981; Simon and Hupp, 1986; Bonneau and Snow, 1992; Hassan and Klein, 2002; Gaeuman *et al.*, 2005].

This paper is concerned with how climate-induced changes in near-future hydrology will affect the stability of, and sediment delivery from, relatively small tributaries of the very large Saint-Lawrence River as it flows through the province of Québec in eastern Canada. The Saint-Lawrence River and its tributaries are a very important fluvial system from both economic and ecological perspectives [Hudon, 2004; Morin *et al.*, 2005]. It is expected that regional changes in hydrology will affect the tributaries in two ways: from upstream through the altered hydrology of their own basins, and from downstream through the base level fall that is predicted to occur because of a decrease in Saint-Lawrence discharge by approximately 20% [Croley, 2003; Ouranos, 2004; Chaumont and Chartier, 2005; Morin *et al.*, 2005]. The latter is mainly due to increased evaporation in the Great Lakes following temperature increases [Croley, 2003; Chaumont and Chartier, 2005].

We tackle the problem using a modelling approach in which output from global climate models (GCMs) drives a hydrological model, and the output of the hydrological model drives a morphodynamic model. We use a single hydrological model (HSAMI) that has been used for operational purposes in this region for many years, and a 1-dimensional morphodynamic model (SEDROUT4-M), but force them with outputs from three alternative GCMs since studies of changes in flow patterns have shown greater sensitivity to the choice of GCM than to greenhouse gas (GHG) emission scenario or climate sensitivity [Prudhomme *et al.*, 2003; Andersson *et al.*, 2006]. Details of the various models are given below. We report results from simulations using all combinations of three GCMs, two GHG-scenarios and three base level scenarios. The response variables discussed are the mean annual bed-material volume transported from three tributaries to the Saint-Lawrence River, and the mean bed elevation in distal and medial sub-reaches of each tributary. By comparing scenarios involving variations in discharge and/or base level we can examine how sensitive rivers are to these two variables taken in combination or in isolation. Modelling several rivers and using alternative climate and base-level scenarios allows us to assess how possible it is to generalize in a robust way the fluvial response to climate change.

4.2 Study areas

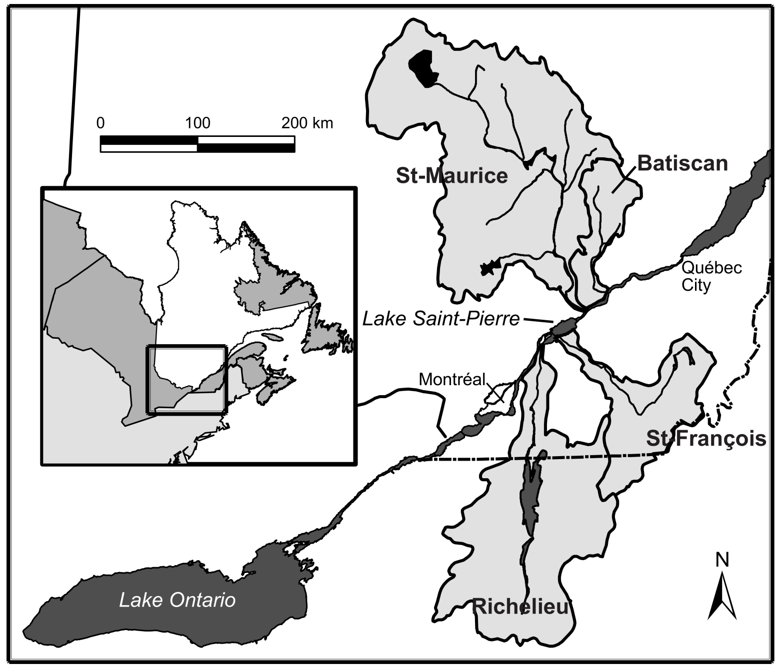

Figure 4.1: Location of the studied Saint-Lawrence River tributaries.

Four tributaries of the Saint-Lawrence River (Batiscan, Richelieu, Saint-François and Saint-Maurice rivers) were originally selected for this study, though technical difficulties (see below) prevented successful modelling of the Saint-Maurice River and led to some gaps in the results from the Saint-François River. The rivers were selected on account of their geometry, availability of data, and importance for navigation. Futhermore, the tributaries selected cover a range of different sizes to cover all sizes of tributaries found in the region and the tributaries are located on both, North and South, shores of the Saint-Lawrence River as climate change effects are expected to be different in the North from the South. They are located in the lower part of the Saint-Lawrence River basin between Montréal and Québec City (Figure 4.1) close to Lake Saint-Pierre (www.geog.umontreal.ca/hydro/TributairesSt-Laurent/). This lake is wide (10–12 km), shallow (mean depth $<$ 3.0 m), and non-tidal. It has been a UNESCO biosphere reserve since 2001 on account of its marginal habitats [Jacques, 1986; Morin and Côté, 2003; Hudon, 2004; Hudon and Carignan, 2008]. The Saint-Lawrence Seaway passes through the lake and navigation depths here are critical, such that any decrease in water level or increase in sedimentation may have important economic consequences. More than half of the suspended sediment input from the south shore tributaries comes from three rivers: the Yamaska, Richelieu and Saint-François rivers [Rondeau *et al.*, 2000].

River dimensions, discharge range and sedimentology are provided in Table 4.1. All of the tributaries contain hydroelectric power dams and their discharge is regulated to a certain extent. The Batiscan and Saint-Maurice rivers, located downstream of Lake Saint-Pierre, are also tidally influenced and the lowest part of the Richelieu River is dredged periodically to

River	Water surface bankfull width (m) mean (min-max)	Length of studied reach (km)	Mean discharge (m^3/s) (Mean annual flood)	Energy slope (-)	Upstream sediment size D_{50}-D_{84} (mm)	Downstream sediment size D_{50}-D_{84} (mm)	Degree of flow regulation
Batiscan	167 (77–277)	17	99(613)	6×10^{-5}	0.52– 1.03	0.37–0.57	Moderate
Richelieu	198 (89–278)	15	346(1045)	5×10^{-5}	0.41– 0.89	0.32–0.48	High
St-François	233 (88–415)	15	208(1421)	3×10^{-5}	8.04–17.57	0.30–0.38	High
St-Maurice	238 (70–507)	14	693(2472)	1×10^{-5}	18.38–2605	0.53–0.89	High

Table 4.1: Characteristics of the studied tributaries

maintain navigation. The upstream end of each study reach was set at a location which on inspection in the field appeared to have been stable for a long time. In the Batiscan, Saint-François and Saint-Maurice rivers it coincided with a marked increase in grain size and slope, and in the Batiscan and Richelieu rivers it was the highest such location before the hydro-electric power dam. Each tributary was surveyed using an echo sounder in 2004/2005 and again in 2006. For the Batiscan River 79 cross sections were used in the model at separations varying from about 100 m in the downstream reach to 300 m upstream; 99 cross sections were taken for the Richelieu River, 60 to 220 m apart; the Saint-François River contains 100 cross sections at 60 to 300 m interval, and the Saint-Maurice River model contains 108 cross sections at 85 to 280 m. On average 700 topographic points were taken at each cross section, but the points used as input in SEDROUT4-M were decimated to an average spacing of 5 m. In the Saint-François River, four branches were used to include in the model a permanent island. The downstream geometry of the Saint-Maurice River is complex and contains multiple bifurcations and confluences, with two main bifurcations and three channels that flow into the Saint-Lawrence River requiring five branches in the model. Longitudinal profiles (Figure 4.2) are markedly different from the theoretical, continuously decreasing smooth curve. It is expected that the effect of a base level fall will be harder to identify in these rivers, because of potential erosion of shallow cross sections and deposition in deep cross sections.

Bed composition was obtained from samples collected from a boat using a grab bucket (Ponar Dredge HB-2, GENEQ Inc.) deployed manually. The bed composition ranges from clay and silt to sand and some gravel in the upstream parts for all the tributaries (Table 4.1). Typically, samples were taken at 5 different points along a cross section at every 2 to 4 cross sections where topography was measured. This resulted in an average of 150 samples for each tributary that were analysed in the laboratory to obtain a grain size distribution from which 10–13 half-phi grain size fractions, starting at a washload limit of 0.125 mm, were extracted.

4.3 Methodology

Climate change will affect the tributaries in two ways: directly through a change in discharge in the tributaries themselves, and indirectly through a discharge change in the Saint-Lawrence River which will affect the base levels of the tributaries. These two effects are assumed to be independent since the watersheds (4700–43 250 km^2) and mean discharges (99–693 m^3/s) of the tributaries are orders of magnitude smaller than those of the Saint-Lawrence River (watershed area 1.3×10^6 km^2, mean discharge 14 000 m^3/s).

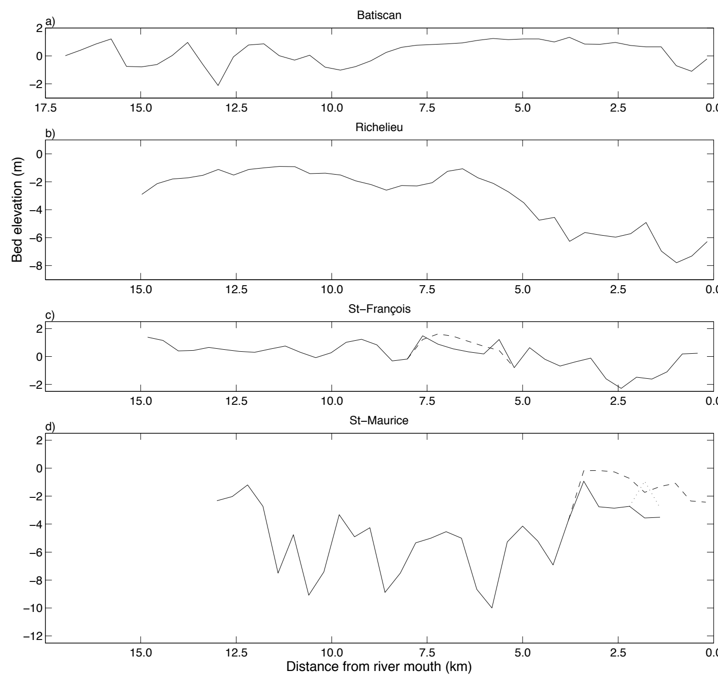

Figure 4.2: Long profile of the tributaries based on the deepest point of each cross section (in meters relative to mean sea level) against the distance from confluence with the Saint-Lawrence River or Lake Saint-Pierre, a) Batiscan River; b) Richelieu River; c) Saint-François River, where the dashed line represents the eastern channel along the island; and d) Saint-Maurice River, with a dashed line representing the eastern channel and a dotted line the middle channel continuous line is the main and western channel.

The morphological model was run with present-day discharge, measured bed topography and bed composition, and base levels for the period between when the topography was measured (2004/5) and the start of the future discharge scenarios (2010). The simulated bed topography and composition is then used as the initial condition for different discharge and base level scenarios that cover the period the 90 year period of 2010 to the end of 2099.

4.3.1 Discharge scenarios

Discharge scenarios were generated by the Ouranos research centre, a consortium on regional climatology and adaptation to climate change [www.ouranos.ca, Chaumont and Chartier, 2005]. Ouranos is the main source of North American regional climate simulations and, as such, is recognized as a leading research centre in climate change in Canada. They simulated two GHG-scenarios (A2(b) and B2(b)) [Nakicenovic *et al.*, 2000; Raupach *et al.*, 2007] with three different GCMs (CSIRO-Mk2, ECHAM4 and HadCM3). The A2 GHG-scenario includes globalized development, whereas the B2 scenario includes regional development. Both GHG-scenarios assume environmental stewardship, but the A2 scenario has a higher GHG-emission rate than the B2 scenario [Merritt *et al.*, 2006]. Current GHG-emissions exceed both the A2 and B2 scenarios, but A2 is closest to the actual emissions [Raupach *et al.*, 2007]. The GCMs were selected based on their differences in predictions of precipitation and temperature: ECHAM4 predicts a moderate increase in temperature and the smallest changes in precipitation; HadCM3 results in the smallest increase in temperature and the highest increase in precipitation; and the CSIRO-Mk2 model has moderate precipitation increase and higher temperature increase for the Québec region [Chaumont and Chartier, 2005].

As in almost all previous model studies of hydrological response to climate change [e.g. Chaumont and Chartier, 2005; Merritt *et al.*, 2006; Graham *et al.*, 2007; Lane *et al.*, 2007; Minville *et al.*, 2008] the GCM outputs were converted to time series of daily temperature and precipitation using the delta method. This uses the difference between a monthly mean temperature or precipitation simulated by a GCM for a 30-year period in the future and for a reference period (1961–1990). This monthly difference (delta value) is then added to daily climatic data synthesized for each watershed. Although alternative downscaling approaches are being developed [e.g. Hay *et al.*, 2000; Diaz-Nieto and Wilby, 2005; Rosberg and Andréasson, 2006; Rydgren *et al.*, 2007], the delta method is the most widely used and has the advantage of simplicity, stability and robustness [Graham *et al.*, 2007]. Although regional simulations from the Canadian Regional Climate Model [CRCM Caya and Laprise, 1999] were available, they did not allow time-mean water budget to be resolved at the required temporal scale for the SEDROUT4-M model; thus, direct output from CRCM could not be used. Using bias correction methods in this case was not deemed appropriate since these methods would not have improved our degree of confidence in the results obtained for precipitation.

Preliminary analyses by Ouranos showed that, in southern Québec where the topography is relatively smooth, using delta values for regional models at a 45 km resolution added little information compared to delta values derived from GCMs at a 250 km resolution. This was also observed by Graham *et al.* [2007] for the Bothnian Bay Basin when comparing RCMs with 25 or 50 km resolution with the GCM HadAM3H at 150 km resolution. The added value of RCMs to the time-mean water budget is relatively modest, as it is contained mainly in the time variability, except where there is a strong local forcing such as near mountains or coastal regions [Laprise, 2008].

The re-computed precipitation and temperature were then used as input in the hydrological model HSAMI [Chaumont and Chartier, 2005; Minville *et al.*, 2008], which is a lumped rain and snowfall runoff model (see Minville *et al.* [2008] for details). It has been successfully used and tested by the hydropower company Hydro-Québec for over twenty years to predict runoff for their reservoirs [St-Hilaire *et al.*, 2003; Chaumont and Chartier, 2005; Minville *et al.*, 2008]. HSAMI is particularly appropriate for this study because it takes into account the locally important processes of snow accumulation, snowmelt, and soil freezing/thawing, as well as evapotranspiration, and because it has already been calibrated to the watersheds concerned [it is used for daily forecasting of natural inflows on 84 watersheds ranging in areas from 160 km^2 to 69 195 km^2: Minville *et al.*, 2008].

For each river, six time series (three GCMs combined with two GHG-scenarios) of daily discharge values were produced by adding the delta values (precipitation and temperature) to the reference period, for three different future time periods or 'horizons': 2010–2039, 2040–2069 and 2070–2099. Delta values were calculated for the years 2020, 2050 and 2080 which were assumed to be representative for the complete horizon. This procedure is similar to that applied by Lane *et al.* [2007]. The hydrological model was calibrated using the reference period 1961–1990. The quality of the calibration was assessed using Nash coefficients, where values above 0.75 are considered good [Nash and Sutcliffe, 1970]. Values of 0.85, 0.79 and 0.83 were obtained for the Batiscan, Richelieu and Saint-François rivers, respectively [Chaumont and Chartier, 2005]. These simulated daily discharges are used as a reference discharge scenario for the morphological modelling by repeatedly using it for the periods 2010–2039, 2040–2069 and 2070–2099, referred to as RefQ hereafter.

Under all tested climate scenarios, spring snowmelt floods in all tributaries are predicted to occur earlier in the year. For the Batiscan, Saint-François and Saint-Maurice rivers, the magnitude remains about the same as in Table 4.1, whereas for the Richelieu River the spring flood increases. Low winter discharge is predicted to increase in all the tributaries. The mean annual discharge remains about the same, with a small increase for the CSIRO-Mk2 and HadCM3 model and a small decrease for the ECHAM4 model. A more detailed description of the different discharge scenarios can be found in Chaumont and Chartier [2005] and Boyer *et al*. [in press].

4.3.2 Base level scenarios

Daily averaged water levels over the period 1996–2005 taken at gauging stations in the Saint-Lawrence River close to the mouths of the tributaries were used as a reference base level scenario, hereafter referred to as RefH. According to Ouranos [2004] and Morin *et al*. [2005] the anticipated decrease in discharge could lead to a decrease in water level of up to 1 m near Montréal. Water release from Lake Ontario is managed to ensure a balance between economic demands and ecological sustainability [LOSL, 2006; IJC, 2008], but there is no available prediction on how the Saint-Lawrence water level will develop over time. Therefore, we used an arbitrary but plausible scenario of a steady decline of 0.01 m per year (0.01m/y hereafter) in the water level of the Saint-Lawrence River from 2010–2099. In order to verify if the results of our simulations are sensitive to this steady decline assumption, we have also tested the impact of a step change in water level, with a sudden decrease of 0.50 m occurring in 2040 (0.50m-2040 hereafter). These two scenarios give us the opportunity to compare the magnitude of base level change (0.50 m vs. 0.90 m in 2099) and the effect of timing since by 2059 both scenarios have a decrease of 0.50 m.

4.3.3 Morphodynamic model

Tributary response to changes in hydrology and base level was simulated using the 1D (width-averaged) morphodynamic model SEDROUT4-M. This is based on the model of Hoey and Ferguson [1994] but with modifications and additions to allow its application to low-gradient divided channels; the changes are described and successfully tested in Verhaar *et al*. [2008]. The model is forced by time series of daily discharges and downstream water levels. It predicts the mean shear stress at each cross section from the step-backwater solution of the width- and depth-averaged flow continuity and momentum equations, using a calibrated constant value of Manning's n, then uses the shear stress to predict the rate of trans-

			2010–39	2040–69	2070–99
Degradation	95%	ref	0.1	3.0	-0.6
		GCM	0.9	2.6	-8.3
		base-level	0.5	0.5	-14.8
	99%	ref	0.1	1.3	-0.9
		GCM	0.4	0.6	-3.0
		base-level	0.2	0.4	-7.5
Aggradation	101%	ref	-0.1	-3.4	-5.1
		GCM	-0.7	-4.5	-9.1*
		base-level	-0.3	-3.6	13.0**

Table 4.2: The influence of the upstream boundary condition (95%, 99% or 101% of transport capacity) on the sediment transport volume at the downstream boundary for the Batiscan River. Data are presented in percentage values compared to the upstream boundary condition at 100% transport capacity for three scenarios: ref (RefQ-RefH), GCM (HadCM3-RefH), base-level (RefQ-0.01m/yr). Note that the 105% aggradation scenarios caused crashing of numerical simulations since flow became too shallow and reached a supercritical state. *2098; **2092 instead of 2099 because the simulation crashed.

				2010–39	2040–69	2070–99
Degradation	95%	middle	ref	-0.03	-0.24	-0.37
			GCM	-0.13	-0.34	-0.51
			base-level	-0.06	-0.26	-0.48
		downstream	ref	0.00	0.00	-0.08
			GCM	0.00	-0.05	-0.17
			base-level	0.00	-0.05	-0.13
	99%	middle	ref	-0.01	-0.10	-0.18
			GCM	-0.06	-0.16	-0.23
			base-level	-0.02	-0.15	-0.25
		downstream	ref	0.00	0.00	-0.04
			GCM	0.00	-0.02	-0.09
			base-level	0.00	-0.02	-0.07
Aggradation	101%	middle	ref	0.02	0.24	0.52
			GCM	0.12	0.43	0.80*
			base-level	0.04	0.33	0.55**
		downstream	ref	0.00	-0.01	0.09
			GCM	0.00	0.05	0.34*
			base-level	0.00	0.03	0.15**

Table 4.3: The influence of the upstream boundary condition (95%, 99% and 101% of transport capacity) on the difference in bed elevation (m) compared to the upstream boundary condition at 100% transport capacity in the Batiscan River at the middle reach (7.5–10 km) and downstream reach (0–2.5 km) for three scenarios: ref (RefQ-RefH), GCM (HadCM3-RefH), base-level (RefQ-0.01m/yr). Note that the 105% aggradation scenarios caused crashing of numerical simulations since flow became too shallow and reached a supercritical state. *2098; **2092 instead of 2099 because the simulation crashed.

port of each of 10–13 half-phi grain size fractions. Bed level and bed grain-size distribution are updated after each time step using overall and fractional conservation of sediment. The time step is variable and needs to satisfy several Courant-Friedrichs-Lewy conditions and is limited to 24h or 1h (when tide is present).

1D morphodynamic models are conceptually inferior to 2D or 3D models which can resolve local spatial differences in flow strength, but higher-dimension models based on the St-Venant or Navier-Stokes flow equations are still computationally too expensive for long-term morphological predictions over extended reaches [Kleinhans *et al.*, 2008; El kadi Abderrezzak and Paquier, 2009]. Rule-based 2D cellular models, which are computationally far more efficient, can generate plausible generic behaviour [e.g. Murray and Paola, 1994] and have been used to simulate the long-term (Holocene) behaviour of specific river systems [e.g. Coulthard *et al.*, 1999, 2005], but they have not yet been shown to yield quantitatively accurate predictions of sediment transport and channel change in specific situations. We preferred, therefore, to stay with a 1D model since such models have been shown to make reasonably accurate quantitative predictions in a variety of specific applications [e.g. Cui *et al.*, 1996; Ferguson *et al.*, 2001; Talbot and Lapointe, 2002; Kleinhans *et al.*, 2008; Ferguson and Church, 2009]. SEDROUT4-M does not include a bank-erosion module but in this study area the banks would contribute mainly washload; moreover, it is not yet clear how best to simulate width adjustment over many years as opposed to bank erosion within single flood events.

Initial bed topography was based on measurements at bankfull stage. Cross sections which were not sampled for bed composition were given the same grain size distribution as their closest upstream cross section. For all simulations, the Ackers and White [1973] total-load transport formula with the White and Day [1982] parameter settings was used since it gave the best match to a limited number of Helley-Smith samples [Verhaar *et al.*, 2008] and allows for the transport of the finest bed material in suspension. We also present here an assessment of the morphological performance of the model based on topographic data taken one year after collecting the input data used to set up the model.

It is well recognized that 1D model response is sensitive to what is assumed about bed-material input to the reach [Simon and Darby, 1997; Hoey and Ferguson, 1997; Ferguson *et al.*, 2001; Lane and Ferguson, 2005]. In the absence of any change in transport capacity an increase in sediment input leads to aggradation whereas reduced supply results in degradation. In rivers with a long history of discharge and bed-material transport measurement one possibility is to use an empirical sediment rating curve [e.g. Gomez *et al*., 2009] but that was not an option in our study area. The bed-material input to each reach was therefore assumed to be at capacity at all times. This is consistent with the view that the immediate controls of this flux (unlike the washload flux, which is supply-limited) are flow strength and bed surface grain size distribution [Wilcock, 2001]. The sediment supply from upstream is relevant only indirectly via its effect on surface size distribution: reduced supply induces surface coarsening which reduces transport rates, and increased supply does the opposite, as demonstrated experimentally or numerically by Dietrich *et al*. [1989], Hoey and Ferguson [1997], and Madej *et al*. [2009] amongst others. A consequence of our assumption of supply at capacity is that there is no change in bed elevation or composition at the head of the reach, but the gradient is free to alter. The input of sediment to the reach will therefore respond to aggradation or degradation within the reach as well as to changes in hydrological regime; this would not be the case if an empirical rating curve was used.

		2010–39	2040–69	2070–99
95%	ref	0.00	0.03	0.04
	GCM	0.01	0.04	0.03
	base-level	0.01	0.03	0.02
105%	ref	0.00	-0.04	-0.07
	GCM	-0.02	-0.06	-0.04
	base-level	-0.01	-0.04	-0.03

Table 4.4: The influence of the upstream boundary grain-size distribution (GSD) (95% or 105% of measured D_{50}) on the sediment transport volume at the downstream boundary for the Batiscan River. Data are presented in percentage values compared to upstream boundary with measured GSD for three scenarios: ref (RefQ-RefH), GCM (HadCM3-RefH), base-level (RefQ-0.01m/yr)).

To test the sensitivity of our results to the choice of upstream boundary condition we tried setting supply to slightly more or less than capacity, thus inducing aggradation or degradation respectively (Tables 4.2 and 4.3), and making the bed at the head of the reach slightly coarser or finer as might happen in the event of changes in supply from further upstream (Table 4.4). Table 4.2 indicates that induced aggradation or degradation at the head of the reach has little effect on sediment output from the reach during the first two horizons, but rather more during the third horizon particularly when combined with a base-level decrease. The impact on bed elevation is similarly larger in the third horizon but it is markedly smaller downstream than in the middle reach (Table 4.3). Table 4.4 shows that changing the upstream GSD has hardly any impact on the sediment output from the reach. The effect on bed elevation is also very minor (< 0.025 m).

4.4 Results

4.4.1 Validation using topographic comparison

Validation of our simulations based on measured changes in topography over approximately one year proved unsuccessful for the Saint-Maurice River. This river exhibits complex planform geometry with two large islands near its mouth, resulting in two bifurcations over a short distance (1650 m). Our measured discharge splits for these bifurcations were 65–34% and 69–31%, respectively, whereas the simulated splits were 76–24% and 88–12%. Several unfruitful attempts were made to modify cross sections in the downstream reach of the branch that receives the smaller discharge; the geometry of two consecutive islands appears too complex to be simplified for application within a 1D model. Thus, results are presented in this paper for only the other three tributaries.

Validation using bed topography changes for these rivers were based on two topographic surveys: on 11 May 2004 and 22 June 2006 for the Batiscan River, on 3–4 May 2005 and 15 June 2006 for the Richelieu River, and on 26–27 April 2005 and 13 June 2006 for the Saint-François River. A comparison of measured and simulated topography was carried out using the average bed level of the main channel over the nearest cross sections. The repeat surveys were always within 10 m of the original sections, i.e. less than 5% of channel width. For the Batiscan and Richelieu rivers, the average differences between measured and simulated bed elevation changes were 0.09 m and 0.13 m, respectively. These values are small and, considering the difficulties in comparing single cross-sectional changes in bed elevation between different years in a 1D model, they are considered in good agreement.

However, the Saint-François River showed much more variability when comparing cross sections at different times, with an average difference of 0.34 m between measured and simulated bed elevation changes. Because of the difficulties of individual cross-sectional comparisons, we have also looked at the overall trend of changes by subtracting DEMs of measured and simulated elevation data from 2005 and 2006. Both the simulated and measured DEMs indicate that the reach is undergoing degradation. However, the amplitude of changes in the measurements is markedly higher than in the simulation. Differences between measured and simulated velocities in the Saint-François River were also greater than for the other two tributaries, particularly at low flow [Verhaar *et al.*, 2008]. This comparison is further complicated by the fact that in the simulations, bed change is equally spread over the submerged part of the cross section, whereas the measured cross sections showed changes in the lateral direction and cross-sectional shape, particularly in the downstream reach which has a large meander loop. Considering the challenges in modelling a complex planform adequately with a 1D model and the good agreement for simulated and measured water levels in this tributary, we believe that these simulations are valid, but that caution is required in interpreting results.

4.4.2 Simulations

The effects of alternative hydrological regime and base level scenarios are examined by averaging the model outputs from each 30-year horizon in each scenario and comparing these averages with those for the same horizon using present-day discharge and base level (RefQ-RefH). The results are interpreted visually and the statistical significance of the difference between each scenario and the RefQ-RefH baseline is assessed relative to the year-to-year variability within each simulation. In most cases the annual bed material transport and the relative bed elevation changes were not normally distributed, so non-parametric tests were used (Kruskal-Wallis and Wilcoxon). Not all the simulations of the Saint-François River cover the full time period of interest because of sedimentation in one of the branches along the island. All simulations with the RefH scenario, as well as the CSIRO-Mk2 and ECHAM4 discharge scenarios in combination with the 0.50m-2040 base level scenario, completed the full simulation (until 2100).

4.4.2.1 Annual bed material transport

The simulated annual flux of bed material entering and leaving each reach is presented in Figures 4.3 and 4.4. The trends for the A2 and B2 GHG-scenarios are very similar in all cases, and differences between these two GHG-scenarios are never statistically different at the 5% significance level. Therefore, Figures 4.3 and 4.4 only present results from the A2 scenario, which is closest to the current GHG-emission rates and which has been used in recent studies on climate change and rivers [Lane *et al.*, 2007, 2008]. Filled symbols in Figures 4.3 and 4.4 are used to indicate values that are significantly different from the RefQ-RefH scenario.

A comparison between incoming and delivery transport rates (Figures 4.3 and 4.4) indicates that the tributaries are in different states, either aggrading, degrading or in equilibrium. Figure 4.5 presents the bed material transport at the up- and downstream boundaries for the reference scenario (RefQ-RefH). Despite the same discharge being applied in each

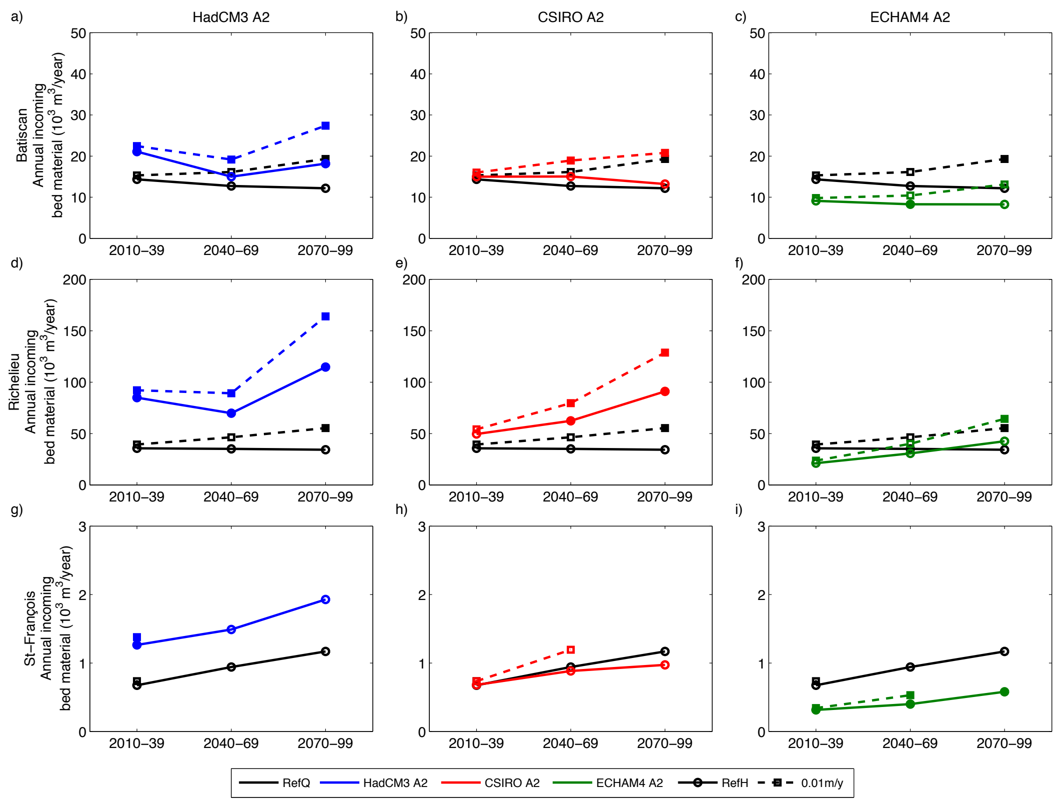

Figure 4.3: Annual bed material transport (m^3/year) at the upstream boundary for all the rivers by climate model scenario for the A2 GHG-scenario: a), b), c): Batiscan River; d), e), f): Richelieu River; and g), h), i): Saint-François River. Black lines represent the annual bed material transport of the RefQ scenarios. Filled symbols indicate significant differences compared to the RefQ-RefH scenario at a 5% significance level. Error bars are not presented in this figure to improve readability.

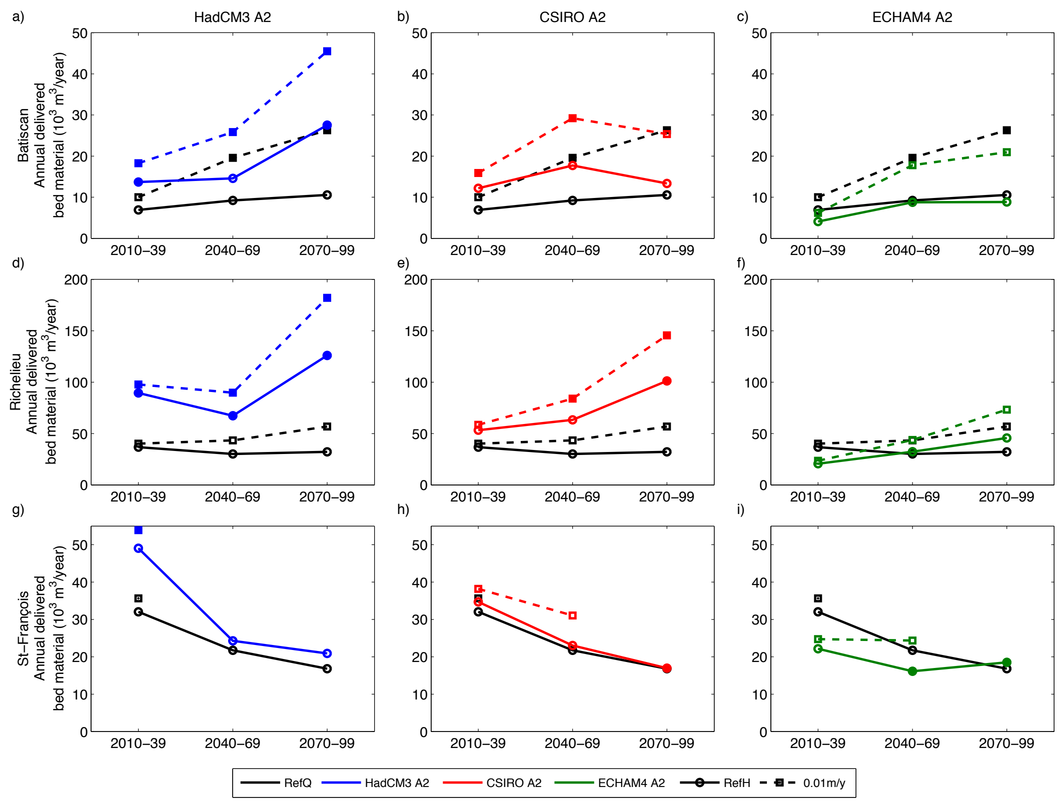

Figure 4.4: Annual bed material transport (m^3/year) at the downstream boundary for all the rivers by climate model scenario for the A2 GHG-scenario: a), b), c): Batiscan River; d), e), f): Richelieu River; and g), h), i): Saint-François River. Black lines represent the annual bed material transport of the RefQ scenarios. Filled symbols indicate significant differences compared to the RefQ-RefH scenario at a 5% significance level. Error bars are not presented in this figure to improve readability.

horizon the upstream boundary transport can be different for each horizon due to morphological changes in the downstream reach that change the transport capacity. The Richelieu River is in a near equilibrium state under the current discharge and base level (Figure 4.5). The Batiscan River is slightly aggrading under the RefQ-RefH scenario, although differences between upstream and downstream boundaries are only statistically significant for the first horizon, and the trend is towards equilibrium towards the 2070–2099 horizon (Figure 4.5). For the Saint-François River, the bed material transport at the upstream boundary is markedly smaller than at the downstream end (Figure 4.5), though it increases over time so that again there is a trend towards equilibrium. One possible reason for this simulated degradation is that grain size composition at the upstream boundary of the Saint-François River is very coarse compared to the rest of the reach ($D_{50} \approx$8 mm compared to $D_{50} \approx$0.3 mm, Table 4.1). The difference in grain size is not as pronounced in the other two tributaries (Table 4.1). Velocities and bed shear stress in the upper reaches are thus not sufficient to transport the active layer coarse material, but they can move the finer sand further downstream, resulting in degradation in this river. Furthermore, this river might be still adapting to a decrease in base level as a consequence of dredging a navigation channel in Lake Saint-Pierre, as observed by its delta propagating into the lake [Bondue *et al.*, 2006]. For the Richelieu this effect is minor as the downstream part is dredged regularly to maintain navigation depths. This could cause increased erosion in the more upstream part, which leads to aggradation in the dredged zone and is therefore not visible in 4.5, where only sediment transport at the model boundaries is presented.

The effect of climate-induced discharge change (continuous coloured lines in Figures 4.3 and 4.4) varies for each river and for each climate model. The HadCM3 model predicts the largest changes in bed material transport for all the rivers. For the Batiscan and Richelieu rivers, the effect is more pronounced in the 2070-2099 horizon. For the Saint-François River, however, the change in annual bed material transport is much smaller. The CSIRO-Mk2 climatic model predicts smaller increases than the HadCM3 model. In most cases the trends follows that of HadCM3, except for the Batiscan River where sediment transport at the downstream boundary decreases in the third horizon (Figure 4.4b). The ECHAM4 model (Figure 4.4c) in general predicts less sediment transport compared to the other two models (Figures 4.3c,f,i, and 4.4c,f,i) and in most cases a decrease compared with RefQ.

For all models, there appears to be a relationship between the equilibrium state of the river and the impact of climate-induced discharge changes. In the Richelieu River (near-equilibrium state), climate changes result in increased sediment delivery at its mouth (Figure 4.4d,e,f). In the slightly aggrading Batiscan River, there is an increase in sediment delivery for the HadCM3 model, a small increase for the CSIRO-Mk2 model, and virtually no change for the ECHAM4 model (Figure 4.4a,b,c). For the Saint-François River, which is degradational, there is an overall decrease in sediment output with time, and the CSIRO-Mk2 and ECHAM4 models show smaller delivery rates than the RefQ scenario (Figure 4.4h,i). The HadCM3 model indicates increases for each horizon, but these are not statistically significant (Figure 4.4g). Simulated changes in input over time (Figure 4.3) also reflect the state of the reach, as can be seen most clearly for the RefQ-RefH scenario: in the near-equilibrium Richelieu River the input is almost stationary, but in the aggrading Batiscan River there is a slight decrease in input as the proximal gradient reduces and in the degrading Saint-François River the input increases as the proximal slope increases. These time trends in input are the opposite of the time trends in output, showing again how within-reach adjustment tends to restore equilibrium.

As would be expected the effect of a base level decrease (dashed lines in Figures 4.3 and 4.4) is to systematically increase the annual bed material transport compared to the RefH scenario, with an increasing impact over time as the magnitude of the base level fall increases. The RefQ simulations show that the effect of falling base

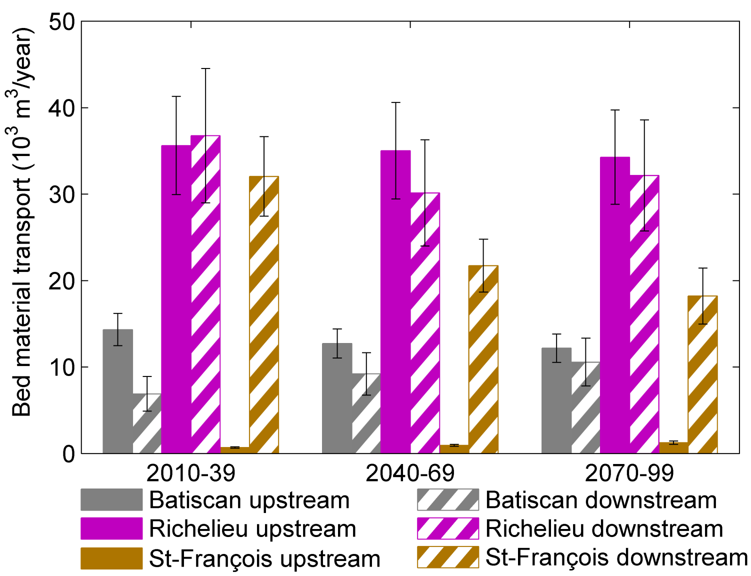

Figure 4.5: Annual bed material transport per horizon at the upstream and downstream boundary for the RefQ-RefH scenario for the three tributaries. Error bars represent +/- one standard error of the variance between years within each horizon.

level reaches the inlet by the second horizon in two of the three rivers (Batiscan and Richelieu rivers).

4.4.2.2 Bed elevation

The effects of discharge and base level changes on bed elevation are compared relative to the RefQ-RefH scenario. Negative values mean lower bed elevation, which could result from either less sedimentation or more erosion. Because data are neither normally distributed nor independent, the Wilcoxon rank test is used to examine differences between GCMs and RefQ scenarios at the end of the simulation period. The lowest points for cross sections over 2.5 km reaches are grouped together to create data sets of multiple values, resulting in 8 to 26 cross sections per reach as the spacing between cross sections is less near the mouth.

Contrary to the bed material transport rates, the bed elevations predicted by the GHG-scenarios are statistically different. The bed elevation for the A2 scenario is consistently lower than the B2 scenario averaged over the whole reach, by about 0.05 m in the Batiscan and Saint-François rivers and 0.20 m in the Richelieu River.

Bed elevation is examined first in 2059 to assess the impact of the two base level scenarios since in both cases the total fall by that date is 0.50 m. The mean differences in bed elevation between the 0.01m/y and 0.50m-2040 base level scenarios are generally small (Figure 4.6), with average values of 0.010, 0.007 and 0.022 m for the Batiscan, Richelieu and Saint-François rivers, respectively. These small values are nevertheless statistically significant in about half the cases. In the Batiscan River, the gradual base level fall produces more erosion in all cases compared to the step fall, whereas in the other two tributaries, the patterns are variable, with only a few cases where the step fall produced significantly more erosion, particularly in the downstream reach of the Saint-François River.

Figures 4.7 and 4.8 show how the mean bed elevation of one sub-reach located at the mouth (0–2.5 km, Figure 4.7) and one in the middle section (7.5–10 km, Figure 4.8) varies over time. The plotted values are differences from the RefQ-RefH scenario in order to eliminate the time trend due to present-day aggradation or degradation. In general the GCMs and base level scenarios result in lower bed elevations than the RefQ-RefH scenario, with the exception of the ECHAM4 model in the Richelieu and Saint-François rivers (Figure 4.7f,i). The future GCM discharge scenarios reduce the aggradation (RefQ) and lead to some erosion (≈ 0.15 m) in the downstream part of the Batiscan River (2010–2099). The equilibrium state of the Richelieu River becomes degradational (≈ 0.30 m) under future climate scenarios. The degradation in Saint-François River is amplified by the HadCM3 scenario, remains similar for the CSIRO-Mk2 scenario and is reduced by the ECHAM4 scenario, with an average degradation for all GCMs of about 1.0–1.5 m over 2010–2099.

Not surprisingly, base level decrease leads to increased degradation for all discharge scenarios for the Batiscan and Saint-François rivers near the mouth, particularly in the last horizon (Figure 4.7). For the Richelieu River, base level decrease does not have a major impact for the RefQ scenario, possibly because bed levels have already been altered by dredging, but it does when combined with climate-induced discharge change. A substantial response to base level fall is also predicted in the Saint-François River, but only for the HadCM3 model near the mouth (Figure 4.7h). In the near-equilibrium Richelieu River, the impact of discharge changes is much greater than that of base level fall, particularly near the mouth (Figure 4.7d,e,f).

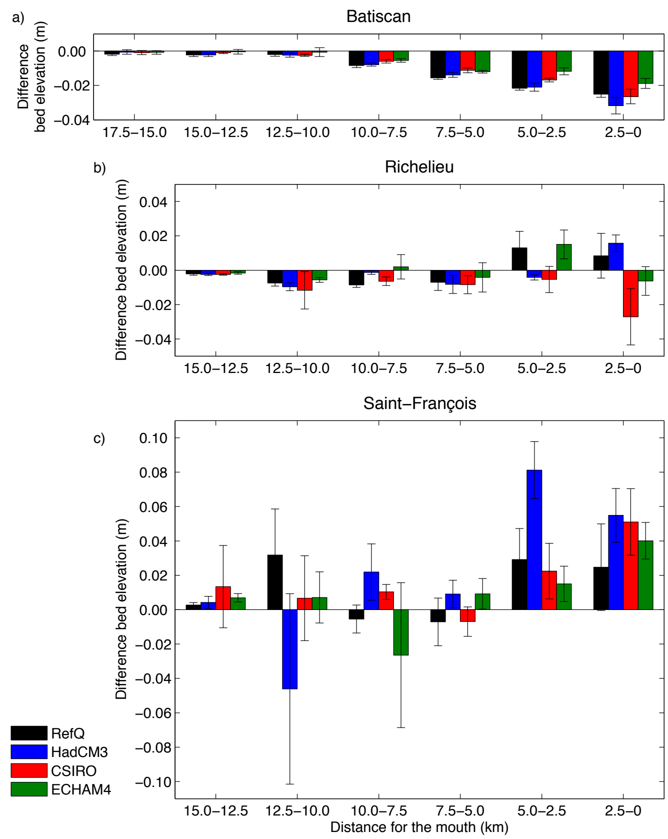

Figure 4.6: Difference in bed elevation between the 0.01m/y and 0.50m-2040 base level scenarios by the end of 2059. Negative values indicate lower bed elevation in the 0.01m/y scenario. The error bars show +/- one standard error. a): Batiscan River; b): Richelieu River; c): Saint-François River.

There is some variation in the distance over which a significant effect of a decrease in the base level only (i.e. for the RefQ scenario) occurs. For the Batiscan River, statistically significant differences are predicted for most of the studied reach, but these changes are only substantial (> 0.25 m) up to 5–7.5 km from the mouth. Bed erosion is 0.17 m in the middle section (7.5–10 km, Figure 4.8a,b,c), and is less than 0.1 m in upstream reaches. For the

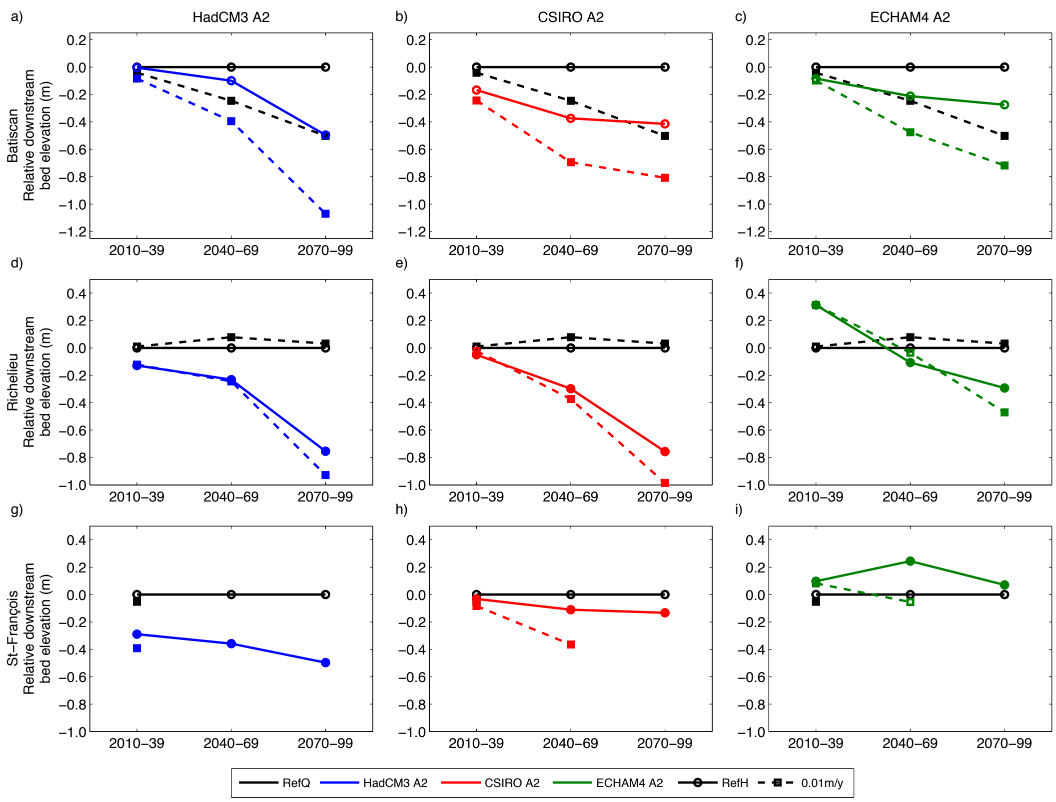

Figure 4.7: Difference in bed elevation averaged near the mouth (0.0–2.5 km interval) between the climate model scenarios and the RefQ-RefH scenario, where negative value indicate lower bed elevations: a), b), c): Batiscan River; e), d), f): Richelieu River; and g), h), i): Saint-François River. Filled symbols indicate significant difference compared to the RefQ-RefH scenario at a 5% significance level. Error bars are not presented in this figure to improve readability.

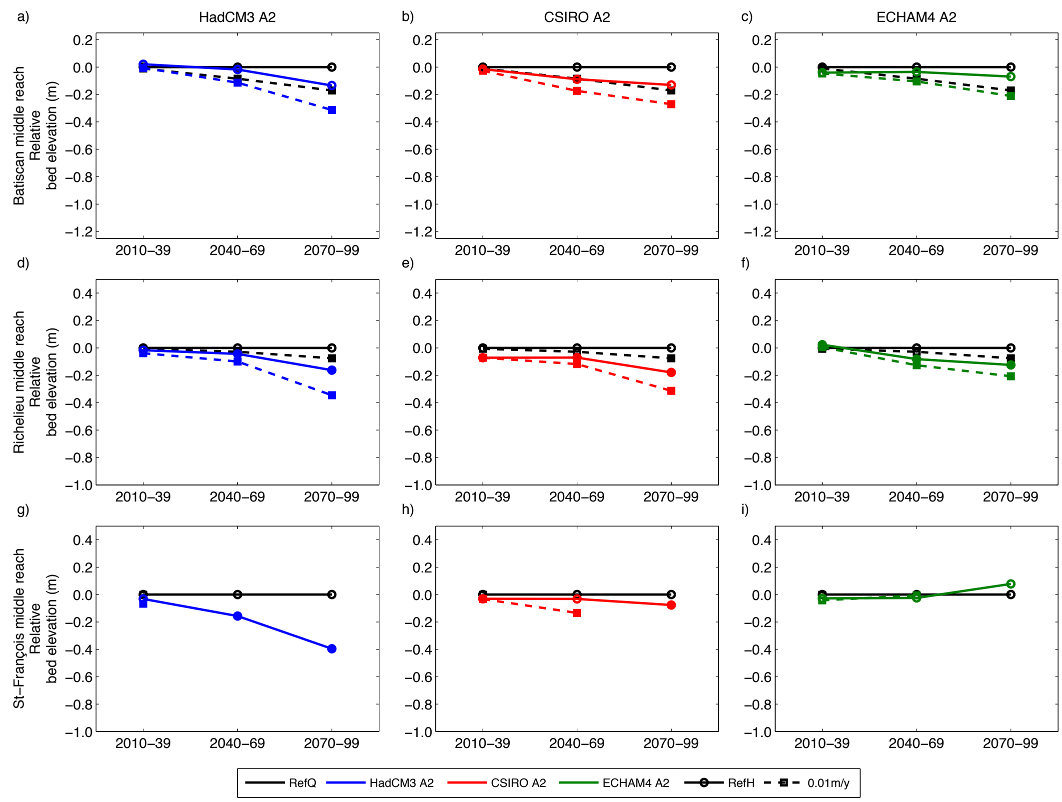

Figure 4.8: Difference in bed elevation averaged over a 7.5–10.0 km interval from the river mouth between the climate model scenarios and the RefQ-RefH scenario, where negative value indicate lower bed elevations: a), b), c): Batiscan River; e), d), f): Richelieu River; and g), h), i): Saint-François River. Filled symbols indicate significant difference compared to the RefQ-RefH scenario at a 5% significance level. Error bars are not presented in this figure to improve readability.

Richelieu River, the impact of a base level fall is much smaller, and does not follow a consistent trend. As already noted the dredged reach close to the mouth is not affected by a base level fall (Figure 4.7d,e,f), but reaches up to distances of 10–12.5 km are significantly different from the RefH scenario (changes ≈ 0.13 m). In the Saint-François River, considerable erosion due to base level drop is simulated in the downstream 5 km (> 0.15 m), and significant differences in bed elevation are found up to 10–12.5 km from the mouth (≈ 0.10 m).

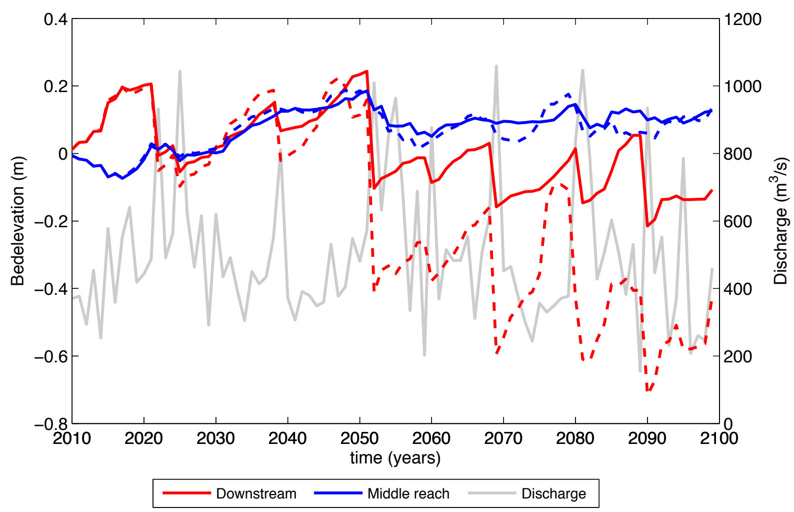

Figure 4.9: Time series showing annual bed elevation variation with discharge for two cross sections, one at the mouth (red) and one in the middle reach (9.4 km upstream from the mouth, in blue) in the Batiscan River for the CSIRO-Mk2 discharge scenario. Continuous lines represent the RefH water level scenario and dashed lines represent the 0.01m/y base-level drop scenario.

Although there are systematic changes in response from one horizon to the next, annual variability can be high within each horizon. Figure 4.9 presents an example of this variability for the Batiscan River, using the CSIRO-Mk2 simulation for a mid-reach and downstream cross section. The impact of a base-level decrease is particularly clear from mid-century for the downstream cross-section where, for a flood of similar magnitude, bed erosion is markedly increased. Only after a relatively long period lacking high magnitude floods are bed levels reaching comparable levels (e.g. around 2070 in Figure 4.9).

The impact on bed elevation of climate variations and base level change varies between reaches, as illustrated by a few examples for the Batiscan River in Figure 4.10. The reach between 10 and 12.5 km is deeper than average, which is why aggradation is greater in this reach than elsewhere. This aggradation in these upstream reaches is slightly reduced by GCM or base-level fall (Figure 4.10b,c). The base-level fall will reduce the aggradation in the downstream reach (2.5–0.0 km) and change into degradation around the year 2050. The bed elevation fluctuates more in the GCM and base-level scenarios than in the RefQ-RefH. Evidently the effect of base-level is more apparent towards 2099, whereas discharge change affects the bed elevation of downstream reaches from the first horizon onwards.

4.5 Discussion

The 1D morphodynamic model predicts that climate-induced changes in discharge and base level will have significant impacts on bed material transport and bed elevation in three tributaries of the Saint-Lawrence River through the 21st century. Ideally, past climate change should be used to validate such a model [e.g. Coulthard *et al*., 2005]. Unfortunately, no historical dataset on sediment accumulation or erosion is available for the studied tributaries. Indeed, there is a surprising lack of both past and modern data on the Saint-Lawrence tributaries, which is why a major field data collection effort was required for this project.

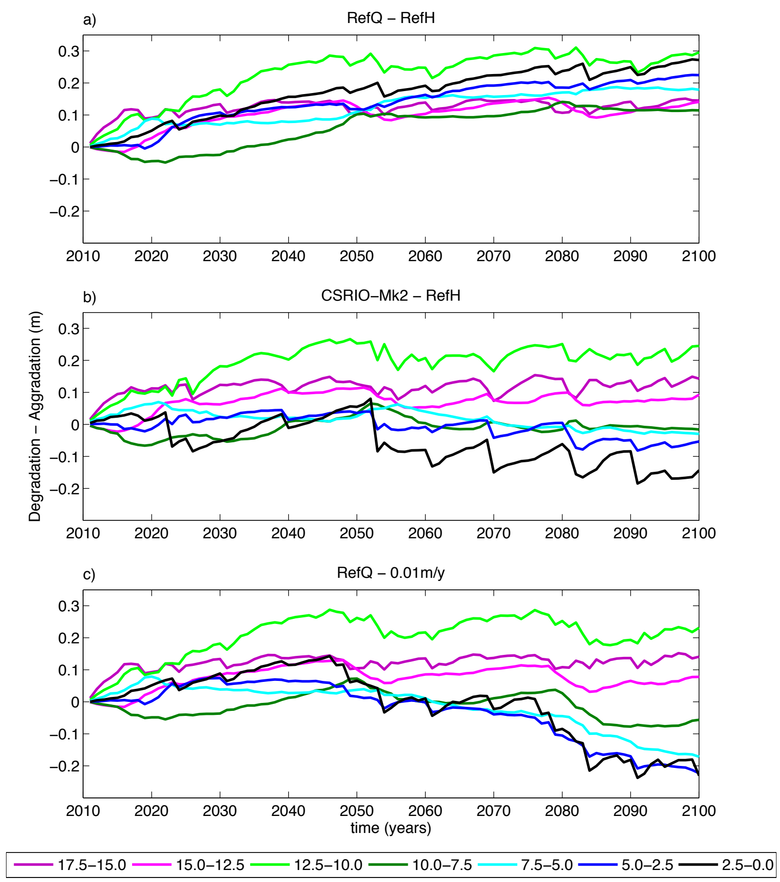

Figure 4.10: Time series showing annual bed aggradation (> 0 m) and degradation (< 0 m) for the 7 reaches in the Batiscan River for a) the reference scenario (RefQ-RefH); b) CSIRO-Mk2 and RefH; c) RefQ-0.01m/y.

Simulations with either climate change or base level held constant show that both types of forcing have an effect on sediment fluxes and channel stability. The general pattern is for degradation to occur. However, the quantitative results are sensitive to the choice of GCM, which is not so surprising considering that the climate models used to generate discharge scenarios in this study were selected based on their marked differences. The choice of GHG-scenarios (A2 or B2) is much less important. It has even less effect on sediment delivery than it has on bed elevation. This may be due to the fact that values of bed elevation were compared only at the end of the simulation, using a spatial average over 2.5 km reaches, whereas sediment transport rates were compared over a 30-year period, at a fixed location. The marked differences between GCMs highlight that conclusions of climate-change studies drawn from only one GCM should be examined with care, as was also noted by Prudhomme *et al.* [2003] who reported that flood magnitude and frequency varied by a factor of nine between different GCMs used in Northern England and Scotland. The low sensitivity of our results to an assumed constant decrease in base level when compared to a step fall also highlights that the choice of a GCM is the key controlling factor in determining future morphological adjustments of rivers.

Climate change impacts on rivers are often seen as impacts on flood risk [Longfield and Macklin, 1999] and their importance for sediment delivery is often overlooked, as pointed out by Lane *et al.* [2007, 2008]. However, the risk of flooding will not be the same if the river is undergoing aggradation or degradation, as flow stage will vary for a given discharge. Aggradation will exacerbate flood risk [Lane *et al.*, 2008], whereas degradation may decrease flood risk but increase bank erosion potential. Running the morphodynamic model using a reference discharge scenario from 2010 to 2099 predicted that the Batiscan River was undergoing slight aggradation, the Richelieu River was in a near-equilibrium state, whereas degradation was the trend for the Saint-François River. The sediment delivery trend for the latter was opposite that in the other two tributaries, with sediment delivery decreasing with time (Figure 4.4). Thus, there are important differences in the impacts of discharge and base level decrease between the three tributaries despite them all being located in the same geomorphic zone (Saint-Lawrence Lowlands) and having very similar characteristics in terms of grain size and slope. High levels of inter-catchment and inter-reach variability have also been observed by Coulthard *et al.* [2005], despite simplified initial conditions. This research is one of the few long-term simulation studies that use real river representations rather than idealized channels to look at the impact of disturbances [e.g. Simon and Darby, 1997; Doyle and Harbor, 2003]. Our results suggest that complex river topography affects adjustment to climate and base level disturbances. Furthermore, aggradation and degradation trends need to be examined carefully when attempting to predict near-future impacts of climate change, and caution is needed when generalizing results obtained from simulations of a single river.

Studying the impacts of climate change on rivers involves dealing with the uncertainty in temperature and precipitation prediction, as well as in the hydrological model to convert these changes into discharge [Prudhomme *et al.*, 2003; Graham *et al.*, 2007]. Furthermore, the delta method used here suffers from limitations with regards to flood recurrence intervals [Graham *et al.*, 2007; Quilbé *et al.*, 2008] which are dependent upon the reference period and so may be biased. For example, if a flood with a 100-year return period occurred during a 30-year reference period it will occur in each predicted horizon, i.e. 3 times in the next 90 years. Thus, modelling near-future discharge and base level changes gives rise to results with very high uncertainty [Andersson *et al.*, 2006; Fowler *et al.*, 2007; Quilbé *et al.*, 2008; Thodsen *et al.*, 2008]. The difficulty of specifying any other upstream boundary condition than sediment supply equal to transport capacity in near-future simulations adds to this uncertainty [Gomez *et al.*, 2009], though our sensitivity tests did not produce radically different results under alternative assumptions. In most cases, these should therefore not be interpreted as absolute quantities, but rather as indicators of trends. However, by comparing differences between scenarios, part of this uncertainty vanishes as the same systematic error affects all of the compared simulations. In other words, comparing scenarios may not provide accurate values, but it gives a good indication of the direction and relative magnitude of change.

The changes in bed material transport in the Richelieu and Saint-François rivers are important for Lake Saint-Pierre. The volume of bed material exiting the Richelieu River will change most in the 2070–2099 horizon (Figure 4.4d,e,f), with values three times the volume from the 2010–2039 horizon RefQ on average, resulting in an increase in the lake's sediment input. On the other hand, the Saint-François River, also draining into Lake Saint-Pierre, will see its sediment delivery decrease by the end of the 21*st* century (on average, 0.59 times the RefQ scenario in the first horizon). Nevertheless, since the volume of transport is much larger in the Richelieu River, there is a potential risk of reduced depth through increased sedimentation in Lake Saint-Pierre in the future. The increase in bed material transport from the Richelieu River also has potential economic consequences as it enters the Saint-Lawrence River close to the navigation channel.

The topography of the tributaries seems to be highly influenced by the base level change, particularly in the Batiscan and Saint-François rivers. As these tributaries have very low energy slopes (Table 4.1), backwater effects persist far upstream, with significant bed elevation changes for distances up to 10 km.

The failed Saint-Maurice River simulation highlighted the limits of our 1D model when islands are present. Clearly in this case a two-dimensional modelling approach is required. The Saint-François island configuration was simpler, but the simulation of several scenarios in combination with base level decrease could nevertheless not be completed for the whole period of interest due to sedimentation in the eastern channel along the island (simulations were stopped as early as 2053). As stated by Wang *et al.* [1995], the stability of bifurcations in one-dimensional modelling depends on the sediment transport condition at the bifurcation. Here, we used a sediment transport ratio identical to the discharge ratio. This ratio may actually vary with discharge and depends on the topography at the bifurcation. Miori *et al.* [2006] showed that, in gravel-bed rivers, the branch which receives most of the discharge is generally the most active in terms of sediment transport and the branch with less base discharge is morphologically less active.

4.6 Conclusion

Morphological simulations for the 21st century of three tributaries of the Saint-Lawrence River based on three GCMs involving changes in both discharge in the tributaries and in the water level of the Saint-Lawrence River (21 scenarios) predicted an overall increase in volumes of bed material that will reach the Saint-Lawrence River and Lake Saint-Pierre, as well as an effect on the longitudinal profile up to 10 km from the confluence with the Saint-Lawrence River.

The GHG-scenarios (A2 or B2) had a much smaller impact on the simulated results than the choice of a climatic model (CSIRO-Mk2, ECHAM4 or HadCM3). The HadCM3 model, which predicts the largest changes in precipitation and moderate change in temperature, produced the largest changes, followed by the CSIRO-Mk2 and ECHAM4 models. This indicates that conclusions drawn from only one climatic model need to be interpreted with caution. By analogy, it would be desirable in future work to determine the sensitivity of the morphodynamic predictions to the choice of hydrological model (here, HSAMI) and the choice of transfer method (here, the delta method) to convert predicted changes in temperature and precipitation into daily discharge.

Alternative base level fall scenarios (an abrupt change versus a progressive fall) indicated that the magnitude of the change is more important than the type of fall. By 2059, both scenarios reached a decrease of 0.50 m, and the difference in simulated bed elevation was on average less than 22 mm for the three tributaries. Note that in applications of this model to other rivers, the base level would be likely to increase due to anticipated sea level rise. This would likely counterbalance the overall increase in bed material transport simulated with the discharge scenarios and lead to sedimentation in the downstream reaches. However, the response of each tributary varied in this study, which highlights the difficulty of generalizing trends in rivers under various climate scenarios and base level change. Sediment delivery from the Saint-François River, which is undergoing degradation, is predicted to decrease over time for all climate models, which is contrary to the trend in the other two tributaries.

Only mean annual bed material transport volumes were examined in this study. As the climate change impacts on discharge affect extreme flows, but not the mean annual flow, a more detailed analysis of bed material transport at the event scale would provide a better insight on the role of extreme events associated with climate change on bed material delivery.

Paragraphe de liason C

The previous chapter (4) showed that sediment transport rates are in general more sensitive to discharge changes than to a base level change. Furthermore, it revealed that the choice of GCM is more important than the GHG scenario or the effect of base level fall. Although the changes in mean daily discharge and mean annual maximum remain close to current values in the GCM scenarios, transport rates change drastically through time. Results in chapter 4 were bulked per horizon to describe general trends. This, however, does not allow a complete understanding of what generates an increase in sediment transport, i.e. does it come from a larger number of relatively frequent events, or from only a few very large storms? Because of the large variability between successive years it was felt that the analysis should focus on a smaller time scale. As the timing of floods as well as the number of floods varies from one scenario to another, a one-on-one comparison is impossible. To investigate what causes this strong non-linear response in sediment transport rates to changes in discharge, chapter 5 examines simulation results of individual sediment transport events and relates them to their associated hydraulic parameters of maximum discharge, duration and recurrence interval. This allows for an assessment of the impact of more extreme events on rivers. The use of the Pearson Type-III distribution is common in the literature and as we are applying this to simulated discharges for relatively short time periods (30 years), it is believed that this method is a relatively accurate tool for our data. It is also possible that the type of distribution would differ between scenarios, thus the use of a widely known and accepted method was deemed best. Furthermore, the recurrence intervals are used as an indication of flood magnitude, not to determine flood risks, for example. The use of recurrence interval is therefore considered a tool that allows us to compare results between the different tributaries.

CHAPTER 5

IMPLICATIONS OF CLIMATE CHANGE FOR THE MAGNITUDE AND FREQUENCY OF BED-MATERIAL TRANSPORT IN TRIBUTARIES OF THE SAINT-LAWRENCE [3]

5.1 Introduction

It is expected that climate change in the 21^{st} century will increase the magnitude and frequency of floods as a result of an increase in rare meteorological events [Middelkoop *et al*., 2001; Reynard *et al*., 2001; Robson, 2002; Milly *et al*., 2002; Prudhomme *et al*., 2002; Lane *et al*., 2007, 2008]. Predicting extremes in a changing climate remains a challenge, particularly in terms of local flooding events [Hunt, 2002; Kundzewicz *et al*., 2005; Kay *et al*., 2006], but irrespective of the precise nature of hydrological change it seems inevitable that it will have consequences for the transport of sediment by rivers. However, the role of climate-induced changes in frequency, duration and seasonality of floods can only be assessed by an event-scale breakdown of the annual average sediment fluxes.

One widely-used approach to understanding how the trade-off between flood magnitude and frequency affects sediment transport is to use the flow duration curve and a transport rating curve to determine the transport magnitude-frequency curve. Wolman and Miller [1960] proposed that the effective discharge (that transports the greatest portion of the annual sediment load) is comparable with the bankfull discharge (with a recurrence interval of about 2 years) and mean annual flood [Wolman and Miller, 1960; Pickup and Warner, 1976; Andrews, 1980; Carling, 1988; Nash, 1994; Emmett and Wolman, 2001; Barry *et al*., 2008]. However, the frequency of effective discharge is known to vary greatly [Pickup and Warner, 1976; Ashmore and Day, 1988; Nash, 1994; Torizzo and Pitlick, 2004]. Furthermore, for a given mean discharge and sediment rating curve, the effective discharge has been shown to be higher when the variability in discharge is greater [Nash, 1994; Vogel *et al*., 2003]. Long-term sediment yield may be dominated by rarer catastrophic events, particularly in steep gravel-bed rivers [Kirchner *et al*., 2001; Lenzi *et al*., 2006], although there is yet no clear consensus on

---

[3] the basis of this chapter is submitted to HYDROLOGICAL PROCESSES. 2009-December-01, HYP-09-0608

this issue. An alternative approach such as the half-load discharge (value above and below which half the long-term sediment load is transported) was also presented by Wolman and Miller [1960], although most of the subsequent literature has only used their effective discharge method. Vogel *et al*. [2003] revived this second approach which they consider more meaningful to determine which discharges are responsible for carrying most of the long-term load. However, very little work has been done on the impacts of the expected increase in high-magnitude floods due to climate change on sediment loads in rivers, particularly with respect to bedload transport [but see Coulthard *et al*., 2005, 2008; Kundzewicz *et al*., 2007; Gomez *et al*., 2009].

We have examined elsewhere the likely impacts of climate change on mean annual sediment transport rates and aggradation/degradation in the lowermost parts of three tributaries of the Saint-Lawrence River [Verhaar *et al*., in press]. A one-dimensional (1D) morphological model using simulated discharges from three Global Climate Models (GCMs) predicted an increase in sediment transport in these sand-bed rivers, and hence an increase in the sediment delivery to the Saint-Lawrence River, with the largest changes occurring during the winter and spring seasons [Boyer *et al*., 2009, in press; Verhaar *et al*., in press]. The objective of this study is to examine climate-change induced changes in the magnitude-frequency-duration relation for bed-material load in these rivers.

5.2 Methodology

5.2.1 Study area

The three tributaries of the Saint-Lawrence River (Batiscan, Richelieu and Saint-François rivers) are located between Montréal and Québec City, Eastern Canada. They have large catchment areas ($> 10\,000$ km^2), low distal gradients ($< 1 \times 10^{-4}$) and predominantly sandy beds. Each river is exploited for hydroelectricity or influenced by dams used for flood control, water intake or recreational activities but the impact of these structures on the natural regime of the river is low for the Batiscan and Richelieu rivers and only moderate for the Saint-François River [Boyer *et al*., in press]. Our simulations indicate that the Batiscan River is currently aggrading, the Saint-François River degrading, and the Richelieu River almost in equilibrium [Verhaar *et al*., in press].

Detailed cross-sectional profiles of topography were taken with an echo sounder from a boat at several cross sections (between 80 and 100) from their confluence with the Saint-Lawrence River to 15–17 km upstream in 2004 and 2005. Bed composition was obtained from samples also collected from a boat using a grab bucket. A detailed description of the field data collection, river characteristics and model validation can be found in Verhaar *et al.* [2008, in press].

5.2.2 Climate scenarios

Three GCMs (CSIRO-Mk2, ECHAM4 and HadCM3) and two greenhouse gas (GHG) emission scenarios [A2 and B2, Nakicenovic *et al.*, 2000; Raupach *et al.*, 2007] were used by the Ouranos research centre, a consortium on regional climatology and adaptation to climate change (www.ouranos.ca), to produce discharge scenarios for the three tributaries [Chaumont and Chartier, 2005; Boyer *et al.*, in press]. Current GHG-emissions exceed both the A2 and B2 scenarios, but A2 is closest to the actual emissions [Raupach *et al.*, 2007] and only these results will be presented here. The GCMs were selected based on their differences in predictions of precipitation and temperature to represent a wide range of outputs when compared to a multimodel dataset [Meehl *et al.*, 2007]. The standard perturbation (or delta) method was used to add predicted changes in precipitation, temperature and evapotranspiration to an observational database which is used as input to a hydrological model to represent future climate [Arnell, 1998; Rosberg and Andréasson, 2006; Graham *et al.*, 2007; Rydgren *et al.*, 2007]. The use of the Canadian Regional Climate Model [CRCM, Caya and Laprise, 1999] was not considered optimal in this case as preliminary analyses by Ouranos showed that, in southern Québec where the topography is relatively smooth and the climate is not influenced by maritime conditions, using delta values for regional models at a 45 km resolution added little information compared to delta values derived from GCMs at a 250 km resolution [Boyer *et al.*, in press].

The hydrological model HSAMI [Chaumont and Chartier, 2005; Minville *et al.*, 2008; Boyer *et al.*, in press], which is a lumped rain and snowfall runoff model used by Hydro-Québec (Québec's national hydro-electricity company), was used by Ouranos to produce six time series (three GCMs combined with two GHG-scenarios) of daily discharge values. The delta values (precipitation and temperature) were added to the reference period (1961–1990) for three different time periods or 'horizons' (2010–2039, 2040–2069 and 2070–2099). The model was calibrated and validated on measured discharge data over the 1961–1990 time period [Chaumont and Chartier, 2005; Boyer *et al.*, in press]. These simulated daily discharges are used as a reference discharge scenario for the morphological modelling by repeatedly using it for the periods 2010–2039, 2040–2069 and 2070–2099, referred to as RefQ hereafter. More details on the simulation scenarios can be found in Boyer *et al.* [in press] and Verhaar *et al.* [in press].

5.2.3 Morphodynamic model

In this study, only sand transport in the lower reaches of the tributaries is considered, not washload supplied from the entire catchments. We have used a morphodynamic model to take into account the possible gain or loss of sediments from the channel bed as well as the throughput from upstream. In the context of climate change simulations for the 21st century, it was felt that running long-term simulations with a daily time-step over long reaches could only be achieved through a 1D morphodynamic model [Gomez *et al.*, 2009].

The 1D uncoupled morphodynamic model SEDROUT4-M [Hoey and Ferguson, 1994; Verhaar *et al.*, 2008] was selected for the simulation of the effects of climate-induced discharge on sediment transport. This model has proven to be capable of simulating morphological changes over various temporal and spatial scales [Talbot and Lapointe, 2002; Ferguson and Church, 2009]. Initial bed topography and bed composition are based on our measurements, with bed composition averaged over the cross section. The upstream limits of our reaches were chosen at locations where long-term stability of bed level could be assumed and bed-material input equated with transport capacity at all times. This, however, does not mean that sediment supply is constant as it will respond to hydrological changes as well as to any change in proximal slope following aggradation or degradation within the reach.

For each tributary the morphological changes for the period between our measurements (2004–2005) and the start of near future time series of discharge (2010) were predicted using observed discharges in the period from 2000 to 2005 and averaged water levels in the Saint-Lawrence River as measured over 1996–2005 at gauging stations close to the river mouths. The results of bed topography and bed composition from these simulations were then used as initial conditions for the near-future simulations over the period 2010–2099. Climate changes are expected to result in a decrease in the Saint-Lawrence River level due to increased evaporation in the Great Lakes following temperature increases [Croley, 2003; Chaumont and Chartier, 2005; Morin *et al.*, 2005]. A steady decline in base level of 0.01 m per year was also used in some simulations [Verhaar *et al*., in press]. Here, we focus on the current daily-averaged Saint-Lawrence water levels, although some simulation results based on a steady base level fall are also discussed later.

Sediment transport rates were simulated with the Ackers and White [1973] total load sediment transport formula and the parameter settings from White and Day [1982]. All particles smaller than 0.125 mm (3ϕ) are assumed to be transported as wash load and are therefore not considered relevant to morphological simulations of the tributary reaches. For various hydraulic conditions SEDROUT4-M was found to accurately simulate water level and mean cross-sectional velocities [Verhaar *et al*., 2008]. The morphological performance of the model was also verified by comparing simulated changes in bed topography over a period of one year with observed changes [Verhaar *et al*., in press].

5.2.4 Event analysis

Differences in mean annual bed-material transport strongly depend on discharge scenarios resulting from different GCMs [Verhaar *et al*., in press]. However, to examine how more extreme events associated with climate change affect bed-material transport, in this study we compare scenarios for different tributaries at the sediment transport event scale instead of the annual scale. Unlike in gravel-bed rivers where sediment transport drops to zero between events, sand-bed rivers are often characterized by very long tails in sediment transport curves [Ferguson *et al*., 2003; Li *et al*., 2008]. To analyze data at the event scale, bed-material transport events were defined here as successive days of transport over 10 m^3/day (approximately 1 g/m/s) with a single peak over 50 m^3/day. These values were determined after examining several sediment transport events associated with several multiple peak floods. Events were separated where the minimum transport between two peaks occurred. For each sediment transport event the maximum discharge, duration and transported volume are calculated.

Discharges are expressed in recurrence intervals to facilitate comparison between the different tributaries and between the climate scenarios. They were calculated by fitting a Pearson-type III distribution approach from the annual maximum discharge time series. For each tributary, the present-day recurrence intervals were computed from the 1932–2004 record (HYDAT, Environment Canada), whereas the future recurrence intervals were obtained from the 2010–2099 series for each GCM scenario. Note that the perturbation method used in this study, which has the advantage of being stable and robust [Graham *et al*., 2007], replicates the inter-annual variability of climate variables of the reference period and can thus not introduce new types of variability which may occur under future climate [Boyer *et al.*, in press]. The variability in precipitation and temperature is therefore stationary and the method cannot predict extreme events very accurately. The frequency/magnitude analysis and calculation of recurrence intervals for future scenarios must therefore be used with caution, knowing that the extreme events may be underestimated. However, the objective here is not to predict future discharge values corresponding to a given recurrence interval, but rather to investigate the relative contributions to sediment transport of events of different recurrence intervals.

5.2.5 Effective and half-load discharge

Wolman and Miller [1960] noted that since transport rate tends to zero in the lowest flows, but flow frequency tends to zero at the highest transport rates, the product of transport rate and frequency must be greatest at some intermediate discharge which they termed the effective discharge. It is known that the estimated value of effective discharge depends on the choice of bin size (or discharge intervals for which the daily sediment transport volumes are summed) [Crowder and Knapp, 2005]. The effective discharge was calculated for about 25 class intervals of discharge, following Crowder and Knapp [2005]. The chosen class intervals have a size of 30, 50 and 70 m^3/s for the Batiscan, Richelieu and Saint-François rivers, respectively, although our tests using various bin sizes did not reveal marked differences. Nevertheless, the effective discharge metric has been criticized as it does not clearly document which discharges are responsible for carrying the bulk of the long-term load [Vogel *et al.*, 2003; Doyle and Shields, 2008]. Hence, an alternative approach using the half-load discharge is also used. This is defined as the discharge value above and below which 50% of the total load is transported [Wolman and Miller, 1960; Vogel *et al.*, 2003].

Recurrence interval	1	2	5	10	20	50	Q_{MAM}
Batiscan	315	587	741	841	936	1059	465
Richelieu	538	1025	1246	1375	1488	1623	1095
Saint-François	661	1360	1755	2012	2255	2567	1277

Table 5.1: Discharge (m^3/s) associated with recurrence intervals of 1, 2, 5, 10, 20 and 50 years for the three tributaries, based on the present-day (1932–2004) records at gauging stations in the downstream part of the tributaries. Q_{MAM} is the mean annual maximum discharge for each series.

5.3 Results

5.3.1 Hydrology

Discharges corresponding to present-day recurrence intervals of 1, 2, 5, 10, 20 and 50 years for the three tributaries are presented in Table 5.1. The mean annual maximum discharge for the RefQ-scenario (1961–1990) in each tributary is close to the 2-year recurrence interval. When comparing each recurrence interval to the present-day 2-year recurrence interval, the tendency for high discharge events (long recurrence intervals) to become more frequent is very obvious, particularly for the Richelieu River (Figure 5.1). For the Batiscan and Saint-François rivers, this trend is less marked, but it is visible for the 50-year recurrence interval, with the exception of the ECHAM4 scenario (Figure 5.1a,c).

The change in mean annual maximum discharge for the three GCMs does not show a consistent trend for all the tributaries and is markedly different from the change in mean daily discharge, with larger variation for the mean annual maximum discharge (-21% to +44%) compared to daily discharges (-10% to +14%) (Table 5.2). However, in most cases (with two exceptions), the direction of change (either increasing or decreasing) remains the same for the two types of discharge. The changes in mean annual maximum discharge are largest for the Richelieu River where it increases in all GCM-scenarios. The ECHAM4 model reduces the mean daily discharge for all tributaries, whereas the HadCM3 model results in the largest differences for both daily and mean annual maximum discharge (Table 5.2). For each GCM-scenario the direction of change in mean annual maximum discharge compared to the RefQ varies from year to year, as illustrated in Figure 5.2 for the Batiscan River. The CSIRO-Mk2 and HadCM3 models generally predict higher floods than ECHAM4. For all tributaries, the timing of flood events also changes for all GCMs, with an expected spring flood in advance by 22 to 34 days by the last horizon (2070–2099) [Boyer *et al.*, in press].

	CSIRO-Mk2		ECHAM4		HadCM3		mean	
	Q_{daily}	Q_{MAM}	Q_{daily}	Q_{MAM}	Q_{daily}	Q_{MAM}	Q_{daily}	Q_{MAM}
Batiscan	6%	8%	-7%	-9%	10%	19%	3%	6%
Richelieu	6%	36%	-9%	5%	14%	44%	4%	28%
Saint-François	4%	-8%	-10%	-21%	9%	6%	1%	-8%
mean	5%	12%	-9%	-8%	11%	23%		

Table 5.2: Percentage of change in mean daily discharge (Q_{daily}) and mean annual maximum discharge (Q_{MAM}) for the period 2010–2099 compared to the RefQ-scenario for three GCMs in each tributary.

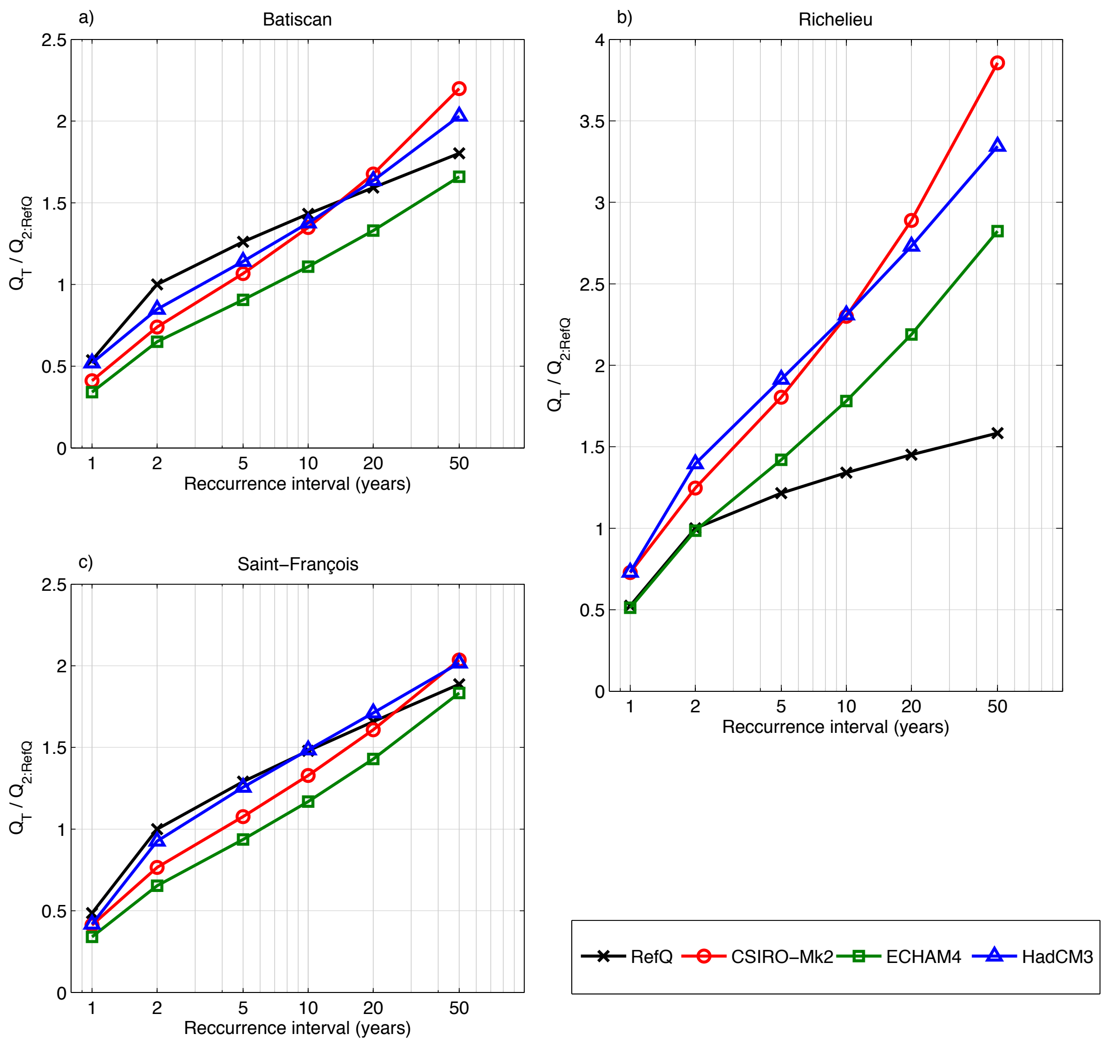

Figure 5.1: Dimensionless flood frequency plots expressed as discharge of a given recurrence interval divided by discharge of a 2-year recurrence interval in the reference scenario (RefQ), against recurrence interval for a) the Batiscan River; b) the Richelieu River; and c) the Saint-François River.

5.3.2 Sediment transport

5.3.2.1 Magnitude-frequency analysis

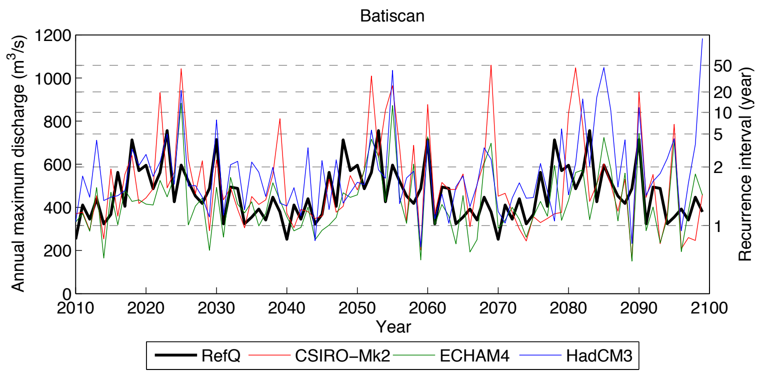

Figure 5.2: Annual maximum discharge over the simulated period (2010–2099) for the RefQ and GCM-scenarios for the Batiscan River. Dashed lines refer to the different discharges associated with recurrence interval of 1, 2, 5, 10, 20 and 50, based on the 1932–2004 records at the Batiscan gauging station.

The impact of GCM scenarios on effective discharge is examined in Figure 5.3. All three tributaries have a bimodal distribution in the RefQ-scenario, which implies that both high- and low-frequency events could be important for maintaining the channel. The effective discharge is around the 2-year (present-day) recurrence discharge for the Richelieu and Saint-François rivers (Figure 5.3b,c) and around the 5-year (present-day) recurrence interval for the Batiscan River (Figure 5.3a). The transported volume varies for the three horizons, with an increase for the Batiscan River, a slight decrease in the Richelieu River and a decrease in the Saint-François River. For the GCM scenarios, the effective discharge increases by several size classes to discharges with present-day recurrence intervals of more than 50 years, with a clear shift towards higher discharge from the first to the last horizon (2070–2099). For all tributaries, the CSIRO-Mk2 and HadCM3 models have similar effective discharges in the low-frequent discharge range. For the ECHAM4 model in the Batiscan River (Figure 5.3g), the effective discharge decreases over time and becomes smaller than the RefQ scenario in the last horizon.

Half-load discharges also increase for all the GCM scenarios over the 2010–2099 period, although less so for the ECHAM4 model (Table 5.3). The half-load discharge for each horizon remains fairly constant within the RefQ scenario, in a similar way to the effective discharge. For GCM scenarios, the overall trend is an increase compared to the RefQ as well as an increase towards the last horizon (Table 5.3). The CSIRO-Mk2 produces the largest increase (33% on average for the three rivers for the entire period), followed by HadCM3

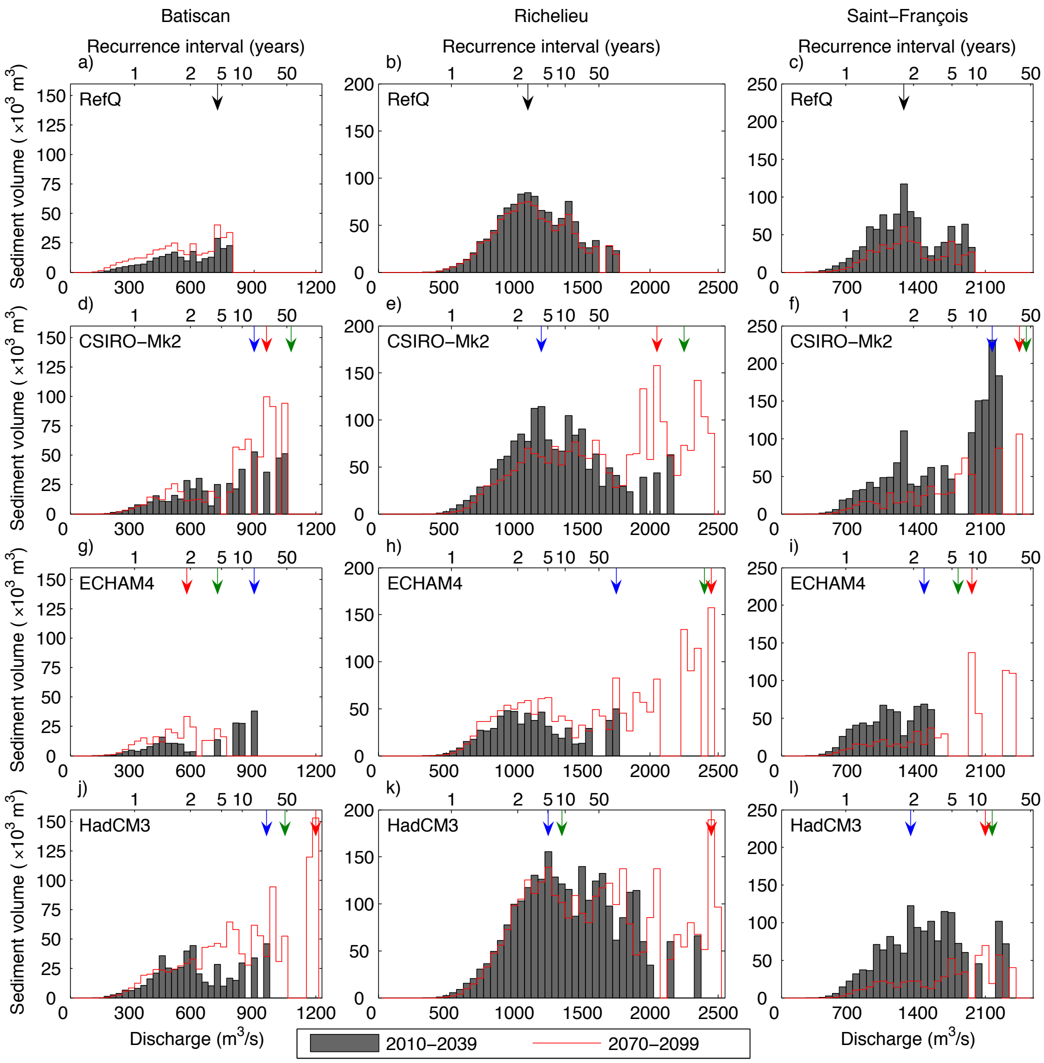

Figure 5.3: Bed-material sediment transport discharge histograms at the downstream boundary for the first (2010–2039) and last (2070–2099) horizons for the Batiscan River (a,d,g,j); Richelieu River (b,e,h,k); and Saint-François River (c,f,i,l) for the RefQ (a,b,c); CSIRO-Mk2 (d,e,f); ECHAM4 (g,h,i); and HadCM3 (j,k,l) models. The arrows indicate the effective discharge for each horizon (black: RefQ, blue: first horizon, green: second horizon and red: third horizon). The upper x-axis represents the present-day recurrence intervals from the 1932–2004 records.

	horizon	RefQ	CSIRO-Mk2	ECHAM4	HadCM3
Batiscan	2010–39	522	623	470	551
	2040–69	506	750	603	567
	2070–99	500	760	516	721
	2010–99	509	717	538	621
Richelieu	2010–39	1112	1233	1052	1370
	2040–69	1102	1353	1175	1293
	2070–99	1093	2022	1366	1711
	2010–99	1102	1516	1203	1464
Saint-François	2010–39	1210	1362	1076	1416
	2040–69	1226	1516	1329	1400
	2070–99	1251	1620	1906	1745
	2010–99	1225	1463	1279	1469

Table 5.3: Half-load discharge (m^3/s) for each discharge scenario for each horizon and for the entire simulated period. Half-load discharge is defined as the value above and below which 50% of the total load is transported.

(25%) and ECHAM4 (6%). Note that changes in half-load discharges exhibit markedly less variability than the effective discharge changes (Figure 5.3).

Bed-material transport rate has a higher variation than water discharge, mainly because of the non-linear character of sediment transport. The change in bed-material volume transported over the whole simulation period (2010–2099) is presented in Figure 5.4. The total bed-material transport increases the most for the HadCM3-scenario, with values 209%, 286% and 134% of the volume in the RefQ-scenario for the Batiscan, Richelieu and Saint-François rivers, respectively. The CSIRO-Mk2 model also results in increased transport, whereas ECHAM4 simulations are usually close to, or slightly less than, the RefQ (Figure 5.4). In the two cases where the changes in mean daily and annual maximum discharge are opposite to each other (Richelieu River, ECHAM4, and Saint-François River, CSIRO-Mk2, Table 5.2), the total bed-material transport remains close to the RefQ-scenario.

In Figure 5.4, sediment volume is split in recurrence interval ranges. For example, bed-material transported during floods with a maximum discharge falling between recurrence intervals of 2 to 5 years were grouped together (green in Figure 5.4). The present-day recurrence intervals are used for the RefQ scenarios of each tributary, whereas the future recurrence intervals are used for the three GCM scenarios. In the RefQ scenario, discharges with a recurrence interval of 2 years or less transport about 50% of the sediments in the Batiscan and Saint-François rivers. In all GCM scenarios, this proportion is reduced for the Batiscan and Saint-François rivers, but it increases for the Richelieu River except for the ECHAM4 sce-

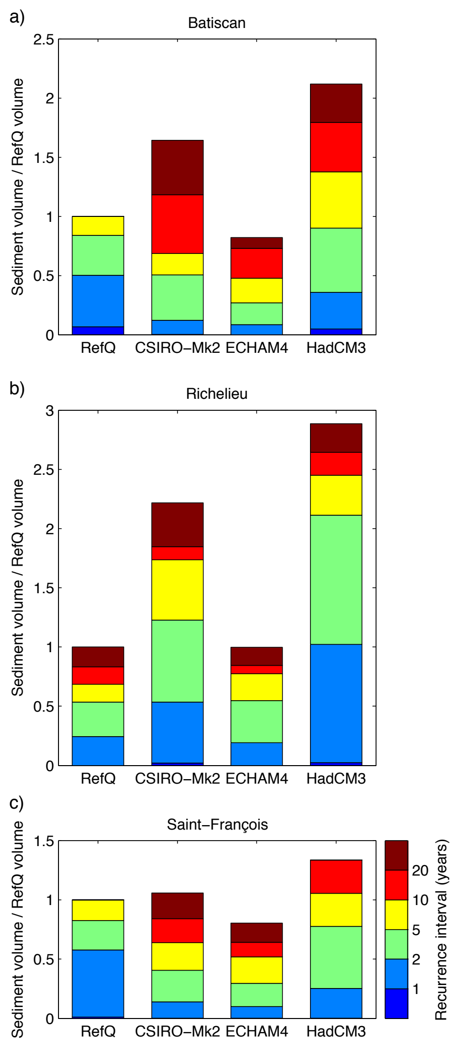

Figure 5.4: Sediment transport volume as a fraction of the total volume transported with the RefQ-scenario for the a) Batiscan River; b) Richelieu River; and c) Saint-François River. Sediment volumes associated with events where the maximum discharge is within the same range of recurrence intervals within the scenario are grouped together. For the RefQ-scenario, the present-day (1932–2004) are used, whereas the future recurrence intervals (2010–2099) are used for each GCM.

nario (Figure 5.4). However, with the CSIRO-Mk2 and HadCM3 scenarios, the total volume of transported sediment increases, thus the proportion of transport associated with discharges of 2-year or less recurrence interval is less (17% on average for all tributaries, with a range from 7 to 35%). In the Richelieu River, discharges with recurrence intervals of 5 years or less contribute to 50% of the total sediment volume transported in the RefQ-scenario. This volume, as well as volumes associated with larger recurrence intervals, remains similar in all GCMs in the Richelieu River (Figure 5.4b). However, in the Batiscan and Saint-François rivers, there is a marked tendency for extreme events (with long future recurrence intervals) to be responsible for a larger proportion of the volume of transported sediments under all GCM scenarios (Figure 5.4a,c). For example, the five largest sediment transport events in the CSIRO-Mk2 transport 36% of the total volume in the Batiscan River, and 29% of the total volume in the Saint-François River. In the RefQ scenario, the five largest events transported only 24 and 13% of the total volume in the Batiscan and Saint-François rivers, respectively.

The threshold discharge for sediment transport in the Richelieu River is estimated at 450 m^3/s. The mean discharge for the RefQ scenario in this river is 437 m^3/s, and is thus very close (97%) to this threshold. The Batiscan and Saint-François rivers have estimated threshold values of approximately 150 and 330 m^3/s, respectively, with mean discharges of 97 and 196 m^3/s for the RefQ scenarios, which correspond to 65% and 60% of the threshold discharge, respectively. The Richelieu River is the only tributary where in the future scenarios the mean discharge exceeds the threshold value for sediment transport, which partly explains why the increase in sediment volume is higher in this river (Figure 5.4b).

5.3.2.2 Event analysis

When events of specific recurrence intervals are examined more closely, the variability of sediment transport volume becomes apparent (Figure 5.5). In Figure 5.5, all flood events (i.e. from RefQ and GCMs simulations) are combined together since no difference in trend was observed between them. In other words, an event with a maximum discharge of, say, 500 m^3/s in the RefQ time series for a given river should result on average in the same volume of bed-material transport as a 500 m^3/s event size in the GCM time series. The variability in sediment transport per event is particularly large for frequent events that occur more than once every 2 years, which is likely due to the large range of event duration for these discharges (Figure 5.5). Floods with a recurrence interval of 2 years generally transport more than the

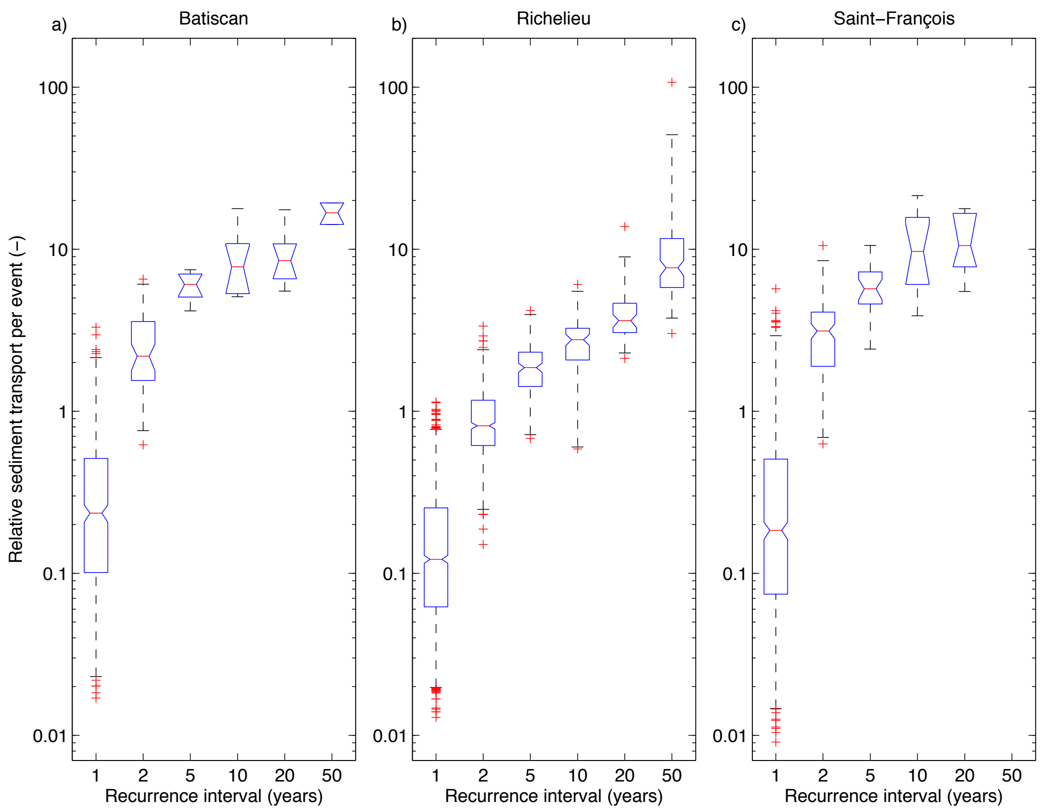

Figure 5.5: Boxplots of the relative sediment transport volume per event grouped by present-day recurrence interval of their maximum discharge for: a) Batiscan River; b) Richelieu River; and c) Saint-François River. Whiskers (–) represent the 1% and 99% percentile and symbols (+) represent outliers. Relative sediment transport volume per event is the volume of each individual event divided by the average volume per event for all events in the river concerned. All simulated maximum discharges (i.e. RefQ and GCMs) are combined in this figure.

mean volume per event and their variability is much less than that of the lower magnitude events. The 2-year events are also less sensitive to the duration as the volume of transport mainly depends on the maximum discharge that largely exceeds the threshold of sediment transport.

The effect of flood peak and duration on bed-material transport volume is further investigated in Figures 5.6, 5.7 and 5.8 for the reference and GCM scenarios. Individual events are plotted in these diagrams as circles of area proportional to the bed-material volume. Vertical dashed lines indicate the half-load discharge over the 2010–2099 period in the RefQ-scenario, which is used to separate 'small' and 'large' events. Note that because the total sediment volume transported for a given event is plotted for the maximum discharge of the event (i.e. it is not plotting daily sediment volume against the associated daily discharge value), the proportion of large events (on the right side of the vertical dashed line in Figures 5.6 to 5.8) is larger than 50% by definition. The median duration of sediment transport events in the RefQ scenario was used as a threshold to separate short from long events.

As expected, there are more small magnitude, short duration events – falling in the lower-left zone in Figures 5.6 to 5.8) – for all tributaries and GCMs. For the Batiscan and Saint-François rivers (Figures 5.6 and 5.8), the relative contribution of short events (below the horizontal dashed line) increases from about 30% in the RefQ scenario to about 50% for all the GCMs, whereas for the Richelieu River (Figure 5.7) the relative contribution remains similar to RefQ (45%) for the CSRIO-Mk2 and HadCM3 scenarios and increases to 56% for the ECHAM4 scenario. The large events for all the tributaries (right of the vertical dashed line) contribute to more sediment volume in all cases, except for the Saint-François River in the ECHAM4 scenario where it remains the same (69%). In general, the relative contribution of large events for the CSIRO-Mk2 and HadCM3 scenarios (77–88%) is similar for all the tributaries, and the ECHAM4 model (68–72%) lies between the RefQ (64–69%) and the other two GCMs.

For the RefQ scenario, the sediment transport during winter is mostly associated with events with small maximum discharge in the Richelieu and Saint-François rivers (no winter events occurred in the RefQ scenario for the Batiscan River - Figure 5.6). In all tributaries and under all GCM scenarios, both the frequency and magnitude of winter events increase. The spring events remain more spread out than the winter events, with both short and long duration and small and large maximum discharge, although for the Richelieu River the winter

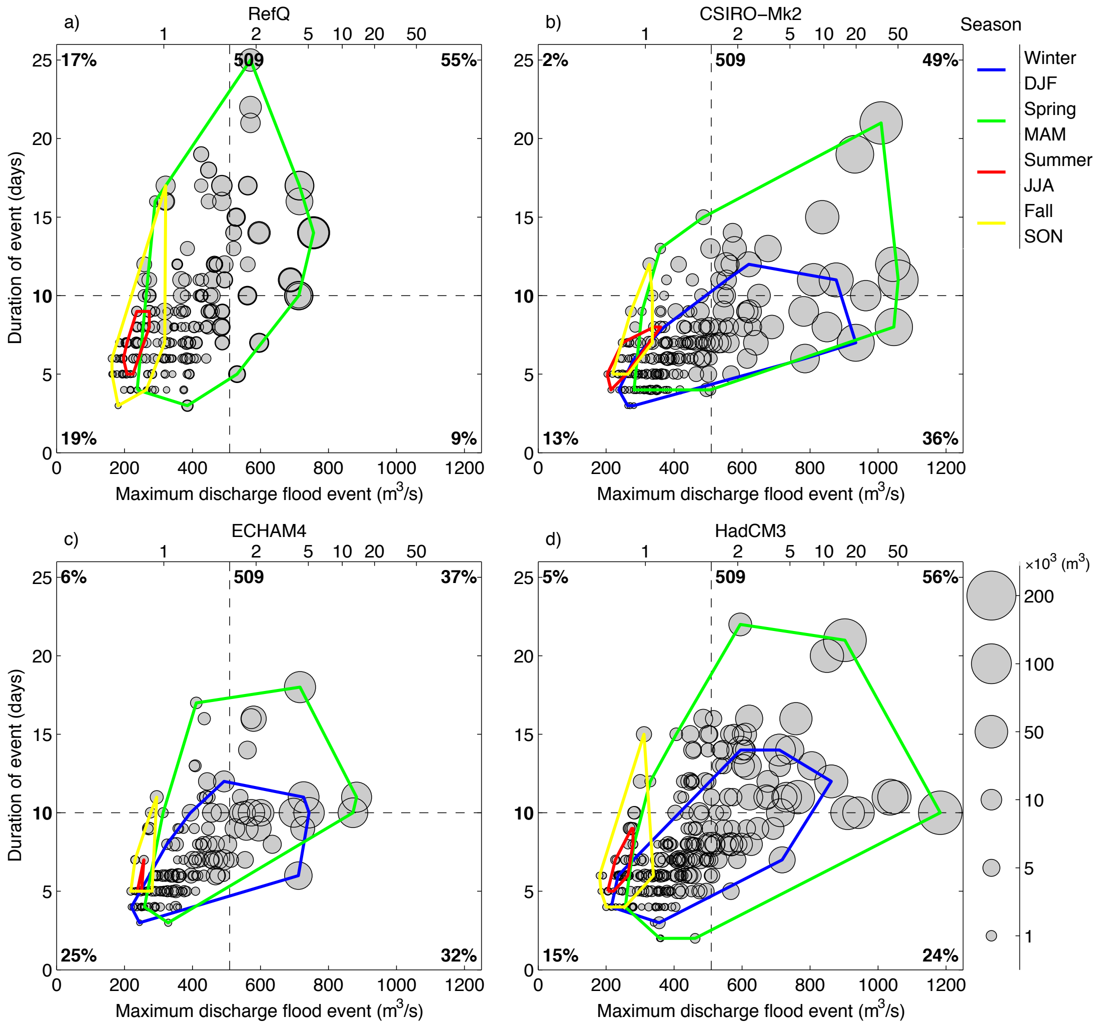

Figure 5.6: Duration/magnitude diagram of sediment transport event duration against maximum discharge for the Batiscan River. Circles are proportional to the volume of sediment transported during the event. The vertical dashed line indicates the half-load discharge for the RefQ scenario for the 2010–2099 period (509 m^3/s). The horizontal dashed line represents the median value of sediment transport event duration (i.e. 50% of the transport events are shorter than this value) in the RefQ scenario (d = 10 days). The percentage in each quadrant gives the contribution to the total sediment transport of short/long and small/large events. The upper x-axis represents the present-day recurrence intervals. The continuous coloured lines indicate 'envelopes' of events occurring within each season. a) RefQ; b) CSIRO-Mk2; c) ECHAM4; d) HadCM3.

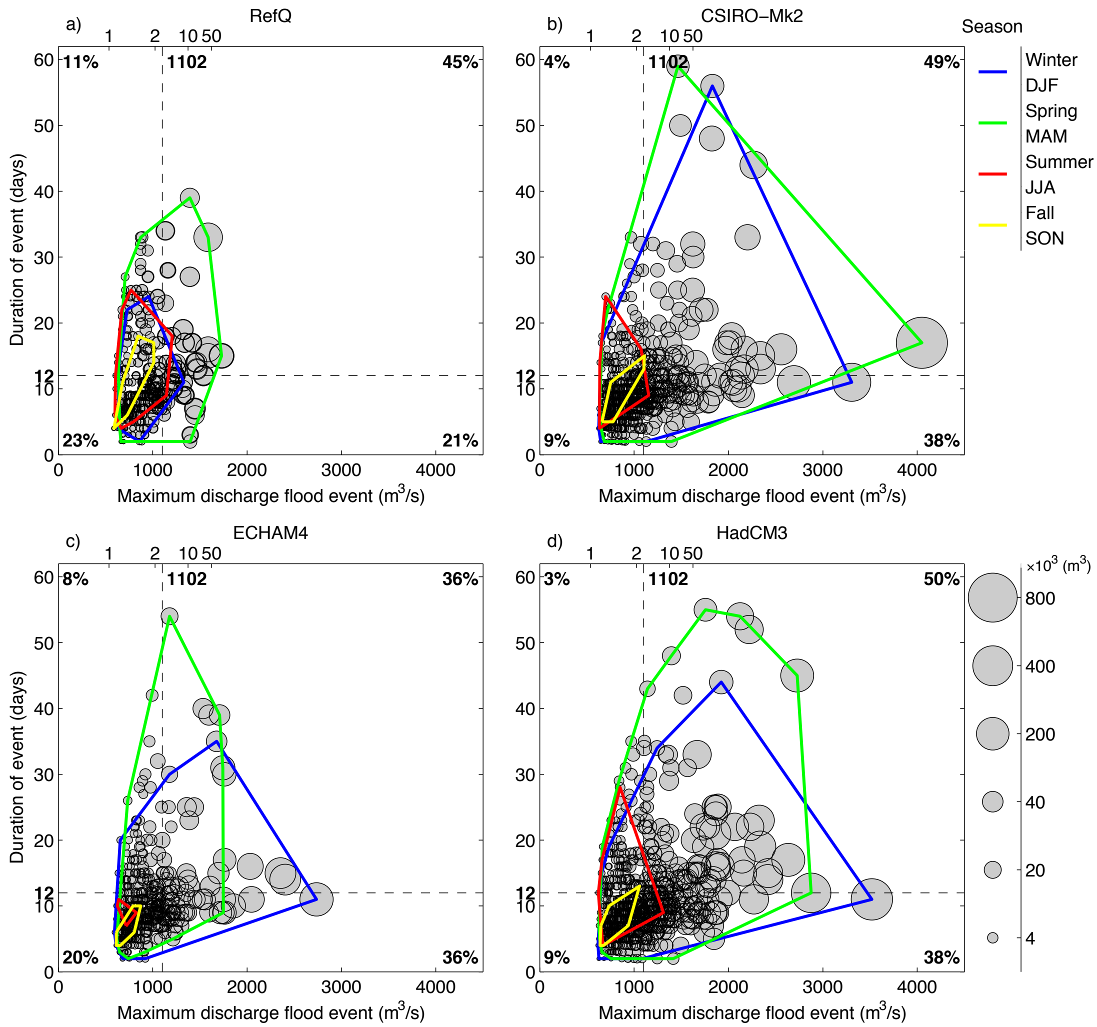

Figure 5.7: Duration/magnitude diagram of sediment transport event duration against maximum discharge for the Richelieu River. Circles are proportional to the volume of sediment transported during the event. The vertical dashed line indicates the half-load discharge for the RefQ scenario for the 2010–2099 period (1102 m^3/s). The horizontal dashed line represents the median value of sediment transport event duration (i.e. 50% of the transport events are shorter than this value) in the RefQ scenario (d = 12 days). The percentage in each quadrant give the contribution to the total sediment transport of short/long and small/large events. The upper x-axis represents the present-day recurrence intervals. The continuous coloured lines indicate 'envelopes' of events occurring within each season. a) RefQ; b) CSIRO-Mk2; c) ECHAM4; d) HadCM3.

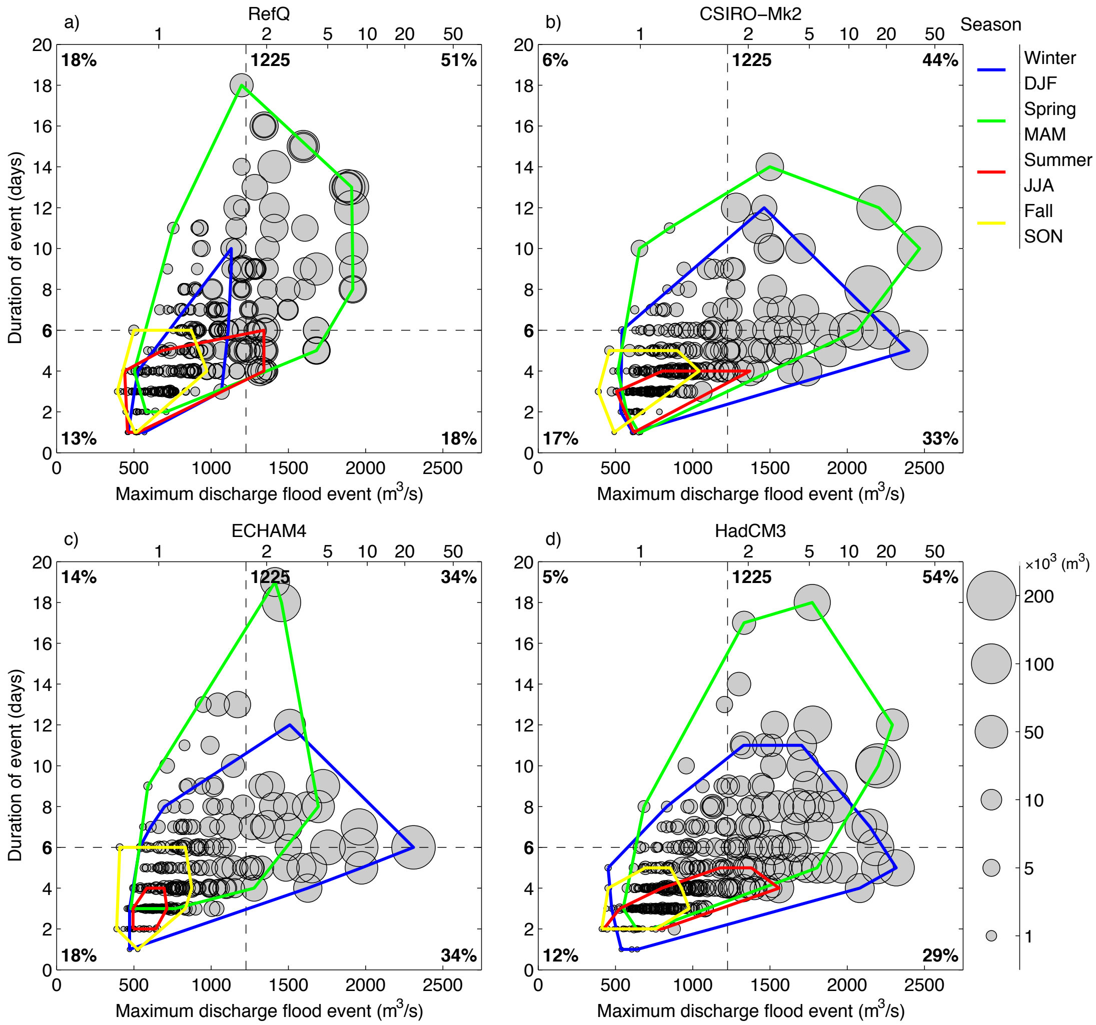

Figure 5.8: Duration/magnitude diagram of sediment transport event duration against maximum discharge for the Saint-François River. Circles are proportional to the volume of sediment transported during the event. The vertical dashed line indicates the half-load discharge for the RefQ scenario for the 2010–2099 period (1225 m^3/s). The horizontal dashed line represents the median value of sediment transport event duration (i.e. 50% of the transport events are shorter than this value) in the RefQ scenario (d = 6 days). The percentage in each quadrant give the contribution to the total sediment transport of short/long and small/large events. The upper x-axis represents the present-day recurrence intervals. The continuous coloured lines indicate 'envelopes' of events occurring within each season. a) RefQ; b) CSIRO-Mk2; c) ECHAM4; d) HadCM3.

and spring events become similar. The events that occur in summer and fall remain similar to the RefQ in terms of duration and maximum discharge for all the tributaries and GCM scenarios.

More sediment transport events occur in the Richelieu River than in the other tributaries. The Richelieu River has a total sediment transport duration ranging from 18% to 28% of the simulated period, whereas in the Batiscan and Saint-François rivers the total sediment transport duration ranges from only 3% to 7%. The Richelieu River also has sediment transport events with a longer median duration (12 days compared to 10 and 6 days for the Batiscan and Saint-François rivers, respectively).

5.4 Discussion

Our study shows that climate-induced changes in discharge in the 21^{st} century are very likely to affect the magnitude and timing of floods in the three studied Saint-Lawrence River tributaries. There is some variability between the three GCM scenarios [which is to be expected since they were specifically chosen to represent a wide range of precipitation and temperature outputs – Chaumont and Chartier, 2005; Boyer *et al.*, in press] but simulations show consistent trends between GCMs and between rivers, with low frequency events becoming more frequent. The largest change in bed material transport can be expected from GCMs that predict the largest change in precipitation. Similar findings in terms of recurrence intervals were found for fall and summer simulations of the Châteauguay River, another tributary of the Saint-Lawrence River [Roy *et al.*, 2001]. However, recurrence intervals can be misleading because they are determined from the peak magnitude of flow and they do not take into account the magnitude and duration of out-of-bank flow [Lane *et al.*, 2007]. In this study, the reliability of the determination of recurrence intervals is also limited by the fact that simulations for the 21^{st} century are based on a 30-year reference period (1961–1990), the same reference period for each of the three horizons and thus any rare events in the reference period could occurw 3 times within the near-future simulation. Furthermore, the perturbation method is known to generate over-prediction of rare events [Lenderink *et al.*, 2007] so a precise analysis of shifts in effective discharge should not be attempted. However, the qualitative trend corresponds well to findings from other studies [e.g. Andrews, 1980; Nash, 1994; Emmett and Wolman, 2001]. To add to this complexity, a clear relationship between discharge and sediment transport cannot be defined [Reid *et al.*, 2007a,b; Coulthard *et al.*, 2008], as highlighted in this study by the large variability in Figure 5.5.

The effective discharge is predicted to increase in all GCM and tributaries, except for the Batiscan River in the ECHAM4 scenario (Figure 5.3). Grain size, flow variability and basin size are considered to be the most important factors influencing effective discharge recurrence interval [Wolman and Miller, 1960; Andrews, 1980; Knighton, 1998; Doyle *et al.*, 2007]. Here the grain size remains about the same and obviously basin size is constant. The shift in effective discharge, towards low-frequency floods, is thus solely a result of increased flow variability. The use of effective discharge has been a topic of debate since it was first introduced by Wolman and Miller [1960], and a lot of uncertainty remains around its calculation [Ashmore and Day, 1988; Lenzi *et al.*, 2006; Doyle and Shields, 2008]. For the three rivers studied here, the effective discharge in the RefQ scenario corresponds to a 2–5 year recurrence interval, which is larger than the 1–2 year value reported in Wolman and Miller [1960], but conforms to observations of Doyle *et al.* [2007] for lowland sand-bed rivers. One of the consequences of climate change modifications to discharge in these rivers is a transition from a relatively simple distribution of effective discharge histograms (Figure 5.3a-c), to a much more complex form of effective discharge histograms with multiple peaks (Figure 5.3d-l). This may also be the case in other rivers, particularly where there is a predicted shift in spring flood discharge. This could indicate a channel maintaining role of near-bankfull flows with recurrence intervals of 2–5 years, with extreme rare events mainly affecting channel bank erosion [Phillips, 2002].

Half-load discharges [Vogel *et al.*, 2003] show similar trends to the effective discharge for the RefQ scenario (Table 5.3 and Figure 5.3), with an overall increase in the 21^{st} century. However, half-load discharge trends for the GCM scenarios are much more consistent than those in the effective discharge. Because the half-load discharge is not dependent on the parameters such as bin size, it provides a more robust indicator of change in morphological behaviour than the effective discharge, and it is also simpler to calculate. However, according to Vogel *et al.* [2003], the half-load discharge for total load corresponds to a relatively rare event compared to the effective discharge of Wolman and Miller [1960], whereas for the lowland rivers studied here, half-load discharges for bed-material in the RefQ scenario correspond to recurrence intervals of about 2 years. The half-load discharge is lower than the effective discharge for the Batiscan and Saint-François rivers, and approximately the same for the Richelieu River.

The increase in frequency and magnitude of winter events results in higher transport rates since for the same discharge, the water surface slope for high magnitude events in the tributaries will be markedly higher in the winter compared to the spring when the Saint-Lawrence River, with highly regulated water levels [Fagherazzi *et al.*, 2005], will reach its maximum level [Boyer *et al.*, 2009]. Because the slopes of the tributaries are very low (3 to 6×10^{-5}), the impact of base level is significant, unlike in small upstream systems with much steeper slopes. The seasonal effect will be enhanced under all GCM scenarios as longer duration, higher magnitude winter events are predicted for all tributaries (Figures 5.6, 5.7 and 5.8). This will be further exacerbated by the predicted 20% decrease in discharge of the Saint-Lawrence River, resulting in a 0.5 to 1 m decrease in it water level, during the 21^{st} century [Croley, 2003]. This effect has been tested using two base-level decrease scenarios in the Saint-Lawrence River (see details in Verhaar *et al.* [in press]). The same winter discharge events when the Saint-Lawrence level was between 0.5 and 1 m lower than their current values resulted in average increases in sediment transport of 40% for the Richelieu and Saint-François rivers and 116% for the Batiscan River.

It is commonly assumed that if climate change leads to a more frequent occurrence of high magnitude, long duration flood events there will be an increased risk of overbank flooding. However, peak-flow magnitude is not the only control on flood risk, as changes in channel geometry, in particular in systems undergoing long-term aggradation, also need to be considered [Lane *et al.*, 2007, 2008]. Our morphodynamic simulations suggest that the Batiscan River is undergoing slight aggradation under the present hydrological regime, the Saint-François River is degrading slightly, and the Richelieu River is almost in equilibrium [Verhaar *et al.*, in press]. However, under all climate-change scenarios increased bed erosion is predicted. This results in reduced aggradation with some erosion in the downstream reaches for the Batiscan River, a switch from equilibrium to a degradational state for the Richelieu River, and increased degradation in the Saint-François River [Verhaar *et al.*, in press]. Thus, the increase in flood risk due to more frequent extreme events is in part compensated by incision of the bed in the three studied tributaries. Higher flood levels which occur more often are predicted for all GCMs and all three tributaries (Figure 5.9). This shows that although lower bed elevation decreases flood risk, the increased frequency of rare events outweighs this effect and the likelihood of observing floods in the range of 1 to 1.25 m above the bankfull level is increased, particularly with the CSIRO-Mk2 model. Note that this increased flood risk is also present for all simulations with a steady fall (0.01 m/yr) in the downstream water levels of the Saint-Lawrence River, with the exception of the ECHAM4 model in the Saint-François River.

Because of the scarce availability of long-term series of sediment transport data to investigate the geomorphic impacts of magnitude-frequency of large floods versus more frequent events, a sediment modelling approach such as that used in this study provides an additional method for validating and comparing the role of different discharges within rivers [Shields *et al*., 2003]. However, ideally, a more sophisticated 2D modelling approach which could simulate bank erosion would be required to assess the role of extreme events on bank erosion and sediment supply. In the Batiscan and Richelieu rivers, banks are stable, but high lateral migration rates were observed in the Saint-François River which cannot be adequately modelled in a 1D approach.

5.5 Conclusion

Morphodynamic simulations for the 21st century based on three GCM scenarios for three tributaries of the Saint-Lawrence River indicate that climate-induced changes in discharge will markedly increase the low-frequency, high-magnitude events which will have a very important impact on both bed-material transport and flood risk. Although mean daily discharge does not alter much in GCM scenarios, there is an increase in flow variability and this results in higher effective and half-load discharges under future scenarios. Very large volumes of sediments are transported by fewer, extreme flood events in most simulations compared to a reference scenario where events of recurrence interval 5 years or less transported most of the sediment. The change in the timing of these events, with much more frequent long duration, high magnitude floods in the winter, will also have a major impact as these events occur during low flow in the Saint-Lawrence River, leading to a greater water surface slope in the tributaries and thus higher transport capacity.

Although the three GCMs predict an increase in large magnitude events, there remains a large variability between these scenarios, with ECHAM4 (dry/warm prediction) resulting in the smallest impact in terms of sediment transport and flood risk, and HadCM3 (largest change in precipitation) having the largest impact on these variables. Future research on

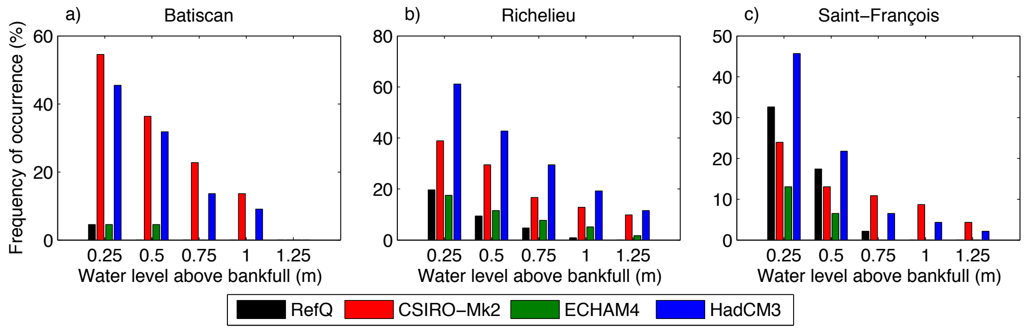

Figure 5.9: Frequency of the number of occurrences per year of five water surface elevations above bankfull level at the upstream boundary for: a) Batiscan River; b) Richelieu River; and c) Saint-François River. Frequency of occurrence is expressed as a percentage of the number of occurrences per year (e.g. 20% is once in 5 years). The bankfull water surface elevations (calculated based on a 2-year recurrence interval) for the Batiscan, Richelieu and Saint-François rivers are 6.47 m, 6.59 m and 7.55 m, respectively.

climate-induced morphodynamic changes in rivers should thus continue to use more than one GCM scenario, unless or until GCM refinement leads to a convergence of climate predictions. Furthermore, there is a need to develop further 2D modelling tools that could run long-term unsteady simulations of bed-material transport and incorporate the impacts of bank erosion on channel evolution.

CHAPTER 6

LIMITS OF 1D NUMERICAL MODELLING: THE NEED TO DEVELOP A 2D APPROACH

Although previous chapters have revealed that plausible results are obtained from SEDROUT4-M, some limitations with the 1D approach have been highlighted by our analysis. The code of SEDROUT4-M can be found in Appendix III and the structure of input-files is given in Appendix IV with the Saint-François River as an example. Some of these limitations may be due to the software itself (i.e. another 1D model may have performed better, that can deal with unsteady flow for example), but some may only be possible to solve through a 2D approach. The first part of this chapter analyses in more detail specific problems that have occurred in the 1D simulations of the Yamachiche, Saint-Maurice and Saint-François rivers (some of which have been briefly mentioned in chapter 4). In the second part of the chapter, adaptations to the 2D model H2D2 that are required to incorporate a bed material transport module are described. This is followed by a comparison between the 1D and 2D simulation results and a discussion on the potential of long-term 2D morphological simulations.

6.1 Complications in 1D modelling of the Saint-Lawrence tributaries

Initially five tributaries of the Saint-Lawrence River were selected. However, two rivers could not be validated: the Yamachiche and Saint-Maurice rivers [Verhaar *et al.*, in press, chapter 4]. The other three tributaries (Batiscan, Richelieu and Saint-François rivers) were

Tributary	Drainage basin (km^2)	Average discharge (m^3/s)	Width (m)	Energy slope (-)	Average depth (m)	Width-to-depth ratio (-)	Sinuosity (-)
Batiscan	4700	99	167	6×10^{-5}	2.72	61.4	1.51
Richelieu	23 720	346	198	5×10^{-5}	7.64	25.9	1.09
Saint-François	10 180	208	233	3×10^{-5}	4.43	52.6	1.20
Saint-Maurice	43 250	693	238	1×10^{-5}	5.65	42.1	1.25
Yamachiche	269	6	25	4.5×10^{-4}	1.50	13.3	1.75

Table 6.1: Characteristics of selected Saint-Lawrence tributaries.

relatively well simulated by SEDROUT4-M. However, the Saint-François River remained problematic due to the complex geometry around the permanent island which caused some of the simulations to crash before 2099 [Verhaar *et al.*, in press, chapter 4]. The problems faced in modelling each of these rivers are different and are therefore described and explained in separate sections.

6.1.1 Yamachiche River: critical flow

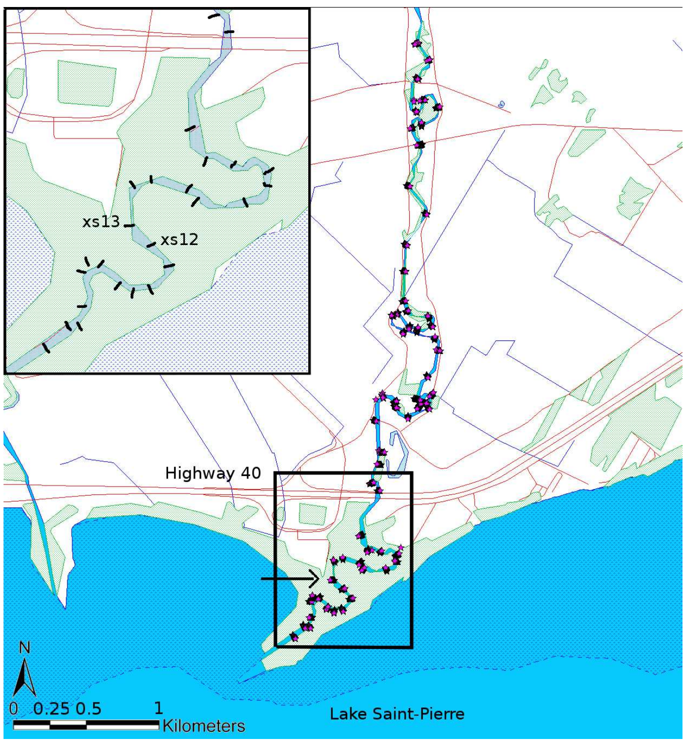

Figure 6.1: Map of cross section locations in the Yamachiche River. The arrow indicates the position of the hydraulic jump in the simulations.

The Yamachiche River is the smallest river selected for this project. It is one to two orders of magnitude smaller in basin size, discharge and water surface width than the other tributaries (Table 6.1). Also, compared to the other tributaries, the width-to-depth ratio of the Yamachiche River is markedly lower (Table 6.1). However, its energy slope is higher compared to the other tributaries, but still low in comparison to other rivers simulated using SEDROUT (0.5–2.2×10^{-2}) [Hoey and Ferguson, 1994; Ferguson *et al.*, 2001; Talbot and Lapointe, 2002]. Although the river is small, it contains large meanders and its sinuosity is high compared to three of the other tributaries (Table 6.1). The downstream end (0.5 km) is almost straight and the river was highly affected by construction of highway 40 (Figure 6.1). However, the sinuosity in a 1-km section downstream of highway 40 is fairly high (2.1). It remains smaller than the sinuosity of 2.5 in the upstream part of the Batiscan River and should therefore not cause a problem for 1D modelling. The most downstream meander of the Yamachiche River has a very stable position [Bondue *et al.*, 2006], although those further upstream within our study-reach are more mobile. This may be problematic in 1D modelling. On the other hand, a far more detailed topographical survey would be needed for 2D modelling of the Yamachiche River, which is practically not feasible as all topography points must be obtained from a total station by wading in this small tributary.

Variable or change	type of change	result
Manning *n*	increase to values of 0.075–0.2	jump occurs further upstream until a value of 0.2 when the upstream boundary is reached
Downstream water level	increased by 0.25 to 1.5 m	jump occurs further upstream
Discharge	increase from 5 up to 30 m^3/s	same effect as Manning *n* and water level
Extra cross section	placed a new cross section downstream of the hydraulic jump to reduce cross sectional distance	hydraulic jump occurred in the same location
Remove cross section	Removed the cross section where hydraulic jump occurred	hydraulic jump shifted to the upstream cross section
Top-down first estimate of water level	Changed the way SEDROUT is estimating the water level for the hydraulic computation	Critical flow still occurred

Table 6.2: Overview of attempts to solve the critical flow occurring in the Yamachiche model.

Compared to the other tributaries, the Yamachiche River has a long profile shape that comes closest to the theoretical concave shape (Figure 6.2, compared with Figure 4.2). However, simulations with a realistic discharge (4 m^3/s) and downstream water level (5 m), but relatively high roughness value ($n = 0.05$) caused supercritical flow to occur at 0.88 km from the mouth (arrow on Figure 6.1). An overview of the various attempts to deal with this problem is given in Table 6.2. All these attempts were unfruitful, although some gave better results in the sense that critical flow did not occur. However, these cases used unrealistic conditions (i.e. high downstream water level and discharge, high roughness value, etc.) and could clearly not be considered meaningful in any simulation of sediment transport rates. Increasing roughness, downstream water levels and/or discharge solved the problem of critical flow at 0.88 km from the mouth, but frequently the hydraulic jump problem occurred further upstream. Simulations with a high roughness value (Manning's $n > 0.1$) were successful, although this value is unrealistic as values of 0.024–0.075 would be expected in this river even if the presence of meanders as well as dunes under high flow conditions should contribute to higher roughness values [Chow, 1950].

It is difficult to understand why it is much more difficult to run sensible simulations for the Yamachiche River compared to the other tributaries. SEDROUT has previously been

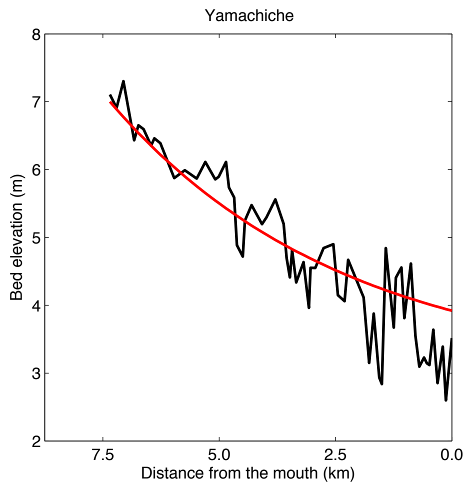

Figure 6.2: Measured longitudinal profiles of the Yamachiche (in black). Approximation of the theoretical profile in red.

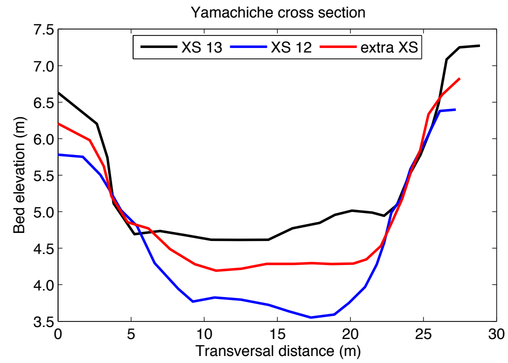

Figure 6.3: Cross sections in the Yamachiche River downstream (xs 12) and at the location of the hydraulic jump (xs 13) as well as the additional cross section that was used in an attempt to solve the hydraulic jump problem.

successfully used in rivers of a size similar to that of the Yamachiche River, for example the Allt-Dubhaig [Hoey and Ferguson, 1994] (Table 6.3). However, unlike the study of Hoey and Ferguson [1994], we have used original cross-sectional shape instead of idealized rectangular cross sections. Cross-sectional shapes are asymmetrical in the meanders, but they are not very complex and should therefore not cause the simulation to crash. The cross-sectional shapes around the point where the hydraulic jump occurs are nearly prismatic (Figure 6.3).

Bed topography measurements in this river were obtained by wading and measuring the profile with a total station instead of echo-sounding from a boat. The difficulty in obtaining topography data partly explains why the distance between cross sections relative to the channel width is six times larger than in other rivers (Table 6.3). SEDROUT uses the slope of the deepest points between cross sections as a first estimation of the water surface elevation at the upstream cross section. As can be seen in Figure 6.3, the cross section where the hydraulic jump occurs (xs13) has a fairly rectangular shape. Thus, the use of a different proxy for the energy slope, such as the mean depth instead of the maximum depth, would give a similar starting point for the hydraulic computation. Tests with an increased water elevation in the first iteration of the hydraulic computation also resulted in the simulation crashing at that same cross section.

The large cross-sectional distance relative to the width in combination with the non-uniform width of the cross sections is believed to be the reason of the occurrence of super-

River	Channel length (m)	Number of cross sections	Average distance (m)	Average width (m)	Distance width ratio (-)
Batiscan	17 174	79	217	167	1.30
Richelieu	15 168	99	153	198	0.77
Saint-François	15 017	72	208	233	0.90
Saint-Maurice	13 487	80	168	238	0.66
Yamachiche	7348	61	120	20	6.03
Allt Dubhaig* [Hoey and Ferguson, 1994]	2800	29	100	10	10.00
Vedder** [Ferguson *et al*., 2001]	8175	49	167	110	1.52
Sainte-Marguerite*** [Talbot and Lapointe, 2002]	12 000	60	200	45	4.44

Table 6.3: Distance between cross sections and the ratio of distance over the width. * used idealized cross-sectional shape and long-profile; ** used idealized cross-sectional shape with constant width; *** assumed prismatic cross sections

critical flow within the Yamachiche River simulations. Other studies conducted with SEDROUT used not only idealized cross-sectional shapes, but also a constant, relatively high, discharge instead of 'real' daily values. The use of real discharge values, which include low flow conditions, can become problematic in simulations of small rivers with large inter cross-sectional distances. However, the relation between cross-sectional distance, river width and energy slope for one-dimensional hydrological and morphological numerical modelling would need further investigation as it was not possible in this study to clearly isolate the cause of the crashing problem in the Yamachiche River.

6.1.2 Saint-Maurice River: discharge distribution in bifurcations

The model of the Saint-Maurice River contains three major channels with two major bifurcations (A and B Figure 6.5) over a short distance (1650 m). A small channel, not included in the model for reasons of simplicity – very little discharge flows through it and the geometry is already complex with two bifurcations – connects the eastern channel with the center channel (Figure 6.5). The convergence of water levels with two bifurcations was a challenge to incorporate in SEDROUT4-M and the details of the bifurcation coding are provided in Appendix III.

The simulated discharge distributions are 76–24% and 88–12% for the upstream (A) and downstream (B) bifurcations, respectively, whereas the measured distributions are 65–34% and 69–31% (Figure 6.5). The absence of the small channel could contribute to the fact that

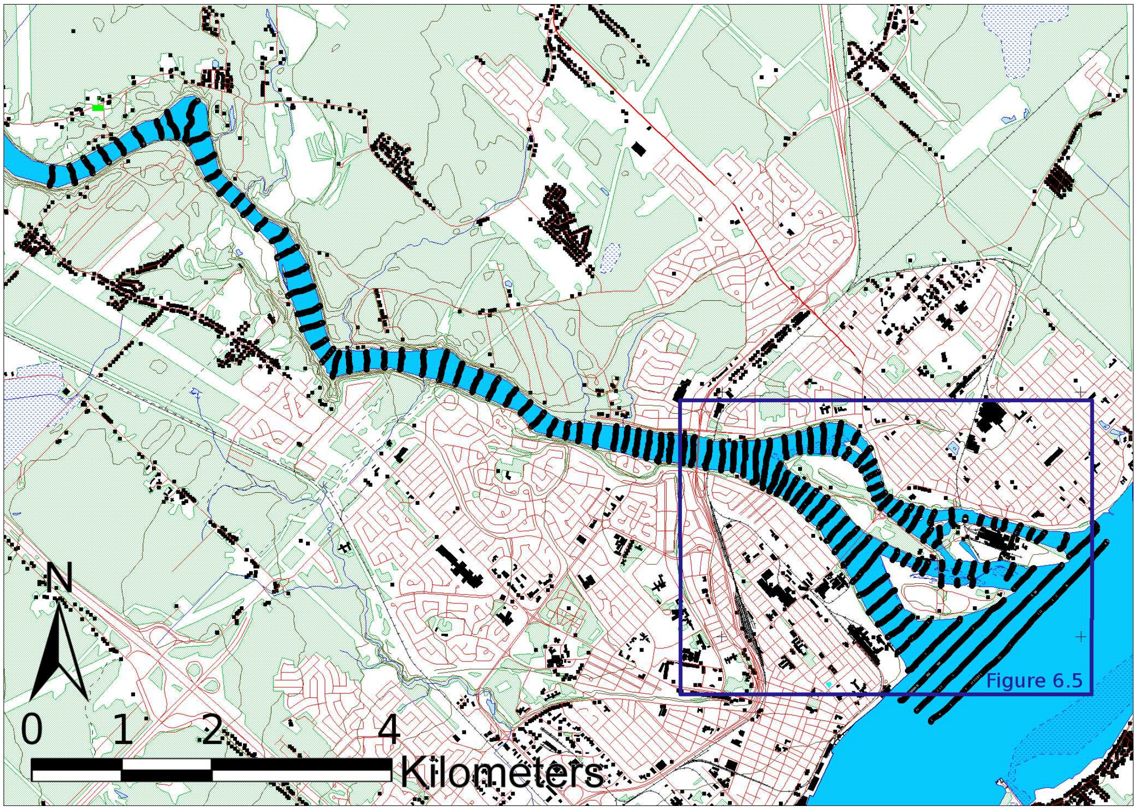

Figure 6.4: The Saint-Maurice River with the measured cross sections.

the eastern channel in the model is receiving less discharge than what was measured, but only about 2% of the total discharge flows through this small channel. To compensate for the absence of the small channel in the model, the cross sections in the eastern channel downstream of bifurcation C (Figure 6.5) were widened to increase their water transport capacity. However, even doubling the width of this part of the river did not result in the correct discharge distribution at the upstream bifurcation – the discharge distribution remained remarkably similar to what it was with the original topography. The most downstream cross section in the eastern channel is slightly further away from the confluence with the Saint-Lawrence River. Therefore, the distance in the model is relatively shorter, but this should lead to a slightly higher discharge in the eastern channel of the model, which is not what is observed.

Another attempt to obtain a more reasonable distribution of the discharge at the upstream bifurcation was to eliminate the center channel. This should have decreased the water transport capacity of the western channel and forced more of the discharge into the eastern channel. This attempt was also unsuccessful; the discharge distribution became closer to the measured values, but was still too far off to be acceptable. An option that was not tested would be to give the channels different roughness values. This option was not implemented for two reasons: first, there is no reason to believe that roughness in the two channels should be very different. Second, it would have required an adaptation of the model and a more complicated calibration/validation procedure which would also have required additional field data that were not available.

The measured distribution is biased by downstream water level changes and discharge fluctuations, as the cross sections of flow measurements were taken at different times. Nevertheless, this cannot account for the large difference observed (the eastern channel only receives 70% of what was measured), as the cross sections at the bifurcation were taken within half an hour from each other and the discharge of both channels added up to the discharge measured upstream of the bifurcation. The channel connecting the eastern and center channel only accounts for 5% of the discharge in the eastern channel (at most 2% of the distribution at the upstream bifurcation A), leaving a 28% variation unexplained.

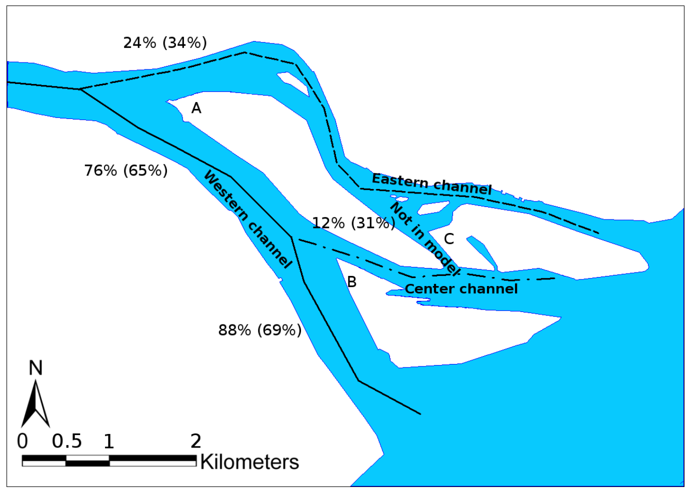

Figure 6.5: Complex geometry of the downstream confluence of the Saint-Maurice River with the Saint-Lawrence River. The black lines in the river indicate the thalweg of the reaches. Numbers give the proportional discharge split at the bifurcations as simulated with SEDROUT4-M with the ADCP measured split in brackets. Letters indicate two major bifurcations (A, B) and a smaller one (C).

A great deal of research on the sediment distribution at bifurcations in 1D models has focussed on determining an appropriate method to specify the ratio between the two downstream branches. However, the Saint-Maurice River example highlights that a good understanding of what determines the water discharge ratio is also a requirement when simulating natural rivers.

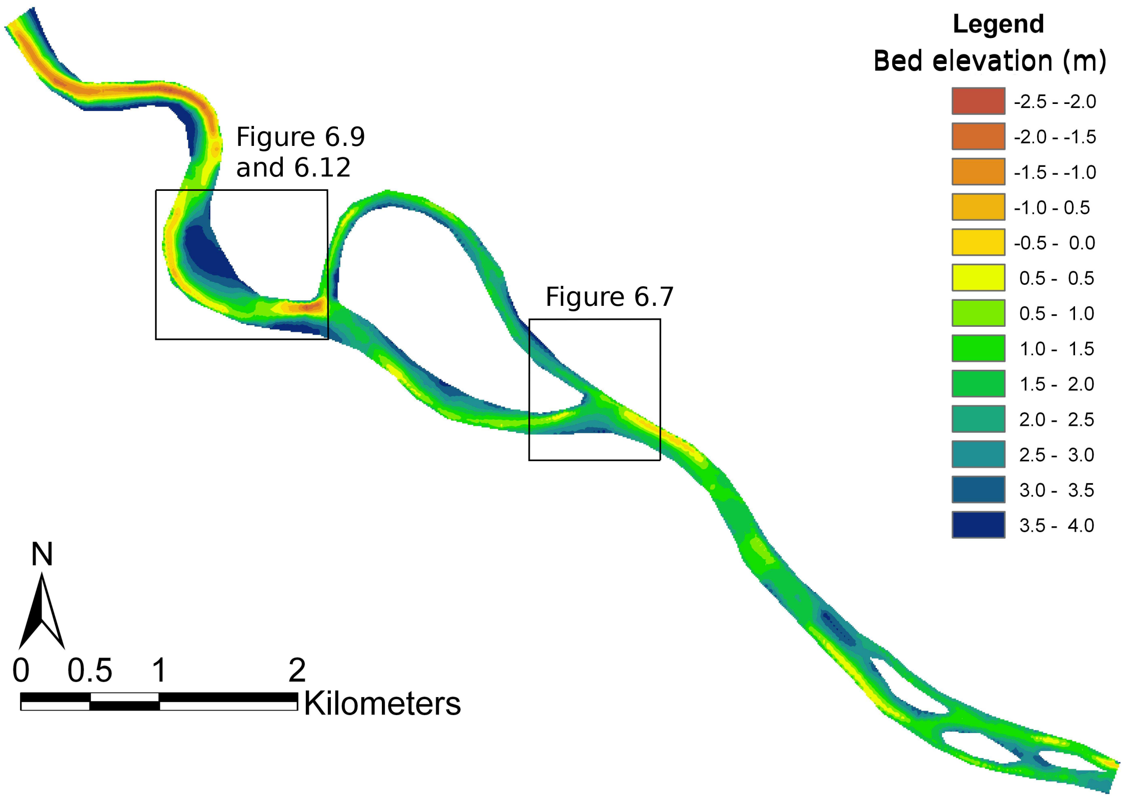

Figure 6.6: The Saint-François River bed topography with the location of detailed figures indicated by black squares.

6.1.3 Saint-François River: sedimentation in a channel branch

The sediment distribution of bed-material at a bifurcation is often unknown and influenced by local topography and near-bed flow patterns. Our simulations with variable discharge and downstream water levels increase the level of complexity as this distribution is not constant over time.

Discharge scenario	RefH	0.01m/y	0.50m-2040
RefQ	2100	2066	2080
CSIRO-Mk2 A2	2100	2075	2100
CSIRO-Mk2 B2	2100	2073	2100
ECHAM4 A2	2100	2082	2100
ECHAM4 B2	2100	2083	2100
HadCM3 A2	2100	2063	2058
HadCM3 B2	2100	2063	2065

Table 6.4: End date of simulations in the Saint-François River.

In the Saint-François River, all the simulations with a smooth base level fall crashed prior to 2099 due to sedimentation in the eastern channel (see Table 6.4 for an overview and Figure 6.6 for location). The RefQ and HadCM3 (A2 and B2) simulations with the sudden drop in 2040 also crashed. The reason for the crash is mainly because of the downstream water level fall which leads to lower water levels in the Saint-François River. The crashing occurred irrespective of the discharge scenarios. The different discharge scenarios only have an influence on the timing of the crash, i.e. when low discharge occurs simultaneously with low downstream water level. HadCM3 crashes earlier than the others but at approximately the same date for both base-level fall scenarios (2058–2065), when the base-level drop is close to 0.50 m in both scenarios.

To solve this problem, the sediment discharge distribution was modified so that the aggrading branch would receive less sediment. This was achieved by setting the sediment transport distribution equal to a different ratio than the water discharge ratio. The following formula was used to calculate the sediment input in the western branch (2 on Figure 6.7) downstream of the bifurcation with the parameter R, which adjusts the sediment transport ratio at the bifurcation (1 results in the same ratio as that of the water discharge):

$$Q_{s2} = \frac{Q_{s1} \times R}{\frac{Q_1}{Q_2} + R - 1} \tag{6.1}$$

The formula generates a sediment input that is always smaller than the total transport in the upstream reach. Equation 6.1 was used to see how sensitive aggradation in the island branch

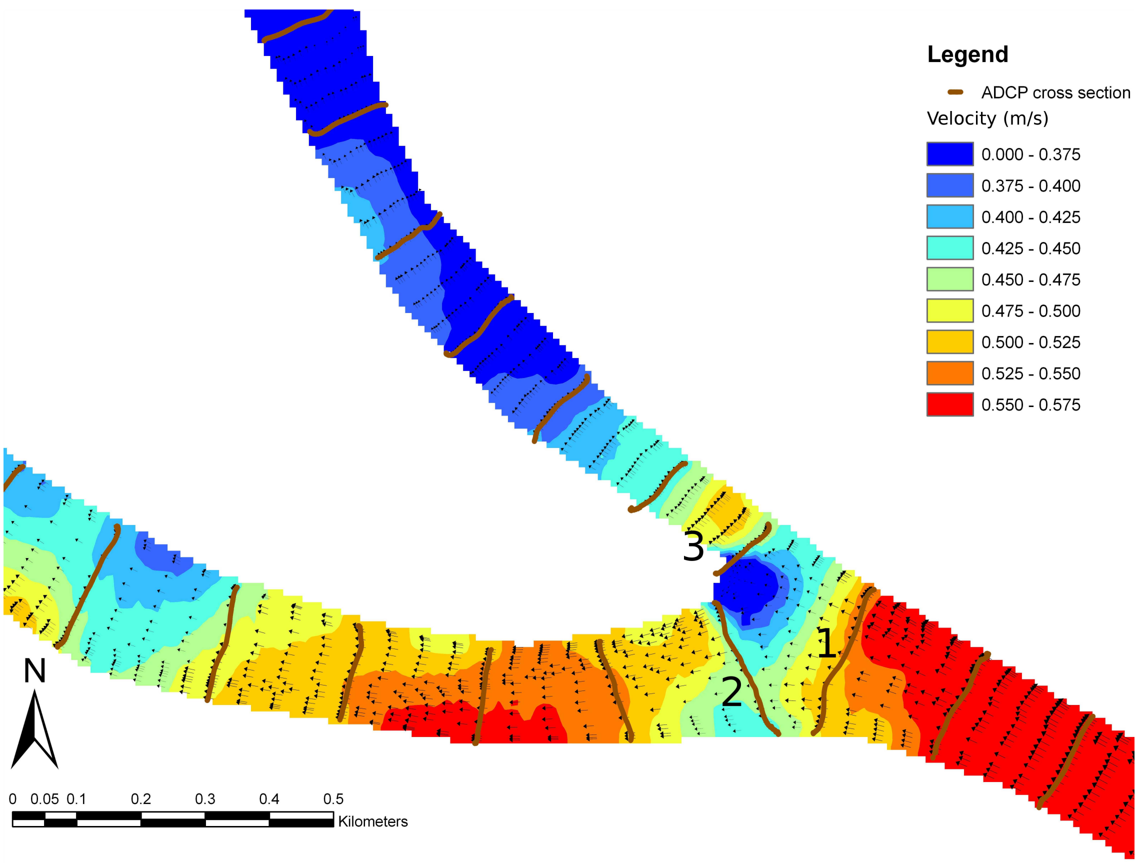

Figure 6.7: Predicted magnitude of flow velocities by H2D2 for bankfull flow conditions.

was to the nodal point relationship – of course the morphological meaning of such a condition would be very questionable. The modified sediment distribution was simulated for the RefQ-0.01m/y scenario, with a range of values for R (Table 6.5). Results show that for higher values of R (= 2, 10) the runs complete the simulation period (Table 6.5). Sedimentation in the eastern channel occurs in all simulations, except for $R = 10$, indicating that this might be a realistic phenomenon and not solely an artefact of the sediment transport relationship at the bifurcation in SEDROUT4-M. This suggests that the crash of SEDROUT4-M could be solved by enabling critical flow or channel cut-off under low water elevations.

The total sediment transport at the downstream boundary remains approximately the same with differences of less than 1.5% for R values of 1.1, 1.5 and 2, and $\pm 4\%$ for $R = 10$. Overall, the ratio of sediment distribution at the island seems to have had a minor effect on our bed material transport analysis of sediment delivery from the Saint-François River, although the morphology within the branches along the island is highly affected.

6.2 2D model: H2D2

The model H2D2, which is an acronym for HydroSim 2 [Heniche *et al.*, 2000] and DisperSim 2 [Secretan *et al.*, 2000a], is used to examine differences in simulations in the island area in the Saint-François River between a 1D and a 2D approach. H2D2 combines a two-dimensional finite element model for the simulation of shallow water flow with a dispersion model for contaminants in the water column, including sediments in suspension. The shallow water equations (or Saint-Venant equations) are solved on a triangular mesh. Flow velocities in two directions and water depths are solved at each corner of the mesh and velocities are calculated half-way each side of the triangles as well.

Approximations used for the hydraulic computation in H2D2 are the following: the water column is well mixed in the vertical direction and the depth is small in comparison to the

R	R_{Qs}	End date	$Q_{s:out}$ (m^3)
1.0	0.70	2066	1 926 819
1.1	0.72	2074	1 937 471
1.5	0.77	2096	1 935 267
2.0	0.82	2100	1 938 422
10.0	0.92	2100	1 980 006

Table 6.5: End date of simulations with different values of R for the sediment transport distribution in the Saint-François River for the RefQ-0.01m/y scenario. $R_{Qs} = \frac{Q_{s2}}{(Q_{s2}+Q_{s3})}$ is given for a discharge distribution that is 70–30%. $Q_{s:out}$ represents the sediment transport volume at the downstream boundary for the period 2010-2066.

width; there is hydrostatic pressure in the vertical, meaning that the vertical component of the acceleration is neglected, so waves are small in amplitude or of long period, like tidal waves; the velocity is constant in the vertical direction (depth averaged); the porosity of the field is taken into account to make a difference between dry and wet area.

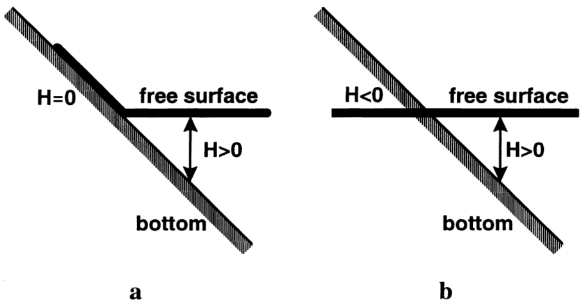

Figure 6.8: Two different concepts of moving boundaries in 2D modelling, a) classic approach, b) new approach, adapted from Heniche *et al.* [2000].

To accurately describe hydraulics in a 2D model under variable flow conditions, a good definition of the model boundaries is critical [Heniche *et al.*, 2000]. Figure 6.8 shows two different approaches for a moving boundary condition. In H2D2, the new approach (Figure 6.8b) is used, allowing the model to have negative water depths. To maintain mass conservation, Manning's *n* is given the normal value for each positive value of water depth, and a high value for each negative water depth. Thus, no water movement can occur in dry areas. Heniche *et al.* [2000] introduced this wetting-drying model in H2D2 and tested it on two artificial cases and a case study. The method has been shown to reproduce complex boundary profiles in stationary and transient flow modelling sufficiently well.

H2D2 has a software tool to set-up the model called Modeleur [Secretan and Leclerc, 1998; Secretan *et al.*, 2000b], which contains a Geographical Information System (GIS) based module to integrate raw data into a numerical terrain model. The strength of this tool is that different data sets can be used together as a basis for the model, for example echo-sounder profiles of the river channel and LIDAR data for the floodplain. Post-processing analysis can also be carried out with Modeleur, and it provides a user-friendly tool to create maps and analyse the results.

A description of the main features and principles of H2D2 can be found in chapter 2 (section 2.5.2), Heniche *et al.* [2000] and Secretan *et al.* [2000a]. The equations for conservation of mass and momentum are also described in this chapter (equations 2.16, 2.17 and 2.18). H2D2 can currently only deal with suspended load sediments over fixed bed topography. The sediment transport is calculated using the methodology of Van Rijn [1987]. H2D2 has proven its efficiency in different types of studies, for example in the Saint-Lawrence River between Montréal and Trois-Rivières [Morin *et al.*, 2000] and to estimate flood risk along the Montmorency River (Québec) [Leclerc *et al.*, 2003; Blin *et al.*, 2005].

6.2.1 Model set-up

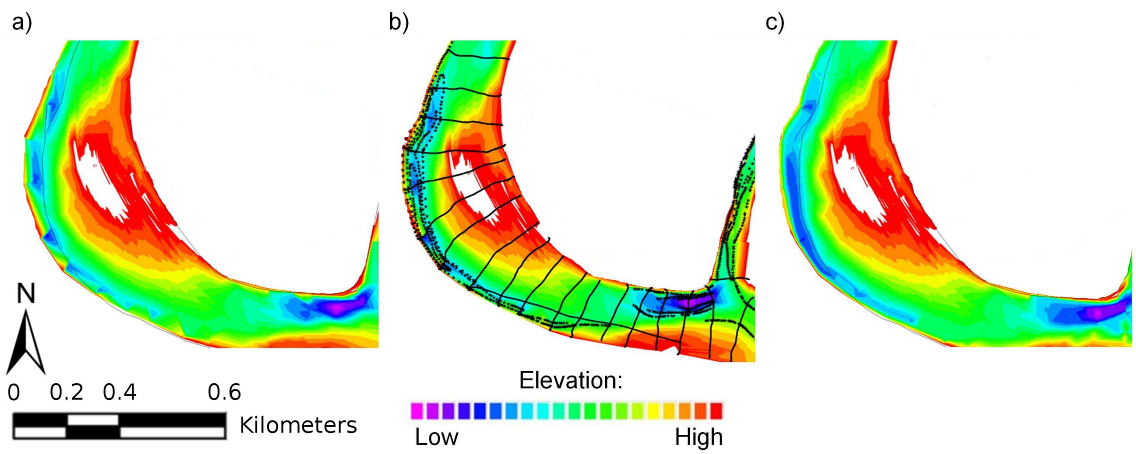

Figure 6.9: Interpolation of echosounder bed topography in Modeleur and the addition of depth contour lines to provide a better interpolation: a) initial interpolation; b) added points and echo sounder data points; c) final interpolation.

The Saint-François River was used as a test case for H2D2. With the use of the Modeleur software tool a model was set up for the main channel of the Saint-François River. The data collection campaign was conducted to set up the 1D model, but cross sections were taken sufficiently close together to be used for the 2D model. However, despite the short distance between cross sections, the interpolation of bed topography resulted in artificial bars, as clearly visible in Figure 6.9a near the outer bend bank. To improve the interpolation, contour lines (based on other topographic data from Environment Canada) perpendicular to the cross section data were added and transformed into points (Figure 6.9b). With the manually created points a new interpolation was performed which resulted in a smoother and more realistic bed topography (Figure 6.9c).

The created mesh contained only the river channel (7582 points and 3575 elements), on

	Low	Moderate	Bankfull
Discharge (m^3/s)	65	200	550
Water level (m)	3.87	4.45	6.35

Table 6.6: Discharge and water level in the Saint-François River for three flow stages.

which later the floodplain and part of the Saint-Lawrence River were added. The first step after creating the topography was to define the boundary conditions and calibrate the model parameters. As the mesh of the channel does not include the floodplains, the first simulations were done with low flow conditions measured on 19 and 20 July 2005 (Table 6.6). A bankfull simulation was done with the flow conditions measured on 26 and 27 April 2005 (Table 6.6). For convergence purposes an intermediate flow stage was used based on discharge and water level measured at gauging stations ($Q = 200$ m^3/s and $h_{ds} = 4.45$ m, Table 6.6). A Manning-n value of 0.02 was used over the entire mesh, which is different from the value used in SEDROUT4-M (0.03) as 1D models represent a river as a straight channel and therefore do not include resistance by meanders. The value of n for dry areas was set to 7. H2D2 allows for a spatially distributed roughness, which is necessary for the simulation of large rivers or for cases that include floodplains with different vegetation types. Full calibration of the model was not carried out as this was a first attempt to develop a model that would incorporate the main channel of the Saint-François River, its floodplain, as well as the Lake Saint-Pierre area to investigate the effects of increased sediment delivery on the morphology of the lake. Unfortunately, due to various reasons this model could not be set up within this thesis and therefore only hydraulic data from the Saint-François River are analysed here. However, the adaptation steps to reach this original objective are described below.

6.2.2 Adapting H2D2 for morphological simulations

The original H2D2 model can only deal with suspended sediment transport over static topography. To use this 2D model for the assessment of climate change impacts on sediment transport and topography, a bed-material or bed load formula needs to be added as well as a module to update bed elevation and bed composition. Identifying zones of primary accumulation within the Lake Saint-Pierre area could theoretically be done by only adding bed material transport, without updating the bed elevation as currently is the case with suspended sediment transport. In such a case, the sediment balance at each point could be used to see if erosion or sedimentation occurred under various hydrological conditions. This would provide a very rough indication of instantaneous erosion/sedimentation patterns, but it would not be possible to quantify the total accumulation.

The first step to incorporate bed-material transport in H2D2 was to add the Ackers and White [1973] total load transport formula to the code. The global and local parameters of

H2D2 were grouped to provide an overview of the information exchanged between the different modules of H2D2: SVC, CD2D, and SED2D, which are respectively the hydraulic, suspended sediment transport and bedload (to be developed) modules (Figure 6.10). The setup for this bedload module and the formulation of the total load formula for the code were carried out, but unfortunately, it was not possible to make the total integration with the code and include transport direction, bed elevation and bed composition updates.

The development of a sediment transport module that includes bed material requires more than just a transport formula. The bed elevation and bed composition need to be updated after each iteration and, more importantly, a 2D model requires the direction of sediment transport. The factors that determine the direction of bed material transport are: 1) the direction of flow near the bottom (caused by secondary flow) and, 2) the transverse bed gradients. The latter is a function of grain size as larger/heavier particles have a higher tendency to move downwards. Thus, contrary to secondary flow that has the same effect for all grain sizes the bed slope contributes to grain sorting in the transverse direction.

Both secondary flow and transverse bed slopes are the reason that bedload transport ratio at a bifurcation is not necessarily the same as the discharge ratio. However, counteracting effects could occur as a result of upstream meander bends or different channel slopes [Kleinhans *et al.*, 2008].

Adaptation of the model to include this phenomenon requires a translation of the depth-averaged flow direction into a direction near the bottom. This can be done through secondary flow intensity, which is computed in H2D2. To fully simulate the direction of bed-material transport, the transverse bed slope is also needed. The formula for the angle between the applied shear stress and the sediment transport for a combination of transverse slope and secondary flow is derived by Struiksma *et al.* [1985]:

$$\tan\beta_{si} = \frac{\sin\beta_\tau - \frac{1}{f(\theta_i)}\frac{\delta z}{\delta y}}{\cos\beta_\tau - \frac{1}{f(\theta_i)}\frac{\delta z}{\delta x}} \tag{6.2}$$

where $\frac{\delta z}{\delta y}$ is the transverse slope, $\frac{\delta z}{\delta x}$ is the longitudinal slope, β_{si} is the direction of sediment transport for size fraction i and β_τ is the direction of the shear stress, where both directions are relative to the longitudinal direction. $f(\theta_i)$ is an empirical function derived from experiments

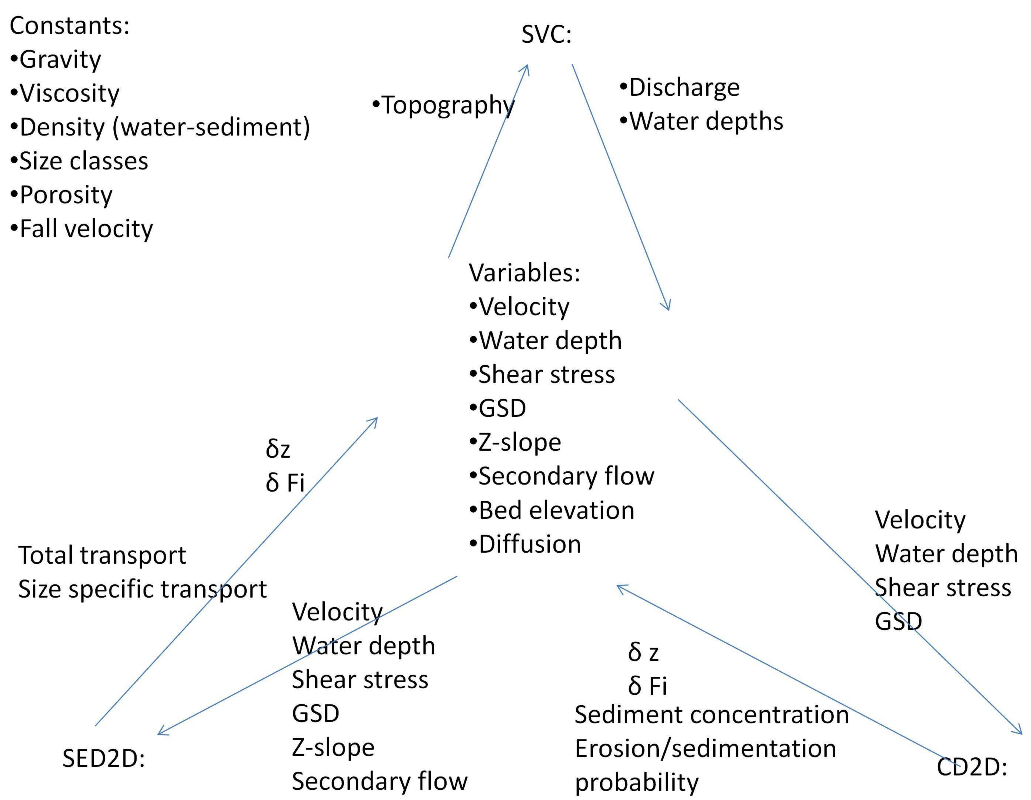

Figure 6.10: Overview of variables and constants that need to be exchanged between the different components of H2D2: SVC, CD2D, SED2D. In the upper-left corner the constants are listed and in the centre the variables that are calculated in post-treatment, and not by the modules themselves, are indicated.

by Talmon *et al*. [1995]:

$$f(\theta_i) = 9\left(\frac{D_i}{H}\right)^{0.3}\sqrt{\theta_i} \tag{6.3}$$

where θ_i is the non dimensional shear stress (Shields number) for size fraction i defined as:

$$\theta_i = \frac{\tau}{(\rho_s - \rho)\, gD_i} \tag{6.4}$$

For the analyses with H2D2, only the hydraulic output of the Saint-François River was available. Sediment transport approximations were based on shear velocity magnitude and direction, although the direction was not corrected for the secondary flow effects as described above, nor is the bed slope effect on the direction of sediment transport.

6.2.3 Saint-François example

To assess the advantage of 2D modelling in the complex topography of the Saint-François River, we have compared our measured ADCP data at low and bankfull flow conditions with the results of simulations of the model created for the main channel of the Saint-François River. The simulations of H2D2 were also compared with those of SEDROUT4-M for these two flow conditions, as well as for an intermediate flow stage (Table 6.6). Overbank flow could not be included in the analysis as the model including the floodplains was not available and no ADCP data were taken at these high flow stages. Note that in the 1D simulations, we used a condition that forced water level in both branches at the bifurcation to be within 0.1 mm and another that fixed sediment transport ratio as being equal to the discharge ratio for all grain size fractions.

No sediment transport occurs at low flow stage. For the moderate and high flow stage, simulated hydraulics from H2D2 is transformed into an approximation of sediment transport rates by using the shear stress at each point and calculating the transport rate with the White and Day [1982] formula and parameters. These calculations were done in MATLAB with a constant grain size distribution that is equal to that measured at the cross sections near the permanent island in the Saint-François River. The direction of sediment transport is equal to the mean velocity of each velocity point and is not corrected for secondary flow and bed slope. The sediment transport rates from this simplified exercise only provide instantaneous transport capacity at the head of the two branches along the island.

6.2.3.1 Hydraulic comparison

	Low flow				Bankfull			
	SEDROUT4-M		H2D2		SEDROUT4-M		H2D2	
Mean difference	0.021	(16%)	-0.019	(-14%)	0.029	(7%)	0.042	(10%)
Mean absolute difference	0.044	(33%)	0.025	(18%)	0.036	(8%)	0.046	(11%)
Standard deviation	0.036		0.016		0.036		0.031	

Table 6.7: Mean difference, mean absolute difference, and standard deviation of cross-sectional average velocities between the models (SEDROUT4-M and H2D2) and the ADCP-measurements (m/s).

Hydraulic simulations with downstream water level and discharge measured during our field campaign show good agreement with water elevation (within 0.001 m). Table 6.7 presents the mean difference, the mean absolute difference and the standard deviation of the average velocity at each cross section between the simulated values by SEDROUT4-M, H2D2 and measured values with the ADCP. At bankfull stage the absolute difference is slightly larger for H2D2 than it is for SEDROUT4-M, but the standard deviation is smaller (also for low flow), meaning that the differences are more similar for each cross section in H2D2. Thus, despite not being fully calibrated, H2D2 is already giving good results. Figure 6.11 presents the relationship between the width-averaged H2D2 velocity and the simulated cross-sectional velocity of SEDROUT4-M at three different flow stages. With increasing flow stage the agreement between the two models is improving, with a regression slope getting close to 1 at bankfull stage. The complex flow field observed in the meander downstream of the island (Figure 6.12) is also well represented by H2D2.

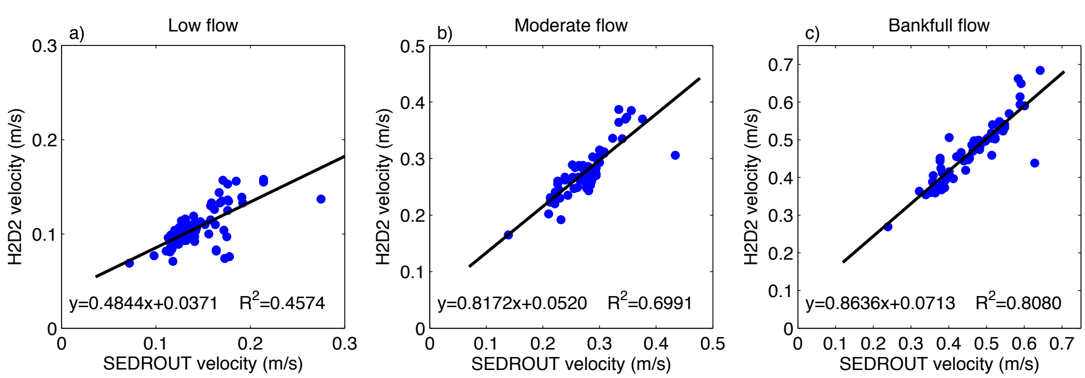

Figure 6.11: Comparison of cross-sectional velocities simulated by SEDROUT4-M with H2D2 simulations three different flow stages: a) low flow; b) moderate flow; c) bankfull flow. Line represents regression the equation and R^2 are given ate the bottom of each graph.

The discharge distribution at the bifurcation around the large island is presented in Figure 6.13a. The discharge split in H2D2 is approximated from the raw data by summing the specific discharge at each point along a cross section and multiplying by the distance between the points. Both the 1D and 2D models overestimate the discharge in the large western branch, with respectively 74–26% and 71–29% ratios, when ADCP measurements indicate a 68–32% split (Figure 6.13a). Under bankfull flow conditions, both models approach the measured ratio of 68–32%, with 70–30% for SEDROUT4-M and 69–31% for H2D2. Both models follow the trend of decreasing ratio with higher flow stage, but H2D2 is closest to the measured ratio than SEDROUT4-M. This can be explained by the fact that the 2D model includes the topography and the momentum of the water discharge at the bifurcation. The good representation of the flow field in the bifurcation zone can be seen in Figure 6.7 at bankfull condition. H2D2 velocities are very similar to the ADCP data that show values of 0.35–0.38 m/s at the cross sections directly downstream of the bifurcation (2 and 3), whereas H2D2 predicts velocities in the range of 0.40–0.43 m/s. Velocities just upstream of the bifurcation (1) are also in the same range (0.47 m/s from ADCP data and 0.50–0.53 m/s in H2D2).

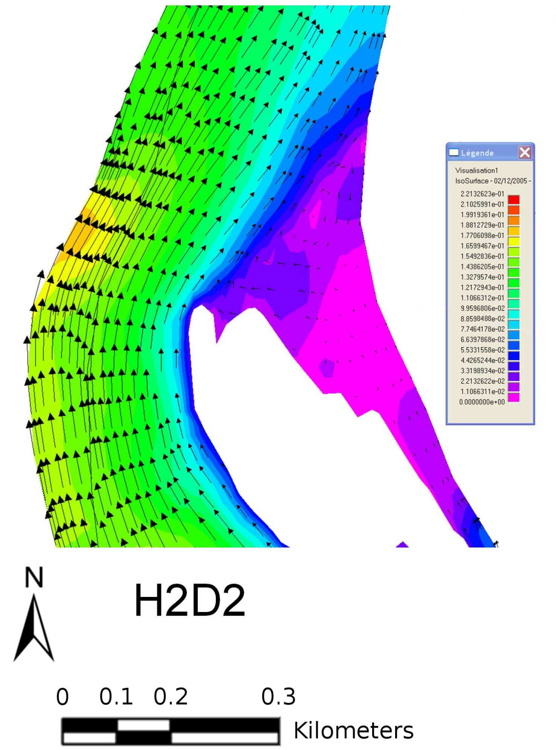

Figure 6.12: Velocity field at low flow conditions (60 m^3/s) as simulated by H2D2.

6.2.3.2 Morphological comparison

The sediment transport rates from H2D2 are instantaneous rates based on a fixed grain size distribution, whereas the SEDROUT4-M rates are the rates over a one-day simulation. By definition, the sediment transport ratio is the same as the discharge ratio for SEDROUT4-M. The ratio for H2D2 is about 0.5 for bankfull flow, which does not seem to be realistic (Figure 6.13b), at lower flow stages no sediment transport occurred around the island. However, this is actually the transport capacity for bed-material at the initial condition, as bed composition changes over time relatively quickly compared to bed elevation which would change after a certain number of iterations. This ratio would likely change through time due to the water sediment interaction and supply from upstream. Indeed, morphological models need some adaptation time at the start-up to correctly represent the sediment transport rates from initial settings because grain size data of the river bed is sparsely sampled and the grain size distribution is averaged over large areas.

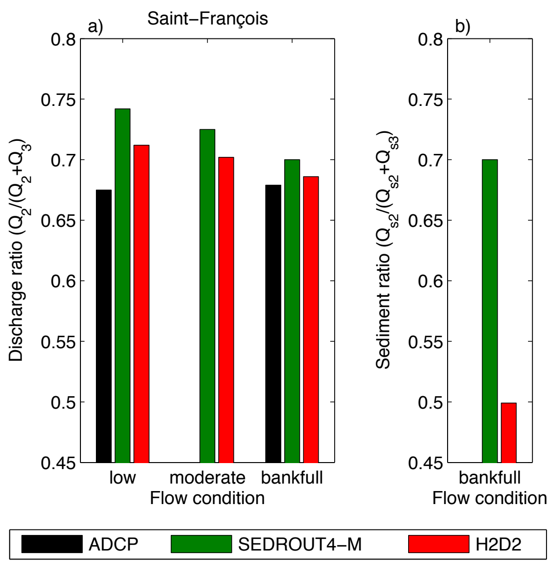

Figure 6.13: a) Ratio of discharge at the bifurcation (large island) for three flow stages as obtained from ADCP measurements, SEDROUT4-M and H2D2 simulations; b) Sediment transport rate at the bifurcation obtained from SEDROUT4-M and H2D2. Q_2 and Q_3 are the discharges in the bifurcated channels.

The ratio of sediment transport between the two channels of the Saint-François River is a good example of the complexity of 2D morphological modelling. Sediment transport distribution cannot simply be subtracted from instantaneous flow fields based on average water velocity directions, the feedback loop of sediment transport on bed elevation and bed composition is not present in the model. It also confirms that the sediment transport rates at the beginning of each simulation are very sensitive to the initial conditions. A more careful integration of sediment transport is required to solve the sediment transport equation, which is currently underway through post-doctoral work carried out at INRS-ETE (Dr. Muluneh Mekonnen, under the supervision of Drs. Yves Secretan and Pascale Biron).

The H2D2 bankfull simulations indicate that velocities drop to values under 0.38 m/s over the entire width of the channel in the eastern branch along the island (Figure 6.7). This zone of low velocities starts at the location where sedimentation occurs in the long-term SEDROUT4-M simulations. This is another indication that the sedimentation that was simulated in 1D is not artificial, but the development over time should be investigated more closely. Island channels are normally relatively stable – compared to, say, multiple channels in gravel braided rivers which are not always morphologically active. However, in this sand-bed river, a similar situation may occur, where one of the channels is markedly less active than the other.

6.2.4 Discussion

Although the hydraulic performance of H2D2 around the island in the Saint-François River seems superior to that of SEDROUT4-M, the morphological results based on the instantaneous flow field are not very promising. Morphodynamic models need some adaptation time at the start-up and, as shown by Ferguson and Church [2009], the model spin-up (alos called zeroing or priming) can have a substantial influence on the results. However, a fully integrated sediment transport module has the potential to overcome this low performance of H2D2. Unfortunately, we have no available measurements of the sediment discharge distribution at the bifurcation of the island to further examine this question.

Sediment distribution at bifurcations in rivers are not fully understood [Bolla Pittaluga *et al.*, 2003; Federici and Paola, 2003; Bertoldi and Tubino, 2007]. Morphodynamic modelling of rivers with bifurcations remains a challenge in both 1D and 2D, nevertheless good results with both 1D and 2D models have been obtained [Zanichelli *et al.*, 2004; Miori *et al.*, 2006]. The analysis here shows that 2D modelling has a better representation of the discharge distribution at the bifurcation in the Saint-François River. Therefore, it has the potential to give better morphological results than SEDROUT4-M.

For 2D models, the grain size distribution in the lateral direction becomes important. This is because, on the one hand, sediment transport is not equally distributed over the river width [Frings and Kleinhans, 2008], which is an important factor in sediment distribution at bifurcations. On the other hand, velocities are variable over the width. As sediment transport is a non-linear function of velocity, good results can only be expected if the correct grain size distribution is used. This is one of the reasons why the transport rates could be different for the approximation of the H2D2 hydraulic results.

It would have been interesting to also be able to investigate the complex multiple bifurcation geometry of the Saint-Maurice River with H2D2. This was unfortunately not possible in this study due to lack of time, but, based on the results of the Saint-François bifurcation, it seems likely that results closer to ADCP measurements would have been obtained.

The debate on the optimal dimension (i.e. 1D, 2D or 3D) of models for river simulations is still open. Clearly, the flow field in complex channels is better represented in 2D and 3D models. As mentioned previously, running long-term simulations for long reaches in 3D remains unrealistic at this point both due to the amount of data required for calibration and validation and to computer processing time limitations. The choice is therefore between a 1D and 2D approach. There is no doubt that 2D models are conceptually superior to 1D models, but in river management, 1D models remain widely used [Ferguson and Church, 2009].

A complex reach of the Fraser River (British Columbia) was modelled with both a 1D model [SEDROUT Ferguson and Church, 2009] and a 2D model using a commercial 2D code [MIKE21C DHI, 1999] in fixed-bed mode [Li and Millar, 2007; Li *et al*., 2008]. Both models used the same transport equation [Parker, 1990b]. Interestingly, the 2D model did not reproduce the aggradation profile as well as the 1D model in this case. Results from the 2D model could have been better if the model had been run in full morphodynamic mode [Ferguson and Church, 2009], but the 2D model still predicted unrealistically large values of bed shear stress around bar margins [Ferguson, 2008; Li *et al*., 2008], which is problematic in this reach of the Fraser River where bar features are ubiquitous.

CHAPTER 7

GENERAL CONCLUSION

This thesis has investigated the morphological effects of climate change on tributaries of the Saint-Lawrence River through changes in discharge and base level. The 1D-morphodynamic model SEDROUT was adapted to deal with these types of changes and to the morphological and topographic settings of the selected tributaries. This concluding chapter first summarizes the key findings from the morphodynamic simulations presented in chapters 3 to 5 and from the investigation of the potential of a 2D-model for long term simulations (chapter 6). A general discussion of these findings is then presented and is followed by suggestions for future research.

7.1 Key findings

The 1D model SEDROUT was chosen for this study because it was felt that it was robust and adaptable – the collaboration with the two researchers who have developed the model (Trevor Hoey and Rob Ferguson) helped in understanding the model and facilitated the implementation of new modules in the existing model. This model has now been used in a variety of geomorphological contexts, ranging from small [Hoey and Ferguson, 1994; Talbot and Lapointe, 2002] to large rivers such as the Fraser River [Ferguson and Church, 2009] and now the tributaries of the Saint-Lawrence River, from gravel [Hoey and Ferguson, 1994; Talbot and Lapointe, 2002] to sand and mixed sand and gravel [Ferguson *et al.*, 2001], and in aggradational [Hoey and Ferguson, 1994; Ferguson *et al.*, 2001; Talbot and Lapointe, 2002] and degradational cases [Talbot and Lapointe, 2002]. The modifications made in this study (chapter 3) broaden even further the types of problems that can now be solved with a strong level of confidence in the results. This is a significant outcome of this thesis as the impacts of near-future climate-induced changes on discharge and base level in large lowland sand-bedded rivers subject to tidal fluctuations will need to be assessed in many parts of the world.

Overall the volume of bed material delivered from the Saint-Lawrence tributaries will increase in the near future regardless of the GCM scenario used to generate discharge time series. The expected water level fall in the Saint-Lawrence River also leads to increased sediment transport, which could have significant consequences for Lake Saint-Pierre as it is already undergoing sedimentation [Carignan and Lorrain, 2000]. Increased bed-material transport is associated with increased maximum discharge and a shift in timing of spring floods towards the winter. More frequent large flood events, with high recurrence intervals, have a dominating impact on the river response (chapter 5). Furthermore, chapter 4 revealed that bed elevations are affected up until relatively large distances upstream. Bed lowering may have consequences for infrastructures within the downstream parts of these rivers, for example for bridge piers. Additionally, the risk of flooding has been shown to increase despite the expected bed erosion because of the predicted increase in frequency and magnitude of large floods (chapter 5).

The analyses of mean annual bed-material transport rates and bed elevations were conducted by comparing the outcome of different scenarios with a reference scenario (chapter 4), in order to minimize the uncertainties in global climate change modelling. Comparison of annual bed-material transport rates and bed elevation revealed that variation from different GCMs is larger than that due to base level drop and GHG scenarios. This raises the question of why these discharge scenarios have such a large influence on the morphological adjustment of rivers when the mean daily and mean annual maximum discharge remained relatively similar. Chapter 5 provides some insight on this question as it reveals that the large change in sediment transport comes partly from an increased variability in the hydrograph and partly because of a change in timing of the spring flood compared to the water levels in the Saint-Lawrence River.

Although the 1D-model has satisfactorily simulated three of the five selected tributaries, the difficulties encountered with the Yamachiche and Saint-Maurice rivers are a good illustration of the challenges that remain in numerical modelling of river morphology (chapter 6). The Yamachiche River problems indicate that the cross-sectional distance relative to the river width is important, although no standard rule is available and therefore it remains a subjective decision to be made by the researcher. The difficulty of adequately capturing a complex river geometry with a 1D model is revealed in both the Saint-Maurice and Saint-François River simulations. There is an obvious advantage in cases of islands and bifurcations to consider the use of a 2D-morphodynamic approach. However, in river management, a 2D approach remains difficult due to the much larger data input requirements.

7.2 Discussion

One of the major challenges in predicting the impacts of climate change on rivers is to deal with the cumulative uncertainty in predicted scenarios and models. In any modelling project, one has to manage uncertainty in measurements, modelling approximations, simplification, assumptions and validation. However, even if this study focussed on the impact of discharge and water level changes on sediment transport of different rivers, an important component of each chapter – chapter 4 in particular – involved justifying the choice of GCMs, of the downscaling approach and of a hydrological model to convert temperature and precipitation changes into daily discharges.

The choice of the GCMs used in this study, CSIRO-Mk2, ECHAM4 and HadCM3, and the use of the perturbation method have an obvious effect on the obtained results. However, the GCM models are covering different possible outputs for near future temperature and precipitation and therefore include most of the possible outputs. For the water level scenarios in the Saint-Lawrence River, only future time series (quarter months) are available for the 2040–2069 horizon [Morin *et al.*, 2009]. These time series were constructed in a similar way as the discharge for the tributaries, but only for the middle horizon and they are therefore not providing information on how the water level decrease will evolve through time. The adopted strategy to use two simple scenarios for the Saint-Lawrence water levels removed any potential bias in the modelling approach, as well as in the natural variability. The latter could have some consequences on the effects of timing, although having scenarios of water levels based on the same time period as the discharge for the tributaries could introduce a dependency on the timing of discharge and water levels that does actually not exist.

Because of the emphasis on the initial steps (which were not strictly speaking part of this study), perhaps less attention has been given in this thesis to the uncertainty in the morphodynamic modelling itself. The latter can be very important as sediment transport formulae are not very precise – bedload formulae that predict transport rates within one-half or twice the observed amounts are sparse [White and Crabbe, 1975; Andrews, 1981; Batalla, 1997; Mueller *et al.*, 2008]. The very good fit between SEDROUT simulations and field measurements in the Fraser River [Ferguson and Church, 2009] strengthens our confidence in SEDROUT results considering that the complexity of the Fraser River is much higher than that of the studied tributaries. Thus, at this point, we feel that the uncertainty in climate modelling was much greater than the uncertainty in morphological modelling. The climate scenarios used in this study, generated in 2005, were chosen to cover a range of GCM outcomes in order to compare their effects. The recent trend in climate change simulations is to use an ensemble of models, from which the average outcome as well as some extremes can be used with a hydrological model to examine discharge impacts [Graham *et al.*, 2007; Leutbecher and Palmer, 2008]. Inherent to future climate change research is the difficulty of translating global trends to local effects on precipitation and temperature. With rapid improvements in reducing the uncertainty in climate modelling and in downscaling at the local scale [Rydgren *et al.*, 2007], it should be possible to obtain in the near future even more reliable predictions of river adjustment to climate change.

Uncertainty comes from the climate models or scenarios, but the use of a hydrological model contributes to the uncertainty as well. The generation of discharge scenarios was beyond the scope of this research, but the fact that only one hydrological model was used could have an influence on the obtained results. Ideally, it other hydrological models should have been tested to verify it similar changes would have been predicted. However, given the high Nash coefficients for all of the tributaries, one could speculate that the differences with other models should be relatively minor.

The lack of field data, particularly on sediment transport, makes it virtually impossible to calibrate and validate thoroughly morphodynamic models [Cao and Carling, 2002b; Gomez *et al.*, 2009]. Examples of extensive field data sets over longer time periods are very sparse, although they exist for the Fraser River [McLean *et al.*, 1999; McLean and Church, 1999; Rice *et al.*, 2009] and Waipaoa River [Gomez *et al.*, 2009]. Long-term data sets on bed and bank topography and sedimentology require considerable efforts, especially when a sufficient spatial and temporal resolution is needed for both model setup and model verification. Considering the economical and ecological importance of the Saint-Lawrence River, it is surprising that virtually no information on either bed topography, grain size distribution or velocity of its tributaries was available at the onset of this project. In contrast, there is a wealth of data on the Saint-Lawrence River [Carignan and Lorrain, 2000; Morin *et al.*, 2000, 2005; Hudon, 2004; Hudon and Carignan, 2008, among others]. However, it will not be possible to make predictions of the future state of the Saint-Lawrence River without knowing what quantities of sediments will be delivered from its tributaries under future climate. In order to make full use of the potential of numerical modelling, a monitoring program should be put in place to at least obtain data on the downstream sections of the key tributaries. With recent technological developments such as the green lidar [McKean and Isaak, 2009], it may be possible to obtain very detailed bed topography datasets under water at a very high spatial resolution. It may not be as simple to collect sedimentological data, although recent photogrammetric findings on automating the characterization of gravel-bed surfaces [Butler *et al*., 2002; Carbonneau *et al*., 2005] are also promising.

Interestingly, the three tributaries for which it was possible to run long-term simulations with the 1D model were in different morphological states according to simulations with the RefQ scenario, i.e aggradation for the Batiscan River, near-equilibrium for the Richelieu River, and degradation for the Saint-François River (chapter 4). This information was not known when the tributaries were selected, but it allowed further generalization of our results. Indeed, if all rivers had been, say, in an aggradational state, wrong conclusions may have been drawn as the variation in the sediment transport trends for different scenarios was considerable between the three rivers. This question probably requires a more systematic investigation.

When generalizing the results obtained in this study to other rivers in the world, it must be remembered that the Saint-Lawrence River may be a special case compared to other watersheds, partly because of the impact of climate change on the Great Lakes (the source of the Saint-Lawrence River), which will result in lower discharges under future climate, and hence provide lower base levels for its tributaries. In many other areas, a sea-level rise, and hence an increase in base level for tributaries, is predicted. Although the modified 1D model SEDROUT4-M should be able to deal with either an increase or a decrease in base level, obviously the conclusion of this study that climate change will in general increase the amount of sediments delivered to the main channel are specific to the base level drop situation. Another characteristic of the Saint-Lawrence watershed is the importance of the spring flood and the impact of climate change on winter temperature and, therefore, on the timing of the peak annual flow. It is possible that climate-induced changes on discharge would be less in a context where spring flood is less dominant in the yearly flood hydrograph.

In general the near-future scenarios lead to an increase in sediment transport towards the Saint-Lawrence River compared to the reference discharge scenarios. However, the ECHAM4 model, which is simulating the smallest change in precipitation and the largest in temperature, predicts similar bedload transport or even a decrease in the future. Furthermore, in general, not only the sediment volume but also the timing is expected to change. This could have consequences for ecology as certain species such as invertebrates depend on sediment transport. The increase in sediment transport volume within the Richelieu has consequences for the harbour in its downstream reach and for the Saint-Lawrence seaway. The increased sediment delivery would likely require more dredging in the near future. As for the Saint-François River, the situation is different. The sediment transport increases compared to the reference scenario, although over time the river approaches the equilibrium state, therefore the volume is actually decreasing over time in all the scenarios. This decrease over time is smaller for the GCM-scenarios than it is for the RefQ-scenario. This would mean that the propagation of its delta as observed in the past [Bondue *et al.*, 2006] will continue at a slower rate than in the past, but for the GCM-scenarios the propagation of the delta would be faster than it would be under the RefQ scenario. The propagation of the delta leads to a diminution in water surface area of Lake Saint-Pierre, on the other hand it increases the perimeter of this lake, as the river mouth reaches further into the lake when the sediment volume is not sufficient to fill in the whole lake.

7.3 Future research

This research focused on in-channel processes, but there is a need for a more integrative modelling approach that would also take into account the connectivity between channels and hillslopes. The connectivity issue was not perceived as essential in this study where lowland rivers were examined, but it is clearly crucial in upland reaches [Lane *et al.*, 2007, 2008; Raven *et al.*, 2009]. Future research should examine the applicability of combining a landscape model such as CAESAR [Coulthard, 2002; Hancock, 2009] with either a 1D or 2D morphodynamic model to be able to simulating the impacts of varying sediment supply on river adjustment. Such a model should incorporate the effects of vegetation changes on sediment delivery and river adjustment.

The importance of extreme events on river adjustment was addressed in this study. However, different downscaling approaches would need to be tested as the perturbation method used here is known to be less accurate for individual floods. Considering the importance of large floods for sediment transport and flood risk, it is essential to test how other methods would affect future discharge time series, and what the resulting impact on river bed elevation and sediment transport delivery would be. Large events are also most likely to generate major planform changes through bank erosion, a process that is still not well integrated in morphodynamic models and that needs to receive more attention in future studies.

Finally, the uncertainty in morphodynamic modelling and the sensitivity of the model to input parameters would need to be addressed more thoroughly in order to provide information to river managers in terms of probability that certain river adjustments would occur under future climate. In all cases, there is a clear requirement for more complete field datasets to calibrate and validate simulation results. This should be facilitated by technological progress in the automation of bed topography and sedimentology data collection, but there also needs to be a political will to fund field monitoring programs as part of climate change adaptation plans.

BIBLIOGRAPHY

Abad JD, Garcia MH, 2006. RVR Meander: A toolbox for re-meandering of channelized streams. *Computers & Geosciences* **32**(1): 92–101. doi:10.1016/j.cageo.2005.05.006.

Ackers P, White WR, 1973. Sediment transport: new approach and analysis. *Journal of Hydraulic Engineering* **99**: 2041–2060.

Adel MM, 2002. Man-made climatic changes in the Ganges basin. *International Journal of Climatology* **22**(8): 993–1016. doi:10.1002/joc.732.

Andersson L, Wilk J, Todd MC, Hughes DA, Earle A, Kniveton D, Layberry R, Savenije HHG, 2006. Impact of climate change and development scenarios on flow patterns in the Okavango River. *Journal of Hydrology* **331**(1-2): 43–57. doi:10.1016/j.jhydrol.2006.04.039.

Andrews ED, 1980. Effective and bankfull discharges of streams in the Yampa River basin, Colorado and Wyoming. *Journal of Hydrology* **46**(3-4): 311–330.

Andrews ED, 1981. Measurement and computation of bed-material discharge in a shallow sand-bed stream, Muddy creek, Wyoming. *Water Resources Research* **17**(1): 131–141.

Andrews ED, 1983. Entrainment of gravel from naturally sorted riverbed material. *Geological Society of America Bulletin* **94**(10): 1225–1231.

Antoine P, 2003. Response of the Selle River to climatic modifications during the Lateglacial and Early Holocene (Somme Basin-northern France). *Quaternary Science Reviews* **22**(20): 2061. doi:10.1016/S0277-3791(03)00180-X.

Armanini A, 1995. Nonuniform sediment transport - dynamics of the active layer. *Journal of Hydraulic Research* **33**(5): 611–622.

Arnell NW, 1998. Climate change and water resources in Britain. *Climate Change* **39**(1): 83–110.

Ashida K, Michiue M, 1971. An investigation of river bed degradation downstream of a dam. In *Proceedings of 14th Congress IAHR 13*. Paris.

Ashmore PE, Day TJ, 1988. Effective discharge for suspended sediment transport in streams of the Saskatchewan River basin. *Water Resources Research* **24**(6): 864–870.

Barnes Jr HH, 1967. Roughness characteristics of natural channels. *U.S. Geological Survey Water-Supply Paper 1849* 213.

Barry JJ, Buffington JM, King JG, 2004. A general power equation for predicting bed load transport rates in gravel bed rivers. *Water Resources Research* **40**(10): W10401. doi:10.1029/2004WR003190.

Barry JJ, Buffington JM, Goodwin P, ASCE M, King JG, Emmett WW, 2008. Performance of bed-load transport equations relative to geomorphic significance: Predicting effective discharge and its transport rate. *Journal of Hydrologic Engineering-ASCE* **134**(5): 601–615. doi:10.1061/(ASCE)0733-9429(2008)134:5(601).

Batalla RJ, 1997. Evaluating bed-material transport equations using field measurements in a sandy gravel-bed stream, Arúcies River, NE Spain. *Earth Surface Processes and Landforms* **22**: 121–130.

Begin ZB, Meyer DF, Schumm SA, 1981. Development of longitudinal profiles of alluvial channels in response to base-level lowering. *Earth Surface Processes and Landforms* **6**(1): 49–68.

Bertoldi W, Tubino M, 2007. River bifurcations: Experimental observations on equilibrium configurations. *Water Resources Research* **43**(10). doi:10.1029/2007WR005907.

Blin B, Leclerc M, Secretan Y, Morse B, 2005. Unit mapping of flood risks for direct damages to single family residences in Quebec (Canada). *Revue des Sciences de l'eau* **18**(4): 427–451.

Blum MD, Törnqvist TE, 2000. Fluvial responses to climate and sea-level change: a review and look forward. *Sedimentology* **47**: 2–48.

Bogaart P, Van Balen RT, Kasse C, Vandenberghe J, 2003. Process-based modelling of fluvial system response to rapid climate change I: model formulation and generic applications. *Quaternary Science Reviews* **22**(20): 2077. doi:10.1016/S0277-3791(03)00143-4.

Bogaart PW, van Balen RT, 2000. Numerical modeling of the response of alluvial rivers to Quaternary climate change. *Global and Planetary Change* **27**(1-4): 147–163.

Bolla Pittaluga M, Repetto R, Tubino M, 2003. Channel bifurcation in braided rivers: Equilibrium configurations and stability. *Water Resources Research* **39**(11): 1046. doi:10.1029/2003WR002754.

Bondue V, 2004. *La réponse des tributaires du Saint-Laurent aux changements environnementaux*. Master's thesis, Département de Géographie, Université de Montréal, Montréal, Canada, in French.

Bondue V, Boyer C, Lamothe M, Roy AG, Ghaleb B, 2006. L'évolution récente du delta de la Yamachiche (Québec): Processus naturel et impacts anthropiques. *Géographie Physique et Quaternaire* **60**: 289–306, (in French).

Bonneau PR, Snow RS, 1992. Character of headwaters adjustment to base-level drop, investigated by digital modeling. *Geomorphology* **5**(3-5): 475–487.

Bonnet S, Crave A, 2003. Landscape response to climate change: Insights from experimental modeling and implications for tectonic versus climatic uplift of topography. *Geology* **31**(2): 123–126.

Bourque A, Simonet G, 2008. *From Impacts to Adaptation in a Changing Climate 2007*, Government of Canada, Ottawa, ON, chap. Québec, 171–226.

Boyer C, Verhaar PM, Roy AG, Biron PM, Morin J, 2009. Impacts of environmental changes on the hydrology and sedimentary processes at the confluences of St-Lawrence tributaries: Potential effect on fluvial ecosystems. *Hydrobiologia* doi:10.1007/s10750-009-9927-1.

Boyer C, Chaumont D, Chartier I, Roy AG, in press. Impact of climate change on the hydrology of St-Lawrence tributaries. *Journal of Hydrology*.

Buffington JM, 1999. The legend of A. F. Shields. *Journal of Hydraulic Engineering-ASCE* **125**(4): 376–387.

Buffington JM, Montgomery DR, 1997. A systematic analysis of eight decades of incipient motion studies, with special reference to gravel-bedded rivers. *Water Resources Research* **33**(8): 1993–2029.

Bulle H, 1926. Untersuchungen über die geschiebeableitung bei der spaltung von wasserläufen. technical report, VDI Verlag, Berlin, in German.

Butler JB, Lane SN, Chandler JH, Porfiri E, 2002. Through-water close range digital photogrammetry in flume and field environments. *Photogrametric Record* **17**(99): 419–439.

Cao Z, Carling PA, 2002a. Mathematical modelling of alluvial rivers: reality and myth. part 2: Special issues.

Proceedings of The Institution of Civil Engineers-water and Maritime Engineering **154**(4): 297–307.

Cao Z, Carling PA, 2002b. Mathematical modelling of alluvial rivers: reality and myth. part i: General review. *Proceedings of The Institution of Civil Engineers-water and Maritime Engineering* **154**(3): 207–219.

Cao ZX, Day R, Egashira S, 2002. Coupled and decoupled numerical modeling of flow and morphological evolution in alluvial rivers. *Journal of Hydraulic Engineering-ASCE* **128**(3): 306–321. doi:10.1061/(ASCE)0733-9429(2002)128:3(306).

Carbonneau PE, Bergeron N, Lane SN, 2005. Automated grain size measurements from airborne remote sensing for long profile measurements of fluvial grain sizes. *Water Resources Research* **41**(11). doi:10.1029/2005WR003994.

Carignan R, Lorrain S, 2000. Sediment dynamics in the fluvial lakes of the st. lawrence river: accumulation rates and characterization of the mixed sediment layer. *Canadian Jouranl of Fisheries and Aquatic Sciences* **57**(Suppl. 1): 63–77.

Carling P, 1988. The concept of dominant discharge applied to 2 gravel-bed streams in relation to channel stability thresholds. *Earth Surface Processes and Landforms* **13**(4): 355–367.

Caya D, Laprise R, 1999. A semi-implicit semi-Lagrangian regional climate model: The Canadian RCM. *Monthly Weather Review* **127**(3): 341–362.

Chaumont D, Chartier I, 2005. Développement de scénarios hydrologiques à des fins de modélisation de la dynamique sédimentaire des tributaires du Saint-Laurent dans un contexte de changements climatiques. Special report, Ouranos, Montréal, Canada, 46 pp. (in French).

Chow VT, 1950. *Open-channel Hydraulics*. McGraw-Hill, New York.

Church M, 1995. Geomorphic response to river flow regulation - case-studies and time-scales. *Regulated Rivers-Research & Management* **11**(1): 3–22.

Coulthard TJ, 2002. A cellular model of holocene upland river basin and alluvial fan evolution. *Earth Surface Processes and Landforms* **27**(3): 269. doi:10.1002/esp.318.

Coulthard TJ, Macklin MG, 2001. How sensitive are river systems to climate and land-use changes?: A model-based evaluation. *Journal of Quaternary Science* **16**(4): 347–351.

Coulthard TJ, Kirkby MJ, Macklin MG, 1999. Modelling the impacts of holocene environmental change in an upland river catchment using a cellular automaton approach. In *Fluvial Processes and Environmental Change*, eds. AG Brown, TM Quine, Wiley, Chichester, 31–46.

Coulthard TJ, Lewin J, Macklin MG, 2005. Modelling differential catchment response to environmental change. *Geomorphology* **69**(1-4): 222–241. doi:10.1016/j.geomorph.2005.01.008.

Coulthard TJ, Lewin J, Macklin MG, 2008. Non-stationarity of basin scale sediment delivery in response to climate change. In *Gravel-Bed Rivers VI: From Process, Understanding to River Restoration*, eds. H Habersack, H Piégay, M Rinaldi, Elsevier, 315–331. doi:10.1016/S0928-2025(07)11131-1.

Croley TEI, 2003. Great Lakes climate change hydrologic impact assessment: I.J.C. Lake Ontario-St. Lawrence River regulation study. Technical memorandum glerl-126, National Oceanic and Atmospheric Administration, Ann Arbor, Michigan.

Crosato A, 2007. Effects of smoothing and regridding in numerical meander migration models. *Water Resources Research* **43**(1). doi:10.1029/2006WR005087.

Crowder DW, Knapp HV, 2005. Effective discharge recurrence intervals of Illinois streams. *Geomorphology* **64**(3-4): 167–184. doi:10.1016/j.geomorph.2004.06.006.

Cudden JR, Hoey TB, 2003. The causes of bedload pulses in a gravel channel: the implications of bedload grain-size distributions. *Earth Surface Processes and Landforms* **28**(13): 1411–1428. doi:10.1002/esp.521.

Cui YT, Parker G, Paola C, 1996. Numerical simulation of aggradation and downstream fining. *Journal of Hydraulic Research* **34**(2): 185–204.

Darby SE, Thorne CR, 1996. Development and testing of riverbank-stability analysis. *Journal of Hydraulic Engineering-ASCE* **122**(8): 443–454.

Darby SE, Alabyan AM, Van de Wiel MJ, 2002. Numerical simulation of bank erosion and channel migration in meandering rivers. *Water Resources Research* **38**(9): 1163. doi:10.1029/2001WR000602.

Darby SE, Rinaldi M, Dapporto S, 2007. Coupled simulations of fluvial erosion and mass wasting for cohesive river banks. *Journal of Geophysical Research* **112**(f3): F03022. doi:10.1029/2006JF000722.

Dargahi B, 2004. Three-dimensional flow modelling and sediment transport in the River Klaralven. *Earth Surface Processes and Landforms* **29**(7): 821–852. doi:10.1002/esp.1071.

De Vriend HJ, Havinga FJ, Havinga H, Visser PJ, Wang ZB, 2000. *Rivierwaterbouwkunde CTwa3340. River Engineering, Lecture notes*. Delft University of Technology, Delft, The Netherlands.

De Wit MJM, van den Hurk B, Warmerdam PMM, Torfs PJJF, Roulin E, van Deursen WPA, 2007. Impact of climate change on low-flows in the river Meuse. *Climatic Change* **82**(3-4): 351–372. doi:10.1007/s10584-006-9195-2.

Dearing JA, 2006. Climate-human-environment interactions: resolving our past. *Climate of The Past* **2**(2): 187–203.

Dearing JA, Battarbee RW, Dikau R, Larocque I, Oldfield F, 2006. Human-environment interactions: learning from the past. *Regional Environmental Change* **6**(1-2): 1–16. doi:10.1007/s10113-005-0011-8.

DHI, 1999. *MIKE21C User'S Guide and Scientific Documentation*. Horsholm, Denmark.

Diaz-Nieto J, Wilby RL, 2005. A comparison of statistical downscaling and climate change factor methods: impacts on low flows in the River Thames, United Kingdom. *Climatic Change* **69**(2-3): 245–268. doi:10.1007/s10584-005-1157-6.

Dietrich WE, Gallinati JD, 1991. *Field Experiment and Measurement Programmes in Geomorphology*, A. A. Balkema, Rotterdam, chap. Fluvial geomorphology, 169–220.

Dietrich WE, Kirchner JW, Ikeda H, Iseya F, 1989. Sediment supply and the development of the coarse surface layer in gravel-bedded rivers. *Nature* **340**(6230): 215–217.

Doyle MW, Harbor JM, 2003. A scaling approximation of equilibrium timescales for sand-bed and gravel-bed rivers responding to base-level lowering. *Geomorphology* **54**(3-4): 217–223. doi:10.1016/S0169-555X(02)00357-4.

Doyle MW, Shields CA, 2008. An alternative measure of discharge effectiveness. *Earthe Surface Processes and Landforms* **33**(2): 308–316. doi:10.1002/esp.1543.

Doyle MW, Shields D, Boyd KF, Skidmore PB, Dominick D, 2007. Channel-forming discharge selection in river restoration design. *Journal of Hydrologic Engineering-ASCE* **133**(7): 831–837.

doi:10.1061/(ASCE)0733-9429(2007)133:7(831).

Duc BM, Wenka TA, Rodi W, 2004. Numerical modeling of bed deformation in laboratory channels. *Journal of Hydraulic Engineering-ASCE* **130**(9): 894–904. doi:10.1061/(ASCE)0733-9429(2004)130:9)894).

Eaton BC, Church M, 2004. A graded stream response relation for bed load-dominated streams. *Journal of Geophysical Research-Earth Surface* **109**(F3). doi:10.1029/2003JF000062.

Eaton BC, Church M, Millar RG, 2004. Rational regime model of alluvial channel morphology and response. *Earth Surface Processes and Landforms* **29**(4): 511–529. doi:10.1002/esp.1062.

Egiazaroff IV, 1965. Calculation of nonunifrom sediment concentrations. *Journal of Hydraulic Division, ASCE* **91**(4): 225–247.

Einstein HA, 1950. The bed-load function for sediment transport in open channel flows. Tech. bull, 1026, Soil Conservation Services, U.S. Dep. of Agric., Washington D.C.

El kadi Abderrezzak K, Paquier A, 2009. One-dimensional numerical modeling of sediment transport and bed deformation in open channels. *Water Resources Research* **45**. doi:10.1029/2008WR007134.

Emmett WW, Wolman MG, 2001. Effective discharge and gravel-bed rivers. *Earth Surface Processes and Landforms* **26**(13): 1369–1380.

Engelund F, 1974. Flow and bed topography in channel beds. *Journal of Hydraulic Division, Proceeding ASCE* **100**: 1631–1648.

Fagherazzi L, Guay R, Sassi T, 2005. Climate Change analysis of the Ottawa River System. Report for the commission mixte internationale - Lake Ontario-St. Lawrence River study on discharge regulation, 72, 72p.

Federici B, Paola C, 2003. Dynamics of channel bifurcations in noncohesive sediments. *Water Resources Research* **39**(6). doi:10.1029/2002WR001434.

Ferguson R, 2003. The missing dimension: effects of lateral variation on 1-D calculations of fluvial bedload transport. *Geomorphology* **56**(1-2): 1. doi:10.1016/S0169-555X(03)00042-4.

Ferguson R, 2008. Gravel-bed rivers at the reach scale. In *Gravel-Bed Rivers VI*, eds. H Habersack, H Piegay, M Rinaldi, Elsevier, chap. Gravel-bed rivers at the reach scale, 33–53.

Ferguson RI, Church M, 2009. A critical perspective on 1D modeling of river processes: gravel load and aggradation in lower Fraser River. *Water Resources Research* doi:10.1029/2009WR007740.

Ferguson RI, Church M, Weatherly H, 2001. Fluvial aggradation in Vedder River: Testing a one-dimensional sedimentation model. *Water Resources Research* **37**(12): 3331–3347.

Ferguson RI, Parsons DR, Lane SN, Hardy RJ, 2003. Flow in meander bends with recirculation at the inner bank. *Water Resources Research* **39**(11). doi:10.1029/2003WR001965.

Fowler HJ, Kilsby CG, Stunell J, 2007. Modelling the impacts of projected future climate change on water resources in north-west England. *Hydrology and Earth System Sciences* **11**(3): 1115–1124.

Frings RM, Kleinhans MG, 2008. Complex variations in sediment transport at three large river bifurcations during discharge waves in the river Rhine. *Sedimentology* **55**(5): 1145–1171. doi:10.1111/j.1365-3091.2007.00940.x.

Gaeuman D, Schmidt JC, Wilcock PR, 2005. Complex channel responses to changes in stream flow and sediment supply on the lower Duchesne River, Utah. *Geomorphology* **64**(3-4): 185–206.

doi:10.1016/j.geomorph.2004.06.007.

Gaudet JM, Roy AG, Best JL, 1994. Effect of orientation and size of Helley-Smith sampler on its efficiency. *Journal of Hydraulic Engineering* **120**(6): 758–766.

Gibson CA, 2005. Flow regime alterations under changing climate in two river basins: implications for freshwater ecosystems. *River Research and Applications* **21**(8): 849. doi:10.1002/rra.855.

Gomez B, Cui Y, Kettner AJ, Peacock DH, Syvitski JPM, 2009. Simulating changes to the sediment transport regime of the Waipaoa River, New Zealand, driven by climate change in the twenty-first century. *Global and Planetary Change* **67**(3-4): 153–166. doi:10.1016/j.gloplacha.2009.02.002.

Goudie AS, 2006. Global warming and fluvial geomorphology. *Geomorphology* **79**(3-4): 384–394. doi:10.1016/j.geomorph.2006.06.023.

Graham LP, Andreasson J, Carlsson B, 2007. Assessing climate change impacts on hydrology from an ensemble of regional climate models, model scales and linking methods - a case study on the Lule River basin. *Climatic Change* **81**(Suppl. 1): 293–307. doi:10.1007/s10584-006-9215-2.

Grass CA, 1970. Initial instability of fine bed sand. *Journal of Hydraulics Division, ASCE* **93**(HY3): 619–627.

Hancock GR, 2009. A catchment scale assessment of increased rainfall and storm intensity on erosion and sediment transport for northern australia. *GEODERMA* **152**(3-4): 350–360. doi:10.1016/j.geoderma.2009.07.003.

Hansen J, Sato M, Ruedy R, Lo K, Lea DW, Medina-Elizade M, 2006. Global temperature change. *Proceedings of the National Academy of Sciences of the United States of America* **103**(39): 14288–14293. doi:10.1073/pnas.0606291103.

Hassan MA, Klein M, 2002. Fluvial adjustment of the Lower Jordan River to a drop in the Dead Sea level. *Geomorphology* **45**(1-2): 21–33.

Havis RN, Alonso CV, King JG, 1996. Modeling sediment in gravel-bedded streams using HEC-6. *Journal of Hydraulic Engineering-ASCE* **122**(10): 559–564.

Hay LE, Wilby RJL, Leavesley GH, 2000. A comparison of delta change and downscaled GCM scenarios for three mountainous basins in the United States. *Journal of the American Water Resources Association* **36**(2): 387–397.

Heniche M, Secretan Y, Boureau P, Leclerc M, 2000. A two-dimensional finite element drying-wetting shallow water model for rivers and estuaries. *Advances in Water Resources* **23**: 359–372.

Hey RD, 1986. River mechanics. *Journal of the Institution of Water Engineers and Scientists* **40**(2): 139–158.

Hodgkins GA, Dudley RW, 2006. Changes in the timing of winter-spring streamflows in eastern North America, 1913-2002. *Geophysical Research Letters* **33**(6). doi:10.1029/2005GL025593.

Hoey TB, Ferguson RI, 1994. Numerical-simulation of downstream fining by selective transport in gravel-bed rivers - model development and illustration. *Water Resources Research* **30**(7): 2251–2260.

Hoey TB, Ferguson RI, 1997. Controls of strength and rate of downstream fining above a river base level. *Water Resources Research* **33**(11): 2601–2608.

Hoey TB, Bishop P, Ferguson RI, 2003. Testing numerical models in geomorphology: How can we ensure critical use of model predictions? In *Prediction in Geomorphology*, eds. P Wilcock, R Iverson, AGU Geophysical Monograph 135, Washington, DC, 241–256. doi:10.1029/135GM017.

Howard A, 1988. *Modelling geomorphological systems*, Wiley, Chichester, chap. Equilibrium models in geomorphology, 49–72.

Hudon C, 2004. Shift in wetland plant composition and biomass following low-level episodes in the St. Lawrence River: looking into the future. *Canadian Journal of Fisheries and Aquatic Sciences* **61**(4): 603–617. doi:10.1139/f04-031.

Hudon C, Carignan R, 2008. Cumulative impacts of hydrology and human activities on water quality in the St. Lawrence River (Lake Saint-Pierre, Quebec, Canada). *Canadian Journal of Fisheries and Aquatic Sciences* **65**(6): 1165–1180. doi:10.1139/F08-069.

Hulse D, Branscomb A, Enright C, Bolte J, 2009. Anticipating floodplain trajectories: a comparison of two alternative futures approaches. *Landscape Ecology* **24**(8): 1067–1090. doi:10.1007/s10980-008-9255-2.

Hunt JCR, 2002. Floods in a changing climate: a review. *Philosophical Transactions of the Royal Society A - Mathematical, Physical and Engineering Sciences* **360**(1796): 1531–1543. doi:10.1098/rsta.2002.1016.

IJC, 2008. A description of plan 2007. Tech. rep., International Joint Commission, http://www.ijc.org/LOSLdocuments/.

IPCC, 2007. *Climate change 2007: the physical science basis*. Contribution of Working Group I to the Fourth Assessment Report of the Intergovernmental Panel on Climate Change. Cambridge University Press, Cambridge, United Kingdom and New York, USA.

Jacques D, 1986. Cartographie des terres humides et des milieux environnants du lac Saint-Pierre. Tech. rep., Rapport présenté à la Corporation pour mise en valeur du Lac St-Pierre (COLASP), (in French).

Jansen PP, Van Bendegom J, Van den Berg J, De Vries M, Zanen A, 1979. *Principles of River Engineering: The non-tidal alluvial River*. Delftse Uitgevers Maatschappij, Delft, The Netherlands.

Kay AL, Reynard NS, Jones RG, 2006. RCM rainfall for UK flood frequency estimation. I. method and validation. *Journal of Hydrology* **318**(1-4): 151–162. doi:10.1016/j.jhydrol.2005.06.012.

Kirchner JW, Finkel RC, Riebe CS, Granger DE, Clayton JL, King JG, Megahan WF, 2001. Mountain erosion over 10 yr, 10 k.y., and 10 m.y. time scales. *Geology* **29**(7): 591–594.

Kleinhans MG, Jagers HRA, Mosselman E, Sloff CJ, 2008. Bifurcation dynamics and avulsion duration in meandering rivers by one-dimensional and three-dimensional models. *Water Resources Research* **44**(8). doi:10.1029/2007WR005912.

Knighton D, 1998. *Fluvial Forms and Processes: a New Perspective*. Arnold, London.

Knox JC, 2000. Sensitivity of modern and Holocene floods to climate change. *Quaternary Science Reviews* **19**(1-5): 439–457.

Komar PD, 1996. Entrainment of sediments from deposits of mixed grain sizes and densities. In *Advances in fluvial dynamics and stratigraphy*, eds. PA Carling, MR Dawson, Wiley, Chichester, New York, 127–269.

Kundzewicz ZW, Ulbrich U, Brucher T, Graczyk D, Kruger A, Leckebusch GC, Menzel L, Pinskwar I, Radziejewski M, Szwed M, 2005. Summer floods in central Europe - Climate change track? *Natural Hazards* **36**(1-2): 165–189. doi:10.1007/s11069-004-4547-6.

Kundzewicz ZW, Mata LJ, Arnell NW, Döll P, Kabat P, Jiménez B, Miller KA, Oki T, Sen Z, Shiklomanov IA, 2007. Freshwater resources and their management. In *Contribution of Working Group II to the Fourth Assessment Report of the Intergouvernemental Panel on Climate Change*, eds. ML Parry, OF Canziani, JP Palutikof, P van der Linden, CE Hanson, Cambridge University Press, Cambridge, UK, 173–210.

Lane SN, Ferguson RI, 2005. Modelling reach-scale fluvial flows. In *Computational Fluid Dynamics: Applications in environmental hydraulics*, eds. PD Bates, SN Lane, RI Ferguson, Wiley. Chichester ed. doi:10.1029/2001WR000602.

Lane SN, Tayefi V, Reid SC, Yu D, Hardy RJ, 2007. Interactions between sediment delivery, channel change, climate change and flood risk in a temperate upland environment. *Earth Surface Processes and Landforms* **32**(3): 429–446. doi:10.1002/esp.1404.

Lane SN, Tayefi V, Reid SC, Yu D, Hardy RJ, 2008. Reconceptualising coarse sediment delivery problems in rivers as catchment-scale and diffuse. *Geomorphology* **98**(3-4): 227–249. doi:10.1016/j.geomorph.2006.12.028.

Langendoen EJ, 2001. Evaluation of the effectiveness of selected computer models of depth-average free surface flow and sediment transport to predict the effect of hydraulic structures and river morphology. Tech. rep., National Sedimentation Laboratory, USDA Agricultural Research Service, Oxford, MS, USA.

Laprise R, 2008. Regional climate modelling. *Journal of Computational Physics* **227**(7): 3641–3666. doi:10.1016/j.jcp.2006.10.024.

Leclerc M, Bellemare JF, Dumas G, Dhatt G, 1990. A finite-element model of estuarian and river flows with moving boundaries. *Advances in Water Resources* **13**(4): 158–168.

Leclerc M, Secretan Y, Heniche M, Ouadra TBMJ, Marion J, 2003. Une méthode prédictive non biaisée et géoréférencée d'estimation des dommages résidentiels d'inondation. *Canadian Journal of Civil Engineering* **30**(5): 914–922. doi:10.1139/l03-065.

Lenderink G, Buishand A, van Deursen W, 2007. Estimates of future discharges of the river Rhine using two scenario methodologies: direct versus delta approach. *Hydrology and Earth System Sciences* **11**(3): 1143–1159.

Lenzi MA, Mao L, Comiti F, 2006. Effective discharge for sediment transport in a mountain river: Computational approaches and geomorphic effectiveness. *Journal of Hydrology* **326**(1-4): 257–276. doi:10.1016/j.jhydrol.2005.10.031.

Leopold LB, Bull WB, 1979. Base level, aggradation, and grade. *Proceedings of The American Philosophical Society* **123**(3): 168–202.

Leutbecher M, Palmer TN, 2008. Ensemble forecasting. *Journal of Computational Physics* **227**(7): 3515–3539. doi:10.1016/j.jcp.2007.02.014.

Li SS, Millar RG, 2007. Simulating bed-load transport in a complex gravel-bed river. *Journal of Hydraulic Engineering-ASCE* **133**(3): 323–328. doi:10.1061/(ASCE)0733-9429(2007)133:3(323).

Li SS, Millar RG, Islam S, 2008. Modelling gravel transport and morphology for the Fraser River Gravel Reach, British Columbia. *Geomorphology* **95**(3-4): 206–222. doi:10.1016/j.geomorph.2007.06.010.

Longfield SA, Macklin MG, 1999. The influence of recent environmental change on flooding and sediment fluxes in the Yorkshire Ouse basin. *Hydrological Processes* **13**: 1051–1066.

LOSL, 2006. Options for managing Lake Ontario and Saint-Lawrence River water levels and flows. Final report, International Lake Ontario-St. Lawrence River Study Board, http://www.losl.org/reports/finalreport-e.html.

Lu Yj, Wang Zy, 2009. 3d numerical simulation for water flows and sediment deposition in dam areas of the three gorges project. *Journal of Hydraulic Engineering-ASCE* **135**(9): 755–769. doi:10.1061/(ASCE)0733-9429(2009)135:9(755).

Madej MA, Sutherland DG, Lisle TE, Pryor B, 2009. Channel responses to varying sediment input: A flume experiment modeled after Redwood Creek, California. *Geomorphology* **103**(4): 507–519. doi:10.1016/j.geomorph.2008.07.017.

McKean J, Isaak D, 2009. Improving stream studies with a samll-footprint green lidar. *EOS* **90**(39): 341–342.

McLean DG, Church M, 1999. Sediment transport along lower Fraser River - 2. estimates based on the long-term gravel budget. *Water Resources Research* **35**(8): 2549–2559.

McLean DG, Church M, Tassone B, 1999. Sediment transport along lower Fraser River - 1. measurements and hydraulic computations. *Water Resources Research* **35**(8): 2533–2548.

Meehl GA, Covey C, Delworth T, Latif M, McAvaney B, Mitchell JFB, Stouffer RJ, Taylor KE, 2007. The WCRP CMIP3 multimodel dataset - a new era in climate change research. *Bulletin of the American Meteorological Society* **88**(9): 1383–1394. doi:10.1175/BAMS-88-9-1383.

Merritt WS, Alila Y, Barton M, Taylor B, Cohen S, Neilsen D, 2006. Hydrologic response to scenarios of climate change in sub watersheds of the Okanagan basin, British Columbia. *Journal of Hydrology* **326**(1-4): 79–108. doi:10.1016/j.jhydrol.2005.10.025.

Middelkoop H, Daamen K, Gellens D, Grabs W, Kwadijk JCJ, Lang H, Parmet BWAH, Schadler B, Schulla J, Wilke K, 2001. Impact of climate change on hydrological regimes and water resources management in the Rhine basin. *Climatic Change* **49**(1-2): 105–128.

Milly P, Wetherald R, Dunne K, Delworth T, 2002. Increasing risk of great floods in a changing climate. *Nature* **415**: 514–517.

Minville M, Brissette F, Leconte R, 2008. Uncertainty of the impact of climate change on the hydrology of a nordic watershed. *Journal of Hydrology* **358**(1-2): 70–83. doi:10.1016/j.jhydrol.2008.05.033.

Miori SR, Repetto R, M Tubino M, 2006. A one-dimensional model of bifurcations in gravel bed channels with erodible banks. *Water Resources Research* **42**(11): W11413. doi:10.1029/2006WR004863.

Molnar P, Anderson RS, Kier G, Rose J, 2006. Relationships among probability distributions of stream discharges in floods, climate, bed load transport, and river incision. *Journal of Geophysical Research-Earth Surface* **111**(F2). doi:10.1029/2005JF000310.

Morin J, Bouchard A, 2001. Les bases de la modélisation du tronçon Montréal / Trois-Rivières. Rapport scientifique smc-hydrométrie rs-100, Environnement Canada, Sainte-Foy, in French.

Morin J, Côté JP, 2003. Modifications anthropiques sur 150 ans au Lac Saint-Pierre: une fenêtre sur les transformations de l’écosystème du Saint-Laurent. *VertigO – La revue en sciences de l’environnement* **4**(3): 1–10, (in French).

Morin J, Boudreau P, Secretan Y, Leclerc M, 2000. Pristine Lake Saint-François, St. Lawrence River: Hydrodynamic simulation and cumulative impact. *Journal of Great Lakes Research* **26**(4): 383–401.

Morin J, Champoux O, Martin S, Turgeon K, 2005. Modélisation intégrée de la response de l'écosystème dans le fleuve Saint-Laurent: Rapport final des activités enterprises dans le cadre du plan d'étude sur la regularisation du lac Ontario et du fleuve Saint-Laurent. Rapport scientifique – RS-108, Environnement Canada, SMC-Hydrologie, Sainte-Foy, Québec, Canada, (in French).

Morin J, Champoux O, Martin S, 2009. Analyse de l'impact des changements climatiques et de travaux de maintient du niveau d'eau sur les indicateurs biotiques du fleuve Saint-Laurent. Rapport scientifique rs-109, Service Météorologique du Canada–Hydrologie, Environnement Canada, Sainte-Foy, Canada, 219p. (in French).

Mosselman E, 1998. Morphological modelling of rivers with erodible banks. *Hydrological Processes* **12**(8): 1357–1370.

Mueller EN, Batalla RJ, Garcia C, Bronstert A, 2008. Modeling bed-load rates from fine grain-size patches during small floods in a gravel-bed river. *Journal of Hydraulic Engineering-ASCE* **134**(10): 1430–1439. doi:10.1061/(ASCE)0733-9429(2008)134:10(1430).

Murray AB, Paola C, 1994. A cellular model of braided rivers. *Nature* **371**(6492): 54–57.

Nagata N, Hosoda T, Nakato T, Muramoto Y, 2005. Three-dimensional numerical model for flow and bed deformation around river hydraulic structures. *Journal of Hydraulic Engineering-ASCE* **131**(12): 1074–1087. doi:10.1061/(ASCE)0733-9429(2005)131:12(1074).

Nakicenovic N, Alcamo J, Davis G, de Vries B, Fenhann J, Gaffin S, Gregory K, Grubler A, Kram TY, Kram T, La Rovere EL, Michaelis L, Moris S, Morita T, Pepper W, Pitcher H, Price L, Raihi K, Roehrl A, Rogner HH, Sankovovski A, Schlesinger M, Shukla P, Smith R Sand Swart, van Rooijen S, Victor N, Dadi Z, 2000. *IPCC Special Report on Emissions Scenarios*. Cambridge University Press, Cambridge, UK.

Nash DB, 1994. Effective sediment-transporting discharge from magnitude-frequency analysis. *Journal of Geology* **102**(1): 79–95.

Nash JE, Sutcliffe JV, 1970. River flow forecasting through conceptual models. *Journal of Hydrology* **10**(3): 282–290.

Nearing MA, Jetten V, Baffaut C, Cerdan O, Couturier A, Hernandez M, Le Bissonnais Y, Nichols MH, Nunes JP, Renschler CS, Souchere V, Van Oost K, 2005. Modeling response of soil erosion and runoff to changes in precipitation and cover. *CATENA* **61**(2-3): 131–154. doi:10.1016/j.catena.2005.03.007.

Olsen NRB, 2003. Three-dimensional CFD modeling of self-forming meandering channel. *Journal of Hydraulic Engineering-ASCE* **129**(5): 366–372. doi:10.1061/(ASCE)0733-9429(2003)129:5(366).

Ouranos, 2004. *Adapting to climate change*. Ouranos, Montréal, Canada. ISBN 2-923292-01-4.

Papanicolaou AN, Elhakeem M, Krallis G, Prakash S, Edinger J, 2008. Sediment transport modeling review - Current and future developments. *Journal of Hydraulic Engineering-ASCE* **134**(1): 1–14.

Park I, Jain AM, 1987. Numerical simulation of degradation of alluvial channel beds. *Journal of Hydraulic Engineering* **113**(7): 845–859.

Parker G, 1990a. The "ACRONYM" series of PASCAL programs for computing bedload transport in gravel rivers. External memo m-220, University of Minneapolis, St. Anthony Falls Hydraulic Laboratoy, Minneapolis, MN, USA, 124 pp.

Parker G, 1990b. Surface-based bedload transport relation for gravel rivers. *Journal of Hydraulic Research* **28**(4): 417–436.

Parker G, 1991. Selective sorting and abrasion of river gravel .1. theory. *Journal of Hydraulic Engineering-ASCE* **117**(2): 131–149.

Parker G, Sutherland AJ, 1990. Fluvial armor. *Journal of Hydraulic Research* **28**(5): 529–544.

Parker G, Klingeman PC, McLean DG, 1982. Bedload and size distribution in paved gravel-bed streams. *Journal of The Hydraulics Division-ASCE* **108**(4): 544–571.

Parrott L, 2002. Complexity and the limits of ecological engineering. *Transactions of The ASAE* **45**(5): 1697–1702.

Phillips JD, 2002. Geomorphic impacts of flash flooding in a forested headwater basin. *Journal of Hydrology* **269**(3-4): 236–250.

Phillips JD, 2003. Sources of nonlinearity and complexity in geomorphic systems. *Progress In Physical Geography* **27**(1): 1–23. doi:10.1191/0309133303pp340ra.

Pickup G, Warner RF, 1976. Effects of hydrologic regime on magnitude and frequency of dominant discharge. *Journal of Hydrology* **29**(1-2): 51–75.

Piégay H, Darby SE, Mosselman E, Surian N, 2005. A review of techniques available for delimiting the erodible river corridor: A sustainable approach to managing bank erosion. *River Research and Applications* **21**(7): 773–789. doi:10.1002/rra.881.

Powell J, 1875. *Exploration of the Colorado River of the West*. Washington, D.C., U.S. Gov. Printing Office.

Proffitt GT, Sutherland AJ, 1983. Transport of non-uniform sediments. *Journal of Hydraulic Research* **21**(1): 33–43.

Prudhomme C, Reynard N, Crooks S, 2002. Downscaling of global climate models for flood frequency analysis: where are we now? *Hydrological Processes* **16**(6, Sp. Iss. SI): 1137–1150. doi:10.1002/hyp.1054.

Prudhomme C, Jakob D, Svensson C, 2003. Uncertainty and climate change impact on the flood regime of small UK catchments. *Journal of Hydrology* **277**(1-2): 1–23. doi:10.1016/S0022-1694(03)00065-9.

Pruski FF, Nearing MA, 2002. Runoff and soil-loss responses to changes in precipitation: A computer simulation study. *Journal of Soil and Water Conservation* **57**(1): 7–16.

Quilbé R, Rousseau AN, Moquet JS, Trinh NB, Dibike Y, Gachon P, Chaumont D, 2008. Assessing the effect of climate change on river flow using general circulation models and hydrological modelling - application to the Chaudière River, Quebec, Canada. *Canadian Water Resources Journal* **33**(1): 73–93.

Rathburn SL, Wohl EE, 2001. One-dimensional sediment transport modeling of pool recovery along a mountain channel after a reservoir sediment release. *Regulated Rivers-Research & Management* **17**(3): 251–273.

Raupach MR, Marland G, Ciais P, Le Quéré C, Canadell JG, Klepper G, Field CB, 2007. Global and regional drivers of accelerating CO2 emissions. *Proc. Natl. Acad. Sci. U.S.A.* **104**(24): 10288–10293.

doi:10.1073/pnas.0700609104.

Raven EK, Lane SN, Ferguson RI, Bracken LJ, 2009. The spatial and temporal patterns of aggradation in a temperate, upland, gravel-bed river. *Earth Surface Processes and Landforms* **34**(9): 1181–1197. doi:10.1002/esp.1783.

Reid SC, Lane SN, Berney JM, Holden J, 2007a. The timing and magnitude of coarse sediment transport events within an upland, temperate gravel-bed river. *Geomorphology* **83**(1-2): 152–182. doi:10.1016/j.geomorph.2006.06.030.

Reid SC, Lane SN, Montgomery DR, Brookes CJ, 2007b. Does hydrological connectivity improve modelling of coarse sediment delivery in upland environments? *Geomorphology* **90**(3-4): 263–282. doi:10.1016/j.geomorph.2006.10.023.

Reynard NS, Prudhomme C, Crooks SM, 2001. The flood characteristics of large UK Rivers: Potential effects of changing climate and land use. *Climatic Change* **48**(2-3): 343–359.

Rhodes DD, 1987. The b-f-m diagram for downstream hydraulic geometry. *Geografiska Annaler Series* **69 A**(1): 147–161.

Riad K, 1961. *Analytical and experimental study of bed load distribution at alluvial diversions*. Ph.D. thesis, Dissertation at Delft University of Technology, Waltman, Delft.

Ribberink JS, 1987. *Mathematical modelling of one-dimensional morphological changes in rivers with non-uniform sediments*. Ph.D. thesis, Delft University of Technology, The Netherlands, communications on Hydraulic and Geotechnical Engineering, No. 87-2, ISSN 0169-1182.

Rice SP, Church M, Wooldridge CL, Hickin EJ, 2009. Morphology and evolution of bars in a wandering gravel-bed river; lower Fraser river, British Columbia, Canada. *Sedimentology* **56**(3): 709–736. doi:10.1111/j.1365-3091.2008.00994.x.

Robson AJ, 2002. Evidence for trends in UK flooding. *Philosophical Transactions of the Royal Society of London Series A - Mathematical, Physical and Engineering Sciences* **360**(1796): 1327–1343. doi:10.1098/rsta.2002.1003.

Rondeau B, Cossa D, Gagnon P, Bilodeau L, 2000. Budget and sources of suspended sediment transported in the St. Lawrence River, Canada. *Hydrological Processes* **14**: 21–36.

Rosberg J, Andréasson J, 2006. From Delta change to Scaling and direct use of RCM output. In *European Conference on Impacts of Climate Change on Renewable Energy Sources*. Reykjavik, Iceland, June 5-9.

Roy L, Leconte R, Brissette FP, Marche C, 2001. The impact of climate change on seasonal floods of a southern Quebec River Basin. *Hydrological Processes* **15**(16): 3167–3179.

Rydgren B, Graham P, Basson M, Wisaeus D, 2007. Addressing climate change-driven increased hydrological variability in environmental assessments for hydropower projects – a scoping study. Tech. rep., Vattenfall Power Consultant AB, Sweden, 41 pp.

Schumm SA, 1977. *The Fluvial System*. Wiley, New York.

Schumm SA, 1993. River response to baselevel change - implications for sequence stratigraphy. *Journal of Geology* **101**(2): 279–294.

Secretan Y, Leclerc M, 1998. Modeleur: a 2D Hydrodynamic GIS and simulation software. In *Proceedings of*

Hydroinformatics Conference. Copenhagen, August.

Secretan Y, Heniche M, Leclerc M, 2000a. DISPERSIM: un outil de modélisation par éléments finis de la dispersion de contaminants en milieu fluvial. Rapport scientifique no. r558, INRS-Eau, in French.

Secretan Y, Roy Y, Ganger M Yand Leclerc, 2000b. Modeleur 1.0a07 – Guide d'utilistion. Rapport inrs-eau r482-g3f, INRS-Eau, in French.

Shields A, 1936. Anwendung der Ähnlichkeitsmechanik und der Turbulenzforschung auf die Geschiebebewegung. *Mitteilungen der Preussischen Versuchsanstalt für Wasserbau und Schiffbau* **Heft 26**, in German.

Shields FD, Copeland RR, Klingeman PC, Doyle MW, Simon A, 2003. Design for stream restoration. *Journal of Hydraulic Engineering-ASCE* **129**(8): 575–584. doi:10.1061/(ASCE)0733-9429(2003)129:8(575).

Simon A, 1989. A model of channel response in disturbed alluvial channels. *Earth Surface Processes and Landforms* **14**(1): 11–26.

Simon A, 1992. Energy, time, and channel evolution in catastrophically disturbed fluvial systems. *Geomorphology* **5**(3-5): 345–372.

Simon A, Darby SE, 1997. Process-form interactions in unstable sand-bed river channels: A numerical modeling approach. *Geomorphology* **21**(2): 85–106.

Simon A, Hupp CR, 1986. Channel evolution in modified Tennessee streams. In *Proceedings, Fourth Federal Interagency Sedimentation Conference*. 71–82.

Slingerland RL, Snow RS, 1988. Stability analysis of a rejuvenated fluvial system. *Zeitschrift für Geomorphologie* **67**: 93–102.

St-Hilaire A, Ouarda TBMJ, Lachance M, Bobee B, Gaudet J, Gignac C, 2003. Assessment of the impact of meteorological network density on the estimation of basin precipitation and runoff: a case study. *Hydrological Processes* **17**(18): 3561–3580. doi:10.1002/hyp.1350.

Struiksma N, Olesen KW, Flokstra C, De Vriend HJ, 1985. Bed deformation in curved alluvial channels. *Journal of Hydraulic Research* **23**(1): 57–79.

Summerfield MM, 1985. Tectonic geomorphology. In *Plate tectonics and landscape development on the African continent*, eds. M Morisawa, J Hack, Allen and Uwin, Boston, vol. 2, 27–51.

Syvitski JP, Morehead MD, Nicholson M, 1998. HYDROTREND: A climate-driven hydrologic-transport model for predicting discharge and sediment load to lakes or oceans. *Computers & Geosciences* **24**(1): 51–68.

Talbot T, Lapointe M, 2002. Numerical modeling of gravel bed river response to meander straightening: The coupling between the evolution of bed pavement and long profile. *Water Resources Research* **38**(6). doi:10.1029/2001WR000330.

Talmon AM, Struiksma N, Van Mierlo MCLM, 1995. Laboratory measurements of the direction of sediment transport on transverse alluvial-bed slopes. *Journal of Hydraulic Research* **33**(4): 495–517.

Thodsen H, Hasholt B, Kjærsgaards JH, 2008. The influence of climate change on suspended sediment transport in Danish rivers. *Hydrological Processes* **22**(6): 764–774. doi:10.1002/hyp.6652.

Tingsanchali T, Supharatid S, 1996. Experimental investigation and analysis of HEC-6 river morphological model. *Hydrological Processes* **10**(5): 747–761.

Toffaleti FB, 1968. A procedure for computation of the total river sand discharge and detailed distribution, bed to surface. Technical rep. no. 5, Committee on Channel Stabilization, Corps of Engineers.

Torizzo M, Pitlick J, 2004. Magnitude-frequency of bed load transport in mountain streams in Colorado. *Journal of Hydrology* **290**(1-2): 137–151. doi:10.1016/j.hydrol.2003.12.001.

Toro-Escobar CM, Parker G, Paola C, 1996. Transfer function for the deposition of poorly sorted gravel in response to streambed aggradation. *Journal of Hydraulic Research* **34**(1): 35–53.

Tucker GE, Slingerland R, 1997. Drainage basin responses to climate change. *Water Resources Research* **33**(8): 2031–2047.

US Army Corps of Engineers, 1996. *HEC6 v4.1 User Manual*. Washington, DC.

Van Den Berg JH, 1995. Prediction of alluvial channel pattern of perennial rivers. *Geomorphology* **12**(4): 259–279.

Van Heijst MWIM, Postma G, 2001. Fluvial response to sea-level changes: a quantitative analogue, experimental approach. *Basin Research* **13**(3): 269–292.

Van Niekerk A, Vogel KR, Slingerland RL, Bridge JS, 1992. Routing of heterogeneous sediments over movable bed - model development. *Journal of Hydraulic Engineering-ASCE* **118**(2): 246–262.

Van Rijn LC, 1984. Sediment transport, part 1: Bed load transport. *Journal of Hydraulic Engineering* **110**(10): 1431–1456.

Van Rijn LC, 1987. *Mathematical modelling of morphological processes in the case of suspended sediment transport*. Ph.D. thesis, Delft University of Technology, delft Hydraulics report no. 382.

Vandenberghe J, 1995. Timescales, climate and river development. *Quaternary Science Reviews* **14**(6): 631–638.

Vandenberghe J, Maddy D, 2001. The response of river systems to climate change. *Quaternary International* **79**: 1–3.

Veldkamp A, Tebbens LA, 2001. Registration of abrupt climate changes within fluvial systems: insights from numerical modelling experiments. *Global and Planetary Change* **28**: 129–144.

Verhaar PM, Biron PM, Ferguson RI, Hoey TB, 2008. A modified morphodynamic model for investigating the response of rivers to short-term climate change. *Geomorphology* **101**(4): 674–682. doi:10.1016/j.geomorph.2008.03.010.

Verhaar PM, Biron PM, Ferguson RI, Hoey TB, in press. Numerical modelling of climate change impacts on Saint-Lawrence River tributaries. *Earth Surface Processes and Landforms*.

Vogel RM, Stedinger JR, Hooper RP, 2003. Discharge indices for water quality loads. *Water Resources Research* **39**(10). doi:10.1029/2002WR001872.

Wallingford, 1990. Sediment transport, the Ackers and White theory revised. Report sr237, HR Wallingford, Wallingford, England.

Wang ZB, Fokkink RJ, DeVries M, Langerak A, 1995. Stability of river bifurcations in 1D morphodynamic models. *Journal of Hydraulic Research* **33**(6): 739–750.

White WR, Day TJ, 1982. Transport of graded gravel bed material. In *Gravel-bed Rivers: Fluvial Processes, Engineering and Management*, eds. RD Hey, JC Bathurst, CR Thorne, Wiley, Chichester, 181–213.

White WR W Rand Milli, Crabbe AD, 1975. Sediment transport theories: a review. *Proceedings of the*

Institution of Civil Engineers **59**(2): 265–292.

Wilcock PR, 2001. The flow, the bed, and the transport: interaction in the flume and field. In *Gravel-bed rivers V*, ed. MP Mosley, Wellington, NZ Hydrol. Soc., 183–219.

Wilcock PR, Crowe JC, 2003. Surface-based transport model for mixed-size sediment. *Journal of Hydraulic Engineering-ASCE* **129**(2): 120–128. doi:10.1061/(ASCE)0733-9429(2003)129:2(120).

Willetts BB, Maizels JK, Florence J, 1987. The simulation of stream bed armouring and its consequences. In *Proceedings Institute of Civil Engineering Part I 82*. 799–814.

Wolman MG, Miller JP, 1960. Magnitude and frequency of forces in geomorphic processes. *Journal of Geology* **68**: 54–74.

Wu WM, Rodi W, Wenka T, 2000. 3D numerical modeling of flow and sediment transport in open channels. *Journal of Hydraulic Engineering-ASCE* **126**(1): 4–15.

Yang C, Simões F, 1999. Sediment transport and river morphologic changes. In *CADAM Proceedings Meeting in Zaragoza 18-19 November*. Spain, paper 18.

Zanichelli G, Caroni E, Fiorotto V, 2004. River bifurcation analysis by physical and numerical modeling. *Journal of Hydraulic Engineering-ASCE* **130**(3): 237–242. doi:10.1061/(ASCE)0733-9429(2004)130:3(237).

Zhang XB, Harvey KD, Hogg WD, Yuzyk TR, 2001. Trends in Canadian streamflow. *Water Resources Research* **37**(4): 987–998.

Appendix I

Accord des coauteurs et permission de l'éditeur

Patrick Michiel Verhaar, PhD, Geography

Article 1

Verhaar PM, Biron PM, Ferguson RI, Hoey TB, A modified morphodynamic model for investigating the response of rivers to short-term climate change, *Geomorphology*, 101(4),674–682, 1 November 2008.

By title of co-author of the article identified above I grand permission to Patrick Verhaar to include this article in his PhD-thesis entitled: *Numerical modelling of the impact of climate change on morphology of the Saint-Lawrence River and its tributaries*, which will be completed at Université de Montréal by the end of 2009.

Patrick Michiel Verhaar, PhD, Geography

Article 2

Verhaar PM, Biron PM, Ferguson RI, Hoey TB, Numerical modelling of climate change impacts on Saint-Lawrence River tributaries, *Earth Surface Processes and Landforms*, in press, accepted on October 14th 2009.

By title of co-author of the article identified above I grand permission to Patrick Verhaar to include this article in his PhD-thesis entitled: *Numerical modelling of the impact of climate change on morphology of the Saint-Lawrence River and its tributaries*, which will be completed at Université de Montréal by the end of 2009.

Patrick Michiel Verhaar, PhD, Geography

Article 3

Verhaar PM, Biron PM, Ferguson RI, Hoey TB, Implications of climate change for the magnitude and frequency of bed-material transport in tributaries of the Saint-Lawrence, *Hydrological Processes*, to be submitted.

By title of co-authors of the article identified above I grand permission to Patrick Verhaar to include this article in his PhD-thesis entitled: *Numerical modelling of the impact of climate change on morphology of the Saint-Lawrence River and its tributaries*, which will be completed at Université de Montréal by the end of 2009.

Appendix II

Bed material transport formulae

II.1 Wilcock and Crowe formula

The similarity collapse has the following form:

$$Q^{\star}_{si} = f(\frac{\tau}{\tau_{ri}}) \tag{II.1}$$

where τ is the bed shear stress, τ_{ri} is the reference shear stress of size fraction i and $Q^{\star}_{si}$ is the dimensionless sediment transport rate of size fraction i defined by:

$$Q^{\star}_{si} = \frac{(s-1)gq_{ib}}{F_i u^3_{\star}} \tag{II.2}$$

where s is the ratio of sediment to water density, g is the acceleration due to gravity, q_{ib} is the volumetric bed material transport per unit width of size i, F_i is the proportion of fraction i in surface size distribution and $u_{\star}$ is the shear velocity.

The shear stress reference value τ_{ri} is scaled against that of the mixture by comparing the grain size diameter:

$$\frac{\tau_{ri}}{\tau_{rs50}} = \left(\frac{D_i}{D_{s50}}\right)^k \tag{II.3}$$

where τ_{rs50} is the shear stress of D_{s50}, D_i is the grain size of fraction i, D_{s50} is the median grain size of bed surface and k, the exponent, is defined by:

$$k = \frac{0.67}{1 + exp\left(1.5 - \frac{D_i}{D_{sm}}\right)} \tag{II.4}$$

where D_{sm} is the mean grain size of bed surface. The function fitted to the transport observations is:

$$Q^{\star}_{si} = \begin{cases} 0.002\psi^{7.5} & \text{for } \psi < 1.35 \\ 14\left(1 - \frac{0.894}{\psi^{0.5}}\right)^{4.5} & \text{for } \psi \geq 1.35 \end{cases} \tag{II.5}$$

where $\psi = {}^{\tau}/_{\tau_{ri}}$.

II.2 Ackers and White formula

It is defined as:

$$Q_{si}^{\star} = C\left\{\frac{F_{gri}}{A_i} - 1\right\}^{d} \tag{II.6}$$

where $F_{gri}$is the mobility number of sediment in the ith fraction and C, A_i and d are empirical coefficients depending on the dimensionless particle size (D_{gri}).

$$Q_{si}^{\star} = \frac{X_i H}{s D_i}\left\{\frac{u_\star}{U}\right\}^{e} \tag{II.7}$$

where X_i is rate of sediment transport in terms of mass flow per unit flow rate for the ith fraction, H is the water depth, U is the mean velocity, e is a transition exponent that is a function of the dimensionless particle size.

$$F_{gri} = \frac{u_\star^{e}}{\left[g D_i (s-1)\right]^{1/2}}\left\{\frac{U}{\sqrt{32}\log_{10}\left(\alpha H / D_i\right)}\right\}^{1-e} \tag{II.8}$$

with $\alpha = 10$ for turbulent flow.

$$D_{gri} = D_i\left\{\frac{g(s-1)}{\nu^2}\right\}^{1/3} \tag{II.9}$$

where D_{gri} is the dimensionless particle size of the ith fraction and ν is the kinematic viscosity of water.

The coefficients e, A_i, d and C are defined as follows depending on the dimensionless particle size.

$D_{gri} > 60$:

$$e = 0.000 \tag{II.10}$$

$$A_i = 0.170 \tag{II.11}$$

$$d = 1.500 \tag{II.12}$$

$$C = 0.025 \tag{II.13}$$

$60 \geq D_{gri} \geq 1$:

$$e = 1.00 - 0.56\log_{10} D_{gri} \tag{II.14}$$

$$A_i = \frac{0.23}{\sqrt{D_{gri}}} + 0.14 \tag{II.15}$$

$$d = \frac{9.66}{D_{gr}} + 1.34 \tag{II.16}$$

$$\log_{10} C = 2.86\log_{10} D_{gri} - \left(\log_{10} D_{gri}\right)^2 - 3.53 \tag{II.17}$$

For Wallingford [1990] d and C are different from the original settings of Ackers and White [1973].

$D_{gri} > 60$: $\quad$ $60 \geq D_{gri} \geq 1$:

$$d = 1.78 \qquad \text{(II.18)}$$

$$d = \frac{6.83}{D_{gri}} + 1.67 \qquad \text{(II.19)}$$

$$\log_{10} C = 2.79 \log_{10} D_{gri} - (0.98 \log_{10} D_{gri})^2 - 3.46 \qquad \text{(II.20)}$$

In equation 2.4 A_i is replaced with A_i' for the White and Day [1982] settings and is calculated as follows:

$$A_i' = \left(0.4 \frac{D_a}{\sqrt{D_{50}}} + 0.6\right) A_i \qquad \text{(II.21)}$$

$$D_a = D_{50} \left(1.62 \left(\frac{D_{84}}{D_{16}}\right)^{0.5}\right)^{-0.55} \qquad \text{(II.22)}$$

where D_a is the particle size that begins to move under the same conditions as uniform material and D_{16}, D_{50} and D_{84} represent the subsurface particle size for which respectively 16%, 50% and 84% of the sediment sample is finer. Finally the sediment transport rate can be calculated from the sediment transport rate in terms of mass per unit flow rate (X_i):

$$Q_{si} = X_i Q \frac{\rho_s}{\rho} \qquad \text{(II.23)}$$

where Q_{si} is the total bed-material transport rate for fraction i, Q is the water discharge, ρ the density of water and ρ_s the density of sediments.

Appendix III

SEDROUT4-M FORTRAN code

In the first part of the SEDROUT4-M code the changes made are shortly described in reversed chronological order. This appendix presents code after describing some changes to the code that are not presented in Verhaar *et al.* [2008]. The version .22 is the one that is described in Verhaar *et al.* [2008] (see chapter 3) under the SEDROUT4-M version, later .22a,b and c were released to write more variables every day, when the daily output option is used. New code (loops and statements) is marked by `C PATRICK` at the start and `C END` at the end, single added or changed lines are just marked `C PATRICK` in the line above, both are accompanied with a short description where possible. Added subroutines are marked at the beginning with `C PATRICK***` with a short description of the routine's function, similar to the original code.

The main changes to the code to allow for variable flow, downstream water level changes including tide, sand-bed rivers and daily output are described in Verhaar *et al.* [2008] (see chapter 3). Some technicalities that are not presented in the paper are described below and include a change in time administration, more detailed information on how the daily discharge and water level are handled and on the adjustment of the definition of transport layer thickness. Also the option to have a backwater curve from the downstream cross section was made available (the original version only allowed for equilibrium water levels at the downstream boundary).

The original version of SEDROUT [Hoey and Ferguson, 1994] based the time administration on keeping track of the cumulative seconds that passed. The input data provided by Ouranos [see Chaumont and Chartier, 2005, for more details] contains daily averaged discharges, therefore the time administration is converted to a calendar date and time format, including leap years. The time step management is changed to assure that the cumulative time by the end of each day will be exactly a multiple of 86400 s ($24\times60\times60$) and the discharge and water level will be updated exactly at midnight of each day. In the case of tide at the downstream boundary a multiple of 3600 s (60×60) is used to have the water level updated exactly every hour. The time module checks every time step if the multiple of 86400 s or 3600 s will be exceeded in the the next two iterations to keep the initial time step for the new boundary conditions as large as possible.

As explained in chapter 3 a quasi-steady flow approach is used in our simulations: in accordance with the data provided by Ouranos the update of the hydrological boundary conditions is done once a day, when there is no tide, otherwise the maximum time step is set to 1 h. Test runs have shown [Verhaar *et al.*, 2008, chapter 3] that this is sufficient for the Batiscan River. Daily discharges are stored in `.qdt`-files covering one calendar year with the last four characters of the file name corresponding to the year (i.e. `FrEA2010.qdt`, `FrEA2011.qdt`, etc.). During the simulation at the end of every year the file of the next year is read and stored in a vector of the memory. The water level file contains a yearly time series of values that is reused throughout the simulation and changed accordingly to the water level scenario and/or tide specified in the `.ini`-file.

If the multiple channel option is used an extra routine is used to assure convergence of the water level and to assure that the discharge redistribution is not oscillating between two values. Also in the case of two bifurcations that are influencing each other it assures that both will find a satisfactory discharge ratio that match the specified accuracy.

Overview of added subroutines:

– ACKERS

– QDATA

– NEWDATE

– READQDATA

– QDISTRIB

– WATERLEVEL

– READWLD

```
C     SEDROUT 4-M 15 April 2008
C
C     CHANGES MADE BY PATRICK VERHAAR AUGUST UNTIL APRIL 2008
C     SEDROUT5 is used as internal name
C     (4M) SEDROUT5.0.22 is published in Geomorphology 2008 as
C     SEDROUT4M, later version a, b and c are added.
C     (22c) write all output in daily files for DAILY in ini-file
C     (22b) Also write water level elevation at each day
C     (22a) Writing sediment transport data at the end of each day
C     and bed elevation
C     (22) Tidal option added if no tide use 0 in .ini file.
C     The downstream water level is updated every hour, the tidal
C     period used is 12 hours. For tide specify the amplitude half the
C     difference between high and low tide.
C     (21) Ackers and White corrected. WLDFILE added. TOL read in
C     .ini-file. Option to write output on first of January.
C     Total sediment volume saved for each section of river.
C     (20) Island (multi-channel) option. Extra input required in
C     .ini-file: Specify number of sections "NSECT"(single channel
C     reaches) after number of xs. (use 1 if no island).
C     specify NSECT-1 times the upstream xs number as located in
C     .sds-file followed by the section number(s) directly downstream
C     of this section two numbers need to be specified if there is
C     1 section downstream last number MUST be 0.
C     All up and downstream xs must be specified tree times in the
C     .sds-file.
C     (19) Grain size distribution with fixed levels for sublayers.
C     (18) Correct the way total bed elevation change is calculated
C     for the use with variable discharge (not devided by width).
C     (17) Friction factor (FF) calculated in SFRICT-subroutine
C     (16) TEXTDATE and TEXTTIME are now stored instead of TIMEYR
C     Outfile (39) for lowest point of each cross section (.LP).
C     (15) RMETHOD option 6 added, specify discharge and calculate DS
C     water level with rating curve.
C     (14) Multiple files with discharge and/or water level data can
C     be used. Data can be stored in a separate folder by specifying
C     the path of the first file to be used in SEDFILE.INI. The start
C     date may be different from the first date in the file, but must
C     appear in that file.
C     (13) Time is converted into date, also a begin and end date need
C     to be specified in .ini-file. Program still uses seconds.
C     (12) Output-files are now stored after each writing to ensure
C     data is also available when program crashes.
C
C     CHANGES MADE BY PATRICK VERHAAR JULY 2005
C     (11) Ackers and White's transport formula, use ACKERS1973,
C     ACKERS1990 or ACKERSDAY to select the values of parameters
C     for the transport equation.
C     (10) Max number in loops with SURV-data changed to 100 instead
C     of 50, all data points are used.
C
C     CHANGES MADE BY TREVOR HOEY AND PATRICK VERHAAR 30 JUNE 2005
C     (9) RMETHOD option 5 added, specified discharge and
C     ds-waterlevel. The EXTEND subroutine is not used with this
C     option.
C     (8) Extention can be done by a specified slope in the ini-file.
C     To avoid problems with rivers with a small or negative slope.
C     (7) Change the water level approximations for sandy rivers
C     a first approximation of the water level must be specified
C     in the .ini-file when using RMETHOD 1.
C     (6) Number of iterations increased for scritcal flow and
C     discharge routine to avoid Froude number 9.99 and not
C     converging discharge or elevation message.
C
C     CHANGES MADE BY PATRICK VERHAAR JUNE 2005
C     All changes within C PATRICK and C END marks
C     (5) Variable discharge option programmed. Read *.qdt file
C     (4) Courant condition changed for constant layer thickness.
C     DZTOL=1% of transport layer. Future change to sand river
C     condition like D84<0.01m or so.
C     (3) Made the constant transport layer thickness working and
C     added output-file with transport layer thickness.
C     and interpolate the discharge at each iteration.
C     (2) Output-file with time step data (elapsed time, time step
C     and critical time step)
C     (1) Constant roughness equation added: n=a
C
C     IMPORTANT CHANGE FEB 2004
C     For all runs a file SEDFILES.INI must be present. This
C     contains a list of the 4 control files for each run as
C     follows. NB the names of input files are not now included
C     in the .ini file.
C     *.ini       name of control file
C     *.sds       name of cross-section data file
C     *.gss       name of grain-size file
C     *.qdt       name of discharge data file
C
C     Changes made September/October 2001 by TBH.
C     (1) Old INFO and SEDINFO arrays are now declared in COMMON
C     blocks, or simply passed as individual variables.
C     (2) Separate subroutine libraries (DLLs) have been removed.
C     All code is now in one file. This makes program compilation
C     and linking easier - so transferability should be improved.
C     (3) The run is now controlled in years so far as the user
C     sees things at both input and output stages. The program
C     still uses seconds. .ini files must contain run lengths
C     and writing intervals in years.
C     (4) Output file formats and options have been modified. The
C     old output files can still be produced and the .res and .inf
C     files are written by default. Additional files for all key
C     variables can be written, with cross-sections in columns and
C     times in rows. The specification of which files to write is
C     located at the end of the .ini file. Note that file code
C     numbers have nearly all been altered.
C     (5) The end of file indicator in .SDS files is now 9999, as
C     the program uses x>9000 as its test for end-of-file.
C
C     Further changes made November 2001.
C     (6) Parker.txt file is no longer needed.
C
C     Further changes September 2002
C     (7) Generalised straining function introduced (w=1+[wo-1][s/so]^c
C     where c=1 (Parker); c=0 (no straining); c<0.4 for poorly sorted
C     beds.
C     (8) Total sediment input (upstream boundary + tributary) and
C     output (downstream boundary) is given in m3 at the end of the
C     .inf file. NB this is summed across the total width.
C
C     Changes made June/July 2003
C     (9) Tributary sediment supply options now extended to include
C     'KXUSMAIN' which is k times the input rate at the u/s boundary
C     in the main stream. 'KXMAIN' gives k times the transport rate
C     at the tributary mouth.
C     (10) Wilcock/Crowe surface-based relation added as a bedload
```

```
C       equation option (.ini file code is 'WILCOCK')
C
C       Changes made August 2003
C       (11) Tributary inputs generalised to up to 5 tributaries.
C       Input format details are in runinfo.ini file.
C
C       Changes made December 2003
C       (12) Option for defining active layer thickness as k.Dgm
C       (surface geometric mean size) added.
C       (13) Dgm now written to .res file, which now contains 18
C       columns (see .inf file for details)
C
C       Changes made September 2004
C       (14) Option to output surface, sub-surface and bedload D90 added
C
C       Arrays that contain information about model nodes.
        REAL ACTSTART(125),
       +BACKBED(125,25),BACKLAYER(125),BACKMAX(125),BACKSED(125,26),
       +BACKSIZE(5,125,25),BEDCH(2,125),BEDFRACT(125,25),
       +CRITWS(250),
       +D165084ACT(4,250),D165084SUB(4,250),D165084BLD(4,250),
       +DGMACT(250),DISTANCE(250),
       +ESLOPE(250),
       +FFACTOR(250),FR(250),
       +MANNING(250),MAXALTDEP(125),MEANDEP(250),
       +NEWSURV(100,500),
       +QBEDLOAD(125),
       +R(250),
       +SCRIT(250),SIZELAYER(5,125,25),SIZESTART(5,125,25),
       +SUBTHICK(125),SURV(100,500),
       +THICKLAYER(125),TRACERS(500,5),
       +VELOCITY(250),VOLCH(2,125),
       +WATSURF(250),WSWIDTH(250)
C
C       Real variables used during calculations and parameter settings
C       etc.
        REAL APP,
       +BACKDT,BACKHDIFF(25),BACKQSECT(25),BEDDS,BEDDS1,
       +DEFREAL(20),DELTAH,DELTAT,DELTATC,DIMTAU,DISPLAY,
       +DSDEPTH(500),DSWATER(500),DXINT,
       +ERR1,ERROR,EXPROP(25),EXTSLOPE,
       +G,
       +HDS1,HDSC,HEST,HLOW,HRAD,HSC(25),HDIFF(25),HCHANGE,
       +INSED(26),
       +KACTIVE,KVISC,
       +MANNINGN,LOWPOINT(125),MSECT,
       +PARKER(36,3),PARAM(5),PCELAPSE,PCSAND(125),
       +Q(250),QBIN,QBFRACTIN(25),QDS(500),QEST,QSECT(25),QSECTMAX(25),
       +QSECTMIN(25),
       +RHO,RHOSED,RDATE(6),RESTDATE,
       +SEDTOTAL(10),SEDCHTOT(25,2),SIZEFINE(25),SS,STRAINC,
       +TAU,TINT,TLENGTH,TELAPSE,TELAPSEYR,THROPUT,TIMEYR,TMAX,TPOS,TOL,
       +TRACEL,TREC,TRIBFRACT(25,5),TRIBK(5),TRIBLOC(5),TRIBQ(5),
       +TRIBQB(5),TRWRITE,TSTART,TTOTAL,TW,TIDE,
       +UBAR,UNITGB,UNITGBIN
C
        INTEGER A,ACTIVE,
       +BIFUR(25),
       +CODE(250),CH,CHECK,CHECKOSS(25),
       +DATE(7),DEBUG,DEFINT(10),DIFF,DTINT,DXTEST,DAILY,
       +ENDDATE(3),EQUATION,EQUCODE,
       +HDATE(5000,2),HT,HTYPE,HYEAR,
       +INF(20),INTERVAL,IDATE,
       +K,KK,
       +L,LL,LENGTH,
       +MAXSEG,
       +N,NCLASS,NMAX,NTOT,NTRAC,NTRIB,NUMSEG,NWRITE,NBIFUR,
       +OFF,OK,
       +PERIOD,PLOT,
       +QDATE(500,3),QTYPE,QT,
       +RECORD,RMETHOD,
       +SCREEN,SED,SET,STOP,SCXS(25,5,2),SECTNEXT,SECTUP,SC,
       +T,TCODE,TIME,TRINT,TRWROUT,TYPE,
       +USB,
       +XS(6),XSM,XSN,XSNUP,
       +WINT,WTYPE,
       +YEARLY,
       +Z
C
        CHARACTER RIVER*20,OPERATOR*20,RUNCODE*8,TIME@*8,EDATE@*8,
       +INFILE(3)*12,OUTFILE(60)*12,OUTPUT(40)*1,SEDC*6,SECTCODE(125)*6,
       +TINPUT(5)*10,TRIBGSD(5)*5,TRIBHERE*4,TRIBSED(5)*5,EXTMETHOD*5,
       +TEXTDATE*10,TEXTTIME*8,QHFILE*62,STARTDATE*8,STARTTIME*8,
       +WLDFILE*62
C
        COMMON /INFO/ CODE,CRITWS,D165084ACT,DISTANCE,ESLOPE,FFACTOR,FR,
       +MANNING,MEANDEP,R,SCRIT,TOL,VELOCITY,WATSURF,WSWIDTH
C
        COMMON /SEDINFO/ D165084SUB,D165084BLD,DGMACT,QBEDLOAD,BEDCH,
       +VOLCH,SEDTOTAL,STRAINC,TRIBFRACT,TRIBK,TRIBQB,TRIBGSD,TRIBHERE,
       +TINPUT
C
        PARAMETER (OFF=0,SET=1)
        PARAMETER (TIME=1,PERIOD=2,YEARLY=3,DAILY=4)
        PARAMETER (OK=1,DIFF=0)
        G=9.81
        RHO=1000
        RHOSED=2650
        SS=RHOSED/RHO
        DISPLAY=5
        NWRITE=0
        CALL DATE_TIME_SEED@
C
C  Assume water temperature of 10C
        KVISC=0.00000131
C PATRICK add variables for different added options
        CALL INITIALISE(RIVER,OPERATOR,RUNCODE,INFILE,QHFILE,QTYPE,DATE,
       +ENDDATE,N,NSECT,NTOT,SCXS,HTYPE,HCHANGE,HYEAR,WLDFILE,TIDE)
        DEBUG=2
        TELINT=0
        JKJK=0
C PATRICK
C open file for storing data on discharge distribution between channels
        OPEN (66,FILE='DATA.XLS')
        WRITE (66,6996)
 6996   FORMAT('ITER         I   SC CO HDIFF(I)          DELTAH(I)          '
       +,'QSECT(I)          BACKQSECT(I)')
        ENDFILE(66)
C END
        CALL CLEAR_SCREEN@
        OPEN (3,FILE=INFILE(2))
        OPEN (4,FILE=INFILE(3))
C PATRICK set variables to read *.qdt file
        IF (QTYPE.EQ.2) THEN
```

```
            LENGTH=INDEX(QHFILE,'.')-1
         ENDIF
C END
         CALL INDATA(N,SIZESTART,SURV,INFILE,TYPE,QTYPE,SIZEFINE,RMETHOD,
        +EQUATION,PARAM,SECTCODE,NCLASS,EXPROP,CODE,DISTANCE,D165084ACT,
        +D165084SUB,DGMACT,TRIBLOC,TRIBQ,TRIBQB,TRIBK,TRIBFRACT,TINPUT,
        +TRIBGSD,TRIBSED,NTRIB,EXTMETHOD,EXTSLOPE)
C
         OUTFILE(7)=RUNCODE//'.dbg'
         OUTFILE(8)=RUNCODE//'.ext'
         OUTFILE(10)=RUNCODE//'.inf'
         OUTFILE(11)=RUNCODE//'.res'
C
         IF (DEBUG.EQ.2) THEN
            DO 4,IFILE=7,8
               OPEN ((IFILE),FILE=OUTFILE(IFILE))
4           CONTINUE
         ENDIF
         OPEN (99,FILE=RUNCODE//'.123')
         WRITE (99,7)
7        FORMAT ('TTOTAL    I   CO HDIFF          QSECT          BACKQSECT')
         END FILE (99)
C
         DO 5,IFILE=10,11
            OPEN ((IFILE),FILE=OUTFILE(IFILE))
5        CONTINUE
C
C Write the initial gs data into the temporary array SIZELAYER.
         IF (TYPE.EQ.1) THEN
            DO 10,XSN=1,N
               DO 15,K=1,5
                  DO 20,I=1,NCLASS
                     SIZELAYER(K,XSN,I)=SIZESTART(K,XSN,I)
20                CONTINUE
15             CONTINUE
10          CONTINUE
         ENDIF
C
C  Set the downstream boundary condition (DISCHARGE) and
C  extend the modelled reach beyond the lowest section
C  (EXTEND) if needed.
C PATRICK set QT for constant discharge to 1 and initial value for
C           variable discharge
         QT=1
         HT=1
C END
C PATRICK variables QT until DATE added
         CALL DISCHARGE (SURV,N,RMETHOD,EQUATION,PARAM,DSDEPTH,DSWATER,
        +QDS,HDS,D165084ACT,DISTANCE,NCLASS,QT,QTYPE,QHFILE,LENGTH,QDATE,
        +DATE,STOP,HT,INFILE,HDATE,TOL,WLDFILE)
         IF (STOP.EQ.999)THEN
            WRITE (*,999)
            READ *,STOP
C              PAUSE
            IF (STOP.EQ.2) GOTO 3001
            IF (STOP.EQ.1) THEN
               QT=1
               HT=1
            ENDIF
         ENDIF
C PATRICK control option for the uses of wld and qdt files
999      FORMAT ('Start date not in first Qdata-file!!',/
        +,'Change start date in .ini file or filename in SEDFILES.INI'
        +,'press 1 to continue with start date',/,'press 2 to stop')
C PATRICK statements for multiple channel option
C Calculate the discharge at each cross-section based on tributary Q
         IF (NSECT.GT.2) THEN
            QSECT(1)=QDS(QT)
            DO I=1,NSECT
               IF (SCXS(I,2,2).NE.0) THEN
                  QSECT(I)=QSECT(SCXS(I,2,1))+QSECT(SCXS(I,2,2))
               ENDIF
               IF (SCXS(I,4,2).NE.0) THEN
                  QSECT(SCXS(I,4,1))=QSECT(I)/2
                  QSECT(SCXS(I,4,2))=QSECT(I)/2
               ENDIF
            END DO
            CALL QDISTRIB(N,NSECT,Q,QSECT,SCXS)
            NBIFUR=0
            J=1
            DO I=1,NSECT
               IF (SCXS(I,4,2).NE.0) THEN
                  NBIFUR=NBIFUR+1
                  BIFUR(J)=SCXS(I,4,1)
                  J=J+1
               ENDIF
            ENDDO
         ELSE
            TCODE=NTRIB
            DO 30,XSN=N,1,-1
               IF (NTRIB.NE.0) THEN
                  IF (TCODE.EQ.0) THEN
                     Q(XSN)=Q(XSN+1)
                  ELSE IF (TRIBLOC(TCODE).LT.DISTANCE(XSN)) THEN
                     IF (XSN.EQ.N) THEN
                        Q(XSN)=QDS(QT)
                     ELSE
                        Q(XSN)=Q(XSN+1)
                     ENDIF
                  ELSE
                     Q(XSN)=Q(XSN+1)-TRIBQ(TCODE)
                     TCODE=TCODE-1
                  ENDIF
               ELSE
                  Q(XSN)=QDS(QT)
               ENDIF
30          CONTINUE
         ENDIF
C END
         IF (RMETHOD.LT.5) THEN
            CALL EXTEND(SURV,Q,HDS,N,D165084ACT,DISTANCE,MEANDEP,
        +   WATSURF,CODE,EXTMETHOD,EXTSLOPE,NMAX,HLOW,EQUATION,PARAM)
         ELSE
C PATRICK ds wl option
            HLOW=HDS
            NMAX=N
            CALL AREA(SURV,HDS,N,AWET,WSB,WP)
            WATSURF(N)=HDS
            WSWIDTH(N)=WSB
            MEANDEP(N)=AWET/WSB
            HRAD=AWET/WP
            CALL SFRICT(Q,N,HRAD,AWET,D165084ACT,ENSL,UBAR,FF,
        +   EQUATION,PARAM)
         ENDIF
```

```
C END
      CALL CLEAR_SCREEN@
      RECORD=SET
C
C  Write the basic run information to the output file .inf
      STARTTIME=TIME@()
      STARTDATE=EDATE@()
      WRITE (10,700) RIVER,OPERATOR,RUNCODE
      WRITE (10,1999)
      WRITE (10,701)
      WRITE (10,710) STARTDATE,STARTTIME
      WRITE (10,720) INFILE(1),INFILE(2)
C
      IF (TYPE.EQ.1) THEN
        WRITE (10,730) INFILE(3)
      ELSE
        WRITE (10,731)
      ENDIF
C
      IF (QTYPE.EQ.1) THEN
        IF (NTRIB.NE.0) THEN
          DO 35,I=1,NTRIB
            QMAIN=QDS(QT)
            DO 34,IM=NTRIB,I,-1
              QMAIN=QMAIN-TRIBQ(IM)
34          CONTINUE
            WRITE (10,742) QDS(QT),QMAIN,I,TRIBQ(I),TRIBLOC(I)
35        CONTINUE
        ELSE
          WRITE (10,740) QDS(QT)
        ENDIF
      ENDIF
C
C  Write information on tributaries in the .inf file
      IF (NTRIB.NE.0) THEN
        DO 38,I=1,NTRIB
          IF (TRIBSED(I).EQ.'SED') THEN
            IF (TINPUT(I).EQ.'KXMAIN') THEN
              WRITE (10,1455) I,TRIBK(I)
            ELSE IF (TINPUT(I).EQ.'KXUSMAIN') THEN
              WRITE (10,1457) I,TRIBK(I)
            ELSE IF (TINPUT(I).EQ.'CONST') THEN
              WRITE (10,1456) I,TRIBQB(I)
            ENDIF
            IF (TRIBGSD(I).EQ.'MAIN') THEN
              WRITE (10,1460)
            ELSE IF (TRIBGSD(I).EQ.'FIXED') THEN
              WRITE (10,1461) I,(TRIBFRACT(J,I),J=1,NCLASS)
            ENDIF
          ELSE
            WRITE (10,1451) I
          ENDIF
38      CONTINUE
      ENDIF
C PATRICK write filenames for daily discharge
      IF (QTYPE.EQ.2) WRITE (10,741) WLDFILE,QHFILE
C PATRICK write the used ds wl condition
      IF (TIDE.LE.0) WRITE (10,745)
      IF (TIDE.GT.0) WRITE (10,746) TIDE
C
      IF (RMETHOD.EQ.1) WRITE (10,750)
      IF (RMETHOD.EQ.2) WRITE (10,752)
      IF (RMETHOD.EQ.3) WRITE (10,751) (PARAM(J),J=3,5)
      IF (RMETHOD.EQ.4) WRITE (10,753)
      IF (RMETHOD.EQ.5) WRITE (10,754)
      IF (RMETHOD.EQ.6) WRITE (10,755) (PARAM(J),J=3,5)
C PATICK
      IF (EQUATION.EQ.1) WRITE (10,760) PARAM(1),PARAM(2)
      IF (EQUATION.EQ.2) WRITE (10,761) PARAM(1),PARAM(2)
      IF (EQUATION.EQ.3) WRITE (10,762) PARAM(1)
      WRITE (10,763) TOL
C END
C
C Now for the calculation of the water surface profile for main channel
C and side channel(s) separately.
      IF (NSECT.EQ.0) THEN
        DO 40,XSN=(NMAX-1),1,-1
          CALL BACKWATER (NMAX,N,XSN,Q,HLOW,SURV,RECORD,EQUATION
     +         ,PARAM)
40      CONTINUE
        GOTO 50
C PATRICK compare wl for multiple channel option
      ELSE
        DO I=1,NSECT
          HDIFF(I)=0
        ENDDO
        DO 60,SC=1,50
          DO I=NSECT,2,-1
            IF (I.EQ.NSECT .OR. SCXS(I,4,1).EQ.0) THEN
              HDSC=HDS
            ELSE
              HDSC=WATSURF(SCXS(I,5,1))
            ENDIF
            XS(1)=SCXS(I,1,1)
            XS(2)=SCXS(I,1,2)
            CALL AREA(SURV,HDSC,XS(2),AWET,WSB,WP)
            WATSURF(XS(2))=HDSC
            WSWIDTH(XS(2))=WSB
            MEANDEP(XS(2))=AWET/WSB
            HRAD=AWET/WP
            CALL SFRICT(Q,XS(2),HRAD,AWET,D165084ACT,ENSL,UBAR,FF,
     +      EQUATION,PARAM)
            DO 65,XSN=XS(2)-1,XS(1),-1
              CALL BACKWATER(XS(2),N,XSN,Q,HDSC,SURV,RECORD,
     +        EQUATION,PARAM)
65          CONTINUE
            SECTUP=SCXS(I,2,1)
            HSC(I)=WATSURF(XS(1))
C Check if upstream end is bifurcation and waterlevel in other channel.
            IF (SCXS(SECTUP,4,2).NE.0) THEN
              IF (SCXS(SECTUP,4,1).EQ.I) THEN
                HDIFF(I)=HSC(SCXS(SECTUP,4,2))-HSC(I)
                IF (ABS(HDIFF(I)).GT.0) THEN
                  IF (SC.GT.1) THEN
                    IF (ABS(BACKHDIFF(I)+HDIFF(I)).LE.0) THEN
                      QSECT(I)=(QSECT(I)+BACKQSECT(I))/2
                      BACKQSECT(I)=2*QSECT(I)-BACKQSECT(I)
                      GOTO 70
                    ENDIF
                  ENDIF
                  BACKQSECT(I)=QSECT(I)
                  BACKHDIFF(I)=HDIFF(I)
                  IF (HDIFF(I).GT.0) THEN
                    SECTNEXT=SCXS(SECTUP,4,2)
```

```
                        XS(1)=SCXS(SECTNEXT,1,1)
                        XS(2)=SCXS(SECTNEXT,1,2)
                        DELTAH=WATSURF(XS(1))-WATSURF(XS(2))
                        QSECT(I)=QSECT(SECTUP)-(
     +                  QSECT(SECTNEXT)*(1-WSWIDTH(XS(1)+1)/
     +                  (WSWIDTH(XS(1)+1)+WSWIDTH(SCXS(I,1,1) +1))*
     +                  HDIFF(I)/DELTAH)**0.5)
                      ELSE
                        DELTAH=HSC(I)-HDSC
                        QSECT(I)=QSECT(I)*(1+(1-WSWIDTH(XS(1)+1)/(
     +                  WSWIDTH(XS(1)+1)+WSWIDTH(SCXS(SECTUP,5,2)+1)
     +                  ))*HDIFF(I)/DELTAH)**0.5
                      ENDIF
 70                   DO J=I,NSECT
                        IF (J.EQ.SCXS(SECTUP,4,2)) THEN
                          QSECT(J)=QSECT(SECTUP)-QSECT(I)
                        ELSE IF (SCXS(J,4,2).NE.0) THEN
                          QSECT(SCXS(J,4,1))=
     +                    QSECT(SCXS(J,4,1))*QSECT(J)/BACKQSECT(J)
                          QSECT(SCXS(J,4,2))=
     +                    QSECT(SCXS(J,4,2))*QSECT(J)/BACKQSECT(J)
                        ELSE IF (SCXS(J,2,2).NE.0) THEN
                          QSECT(J)=QSECT(SCXS(J,2,1))+
     +                    QSECT(SCXS(J,2,2))
                        ENDIF
                      ENDDO
                      CALL QDISTRIB (N,NSECT,Q,QSECT,SCXS)
                    ENDIF
                  ENDIF
                ENDIF
                IF (I.EQ.2) THEN
                  CHECK=0
                  DO J=1,NSECT
                    IF (ABS(HDIFF(J)).GT.0) CHECK=1
                  ENDDO
                  IF (CHECK.EQ.0) GOTO 55
                ENDIF
              ENDDO
 60         CONTINUE
 55         I=1
            HDSC=WATSURF(SCXS(I,5,1))
            XS(1)=SCXS(I,1,1)
            XS(2)=SCXS(I,1,2)
            CALL AREA(SURV,HDSC,XS(2),AWET,WSB,WP)
            WATSURF(XS(2))=HDSC
            WSWIDTH(XS(2))=WSB
            MEANDEP(XS(2))=AWET/WSB
            HRAD=AWET/WP
            CALL SFRICT(Q,XS(2),HRAD,AWET,D165084ACT,ENSL,UBAR,FF,
     +      EQUATION,PARAM)
            DO 66,XSN=XS(2)-1,XS(1),-1
              CALL BACKWATER(XS(2),N,XSN,Q,HDSC,SURV,RECORD,EQUATION,
     +        PARAM)
 66         CONTINUE
          ENDIF
C END
C   Draw the water surface profile on the screen if requested
 50       CALL CLEAR_SCREEN@
          WRITE (*,850)
C          use next line when manual start use plot=2 of batch file simulation
C          READ *,PLOT
          PLOT=2
C
          IF (PLOT.EQ.1) THEN
            CALL DRAW(DISTANCE,MEANDEP,WATSURF,N,TRIBLOC,TRIBQ,NTRIB)
            CALL SLEEP@(DISPLAY)
            CALL TEXT_MODE@
          ENDIF
C
C   Print a warning and exit the program if sediment routing cannot be
C   used with the input data format used.
          IF (TYPE.EQ.2) THEN
            WRITE (*,890)
            GOTO 3001
          ENDIF
          CALL CLEAR_SCREEN@
C
C   Report the size classes used herein, and the initial
C   surface and sub-surface gsd's
          WRITE (10,1100)
          WRITE (10,1105) (-1*SIZEFINE(L),L=1,NCLASS)
          WRITE (10,1101)
          WRITE (10,1105) (EXPROP(L),L=1,NCLASS)
C
          READ (5,'(A)') SEDC
C
          IF (SEDC.EQ.'SED') THEN
            SED=1
C   The sediment routing routine is to be used.
C   Read the relevant sediment parameters from the input
C   files. TLENGTH= length of run (s); DELTAT= initial timestep(s);
C   WTYPE= output recorded after time[1] or iterations[2]; INTERVAL=
C   constant[1] or variable[2] computation interval; ACTIVE= active
C   layer is constant*D84 [1] or fixed [2] depth; KACTIVE= value
C   of constant for active layer; TINT= time interval for writing
C   to output files; EQUCODE= which bedload equation to be used
C   [1=Parker,1990; 2=Einstein; 3=Wilcock; 4=Ackers,1973;5=Ackers,1990;
C   6=Ackers and Day]; WINT= the number of iterations between writing
C   to output files (if WTYPE=2);
          DO 41,I=1,10
            SEDTOTAL(I)=0
 41       CONTINUE
C PATRICK keep track of sediment volume at the limits of each section
          DO 42,I=1,25
            SEDCHTOT(I,1)=0
            SEDCHTOT(I,2)=0
 42       CONTINUE
C
          CALL SEDDEF(DEFREAL,DEFINT,NCLASS,INSED)
          TLENGTH=DEFREAL(1)
          TLENGTH=(((ENDDATE(1)-DATE(1))*365.25+
         +(ENDDATE(2)-DATE(2))*365.25/12)+(ENDDATE(3)-DATE(3)))*24*60*60
          DELTAT=DEFREAL(2)
          WTYPE=DEFINT(2)
          INTERVAL=DEFINT(1)
          ACTIVE=DEFINT(5)
          KACTIVE=DEFREAL(5)
          TINT=DEFREAL(7)
          EQUCODE=DEFINT(9)
          USB=DEFINT(3)
          IF (WTYPE.EQ.2) WINT=DEFINT(6)
C
C   Report the variable settings to the .inf file
          WRITE (10,770) (DATE(J),J=1,3),(ENDDATE(J),J=1,3)
```

```
      IF (INTERVAL.EQ.1) WRITE (10,771) DELTAT
      IF (INTERVAL.EQ.2) WRITE (10,772)
      IF (WTYPE.EQ.1) WRITE (10,773) (TINT/60/60/24/365.25)
      IF (WTYPE.EQ.2) WRITE (10,774) WINT
      IF (WTYPE.EQ.3) WRITE (10,775)
      IF (WTYPE.EQ.4) WRITE (10,776)
      IF (INTERVAL.EQ.1) NUMSEG=INT(TLENGTH/DELTAT)
      IF (INTERVAL.EQ.2) NUMSEG=1000
C
c  Check the output files that have been requested
C PATRICK 36 REPLACED BY 40 for extra output files (.DT and .LA)
      DO 125 K=1,40
        READ (5,'(A)') OUTPUT(K)
125   CONTINUE
C
      IF (OUTPUT(1).EQ.'Y') OUTFILE(21)=RUNCODE//'.sed'
      IF (OUTPUT(2).EQ.'Y') OUTFILE(22)=RUNCODE//'.tpt'
      IF (OUTPUT(3).EQ.'Y') OUTFILE(23)=RUNCODE//'.sur'
      IF (OUTPUT(4).EQ.'Y') OUTFILE(24)=RUNCODE//'.sub'
      IF (OUTPUT(5).EQ.'Y') OUTFILE(25)=RUNCODE//'.bld'
      IF (OUTPUT(6).EQ.'Y') OUTFILE(26)=RUNCODE//'.hyd'
      IF (OUTPUT(7).EQ.'Y') OUTFILE(27)=RUNCODE//'.50a'
      IF (OUTPUT(8).EQ.'Y') OUTFILE(28)=RUNCODE//'.84a'
      IF (OUTPUT(9).EQ.'Y') OUTFILE(29)=RUNCODE//'.qb'
      IF (OUTPUT(10).EQ.'Y') OUTFILE(30)=RUNCODE//'.50b'
      IF (OUTPUT(11).EQ.'Y') OUTFILE(31)=RUNCODE//'.S'
      IF (OUTPUT(12).EQ.'Y') OUTFILE(32)=RUNCODE//'.tau'
      IF (OUTPUT(13).EQ.'Y') OUTFILE(33)=RUNCODE//'.zz'
      IF (OUTPUT(14).EQ.'Y') OUTFILE(34)=RUNCODE//'.R'
      IF (OUTPUT(15).EQ.'Y') OUTFILE(35)=RUNCODE//'.FR'
      IF (OUTPUT(16).EQ.'Y') OUTFILE(36)=RUNCODE//'.ff'
      IF (OUTPUT(17).EQ.'Y') OUTFILE(37)=RUNCODE//'.16a'
      IF (OUTPUT(18).EQ.'Y') OUTFILE(38)=RUNCODE//'.16s'
      IF (OUTPUT(19).EQ.'Y') OUTFILE(39)=RUNCODE//'.50s'
      IF (OUTPUT(20).EQ.'Y') OUTFILE(40)=RUNCODE//'.84s'
      IF (OUTPUT(21).EQ.'Y') OUTFILE(41)=RUNCODE//'.16b'
      IF (OUTPUT(22).EQ.'Y') OUTFILE(42)=RUNCODE//'.84b'
      IF (OUTPUT(23).EQ.'Y') OUTFILE(43)=RUNCODE//'.n'
      IF (OUTPUT(24).EQ.'Y') OUTFILE(44)=RUNCODE//'.h'
      IF (OUTPUT(25).EQ.'Y') OUTFILE(45)=RUNCODE//'.dz'
      IF (OUTPUT(26).EQ.'Y') OUTFILE(46)=RUNCODE//'.Sdz'
      IF (OUTPUT(27).EQ.'Y') OUTFILE(47)=RUNCODE//'.dA'
      IF (OUTPUT(28).EQ.'Y') OUTFILE(48)=RUNCODE//'.SdA'
      IF (OUTPUT(29).EQ.'Y') OUTFILE(49)=RUNCODE//'.pcs'
      IF (OUTPUT(30).EQ.'Y') OUTFILE(50)=RUNCODE//'.u'
      IF (OUTPUT(31).EQ.'Y') OUTFILE(51)=RUNCODE//'.wws'
      IF (OUTPUT(32).EQ.'Y') OUTFILE(52)=RUNCODE//'.lat'
      IF (OUTPUT(33).EQ.'Y') OUTFILE(53)=RUNCODE//'.dgm'
      IF (OUTPUT(34).EQ.'Y') OUTFILE(54)=RUNCODE//'.90a'
      IF (OUTPUT(35).EQ.'Y') OUTFILE(55)=RUNCODE//'.90s'
      IF (OUTPUT(36).EQ.'Y') OUTFILE(56)=RUNCODE//'.90b'
C PATRICK
      IF (OUTPUT(37).EQ.'Y') OUTFILE(57)=RUNCODE//'.DT'
      IF (OUTPUT(38).EQ.'Y') OUTFILE(58)=RUNCODE//'.LA'
      IF (OUTPUT(39).EQ.'Y') OUTFILE(59)=RUNCODE//'.LP'
      IF (OUTPUT(40).EQ.'Y') OUTFILE(60)=RUNCODE//'.YQS'
C
      DO 129,IFILE=21,60
C END 56 REPLACED BY 60 for extra output files
        IF (OUTPUT(IFILE-20).EQ.'Y')
     +  OPEN ((IFILE),FILE=OUTFILE(IFILE))
129   CONTINUE
C
C  Initialise the active layer thickness arrays
      IF (ACTIVE.EQ.1) THEN
        DO 130,XSN=1,N
          ACTSTART(XSN)=KACTIVE*D165084ACT(3,XSN)
          THICKLAYER(XSN)=ACTSTART(XSN)
          MAXALTDEP(XSN)=ACTSTART(XSN)
130     CONTINUE
      ELSE IF (ACTIVE.EQ.2) THEN
        DO 135,XSN=1,N
          ACTSTART(XSN)=2*KACTIVE
          THICKLAYER(XSN)=0.5*ACTSTART(XSN)
          MAXALTDEP(XSN)=0.5*ACTSTART(XSN)
          SUBTHICK(XSN)=ACTSTART(XSN)
135     CONTINUE
      ELSE IF (ACTIVE.EQ.3) THEN
        DO 136,XSN=1,N
          ACTSTART(XSN)=KACTIVE*DGMACT(XSN)
          THICKLAYER(XSN)=ACTSTART(XSN)
          MAXALTDEP(XSN)=ACTSTART(XSN)
136     CONTINUE
      ENDIF
C
      IF (INTERVAL.EQ.1) DTINT=DELTAT
C
C  If Parker (1990) equation to be used, read relevant array.
      IF (EQUCODE.EQ.1) THEN
        PARKER(1,1) = 0.6684
        PARKER(1,2) = 1.011
        PARKER(1,3) = 0.8157
        PARKER(2,1) = 0.7639
        PARKER(2,2) = 1.011
        PARKER(2,3) = 0.8157
        PARKER(3,1) = 0.8601
        PARKER(3,2) = 1.010
        PARKER(3,3) = 0.8182
        PARKER(4,1) = 0.9096
        PARKER(4,2) = 1.008
        PARKER(4,3) = 0.8233
        PARKER(5,1) = 0.9615
        PARKER(5,2) = 1.004
        PARKER(5,3) = 0.8333
        PARKER(6,1) = 1.00
        PARKER(6,2) = 0.9997
        PARKER(6,3) = 0.8439
        PARKER(7,1) = 1.055
        PARKER(7,2) = 0.9903
        PARKER(7,3) = 0.8621
        PARKER(8,1) = 1.108
        PARKER(8,2) = 0.9789
        PARKER(8,3) = 0.8825
        PARKER(9,1) = 1.197
        PARKER(9,2) = 0.9567
        PARKER(9,3) = 0.9214
        PARKER(10,1) = 1.302
        PARKER(10,2) = 0.9273
        PARKER(10,3) = 0.9723
        PARKER(11,1) = 1.407
        PARKER(11,2) = 0.8964
        PARKER(11,3) = 1.025
        PARKER(12,1) = 1.529
        PARKER(12,2) = 0.8604
```

```
      PARKER (12,3) = 1.083
      PARKER (13,1) = 1.641
      PARKER (13,2) = 0.8287
      PARKER (13,3) = 1.13
      PARKER (14,1) = 1.702
      PARKER (14,2) = 0.8123
      PARKER (14,3) = 1.153
      PARKER (15,1) = 1.832
      PARKER (15,2) = 0.7796
      PARKER (15,3) = 1.196
      PARKER (16,1) = 1.937
      PARKER (16,2) = 0.7554
      PARKER (16,3) = 1.225
      PARKER (17,1) = 2.044
      PARKER (17,2) = 0.7326
      PARKER (17,3) = 1.25
      PARKER (18,1) = 2.261
      PARKER (18,2) = 0.6928
      PARKER (18,3) = 1.287
      PARKER (19,1) = 2.499
      PARKER (19,2) = 0.6585
      PARKER (19,3) = 1.313
      PARKER (20,1) = 2.732
      PARKER (20,2) = 0.6345
      PARKER (20,3) = 1.333
      PARKER (21,1) = 2.993
      PARKER (21,2) = 0.615
      PARKER (21,3) = 1.352
      PARKER (22,1) = 3.477
      PARKER (22,2) = 0.5877
      PARKER (22,3) = 1.38
      PARKER (23,1) = 4.075
      PARKER (23,2) = 0.564
      PARKER (23,3) = 1.403
      PARKER (24,1) = 4.469
      PARKER (24,2) = 0.5523
      PARKER (24,3) = 1.414
      PARKER (25,1) = 5.016
      PARKER (25,2) = 0.5395
      PARKER (25,3) = 1.426
      PARKER (26,1) = 6.158
      PARKER (26,2) = 0.5209
      PARKER (26,3) = 1.444
      PARKER (27,1) = 7.821
      PARKER (27,2) = 0.5045
      PARKER (27,3) = 1.458
      PARKER (28,1) = 10.06
      PARKER (28,2) = 0.4917
      PARKER (28,3) = 1.469
      PARKER (29,1) = 14.38
      PARKER (29,2) = 0.479
      PARKER (29,3) = 1.48
      PARKER (30,1) = 19.97
      PARKER (30,2) = 0.4712
      PARKER (30,3) = 1.469
      PARKER (31,1) = 25.79
      PARKER (31,2) = 0.4668
      PARKER (31,3) = 1.49
      PARKER (32,1) = 38.57
      PARKER (32,2) = 0.462
      PARKER (32,3) = 1.493
      PARKER (33,1) = 68.74
      PARKER (33,2) = 0.4578
      PARKER (33,3) = 1.497
      PARKER (34,1) = 91.95
      PARKER (34,2) = 0.4564
      PARKER (34,3) = 1.498
      PARKER (35,1) = 231.2
      PARKER (35,2) = 0.4541
      PARKER (35,3) = 1.499
      PARKER (36,1) = 2320.0
      PARKER (36,2) = 0.4527
      PARKER (36,3) = 1.5
    ENDIF
C
    IF (DEFINT(8).EQ.2) THEN
C
C   The tracing routine is to be used.  Initialisation follows.
      CALL TRACINIT (TRACERS,TPOS,NTRAC,TSTART,TREC,THROPUT)
      OPEN (20,FILE='TRACERS.TXT')
      TRACEL=0
      TRWRITE=0
      TRWROUT=0
    ENDIF
C
    TELAPSE=0
    PCELAPSE=0
    TW=0
    DXTEST=OK
    Z=1
    TTOTAL=0
    PULSE=0
C
C  Report the sediment routing settings to the .inf file
    WRITE (10,780) DEFREAL(3)
    IF (DEFINT(5).EQ.1) WRITE (10,781) KACTIVE
    IF (DEFINT(5).EQ.2) WRITE (10,782) KACTIVE
    IF (DEFINT(5).EQ.3) WRITE (10,783) KACTIVE
    IF (EQUCODE.EQ.1) WRITE (10,784) DEFREAL(6),DEFREAL(8),
   +DEFREAL(9)
    IF (EQUCODE.EQ.1) THEN
      STRAINC=DEFREAL(10)
      IF (STRAINC.LT.0.000001) THEN
        WRITE (10,787)
      ELSE IF (STRAINC.GT.0.99999) THEN
        WRITE (10,788)
      ELSE
        WRITE (10,789) STRAINC
      ENDIF
    ENDIF
    IF (EQUCODE.EQ.2) WRITE (10,785)
    IF (EQUCODE.EQ.3) WRITE (10,786)
    IF (EQUCODE.EQ.4) WRITE (10,801)
    IF (EQUCODE.EQ.5) WRITE (10,802)
    IF (EQUCODE.EQ.6) WRITE (10,803)
    IF (USB.EQ.1) WRITE (10,791)
    IF (USB.EQ.2) WRITE (10,792) (INSED(J),J=1,17)
    IF (USB.EQ.3) WRITE (10,793) DEFREAL(4)
    IF (USB.EQ.5) WRITE (10,794) INSED(1)
C  Confirm the formats for the output files, in the .inf file
    WRITE (10,1400) OUTFILE(11)
    WRITE (10,1409)
    IF (OUTPUT(1).EQ.'Y')WRITE (10,1402) OUTFILE(21)
    IF (OUTPUT(2).EQ.'Y')WRITE (10,1403) OUTFILE(22)
```

```
      IF (OUTPUT(3).EQ.'Y')WRITE (10,1404) OUTFILE(23)
      IF (OUTPUT(4).EQ.'Y')WRITE (10,1405) OUTFILE(24)
      IF (OUTPUT(5).EQ.'Y')WRITE (10,1406) OUTFILE(25)
      IF (OUTPUT(6).EQ.'Y')WRITE (10,1401) OUTFILE(26)
C
C PATRICK REPLACED 28 BY 27 AND 53 BY 60
      DO 480,IFILE=27,60
        IF (OUTPUT(IFILE-20).EQ.'Y') WRITE (10,1408) OUTFILE(IFILE)
 480  CONTINUE
C
      WRITE (10,1610)
      MAXSEG=31999
 494  T=1
C  for fixed timesteps
C
C      IF (INTERVAL.EQ.1) THEN
C        IF (TTOTAL.GE.MAXSEG) NUMSEG=NUMSEG-MAXSEG
C        IF (NUMSEG.LT.MAXSEG) MAXSEG=NUMSEG
C      ENDIF
C
      DO 500,T=1,100
        TTOTAL=TTOTAL+1
        DO 600,XSN=1,N
          BACKLAYER(XSN)=THICKLAYER(XSN)
          BACKMAX(XSN)=MAXALTDEP(XSN)
          DO 610,K=1,5
            DO 620,I=1,NCLASS
              BACKSIZE(K,XSN,I)=SIZELAYER(K,XSN,I)
 620        CONTINUE
 610      CONTINUE
          BACKSED(XSN,1)=QBEDLOAD(XSN)
          BACKSED(XSN,2)=VOLCH(1,XSN)
          BACKSED(XSN,3)=VOLCH(2,XSN)
          BACKSED(XSN,4)=BEDCH(1,XSN)
          BACKSED(XSN,5)=BEDCH(2,XSN)
          BACKSED(XSN,7)=D165084ACT(1,XSN)
          BACKSED(XSN,8)=D165084ACT(2,XSN)
          BACKSED(XSN,9)=D165084ACT(3,XSN)
          BACKSED(XSN,10)=D165084SUB(1,XSN)
          BACKSED(XSN,11)=D165084SUB(2,XSN)
          BACKSED(XSN,12)=D165084SUB(3,XSN)
          BACKSED(XSN,13)=D165084BLD(1,XSN)
          BACKSED(XSN,14)=D165084BLD(2,XSN)
          BACKSED(XSN,15)=D165084BLD(3,XSN)
          DO 640,I=1,NCLASS
            BACKBED(XSN,I)=BEDFRACT(XSN,I)
 640      CONTINUE
 600    CONTINUE
        JCHECK=0
        IF (TTOTAL.LT.1.05) JCHECK=1
        IF (SCREEN.EQ.15) JCHECK=1
        IF (JCHECK.EQ.1) THEN
          SCREEN=0
          WRITE (*,1999)
          WRITE (*,710) STARTDATE,STARTTIME
          WRITE (*,1999)
          WRITE (*,1650)
          WRITE (*,1999)
          WRITE (*,1655)
          WRITE (*,2001)
        ENDIF
        IF (INTERVAL.EQ.1) DELTAT=DTINT
        TELAPSE=TELAPSE+DELTAT
        TW=TW+DELTAT
 499    BACKDT=DELTAT
        IF (NTRIB.EQ.0) THEN
          TCODE=0
        ELSE
          TCODE=1
        ENDIF
        DO 200,XSN=1,N
          TRIBHERE='NO'
          IF (NTRIB.GT.0) THEN
C PATRICK control block for tributary option
C     WRITE (*,9997) TRIBLOC(TCODE),TCODE
C9997 FORMAT (F9.2,1X,I2)
C     PAUSE
C END
              IF (TRIBLOC(TCODE).LT.(DISTANCE(XSN)+0.1)) THEN
                IF (TRIBLOC(TCODE).GT.DISTANCE(XSN-1)) THEN
                  IF (TRIBSED(TCODE).EQ.'SED') THEN
                    TRIBHERE='TRIB'
                  ELSE
                    TRIBHERE='NSED'
                  ENDIF
                ENDIF
              ENDIF
            ENDIF
C PATRICK control block for variable discharge
C     WRITE (*,9998) TTOTAL,XSN,Q(XSN),TRIBHERE
C9998 FORMAT ('# iteration:',F6.1,'  XSN:',I2,'  Q:',F6.1,
C    +'  TRIBHERE:',A5)
C     IF (XSN.EQ.82) PAUSE
C END
C PATRICK statements for multiple channel option
          IF (XSN.EQ.1) CH=1
          IF (NSECT.GE.2) THEN
C Check if there's a bifurcation or confluence
            XS(1)=SCXS(CH,1,1)
            XS(2)=SCXS(CH,1,2)
            IF (XSN.EQ.XS(1) .AND. XSN.NE.1) THEN
C if it is a bifurcation then calculate bedload out of discharge ratio
              IF (SCXS(CH,2,2).EQ.0) THEN
                SECTUP=SCXS(CH,2,1)
                XSNUP=SCXS(CH,3,1)
                QBEDLOAD(XSN)=QBEDLOAD(XSNUP)*Q(XSN+1)/Q(XSN)
                DO I=1,NCLASS
                  BEDFRACT(XSN,I)=
     +            BEDFRACT(XSNUP,I)*Q(XSN+1)/Q(XSN)
                ENDDO
                GOTO 199
C if it is a confluence sum the bedload of the upstream channels
              ELSE IF (SCXS(CH,2,2).NE.0) THEN
                QBEDLOAD(XSN)=QBEDLOAD(SCXS(CH,3,1)-1)+
     +          QBEDLOAD(SCXS(CH,3,2)-1)
c     WRITE (*,9876) QBEDLOAD(XSN),QBEDLOAD(SCXS(CH,3,1)-1),
c    +          QBEDLOAD(SCXS(CH,3,2)-1)
c9876 FORMAT(F10.7,2(1X,F10.7))
c     PAUSE
                DO I=1,NSECT
                  BEDFRACT(XSN,I)=BEDFRACT(SCXS(CH,3,1)-1,I)+
     +            BEDFRACT(SCXS(CH,3,2)-1,I)
                ENDDO
              ENDIF
```

```
C if downstream is confluence, no need to calculate bedload for last xs
                ELSE IF (XSN.EQ.XS(2) .AND. SCXS(CH,4,1).NE.0) THEN
                   IF (SCXS(CH,4,2).EQ.0) GOTO 199
                ENDIF
             ENDIF
C END
C PATRICK Q added for Ackers and White's transport formula
             IF (TTOTAL.LT.1.05) THEN
                CALL SEDROUT (ACTSTART,SIZESTART,SIZELAYER,THICKLAYER,
     +          DELTAT,N,SURV,TTOTAL,XSN,PARKER,MAXALTDEP,
     +          BEDFRACT,QBIN,QBFRACTIN,DXTEST,DXINT,INF,JKJK,DEFINT,
     +          DEFREAL,SIZEFINE,INSED,KVISC,SS,RHOSED,NCLASS,EXPROP,
     +          TRIBLOC,TCODE,SUBTHICK,Q,CH,SCXS,NSECT)
             ELSE
                CALL SEDROUT (ACTSTART,SIZESTART,SIZELAYER,THICKLAYER,
     +          DELTAT,N,NEWSURV,TTOTAL,XSN,PARKER,MAXALTDEP,
     +          BEDFRACT,QBIN,QBFRACTIN,DXTEST,DXINT,INF,JKJK,DEFINT,
     +          DEFREAL,SIZEFINE,INSED,KVISC,SS,RHOSED,NCLASS,EXPROP,
     +          TRIBLOC,TCODE,SUBTHICK,Q,CH,SCXS,NSECT)
             ENDIF
             IF (TRIBHERE.EQ.'TRIB'.OR.TRIBHERE.EQ.'NSED') THEN
                IF (TCODE.EQ.NTRIB) THEN
                   TCODE=1
                ELSE
                   TCODE=TCODE+1
                ENDIF
             ENDIF
             IF (DXTEST.EQ.DIFF .AND. INTERVAL.NE.1) THEN
                DELTAT=DXINT
                TELAPSE=TELAPSE+DXINT-BACKDT
                TW=IW+DXINT-BACKDT
                DO 650,XSM=1,N
                   THICKLAYER(XSM)=BACKLAYER(XSM)
                   MAXALTDEP(XSM)=BACKMAX(XSM)
                   DO 660,K=1,5
                      DO 670,I=1,NCLASS
                         SIZELAYER(K,XSM,I)=BACKSIZE(K,XSM,I)
670                   CONTINUE
660                CONTINUE
                   QBEDLOAD(XSM)=BACKSED(XSM,1)
                   VOLCH(1,XSM)=BACKSED(XSM,2)
                   VOLCH(XSM,2)=BACKSED(XSM,3)
                   BEDCH(1,XSM)=BACKSED(XSM,4)
                   BEDCH(2,XSM)=BACKSED(XSM,5)
                   D165084ACT(1,XSM)=BACKSED(XSM,7)
                   D165084ACT(2,XSM)=BACKSED(XSM,8)
                   D165084ACT(3,XSM)=BACKSED(XSM,9)
                   D165084SUB(1,XSM)=BACKSED(XSM,10)
                   D165084SUB(2,XSM)=BACKSED(XSM,11)
                   D165084SUB(3,XSM)=BACKSED(XSM,12)
                   D165084BLD(1,XSM)=BACKSED(XSM,13)
                   D165084BLD(2,XSM)=BACKSED(XSM,14)
                   D165084BLD(3,XSM)=BACKSED(XSM,15)
                   DO 690,I=1,NCLASS
                      BEDFRACT(XSM,I)=BACKBED(XSM,I)
690                CONTINUE
650             CONTINUE
                DXTEST=OK
                GOTO 499
             ENDIF
199          IF (XSN.EQ.SCXS(CH,1,2) .AND. XSN.LT.N) CH=CH+1
200       CONTINUE
C PATRICK statements for multiple channel option
          DO CH=1,NSECT
             XS(1)=SCXS(CH,1,1)
             SEDCHTOT(CH,1)=SEDCHTOT(CH,1)+QBEDLOAD(XS(1))*DELTAT
             XS(2)=SCXS(CH,1,2)-1
             SEDCHTOT(CH,2)=SEDCHTOT(CH,2)+QBEDLOAD(XS(2))*DELTAT
             IF (SCXS(CH,2,2).NE.0 .AND. SCXS(CH,4,2).NE.0) THEN
                XS(1)=SCXS(CH,1,1)
                XS(2)=SCXS(CH,1,2)
                XS(3)=SCXS(CH,3,1)
                XS(4)=SCXS(CH,3,2)
                XS(5)=SCXS(CH,5,1)
                XS(6)=SCXS(CH,5,2)
                KK=2
             ELSE IF (SCXS(CH,2,2).NE.0) THEN
                XS(1)=SCXS(CH,1,1)
                XS(3)=SCXS(CH,3,1)
                XS(4)=SCXS(CH,3,2)
                KK=1
             ELSE IF (SCXS(CH,4,2).NE.0) THEN
                XS(1)=SCXS(CH,1,2)
                XS(3)=SCXS(CH,5,1)
                XS(4)=SCXS(CH,5,2)
                KK=1
             ENDIF
             DO L=1,KK
                IF(L.EQ.1) LL=3
                IF(L.EQ.2) LL=5
                DO K=LL,LL+1
                   DO J=1,2
                      BEDCH(J,XS(K))=BEDCH(J,XS(L))
                      VOLCH(J,XS(K))=VOLCH(J,XS(L))
                   END DO
                   DO J=1,4
                      D165084ACT(J,XS(K))=D165084ACT(J,XS(L))
                      D165084SUB(J,XS(K))=D165084SUB(J,XS(L))
                      D165084BLD(J,XS(K))=D165084BLD(J,XS(L))
                   END DO
                   IF (SCXS(CH,2,2).NE.0) THEN
                      DO I=1,NCLASS
                         BEDFRACT(XS(K),I)=BEDFRACT(XS(L),I)
                      END DO
                   ENDIF
                END DO
             END DO
          END DO
          IF (DEFINT(8).EQ.2 .AND. TELAPSE.GE.TSTART) THEN
             TRACEL=TRACEL+DELTAT
             TRWRITE=TRWRITE+DELTAT
             IF (TRWRITE.GE.TREC) THEN
                TRWROUT=1
                TRWRITE = 0
             ENDIF
C END
             CALL TRACING (TRACERS,TPOS,NTRAC,THROPUT,DELTAT,BEDFRACT,
     +       SIZELAYER,THICKLAYER,DISTANCE,WSWIDTH,QBEDLOAD)
          ENDIF
          PCELAPSE=TELAPSE*100/TLENGTH
          TELAPSEYR=TELAPSE/60/60/24/365.25
          CALL NEWDATE (DATE,DELTAT,MSECT)
          IF (TTOTAL.LT.1.05) THEN
             RECORD=SET
```

```
              Z=Z+1
C          ELSE IF (TELAPSE.GT.TLENGTH) THEN
C PATRICK new stop criterium for date
              ELSE IF (DATE(1).GE.ENDDATE(1)) THEN
                 IF (DATE(2).GE.ENDDATE(2)) THEN
                    IF (DATE(3).GE.ENDDATE(3)) THEN
                       RECORD=SET
                    ENDIF
                 ENDIF
C END          ENDIF

           ELSE IF (WTYPE .EQ. PERIOD .AND. Z.GE.DEFINT(6)) THEN
              RECORD=SET
           IF (TELAPSEYR.LT.1.0) THEN
              WRITE (*,1801) (0.001*TTOTAL),TELAPSEYR,PCELAPSE,TIME@()
           ELSE
              IF (TTOTAL.LT.1000000) THEN
                 WRITE (*,1800) (0.001*TTOTAL),TELAPSEYR,PCELAPSE,TIME@()
              ELSE
                 WRITE (*,1800) (0.000001*TTOTAL),TELAPSEYR,PCELAPSE,
     +           TIME@()
              ENDIF
           ENDIF
           SCREEN=SCREEN+1
           Z=1
           ELSE IF (WTYPE .EQ. TIME .AND. TW .GT. TINT) THEN
              RECORD=SET
              IF (TELAPSEYR.LT.1.0) THEN
                 WRITE (*,1801) (0.001*TTOTAL),TELAPSEYR,PCELAPSE,TIME@()
              ELSE
                 WRITE (*,1800) (0.001*TTOTAL),TELAPSEYR,PCELAPSE,TIME@()
              ENDIF
              TW=TW-TINT
              SCREEN=SCREEN+1
C PATRICK new option for time administration
           ELSEIF (WTYPE.EQ.YEARLY .OR. WTYPE.EQ.DAILY) THEN
              IF (DATE(2).EQ.1 .AND. DATE(3).EQ.1) THEN
                 IF (DATE(4).EQ.0 .AND. DATE(5).EQ.0 .AND. DATE(6).EQ.0)
     +           THEN
                    RECORD=SET
                    IF (TELAPSEYR.LT.1.0) THEN
                       WRITE (*,1801) (0.001*TTOTAL),TELAPSEYR,PCELAPSE,
     +                 TIME@()
                    ELSE
                       WRITE (*,1800) (0.001*TTOTAL),TELAPSEYR,PCELAPSE,
     +                 TIME@()
                    ENDIF
                    SCREEN=SCREEN+1
                 ELSE
                    RECORD=OFF
                    Z=Z+1
                 ENDIF
              ELSE
                 RECORD=OFF
                 Z=Z+1
           ENDIF
C Write data on daily basis when selected
C except for .inf;.res (1) .sed (2) .tpt (3) .sur (4) .sub
C (5) .bld and (6) .hyd
              IF (WTYPE.EQ.DAILY) THEN
                 IF (DATE(4).EQ.0 .AND. DATE(5).EQ.0 .AND. DATE(6).EQ.0)
     +           THEN
C Convert array with date to a single text-variable
                 DO 219,A=1,6
                    RDATE(A)=DATE(A)
219              CONTINUE
                 IDATE=AINT(RDATE(1)/1000)
                 TEXTDATE(1:1)=CHAR(48+IDATE)
                 RESTDATE=RDATE(1)-IDATE*1000
                 IDATE=AINT(RESTDATE/100)
                 TEXTDATE(2:2)=CHAR(48+IDATE)
                 RESTDATE=RESTDATE-IDATE*100
                 IDATE=AINT(RESTDATE/10)
                 TEXTDATE(3:3)=CHAR(48+IDATE)
                 RESTDATE=RESTDATE-IDATE*10
                 IDATE=RESTDATE
                 TEXTDATE(4:4)=CHAR(48+IDATE)
                 TEXTDATE(5:5)=CHAR(45)
                 IDATE=AINT(RDATE(2)/10)
                 TEXTDATE(6:6)=CHAR(48+IDATE)
                 RESTDATE=RDATE(2)-IDATE*10
                 IDATE=RESTDATE
                 TEXTDATE(7:7)=CHAR(48+IDATE)
                 TEXTDATE(8:8)=CHAR(45)
                 IDATE=AINT(RDATE(3)/10)
                 TEXTDATE(9:9)=CHAR(48+IDATE)
                 RESTDATE=RDATE(3)-IDATE*10
                 IDATE=RESTDATE
                 TEXTDATE(10:10)=CHAR(48+IDATE)
                 IDATE=AINT(RDATE(4)/10)
                 TEXTTIME(1:1)=CHAR(48+IDATE)
                 RESTDATE=RDATE(4)-IDATE*10
                 IDATE=RESTDATE
                 TEXTTIME(2:2)=CHAR(48+IDATE)
                 TEXTTIME(3:3)=CHAR(58)
                 IDATE=AINT(RDATE(5)/10)
                 TEXTTIME(4:4)=CHAR(48+IDATE)
                 RESTDATE=RDATE(5)-IDATE*10
                 IDATE=RESTDATE
                 TEXTTIME(5:5)=CHAR(48+IDATE)
                 TEXTTIME(6:6)=CHAR(58)
                 IDATE=AINT(RDATE(6)/10)
                 TEXTTIME(7:7)=CHAR(48+IDATE)
                 RESTDATE=RDATE(6)-IDATE*10
                 IDATE=RESTDATE
                 TEXTTIME(8:8)=CHAR(48+IDATE)
                 DO 244,IFILE=21,60
                    IF (OUTPUT(IFILE-20).EQ.'Y') BACKSPACE (IFILE)
244              CONTINUE
              IF (OUTPUT(7).EQ.'Y') WRITE (27,1420)
     +        (1000*D165084ACT(2,XSN),XSN=1,N)
              IF (OUTPUT(8).EQ.'Y') WRITE (28,1420)
     +        (1000*D165084ACT(3,XSN),XSN=1,N)
              IF (OUTPUT(9).EQ.'Y') WRITE (29,1421)
     +        ((QBEDLOAD(XSN)/WSWIDTH(XSN)),XSN=1,N)
              IF (OUTPUT(10).EQ.'Y') WRITE (30,1420)
     +        (1000*D165084BLD(2,XSN),XSN=1,N)
              IF (OUTPUT(11).EQ.'Y') WRITE (31,1422)
     +        (ESLOPE(XSN),XSN=1,N)
              IF (OUTPUT(12).EQ.'Y') WRITE (32,1423)
     +        ((R(XSN)*ESLOPE(XSN)/(SS-1)/D165084ACT(2,XSN)),XSN=1,N)
              IF (OUTPUT(13).EQ.'Y') WRITE (33,1424)
     +        ((WATSURF(XSN)-MEANDEP(XSN)),XSN=1,N)
              IF (OUTPUT(14).EQ.'Y') WRITE (34,1425) (R(XSN),XSN=1,N)
```

```
                 IF (OUTPUT(15).EQ.'Y') WRITE (35,1425) (FR(XSN),XSN=1,N)
                 IF (OUTPUT(16).EQ.'Y') WRITE (36,1426)
     +           (FFACTOR(XSN),XSN=1,N)
                 IF (OUTPUT(17).EQ.'Y') WRITE (37,1420)
     +           (1000*D165084ACT(1,XSN),XSN=1,N)
                 IF (OUTPUT(18).EQ.'Y') WRITE (38,1420)
     +           (1000*D165084SUB(1,XSN),XSN=1,N)
                 IF (OUTPUT(19).EQ.'Y') WRITE (39,1420)
     +           (1000*D165084SUB(2,XSN),XSN=1,N)
                 IF (OUTPUT(20).EQ.'Y') WRITE (40,1420)
     +           (1000*D165084SUB(3,XSN),XSN=1,N)
                 IF (OUTPUT(21).EQ.'Y') WRITE (41,1420)
     +           (1000*D165084BLD(1,XSN),XSN=1,N)
                 IF (OUTPUT(22).EQ.'Y') WRITE (42,1420)
     +           (1000*D165084BLD(3,XSN),XSN=1,N)
                 IF (OUTPUT(23).EQ.'Y') WRITE (43,1426)
     +           (MANNING(XSN),XSN=1,N)
                 IF (OUTPUT(24).EQ.'Y') WRITE (44,1425)
     +           (MEANDEP(XSN),XSN=1,N)
                 IF (OUTPUT(25).EQ.'Y') WRITE (45,1426)
     +           (BEDCH(1,XSN),XSN=1,N)
                 IF (OUTPUT(26).EQ.'Y') WRITE (46,1420)
     +           (BEDCH(2,XSN),XSN=1,N)
                 IF (OUTPUT(27).EQ.'Y') WRITE (47,1420)
     +           (VOLCH(1,XSN),XSN=1,N)
                 IF (OUTPUT(28).EQ.'Y') WRITE (48,1420)
     +           (VOLCH(2,XSN),XSN=1,N)
                 IF (OUTPUT(29).EQ.'Y') WRITE (49,1420)
     +           (PCSAND(XSN),XSN=1,N)
                 IF (OUTPUT(32).EQ.'Y') THEN
                   DO 7900,IT=1,NTRIB
                     WRITE (52,1427)IT,TRIBQB(IT),
     +               (TRIBFRACT(II,IT),II=1,NCLASS)
 7900              CONTINUE
                 ENDIF
                 IF (OUTPUT(33).EQ.'Y')
     +           WRITE (53,1420) (1000*DGMACT(XSN),XSN=1,N)
                 IF (OUTPUT(34).EQ.'Y') WRITE (54,1420)
     +           (1000*D165084ACT(4,XSN),XSN=1,N)
                 IF (OUTPUT(35).EQ.'Y') WRITE (55,1420)
     +           (1000*D165084SUB(4,XSN),XSN=1,N)
                 IF (OUTPUT(36).EQ.'Y') WRITE (56,1420)
     +           (1000*D165084BLD(4,XSN),XSN=1,N)
C PATRICK write data to added output-files
                 IF (OUTPUT(37).EQ.'Y' .AND. TELAPSE.GT.3600)
     +           WRITE (57,1428) TELAPSE,DELTAT,DELTATC
                 IF (OUTPUT(38).EQ.'Y') WRITE (58,1425)
     +           (THICKLAYER(XSN),XSN=1,N)
                 IF (OUTPUT(30).EQ.'Y')
     +           WRITE (50,1426) (VELOCITY(XSN),XSN=1,N)
                 IF (OUTPUT(31).EQ.'Y')
     +           WRITE (51,1420) (WATSURF(XSN),XSN=1,N)
                 IF (OUTPUT(39).EQ.'Y')
     +           WRITE (59,1431) TEXTDATE,(LOWPOINT(XSN),XSN=1,N)
                 IF (OUTPUT(40).EQ.'Y') THEN
                   IF (NSECT.GE.2) THEN
                     WRITE (60,1430) TEXTDATE,(SEDCHTOT(CH,1),CH=1
     +                 ,NSECT),(SEDCHTOT(CH,2),CH=1,NSECT)
                   ELSE
                     WRITE (60,1429) TEXTDATE,SEDTOTAL(1)
     +                 ,SEDTOTAL(2)
                   ENDIF
                 ENDIF
                 DO 259,IFILE=21,60
                   IF (OUTPUT(IFILE-20).EQ.'Y') END FILE(IFILE)
 259             CONTINUE
               ENDIF
             ENDIF
           ELSE
C END
             RECORD=OFF
             Z=Z+1
           ENDIF
C   Write the results to output files
           IF (RECORD.EQ.SET) THEN
C PATRICK Convert array with date to a single text-variable
             DO 220,A=1,6
               RDATE(A)=DATE(A)
 220         CONTINUE
             IDATE=AINT(RDATE(1)/1000)
             TEXTDATE(1:1)=CHAR(48+IDATE)
             RESTDATE=RDATE(1)-IDATE*1000
             IDATE=AINT(RESTDATE/100)
             TEXTDATE(2:2)=CHAR(48+IDATE)
             RESTDATE=RESTDATE-IDATE*100
             IDATE=AINT(RESTDATE/10)
             TEXTDATE(3:3)=CHAR(48+IDATE)
             RESTDATE=RESTDATE-IDATE*10
             IDATE=RESTDATE
             TEXTDATE(4:4)=CHAR(48+IDATE)
             TEXTDATE(5:5)=CHAR(45)
             IDATE=AINT(RDATE(2)/10)
             TEXTDATE(6:6)=CHAR(48+IDATE)
             RESTDATE=RDATE(2)-IDATE*10
             IDATE=RESTDATE
             TEXTDATE(7:7)=CHAR(48+IDATE)
             TEXTDATE(8:8)=CHAR(45)
             IDATE=AINT(RDATE(3)/10)
             TEXTDATE(9:9)=CHAR(48+IDATE)
             RESTDATE=RDATE(3)-IDATE*10
             IDATE=RESTDATE
             TEXTDATE(10:10)=CHAR(48+IDATE)
             IDATE=AINT(RDATE(4)/10)
             TEXTTIME(1:1)=CHAR(48+IDATE)
             RESTDATE=RDATE(4)-IDATE*10
             IDATE=RESTDATE
             TEXTTIME(2:2)=CHAR(48+IDATE)
             TEXTTIME(3:3)=CHAR(58)
             IDATE=AINT(RDATE(5)/10)
             TEXTTIME(4:4)=CHAR(48+IDATE)
             RESTDATE=RDATE(5)-IDATE*10
             IDATE=RESTDATE
             TEXTTIME(5:5)=CHAR(48+IDATE)
             TEXTTIME(6:6)=CHAR(58)
             IDATE=AINT(RDATE(6)/10)
             TEXTTIME(7:7)=CHAR(48+IDATE)
             RESTDATE=RDATE(6)-IDATE*10
             IDATE=RESTDATE
             TEXTTIME(8:8)=CHAR(48+IDATE)
             BACKSPACE (10)
             BACKSPACE (11)
C END
             DO 245,IFILE=21,60
               IF (OUTPUT(IFILE-20).EQ.'Y') BACKSPACE (IFILE)
```

```
 245        CONTINUE
            NWRITE=NWRITE+1
            TIMEYR=TELAPSE/60/60/24/365.25
            WRITE (10,1611) NWRITE,TIMEYR,(TTOTAL/1000),
     +      TEXTDATE,TEXTTIME
            DO 250,XSN=1,N
               TAU=RHO*G*R(XSN)*ESLOPE(XSN)
               DIMTAU=R(XSN)*ESLOPE(XSN)/(SS-1)/D165084ACT(2,XSN)
               IF (TTOTAL.LT.1.01) THEN
                  CALL LOWBED (SURV,XSN,BEDMIN)
                  LOWPOINT(XSN)=BEDMIN
               ELSE
                  CALL LOWBED (NEWSURV,XSN,BEDMIN)
                  LOWPOINT(XSN)=BEDMIN
               ENDIF
               PCSAND(XSN)=0
               DO 251,IC=1,NCLASS
                  IF (SIZEFINE(IC).LT.1.01) THEN
                     PCSAND(XSN)=PCSAND(XSN)+SIZELAYER(1,XSN,IC)
                  ELSE
                     GOTO 252
                  ENDIF
 251           CONTINUE
 252           WRITE (11,1710) SECTCODE(XSN),TEXTDATE,TEXTTIME,
     +         DISTANCE(XSN),WSWIDTH(XSN),R(XSN),ESLOPE(XSN),TAU,
     +         DIMTAU,(1000*D165084ACT(J,XSN),J=2,3),1000*DGMACT(XSN),
     +         (1000*D165084SUB(2,XSN)),1000*D165084BLD(2,XSN),
     +         QBEDLOAD(XSN)/WSWIDTH(XSN),PCSAND(XSN),WATSURF(XSN),
     +         (WATSURF(XSN)-MEANDEP(XSN)),LOWPOINT(XSN),BEDCH(2,XSN)
               IF (OUTPUT(6).EQ.'Y') THEN
C PATRICK write discharge to .hyd file, if there are tributaries and/or
C variable discharge is used.
                  IF (NTRIB.NE.0 .OR. QTYPE.EQ.2) THEN
                     WRITE (26,1721) SECTCODE(XSN),
     +               TEXTDATE,TEXTTIME,DISTANCE(XSN),Q(XSN),
     +               WSWIDTH(XSN),MEANDEP(XSN),VELOCITY(XSN),R(XSN),
     +               ESLOPE(XSN),FFACTOR(XSN),MANNING(XSN),FR(XSN)
                  ELSE
                     WRITE (26,1720)
     +               SECTCODE(XSN),TEXTDATE,TEXTTIME,DISTANCE(XSN),
     +               WSWIDTH(XSN),MEANDEP(XSN),VELOCITY(XSN),R(XSN),
     +               ESLOPE(XSN),FFACTOR(XSN),MANNING(XSN),FR(XSN)
                  ENDIF
               ENDIF
               IF (OUTPUT(1).EQ.'Y') WRITE (21,1730)
     +         SECTCODE(XSN),TEXTDATE,TEXTTIME,
     +         (1000*D165084ACT(J,XSN),J=1,3),
     +         (1000*D165084SUB(J,XSN),J=1,3),
     +         (1000*D165084BLD(J,XSN),J=1,3)
               UNITGB=(QBEDLOAD(XSN)/WSWIDTH(XSN))*RHOSED*1000
               IF (XSN.EQ.1) THEN
                  IF (OUTPUT(2).EQ.'Y') THEN
                     UNITGBIN=(QBIN/WSWIDTH(XSN))*RHOSED*1000
                     WRITE (22,1739) TEXTDATE,TEXTTIME,QBIN,
     +               QBIN/WSWIDTH(XSN),UNITGBIN
                  ENDIF
               ENDIF
               IF (OUTPUT(2).EQ.'Y') WRITE (22,1740) SECTCODE(XSN),
     +         TEXTDATE,TEXTTIME,QBEDLOAD(XSN),
     +         QBEDLOAD(XSN)/WSWIDTH(XSN),UNITGB,
     +         BEDCH(2,XSN),VOLCH(2,XSN),(WATSURF(XSN)-MEANDEP(XSN))
               IF (OUTPUT(3).EQ.'Y') WRITE (23,1750) SECTCODE(XSN),
     +         TEXTDATE,TEXTTIME,(SIZELAYER(1,XSN,I),I=1,NCLASS)
               IF (OUTPUT(4).EQ.'Y') WRITE (24,1750) SECTCODE(XSN),
     +         TEXTDATE,TEXTTIME,(SIZELAYER(2,XSN,I),I=1,NCLASS)
C PATRICK if statement to avoid divide by zero
               IF (XSN.EQ.1) THEN
                  IF (QBIN.GT.0) THEN
                     IF (OUTPUT(5).EQ.'Y') WRITE (25,1749) TEXTDATE,
     +               TEXTTIME,(100*QBFRACTIN(I)/QBIN,I=1,NCLASS)
                  ELSE
                     IF (OUTPUT(5).EQ.'Y') WRITE (25,1749) TEXTDATE,
     +               TEXTTIME,QBIN
                  ENDIF
               ENDIF
               IF (OUTPUT(5).EQ.'Y') THEN
                  IF (QBEDLOAD(XSN).GT.0) THEN
                     WRITE (25,1750) SECTCODE(XSN),TEXTDATE,TEXTTIME,
     +               (0.1*BEDFRACT(XSN,I)/QBEDLOAD(XSN),I=1,NCLASS)
                  ELSE
                     WRITE (25,1750)
     +               SECTCODE(XSN),TEXTDATE,TEXTTIME,QBEDLOAD(XSN)
                  ENDIF
               ENDIF
 250        CONTINUE
            IF (WTYPE.NE.DAILY) THEN
            IF (OUTPUT(7).EQ.'Y') WRITE (27,1420)
     +      (1000*D165084ACT(2,XSN),XSN=1,N)
            IF (OUTPUT(8).EQ.'Y') WRITE (28,1420)
     +      (1000*D165084ACT(3,XSN),XSN=1,N)
            IF (OUTPUT(9).EQ.'Y') WRITE (29,1421)
     +      ((QBEDLOAD(XSN)/WSWIDTH(XSN)),XSN=1,N)
            IF (OUTPUT(10).EQ.'Y') WRITE (30,1420)
     +      (1000*D165084BLD(2,XSN),XSN=1,N)
            IF (OUTPUT(11).EQ.'Y') WRITE (31,1422)
     +      (ESLOPE(XSN),XSN=1,N)
            IF (OUTPUT(12).EQ.'Y') WRITE (32,1423)
     +      ((R(XSN)*ESLOPE(XSN)/(SS-1)/D165084ACT(2,XSN)),XSN=1,N)
            IF (OUTPUT(13).EQ.'Y') WRITE (33,1424)
     +      ((WATSURF(XSN)-MEANDEP(XSN)),XSN=1,N)
            IF (OUTPUT(14).EQ.'Y') WRITE (34,1425) (R(XSN),XSN=1,N)
            IF (OUTPUT(15).EQ.'Y') WRITE (35,1425) (FR(XSN),XSN=1,N)
            IF (OUTPUT(16).EQ.'Y') WRITE (36,1426)
     +      (FFACTOR(XSN),XSN=1,N)
            IF (OUTPUT(17).EQ.'Y') WRITE (37,1420)
     +      (1000*D165084ACT(1,XSN),XSN=1,N)
            IF (OUTPUT(18).EQ.'Y') WRITE (38,1420)
     +      (1000*D165084SUB(1,XSN),XSN=1,N)
            IF (OUTPUT(19).EQ.'Y') WRITE (39,1420)
     +      (1000*D165084SUB(2,XSN),XSN=1,N)
            IF (OUTPUT(20).EQ.'Y') WRITE (40,1420)
     +      (1000*D165084SUB(3,XSN),XSN=1,N)
            IF (OUTPUT(21).EQ.'Y') WRITE (41,1420)
     +      (1000*D165084BLD(1,XSN),XSN=1,N)
            IF (OUTPUT(22).EQ.'Y') WRITE (42,1420)
     +      (1000*D165084BLD(3,XSN),XSN=1,N)
            IF (OUTPUT(23).EQ.'Y') WRITE (43,1426)
     +      (MANNING(XSN),XSN=1,N)
            IF (OUTPUT(24).EQ.'Y') WRITE (44,1425)
     +      (MEANDEP(XSN),XSN=1,N)
            IF (OUTPUT(25).EQ.'Y') WRITE (45,1426)
     +      (BEDCH(1,XSN),XSN=1,N)
            IF (OUTPUT(26).EQ.'Y') WRITE (46,1420)
     +      (BEDCH(2,XSN),XSN=1,N)
```

```
      IF (OUTPUT(27).EQ.'Y') WRITE (47,1420)
     + (VOLCH(1,XSN),XSN=1,N)
      IF (OUTPUT(28).EQ.'Y') WRITE (48,1420)
     + (VOLCH(2,XSN),XSN=1,N)
      IF (OUTPUT(29).EQ.'Y') WRITE (49,1420)
     + (PCSAND(XSN),XSN=1,N)
      IF (OUTPUT(32).EQ.'Y') THEN
        DO 790,IT=1,NTRIB
          WRITE (52,1427)IT,TRIBQB(IT),
     +    (TRIBFRACT(II,IT),II=1,NCLASS)
790     CONTINUE
      ENDIF
      IF (OUTPUT(33).EQ.'Y')
     + WRITE (53,1420) (1000*DGMACT(XSN),XSN=1,N)
      IF (OUTPUT(34).EQ.'Y') WRITE (54,1420)
     + (1000*D165084ACT(4,XSN),XSN=1,N)
      IF (OUTPUT(35).EQ.'Y') WRITE (55,1420)
     + (1000*D165084SUB(4,XSN),XSN=1,N)
      IF (OUTPUT(36).EQ.'Y') WRITE (56,1420)
     + (1000*D165084BLD(4,XSN),XSN=1,N)
C PATRICK write data to added output-files
      IF (OUTPUT(37).EQ.'Y' .AND. TELAPSE.GT.3600)
     + WRITE (57,1428) TELAPSE,DELTAT,DELTATC
      IF (OUTPUT(38).EQ.'Y') WRITE (58,1425)
     + (THICKLAYER(XSN),XSN=1,N)
        IF (OUTPUT(30).EQ.'Y') WRITE (50,1423)
     +  (VELOCITY(XSN),XSN=1,N)
        IF (OUTPUT(31).EQ.'Y') WRITE (51,1424)
     +  (WATSURF(XSN),XSN=1,N)
        IF (OUTPUT(39).EQ.'Y') WRITE (59,1424)
     +  (LOWPOINT(XSN),XSN=1,N)
        IF (OUTPUT(40).EQ.'Y') THEN
          IF (NSECT.GE.2) THEN
            WRITE (60,1430) TEXTDATE,(SEDCHTOT(CH,1),CH=1
     +      ,NSECT),(SEDCHTOT(CH,2),CH=1,NSECT)
          ELSE
            WRITE (60,1429) TEXTDATE,SEDTOTAL(1),SEDTOTAL(2)
          ENDIF
        ENDIF
      ENDIF
C END
      END FILE (10)
      END FILE (11)
      DO 260,IFILE=21,60
        IF (OUTPUT(IFILE-20).EQ.'Y') END FILE(IFILE)
260   CONTINUE
     ENDIF
     IF (TRWROUT.EQ.1) THEN
      TRINT = INT(TRACEL/60)
      WRITE (20,4000) (TELAPSE/60),TRINT
      WRITE (20,4001) TPOS
      DO 800,IT=1,NTRAC
        WRITE (20,4010)
     +  INT(TRACERS(IT,1)),INT(TRACERS(IT,2)),TRACERS(IT,4)
800   CONTINUE
      TRWROUT=0
     ENDIF
C PATRICK redefines the discharge when .qdt file is used
     IF (QTYPE.EQ.2) CALL QDATA (DATE,DISTANCE,DSDEPTH,DSWATER,HDS,
     + LENGTH,MSECT,N,NTRIB,NSECT,PARAM,Q,QDATE,QDS,QHFILE,QT,
     + RMETHOD,TCODE,TMAX,TRIBLOC,TRIBQ,XSN,QSECT,SCXS)
     IF (QTYPE.EQ.2) CALL WATERLEVEL (DSWATER,HDATE,HDS,HT,DATE,
     + HTYPE,HCHANGE,HYEAR,TMAX,MSECT,TIDE)
C END
      CALL DISTRIB (N,NEWSURV,SURV,TTOTAL,BEDCH,WATSURF)
      ERR1=0
      CALL LOWBED(NEWSURV,N,BEDDS)
      CALL LOWBED(NEWSURV,N-1,BEDDS1)
      HDS1=HDS+BEDDS1-BEDDS
      CALL AREA(NEWSURV,HDS,N,AWET,WSB,WP)
      BEDMEAN=HDS-(AWET/WSB)
      CALL AREA(NEWSURV,HDS1,N-1,AWET,WSB,WP)
      BEDMEAN1=HDS1-(AWET/WSB)
      SLOPE=(BEDMEAN1-BEDMEAN)/(DISTANCE(N)-DISTANCE(N-1))
C       SLOPE1=(HDS1-HDS)/(DISTANCE(N)-DISTANCE(N-1))
C       WRITE (*,9999) SLOPE1,SLOPE
C9999   FORMAT (F12.9,F12.9)
C       PAUSE
      HEST=HDS
C PATRICK for specific ds water level
      IF (RMETHOD.LT.5) THEN
        DO 280,K=1,50
          CALL AREA(NEWSURV,HEST,N,AWET,WSB,WP)
          HRAD=AWET/WP
          D84=D165084ACT(3,N)
          IF (EQUATION.EQ.1) THEN
            UBAR=(PARAM(1)*LOG10(HRAD/D84)+PARAM(2))
     +      *((8*G*HRAD*SLOPE)**0.5)
          ELSE IF (EQUATION.EQ.2) THEN
            MANNINGN=PARAM(1)*(D84**PARAM(2))
            UBAR=(1/MANNINGN)*(HRAD**(0.667))*(SLOPE**0.5)
C PATRICK
          ELSE IF (EQUATION.EQ.3) THEN
            MANNINGN=PARAM(1)
            UBAR=(1/MANNINGN)*(HRAD**(0.667))*(SLOPE**0.5)
C END
          ENDIF
          QEST=UBAR*AWET
          ERROR=(QEST-QDS(QT))/(QEST+QDS(QT))
          IF (ABS(ERROR).LT.0.001) GOTO 281
          IF (K.EQ.1) THEN
            HEST=HEST+0.001
            ERR1=ERROR
          ELSE IF (K.EQ.2) THEN
            IF (ERROR*ERR1.LT.0) THEN
              HEST=HEST-0.0005
              GOTO 281
            ENDIF
            IF (ABS(ERROR).GT.ABS(ERR1)) THEN
              APP=-1
            ELSE
              APP=1
            ENDIF
            HEST=HEST+APP*0.001
          ELSE
            HEST=HEST+APP*0.001
          ENDIF
          IF (ERR1*ERROR.LT.0) THEN
            HEST=HEST-APP*0.001
            GOTO 281
          ENDIF
280     CONTINUE
281     IF (K.GT.50) PRINT *,'DISCHARGE/ELEVATION NOT CONVERGED!!'
        HDS=HEST
```

```
                CALL EXTEND(NEWSURV,Q,HDS,N,D165084ACT,DISTANCE,MEANDEP,
     +          WATSURF,CODE,EXTMETHOD,EXTSLOPE,NMAX,HLOW,EQUATION,PARAM)
              ELSE
                NMAX=N
                HLOW=HDS
                CALL AREA(NEWSURV,HDS,N,AWET,WSB,WP)
                HRAD=AWET/WP
                WSWIDTH(N)=WSB
                MEANDEP(N)=AWET/WSB
                WATSURF(N)=HDS
                CALL SFRICT(Q,N,HRAD,AWET,D165084ACT,ENSL,UBAR,FF,
     +          EQUATION,PARAM)
              ENDIF
C END
              IF (RECORD.EQ.SET) THEN
                OPEN (17,FILE='NEWSTART.SDS')
                OPEN (18,FILE='NEWSTART.GSS')
                DO 400,K=1,N
                  WRITE (17,'(A6)') SECTCODE(K)
                  WRITE (18,'(A6)') SECTCODE(K)
                  WRITE (17,1690) DISTANCE(K)
                  DO 380,L=1,NCLASS
                    WRITE (18,1685) (SIZELAYER(II,K,L),II=1,5)
380               CONTINUE
                  DO 390,I=1,100
                    WRITE (17,1700) (NEWSURV(I,J),J=((2*K)-1),(2*K))
                    IF (NEWSURV(I,2*K).GT.9000) GOTO 400
390               CONTINUE
400             CONTINUE
              ENDIF
C Now for the calculation of the water surface profile for main channel
C and side channel(s) separately.
              IF (NSECT.EQ.0) THEN
                DO 350,XSN=(NMAX-1),1,-1
                  CALL BACKWATER (NMAX,N,XSN,Q,HLOW,NEWSURV,RECORD,
     +            EQUATION,PARAM)
350             CONTINUE
                GOTO 450
              ELSE
C PATRICK statements for multiple channel option
                DO I=1,NSECT
                  HDIFF(I)=0
                  QSECTMAX(I)=Q(1)
                  QSECTMIN(I)=0
                  CHECKOSS(I)=0
                ENDDO
                K=0
459             DO 460,SC=1,10
                  DO I=NSECT,2,-1
                    IF (I.EQ.NSECT .OR. SCXS(I,4,1).EQ.0) THEN
                      HDSC=HDS
                    ELSE
                      HDSC=WATSURF(SCXS(I,5,1))
                    ENDIF
                    XS(1)=SCXS(I,1,1)
                    XS(2)=SCXS(I,1,2)
                    CALL AREA(NEWSURV,HDSC,XS(2),AWET,WSB,WP)
                    WATSURF(XS(2))=HDSC
                    WSWIDTH(XS(2))=WSB
                    MEANDEP(XS(2))=AWET/WSB
                    HRAD=AWET/WP
                    CALL SFRICT(Q,XS(2),HRAD,AWET,D165084ACT,ENSL,UBAR,
     +              FF,EQUATION,PARAM)
                    DO 465,XSN=XS(2)-1,XS(1),-1
                      CALL BACKWATER(XS(2),N,XSN,Q,HDSC,NEWSURV,RECORD,
     +                EQUATION,PARAM)
465                 CONTINUE
                    SECTUP=SCXS(I,2,1)
                    HSC(I)=WATSURF(XS(1))
C Check if upstream end is bifurcation and waterlevel in other channel.
                    IF (SCXS(SECTUP,4,2).NE.0) THEN
                      IF (SCXS(SECTUP,4,1).EQ.I) THEN
                        HDIFF(I)=HSC(SCXS(SECTUP,4,2))-HSC(I)
                        IF (ABS(HDIFF(I)).GT.0) THEN
                          IF (SC.GT.1) THEN
                            IF (ABS(BACKHDIFF(I)+HDIFF(I)).LE.TOL .OR.
     +                      CHECKOSS(I).EQ.1 .OR. K.EQ.9) THEN
                              CHECKOSS(I)=1
                              IF (HDIFF(I).GT.0) THEN
                                QSECTMIN(I)=QSECT(I)
                                BACKQSECT(I)=QSECT(I)
                              ELSE
                                QSECTMAX(I)=QSECT(I)
                                BACKQSECT(I)=QSECT(I)
                              ENDIF
                              QSECT(I)=(QSECTMAX(I)+QSECTMIN(I))/2
                              GOTO 470
                            ENDIF
                          ENDIF
                          DELTAH=HSC(I)-HDSC
                          BACKQSECT(I)=QSECT(I)
                          BACKHDIFF(I)=HDIFF(I)
                        IF (HDIFF(I).GT.0) THEN
                          SECTNEXT=SCXS(SECTUP,4,2)
                          XS(1)=SCXS(SECTNEXT,1,1)
                          XS(2)=SCXS(SECTNEXT,1,2)
                          DELTAH=WATSURF(XS(1))-WATSURF(XS(2))
                          QSECT(I)=QSECT(SECTUP)-(
     +                    QSECT(SECTNEXT)*(1-WSWIDTH(XS(1)+1)/
     +                    (WSWIDTH(XS(1)+1)+WSWIDTH(SCXS(I,1,1) +1))*
     +                    HDIFF(I)/DELTAH)**0.5)
                          IF (QSECT(I).LT.QSECTMIN(I)) THEN
                            QSECT(I)=QSECTMIN(I)
                            CHECKOSS(I)=1
                          ENDIF
                        ELSE
                          DELTAH=HSC(I)-HDSC
                          QSECT(I)=QSECT(I)*(1+(1-WSWIDTH(XS(1)+1)/(
     +                    WSWIDTH(XS(1)+1)+WSWIDTH(SCXS(SECTUP,5,2)+1)
     +                    ))*HDIFF(I)/DELTAH)**0.5
                          IF (QSECT(I).GT.QSECTMAX(I)) THEN
                            QSECT(I)=QSECTMAX(I)
                            CHECKOSS(I)=1
                          ENDIF
                        ENDIF
470                     DO J=I,NSECT
                          IF (J.EQ.SCXS(SECTUP,4,2)) THEN
                            QSECT(J)=QSECT(SECTUP)-QSECT(I)
                          ELSE IF (SCXS(J,4,2).NE.0) THEN
                            QSECT(SCXS(J,4,1))=QSECT(SCXS(J,4,1))
     +                      *QSECT(J)/BACKQSECT(J)
                            QSECT(SCXS(J,4,2))=QSECT(SCXS(J,4,2))
     +                      *QSECT(J)/BACKQSECT(J)
                          ELSE IF (SCXS(J,2,2).NE.0) THEN
```

```
                              QSECT(J)=QSECT(SCXS(J,2,1))+
     +                        QSECT(SCXS(J,2,2))
                           ENDIF
                        ENDDO
                        CALL QDISTRIB (N,NSECT,Q,QSECT,SCXS)
                     ENDIF
      BACKSPACE(66)
      WRITE (66,6999) TTOTAL,I,K*10+SC,CHECKOSS(I),HDIFF(I),DELTAH,
     +QSECT(I),BACKQSECT(I),QSECTMAX(I),QSECTMIN(I)
 6999 FORMAT (F10.0,1X,I2,1X,I3,1X,I1,1X,6(F14.9,1X))
      ENDFILE(66)
                  ENDIF
               ENDIF
               IF (I.EQ.2) THEN
                  CHECK=0
                  DO J=1,NSECT
                     IF (ABS(HDIFF(J)).GT.TOL) THEN
                        IF (ABS(QSECT(J)-BACKQSECT(J)).GT.0)
     +                  CHECK=1
                     ENDIF
                  ENDDO
                  IF (CHECK.EQ.0) GOTO 455
               ENDIF
            ENDDO
  460    CONTINUE
         CHECK=0
         DO J=1,NSECT
            IF (ABS(HDIFF(J)).GT.TOL) THEN
               IF (ABS((QSECT(J)-BACKQSECT(J))/QSECT(J)).GT.0.001)
     +         CHECK=1
            ENDIF
         ENDDO
         IF (CHECK.EQ.1) THEN
            IF (K.EQ.9) THEN
               WRITE (7,467) TTOTAL*0.001,K*10+SC,
     +         (HDIFF(BIFUR(N)),N=1,NBIFUR)
  467 FORMAT('Waterlevel at bifurcation not converged',/,
     +F12.3,1X,I3,25(F12.9,2X))
               GOTO 455
            ENDIF
            K=K+1
            GOTO 459
         ENDIF
  455    I=1
         HDSC=(WATSURF(SCXS(I,5,1))+WATSURF(SCXS(I,5,2)))/2
         XS(1)=SCXS(I,1,1)
         XS(2)=SCXS(I,1,2)
         CALL AREA(NEWSURV,HDSC,XS(2),AWET,WSB,WP)
         WATSURF(XS(2))=HDSC
         WSWIDTH(XS(2))=WSB
         MEANDEP(XS(2))=AWET/WSB
         HRAD=AWET/WP
         CALL SFRICT(Q,XS(2),HRAD,AWET,D165084ACT,ENSL,UBAR,
     +   FF,EQUATION,PARAM)
         DO 466,XSN=XS(2)-1,XS(1),-1
            CALL BACKWATER(XS(2),N,XSN,Q,HDSC,NEWSURV,RECORD,
     +      EQUATION,PARAM)
  466    CONTINUE
      ENDIF
  450 IF (INTERVAL.EQ.2) THEN
         IF (DATE(1).GE.ENDDATE(1)) THEN
            IF (DATE(2).GE.ENDDATE(2)) THEN
```

```
               IF (DATE(3).GE.ENDDATE(3)) THEN
                  GOTO 501
               ENDIF
            ENDIF
         ENDIF
C           IF (TELAPSE.GT.TLENGTH) GOTO 501
C PATRICK THICKLAYER AND DEFINT ADDED
         CALL COURANT(N,DELTAT,DISTANCE,BEDCH,D165084ACT,ESLOPE,
     +   QBEDLOAD,WSWIDTH,DELTATC,THICKLAYER,DEFINT,SCXS)
C PATRICK max time step for variable discharge option, prevent program
C to step over specified data (now daily discharge)
         IF (2*DELTAT.GT.DELTATC) THEN
            DELTAT=DELTATC
         ELSE
            DELTAT=DELTAT*2
         ENDIF
         IF (QTYPE.EQ.2) THEN
            IF (2*DELTAT.GT.TMAX .AND. DELTAT.LT.TMAX) DELTAT=TMAX/2
            IF (DELTAT.GT.TMAX) DELTAT=TMAX
         ENDIF
C PATRICK write the used timestep to .DT file for the first hour
         IF (OUTPUT(37).EQ.'Y' .and. TELAPSE.LT.3601) THEN
            BACKSPACE (57)
            WRITE (57,1428) TELAPSE,DELTAT,DELTATC
            END FILE (57)
         ENDIF
      ENDIF
C END
C        IF (INTERVAL.EQ.2) THEN
C           IF (T.EQ.1000 .AND. TELAPSE.LT.TLENGTH) GOTO 495
C        ENDIF
      IF (T.GE.100) THEN
         GOTO 494
      ENDIF
C END
 500  CONTINUE
      ELSE
         SED=2
 501  ENDIF
C PATRICK reset position so file is accessable when simulation crashes
      BACKSPACE (10)
      WRITE (10,795) SEDTOTAL(1)
      WRITE (10,796) SEDTOTAL(2)
C PATRICK write end date to have an idea of comutation time needed
      WRITE (10,711) EDATE@(),TIME@()
C
      IF (NTRIB.GT.0) THEN
         DO 2200,IT=1,NTRIB
            WRITE (10,797) IT,SEDTOTAL(5+IT)
 2200    CONTINUE
      ENDIF
C
      END FILE (10)
C
 700  FORMAT ('River: ',A20,4X,'Operator: ',A20,/,'Run Code: ',A8)
 701  FORMAT ('This run with VERSION 4-M of program SEDROUT',/,' ')
 710  FORMAT ('Date of run:  ',A8,4X,'Run started at:  ',A8)
C PATRICK added 711
 711  FORMAT ('Date end of run:  ',A8,3X,'Run ended at:  ',A8)
 720  FORMAT ('Control file: ',A12,4X, 'Cross-section data file: ',A12)
 730  FORMAT ('Full grain size distributions input from:  ',A12,/,' ')
 731  FORMAT
```

```
      +('D84 only (no sediment routing option) in file:   ',A12,/,' ')
 740  FORMAT ('Discharge is constant at ',F8.2, 'm3/s')
 741  FORMAT ('D/s condition varies with time, read from files:',/,
      +A62,/,A62)
 742  FORMAT ('Total discharge at downstream end is ',F9.2,' m3/s',/
      +,'Mainstream discharge is ',F9.2,' m3/s',/
      +,'Tributary ',I2,' discharge is ',F9.2,' m3/s',/
      +,'Tributary enters at ',F7.1,'m along the reach',/,' ')
C PATRICK added 745,746
 745  FORMAT('No correction for tide is made at d/s boundary')
 746  FORMAT('Bi-daily tide is applied d/s boundary with amplitude:'
      +,F5.3,'m.')
 750  FORMAT(' ',/
      +,'D/s boundary condition:  roughness law, specified discharge')
 752  FORMAT
      +('D/s boundary condition:  roughness law, specified water depth')
 751  FORMAT ('D/s boundary condition:  rating curve, Q=a+bh^c,',/
      +,'a=',F6.3, 'b=',F6.3, 'c=',F6.3)
 753  FORMAT (' ',/
      +,'D/s boundary condition: specified depth and discharge')
C PATRICK added 754,755
 754  FORMAT (' ',/
      +,'D/s boundary condition: specified water level and discarge')
 755  FORMAT (' ',/
      +,'D/s boundary condition: specified discharge and rating curv:'
      +,/,'h=((q-a)/b)^(1/c)',/,'a=',F6.3, 'b=',F6.3, 'c=',F6.3)
 760  FORMAT ('Roughness equation is (1/f^.5)=a.log(R/D84)+b',/
      +,'where a=',F6.3,2X,'b=',F6.3)
 761  FORMAT ('Roughness equation is n=a.D84^b where a=',F6.3
      +,2X,'b=',F6.3)
C PATRICK added 762,763
 762  FORMAT ('Roughness is constant manning-value n=',F6.3)
 763  FORMAT ('The tolerance for water level calculation:',F8.6)
 770  FORMAT (' ',/,'Simulation period: ',I4,2(1X,I2),' until: ',
      +I4,2(1X,I2))
 771  FORMAT ('A constant timestep of  ',F5.1,' seconds is used')
 772  FORMAT ('A variable timestep is used')
 773  FORMAT
      +('Data written to output files after every ',F8.3,' years')
 774  FORMAT
      +('Data written to output files after every ',I8,' iterations')
C PATRICK added 775,776
 775  FORMAT ('Data written to output files every first of January')
 776  FORMAT ('Data written to output files every first of January',/
      +,'sediment transport written every day')
 780  FORMAT (' ',/,'Bed porosity:  ',F5.2)
 781  FORMAT ('Active layer defined as k.D84, where k= ',F6.2)
 782  FORMAT ('Active layer is constant at ',F5.2,'m')
 783  FORMAT ('Active layer defined as k.Dgm, where k= ',F5.2)
 784  FORMAT ('Parker [1990] bedload equation used, with Beta= ',F7.3
      +,/,'for Gravel, Beta= ',F7.3,' for Sand, and tau*ref= ',F6.3)
 785  FORMAT ('Einstein bedload equation used')
 786  FORMAT ('Wilcock & Crowe bedload equation used')
 787  FORMAT ('No straining used',/,' ')
 788  FORMAT ('Parker straining function used',/,' ')
 789  FORMAT ('Modified Parker straining function used with',/
      +,'straining exponent = ',F5.3,/,' ')
 791  FORMAT ('Upstream boundary condition is fixed elevation')
 792  FORMAT ('Upstream boundary condition is constant input rate of'
      +,/,F12.8,'m3/m/s.  Percentages in the grain size classes are:'
      +,/,25(F4.1,1X))
 793  FORMAT ('Upstream boundary condition is k.bedload transport',/
      +,'rate at upstream cross-section, where k= ',F7.4)
 794  FORMAT ('Upstream boundary condition is constant input rate of'
      +,/,F12.8,'m3/m/s.  GSD is the same as at cross-section 2')
 795  FORMAT (' ',/,'Total sediment input at upstream boundary'
      +,/,'throughout the run is ',E10.3,' m3.',/,' ')
 796  FORMAT ('Total sediment output from the downstream boundary',/
      +,'throughout the run is ',E10.3,' m3.',/,' ')
 797  FORMAT ('Total sediment input from tributary',I2,' throughout',/
      +,'the run is ',E10.3,' m3.',/,' ')
C PATRCIK added 801,802,803
 801  FORMAT ('Ackers and White's total load equation is used',/
      +,'with 1973 parameters')
 802  FORMAT ('Ackers and White's total load equation is used',/
      +,'with 1990 parameters')
 803  FORMAT ('Ackers and White's total load equation is used',/
      +,'with Ackers an Day's (1982) parameters')
 850  FORMAT ('    ***   WATER SURFACE PROFILE PLOT   ***',/,' ',/
      +,'Before entering the sediment routing module a check on the ',/
      +,'surface profile can be useful',/,' ',/
      +,'Do you want to see a plot of the water surface profile on',/
      +,'the screen?  Type the number of the required option, and',/
      +,'press "ENTER"',/,' ',/,'1. Yes',/,'2. No',/,' ',/,' ')
 890  FORMAT ('The sediment routing routine cannot be used with this'
      +,/,'input data format.')
 1100 FORMAT (' ',/,'Size classes used have upper limits at the',/
      +,'following phi sizes')
 1101 FORMAT (' ',/
      +,'Values of exchange parameter for each size classe are:')
 1105 FORMAT (25(F4.1,1X))
 1400 FORMAT (' ',/
      +,'The key results file is ',A12,' with 18 columns',/
      +,'1. section code;  2. run time (yrs); 3. distance along',/
      +,'reach [m]; 4.water surface width [m];  5. hydraulic radius [m];'
      +,/,'6. energy slope; 7. shear stress [N/m2]; 8. dimensionless'
      +,/,'stress - surface D50; 9. surface D50[mm]; 10. surface D84'
      +,/,'[mm]; 11. surface geometric mean size [mm]; 12. sub-surface'
      +,/,'D50 [mm]; 13. bedload D50 [mm]; 14. unit bedload transport'
      +,/,'rate [m3/m/s]; 15. %sand in surface(<2mm); 16. water surface'
      +,/,'elevation [m]; 17. mean bed elevation [m]; 18. total'
      +,/,'elevation change during run[m].',/,' ')
C PATRICK discharge also stored when variable in time
 1401 FORMAT (' ',/,'The hydraulics results are in file  ',A12,/
      +,'containing 12 columns: 1.  section code; 2. run time (yrs);'
      +,/,'3. distance along channel [m]; [3a - Discharge (m3/s) only'
      +,/,'in runs with tributary inflow or variable discharge];'
      +,/,'4. water surface width [m]; 5. mean depth [m]; 6. mean'
      +,/,'velocity [m/s]; 7. hydraulic radius [m]; 8. energy slope;'
      +,/,'9. friction factor; 10. Mannings n 11. Froude Number')
 1402 FORMAT (' ',/,'Summary grain size statistics are in file  ',A12
      +,/,'containing 11 columns: 1. section code; 2. run time (yrs);'
      +,/,'3-5. surface d16, d50, d84 [mm]; 6-8. sub-surface d16, d50,'
      +,/,'d84 [mm]; 9-11. bedload d16, d50, d84 [mm]')
 1403 FORMAT (' ',/
      +,'Sediment transport/ storage results are in file  ',A12,/
      +,'containing 8 columns: 1. section code; 2. run time (yrs);'
      +,/,'3. bedload transport rate [m3/s]; 4. unit bedload transport'
      +,/,'rate [m3/m/s]; 5. unit mass bedload transport rate [g/m/s];'
      +,/,'6. overall mean elevation change at the node [m]; 7. overall'
      +,/,'area of deposition/erosion at the node [m2]; 8.mean bed',/
      +,'elevation [m]')
 1404 FORMAT (' ',/
      +,'Active layer grain size distributions are in file  ',A12
```

```
      +,/,'with 18 columns: 1. section code; 2. run time (yrs);'
      +,/,'3-17. % in size classes given in the file .inf')
 1405 FORMAT (' ',/
      +,'Subsurface grain size distributions are in file ',A12
      +,/,' with format as for active layer.')
 1406 FORMAT (' ',/
      +,'Grain size distributions of bedload are in file ',A12
      +,/,'with format as for active layer.')
 1408 FORMAT ('           ',A12)
 1409 FORMAT ('The following files were selected for output:',/,' ')
 1420 FORMAT (125(F8.4,1X))
 1421 FORMAT (125(F10.8,1X))
 1422 FORMAT (125(F8.6,1X))
 1423 FORMAT (125(F5.3,1X))
 1424 FORMAT (125(F8.3,1X))
 1425 FORMAT (125(F6.3,1X))
 1426 FORMAT (125(F6.4,1X))
 1427 FORMAT (I2,1X,F10.8,1X,25(F5.2,1X))
C PARTICK added 1428,1429,1430,1431
 1428 FORMAT (F12.1,1X,F9.3,1X,F9.3)
 1429 FORMAT (A10,2(1X,F12.0))
 1430 FORMAT (A10,50(1X,F12.0))
 1431 FORMAT (A10,125(F8.3,1X))
 1451 FORMAT (' ',/,'Tributary ',I2,' brings in no sediment.')
 1455 FORMAT ('Tributary ',I2
      +,' sediment input is K times bedload discharge in'
      +,/,'the main channel, where K = ',F6.3)
 1456 FORMAT ('Tributary ',I2,' sediment input is fixed at ',F12.10,/
      +,'m3/s.')
 1457 FORMAT ('Tributary ',I2
      +,' sediment input is K times bedload discharge at'
      +,/,'the upstream boundary [main channel], where K = ',F6.3)
 1460 FORMAT ('Tributary ',I2
      +,'input grain size distribution is identical to'
      +,/,'that in the main channel at the point of entry.',/,' ')
 1461 FORMAT ('Tributary ',I2
      +,' grain size distribution is specified as',/
      +,'follows: [% in each class, in the same order as size classes',/
      +,'are defined above:]',/,25(F5.2,1X),/,' ')
 1610 FORMAT (' ',/
      +,'Data written to output files at the following elapsed times:'
      +,/,'   Result block code       Years     000s Iterations')
 1611 FORMAT (5X,I3,15X,F8.3,4X,F10.3,1X,A10,1X,A8)
 1650 FORMAT ('Press "Ctrl" and "Pause" together to interrupt the'
      +,/,'run if required')
 1655 FORMAT ('# iterations   Elapsed    % of run      Time',/
      +,'  000s:M          time         elapsed',/,'              [years]')
 1685 FORMAT (10(F7.4,2X))
 1690 FORMAT (F10.2)
 1700 FORMAT (2(F12.6,1X))
 1710 FORMAT (A6,1X,A10,1X,A8,1X,F8.2,1X,F6.2,1X,F5.2,1X,F8.6,1X,F4.1,
      +1X,F6.3,1X,F8.4,1X,F8.4,1X,F8.4,1X,F8.4,1X,F8.4,1X,F9.7,1X,F6.2,
      +1X,F8.3,1X,F8.3,1X,F8.3,1X,F8.4)
 1720 FORMAT (A6,1X,A10,1X,A8,1X,F7.1,1X,F5.1,3(1X,F5.2),1X,F8.6,1X,
      +F6.4,1X,F6.4,1X,F4.2)
 1721 FORMAT (A6,1X,A10,1X,A8,1X,F7.1,1X,F7.2,1X,F5.1,3(1X,F5.2),1X,
      +F8.6,1X,F6.4,1X,F6.4,1X,F4.2)
 1730 FORMAT (A6,1X,A10,1X,A8,1X,9(1X,F7.2))
 1739 FORMAT ('Input   ',A10,1X,A8,2X,F8.5,2X,F8.6,2X,F8.2)
 1740 FORMAT
      +(A6,1X,A10,1X,A8,2X,F8.5,2X,F8.6,2X,F8.2,2X,F6.2,2X,F7.2,2X,F9.3)
 1749 FORMAT ('Input   ',A10,1X,A8,25(1X,F5.2))
 1750 FORMAT (A6,1X,A10,1X,A8,25(1X,F5.2))
 1800 FORMAT (F7.3,2X,F10.1,7X,F5.1,5X,A8)
 1801 FORMAT (F7.3,2X,F10.4,7X,F5.1,5X,A8)
 1999 FORMAT (' ')
 2001 FORMAT('_____________________________________________')
 4000 FORMAT(' ',/
      +,'Tracer position data after run time',F10.1,'  minutes',/
      +,'corresponding to',I10,'  minutes after tracer introduction'
      +,/,'  ',/,' ')
 4001 FORMAT('Starting position for all tracers was ',F8.2
      +,'m along the reach',/,' ')
 4010 FORMAT (I4,2X,I4,2X,F8.2)
C
      IF (TELAPSEYR.LT.1.0) THEN
        WRITE (*,1801) (0.001*TTOTAL),TELAPSEYR,PCELAPSE,TIME@()
      ELSE
        WRITE (*,1800) (0.001*TTOTAL),TELAPSEYR,PCELAPSE,TIME@()
      ENDIF
C
      DO 3000,I=7,18
        CLOSE (I)
 3000 CONTINUE
C
      CLOSE(4)
      CLOSE(20)
C
 3001 END
C
C_______________________BWLIB ROUTINES_________________________
C  These subroutines perform the hydraulic computations.
C
C  This routine calculates the water discharge from supplied stage,
C  or stage from supplied discharge, according to the method
C  specified.
C
C     *****************************************************************
      SUBROUTINE DISCHARGE (SURV,N,RMETHOD,EQUATION,PARAM,DSDEPTH
      +,DSWATER,QDS,HDS,D165084ACT,DISTANCE,NCLASS,QT,QTYPE
      +,QHFILE,LENGTH,QDATE,DATE,STOP,HT,INFILE,HDATE,TOL,WLDFILE)
C
      INTEGER DATE(7),EQUATION,I,LENGTH,NCLASS,NN,QDATE(500,3),QT
      +,QTYPE,RMETHOD,STOP,Y,HT,HDATE(500,2)
C
      REAL AWET,BEDMEAN(5),BEDMIN,D165084ACT(4,250),D84,DIST(5),
      +DISTANCE(250),DSDEPTH(500),DSDEPTHEST,DSWATER(500),
      +ERROR,EST(3),G,HDS,HEST,HRAD,MANNINGN,
      +PARAM(5),QDS(500),QEST,
      +SLOPE,SURV(100,500),TOL,UBAR,WSB,WP
C
      CHARACTER QHFILE*62,SMETH*15,INFILE(3)*12,WLDFILE*62
C
      G=9.81
C
C PATRICK QTYPE condition for reading  .qdt-file
C  Reading the water depth at the d/s boundary and/or the discharge.
      IF (QTYPE.EQ.1) THEN
        IF (RMETHOD.EQ.1) THEN
          READ (5,*) DSDEPTHEST,QDS(1)
        ELSE IF (RMETHOD.EQ.2) THEN
          READ (5,*) DSDEPTH(1)
        ELSE IF (RMETHOD.EQ.3) THEN
          READ (5,*) DSDEPTH(1)
```

```
            ELSE IF (RMETHOD.EQ.4) THEN
               READ (5,*) DSDEPTH(1),QDS(1)
C                DSDEPTH(QT)=PARAM(1)
            ELSE IF (RMETHOD.EQ.5) THEN
               READ (5,*) DSWATER(1),QDS(1)
            ELSE IF (RMETHOD.EQ.6) THEN
               READ (5,*) QDS(1)
            ENDIF
         ELSE IF (QTYPE.EQ.2) THEN
            CALL READQDATA (DATE,DSDEPTH,DSWATER,I,LENGTH,
     +      QHFILE,QDS,QDATE,RMETHOD)
C set QT if start date not equals first date in .qdt-file
            DO 20,J=1,I
               IF (DATE(1).EQ.QDATE(J,1)) THEN
                  IF (DATE(2).EQ.QDATE(J,2)) THEN
                     IF (DATE(3).EQ.QDATE(J,3)) THEN
                        QT=J
                        IF (QT.GE.I) STOP=999
                        GOTO 95
                     ENDIF
                  ENDIF
               ENDIF
 20         CONTINUE
            STOP=999
 95         READ (5,*) DSWATER(1)
            CALL READWLD (DATE,DSWATER,HI,WLDFILE,HDATE)
            DO J=1,HI
               IF (HDATE(J,1).LT.HDATE(J+1,1)) THEN
                  IF (HDATE(J,1).LE.DATE(2) .AND.
     +            DATE(2).LE.HDATE(J+1,1)) THEN
                     IF (DATE(2).EQ.HDATE(J,1) .AND.
     +               DATE(3).GE.HDATE(J,2)) THEN
                        HT=J
                        GOTO 96
                     ELSE IF (DATE(2).EQ.HDATE(J+1,1) .AND.
     +               DATE(3).LT.HDATE(J+1,2)) THEN
                        HT=J
                        GOTO 96
                     ELSE IF (HDATE(J,1).LT.DATE(2) .AND.
     +               DATE(2).LT.HDATE(J+1,1)) THEN
                        HT=J
                        GOTO 96
                     ENDIF
                  ENDIF
               ELSE IF (DATE(2).EQ.HDATE(J,1)) THEN
                  IF (DATE(3).GE.HDATE(J,2) .AND.
     +            DATE(3).LT.HDATE(J+1,2)) THEN
                     HT=J
                     GOTO 96
                  ENDIF
               ENDIF
            END DO
         ENDIF
C END
C How is the slope at the d/s boundary to be determined? From file,
C in which case read its value, or from program via survey data?
C
 96      READ (5,*) TOL
         READ (5,'(A)') SMETH
C
         IF (SMETH.EQ.'SLOPE') THEN
            READ (5,*) SLOPE
         ELSE
C For closely spaced sections (<95m) calculate a reach average
C slope over 5 sections.
            Y=0
            IF (RMETHOD.EQ.1) Y=1
            IF (RMETHOD.EQ.2) Y=1
            IF (Y.EQ.1) THEN
               IF ((DISTANCE(N)-DISTANCE(N-1)).LT.95) THEN
                  DO 50,M=1,5
                     CALL LOWBED(SURV,(N+1-M),BEDMIN)
                     IF (RMETHOD.EQ.1) THEN
                        HDS1=BEDMIN+ DSDEPTHEST
                     ELSE IF (RMETHOD.EQ.2) THEN
                        HDS1=BEDMIN+DSDEPTH(QT)
                     ENDIF
                     CALL AREA(SURV,HDS1,(N+1-M),AWET,WSB,WP)
                     BEDMEAN(M)=HDS1-(AWET/WSB)
                     DIST(M)=DISTANCE(N+1-M)
 50               CONTINUE
                  NN=5
                  CALL SLOPEST (NN,BEDMEAN,DIST,SLOPE)
                  SLOPE=SLOPE*(-1)
               ELSE
C  Calculate slope between bottom 2 sections
                  CALL LOWBED(SURV,N,BEDMIN)
                  IF (RMETHOD.EQ.1) THEN
                     HDS=BEDMIN+ DSDEPTHEST/2
                  ELSE IF (RMETHOD.EQ.2) THEN
                     HDS=BEDMIN+DSDEPTH(QT)
                  ENDIF
                  CALL AREA (SURV,HDS,N,AWET,WSB,WP)
                  BEDMEAN(1)=HDS-(AWET/WSB)
                  CALL LOWBED(SURV,N-1,BEDMIN)
                  IF (RMETHOD.EQ.1) THEN
                     HDS1=BEDMIN+ DSDEPTHEST/2
                  ELSE IF (RMETHOD.EQ.2) THEN
                     HDS1=BEDMIN+DSDEPTH(QT)
                  ENDIF
                  CALL AREA (SURV,HDS1,N-1,AWET,WSB,WP)
                  BEDMEAN(2)=HDS1-(AWET/WSB)
                  SLOPE=(BEDMEAN(2)-BEDMEAN(1))/(DISTANCE(N)-DISTANCE(N-1))
                  IF (SLOPE.LT.0) SLOPE=0.01
               ENDIF
            ENDIF
         ENDIF
C
         IF (RMETHOD.EQ.1) THEN
            D84=D165084ACT(3,N)
            CALL LOWBED(SURV,N,BEDMIN)
C  Guess a water surface elevation from roughness approximation.
            HGUESS=BEDMIN+ DSDEPTHEST/2
            CALL AREA (SURV,HGUESS,N,AWET,WSB,WP)
            HRAD=AWET/WP
            IF (EQUATION.EQ.1) THEN
               UBAR=(PARAM(1)*LOG10(HRAD/D84)+PARAM(2))
     +         *((8*G*HRAD*SLOPE)**0.5)
            ELSE IF (EQUATION.EQ.2) THEN
               MANNINGN=PARAM(1)*(D84**PARAM(2))
               UBAR=(1/MANNINGN)*(HRAD**(0.667))*(SLOPE**0.5)
C PATRICK
            ELSE IF (EQUATION.EQ.3) THEN
               MANNINGN=PARAM(1)
```

```
                  UBAR=(1/MANNINGN)*(HRAD**(0.667))*(SLOPE**0.5)
C END
              ENDIF
              QEST=UBAR*AWET
              IF (QEST .LT. QDS(QT)) THEN
                  HEST=HGUESS+(HGUESS-BEDMIN)*(ABS(QEST-QDS(QT))/
     +            (QEST+QDS(QT)))**0.5
              ELSE
                  HEST=HGUESS-(HGUESS-BEDMIN)*(ABS(QEST-QDS(QT))/
     +            (QEST+QDS(QT)))**0.5
              ENDIF
              DO 100,K=1,100
                  CALL AREA (SURV,HEST,N,AWET,WSB,WP)
                  HRAD=AWET/WP
                  IF (EQUATION.EQ.1) THEN
                      UBAR=(PARAM(1)*LOG10(HRAD/D84)+PARAM(2))
     +                *((8*G*HRAD*SLOPE)**0.5)
                  ELSE IF (EQUATION.EQ.2) THEN
                      MANNINGN=PARAM(1)*(D84**PARAM(2))
                      UBAR=(1/MANNINGN)*(HRAD**(0.667))*(SLOPE**0.5)
C PATRICK
                  ELSE IF (EQUATION.EQ.3) THEN
                      MANNINGN=PARAM(1)
                      UBAR=(1/MANNINGN)*(HRAD**(0.667))*(SLOPE**0.5)
C END
                  ENDIF
                  QEST=UBAR*AWET
                  ERROR=(QEST-QDS(QT))/(QEST+QDS(QT))
                  IF (ABS(ERROR).LT.0.0005) GOTO 101
                  IF (K.EQ.1) THEN
                      EST(1)=HEST
                      EST(2)=QEST
                      EST(3)=ERROR
                      IF (ERROR.GT.0) HEST=HEST-0.1*DSDEPTHEST
                      IF (ERROR.LT.0) HEST=HEST+0.1*DSDEPTHEST
                  ELSE
                      IF (EST(3)*ERROR.LT.0) THEN
                          IF (EST(3).LT.0) THEN
                              HEST=EST(1)+ABS(EST(2)-QDS(QT))*(HEST-EST(1))/
     +                        (ABS(EST(2)-QDS(QT))+ABS(QEST-QDS(QT)))
                          ELSE
                              HEST=HEST+ABS(ERROR)*(EST(1)-HEST)/
     +                        (ABS(EST(3))+ABS(ERROR))
                          ENDIF
                          IF (ABS(ERROR).LT.ABS(EST(3))) THEN
                              EST(1)=HEST
                              EST(2)=QEST
                              EST(3)=ERROR
                          ENDIF
                      ELSE
                          IF (ABS(ERROR).LT.ABS(EST(3))) THEN
                              EST(1)=HEST
                              EST(2)=QEST
                              EST(3)=ERROR
                              IF (ERROR.GT.0) HEST=HEST-((HRAD*ABS(ERROR))**0.5)
                              IF (ERROR.LT.0) HEST=HEST+((HRAD*ABS(ERROR))**0.5)
                          ELSE
                              IF (EST(3).GT.0) HEST=EST(1)-((HRAD*ABS(ERROR))
     +                        **0.5)
                              IF (EST(3).LT.0) HEST=EST(1)+((HRAD*ABS(ERROR))
     +                        **0.5)
                          ENDIF
                      ENDIF
                  ENDIF
100           CONTINUE
101           IF (K.GT.100) PRINT *,'DISCHARGE/ELEVATION NOT CONVERGED!!'
              HDS=HEST
          ELSE IF (RMETHOD.EQ.2) THEN
              CALL LOWBED(SURV,N,BEDMIN)
              HDS=DSDEPTH(QT)+BEDMIN
              CALL AREA(SURV,HDS,N,AWET,WSB,WP)
              D84=D165084ACT(3,N)
              HRAD=AWET/WP
              IF (EQUATION.EQ.1) THEN
                  UBAR=(PARAM(1)*LOG10(HRAD/D84)+PARAM(2))
     +            *((8*G*HRAD*SLOPE)**0.5)
              ELSE IF (EQUATION.EQ.2) THEN
                  MANNINGN=PARAM(1)*(D84**PARAM(2))
                  UBAR=(1/MANNINGN)*(HRAD**(0.667))*(SLOPE**0.5)
C PATRICK
              ELSE IF (EQUATION.EQ.3) THEN
                  MANNINGN=PARAM(1)
                  UBAR=(1/MANNINGN)*(HRAD**(0.667))*(SLOPE**0.5)
C END
              ENDIF
              QDS(1)=UBAR*AWET
          ELSE IF (RMETHOD.EQ.3) THEN
              QDS(1)=PARAM(3)+PARAM(4)*(DSDEPTH(1)**PARAM(5))
              CALL LOWBED(SURV,N,BEDMIN)
              HDS=DSDEPTH(QT)+BEDMIN
          ELSE IF (RMETHOD.EQ.4) THEN
              CALL LOWBED(SURV,N,BEDMIN)
              HDS=DSDEPTH(QT)+BEDMIN
          ELSE IF (RMETHOD.EQ.5) THEN
              HDS=DSWATER(1)
          ELSE IF (RMETHOD.EQ.6) THEN
              HDS=PARAM(3)*(QDS(QT)/PARAM(4))**(1/PARAM(5))
          ENDIF
C
          END
C
C     ****************************************************************
C  Subroutine to calculate the wetted area for given cross-sectional
C  bed elevation data and water surface elevation.
C
          SUBROUTINE AREA (SURV,WSURF,M,AWET,WSB,WP)
C
          REAL SURV(100,500),WSURF,AWET,WSB,WSI,WP
          INTEGER M
          AWET=0
          WSB=0
          WP=0
C
          DO 200,I=1,99
              J=I+1
              IF (SURV(J,(2*M-1)).LT.9000)THEN
                  IF ((SURV(I,2*M)-WSURF).GT.0.01) THEN
                      IF (WSURF-SURV(J,2*M).GT.0.009) THEN
                          WSI=SURV(I,(2*M-1))+((SURV(I,2*M)-WSURF)*
     +                    (SURV(J,(2*M-1))-SURV(I,(2*M-1)))/
     +                    (SURV(I,2*M)-SURV(J,2*M)))
                          AWET=AWET+
     +                    ((SURV(J,(2*M-1))-WSI)*(WSURF-SURV(J,2*M))/2)
                          WSB=WSB+(SURV(J,(2*M-1))-WSI)
```

```
                  WP=WP+((((WSURF-SURV(J,2*M))**2)+
     +             ((SURV(J,2*M-1)-WSI)**2))**0.5)
                ENDIF
              ELSE IF ((SURV(J,2*M)-WSURF).GT.0.01) THEN
                IF ((SURV(I,2*M)-WSURF).LT.0.00) THEN
                  WSI=SURV(I,(2*M-1))+((WSURF-SURV(I,2*M))*
     +             (SURV(J,(2*M-1))-SURV(I,(2*M-1)))/
     +             (SURV(J,2*M)-SURV(I,2*M)))
                  AWET=AWET+
     +             ((WSI-SURV(I,(2*M-1)))*((WSURF-SURV(I,2*M))/2))
                  WSB=WSB+(WSI-SURV(I,(2*M-1)))
                  WP=WP+((((WSURF-SURV(I,2*M))**2)+
     +             ((WSI-SURV(I,(2*M-1)))**2))**0.5)
                ENDIF
              ELSE
                IF (ABS(SURV(I,2*M)-WSURF).LT.0.01 .AND.
     +          ABS(SURV(J,2*M)-WSURF).LT.0.01) GOTO 200
                AWET=AWET+((SURV(J,(2*M-1))-SURV(I,(2*M-1)))*
     +          ((2*WSURF-SURV(I,2*M)-SURV(J,2*M))/2))
                WSB=WSB+(SURV(J,(2*M-1))-SURV(I,(2*M-1)))
                WP=WP+((((SURV(J,(2*M-1))-SURV(I,(2*M-1)))**2)+
     +          ((SURV(J,2*M)-SURV(I,2*M))**2))**0.5)
              ENDIF
            ELSE
              GOTO 201
            ENDIF
200   CONTINUE
C
201   END
C
C     ******************************************************************
C   Routine to calculate the friction slope.
C
      SUBROUTINE SFRICT (Q,XSN,HRAD,AWET,D165084ACT,
     +ENSL,UBAR,FF,EQUATION,PARAM)
C
      REAL AWET,D165084ACT(4,250),D84,ENSL,FF,G,HRAD,MANNINGN,PARAM(5)
     +,Q(250),UBAR
C
      INTEGER EQUATION,XSN
C
      G=9.81
      D84= D165084ACT(3,XSN)
      UBAR=Q(XSN)/AWET
C
      IF (EQUATION.EQ.1) THEN
          FF=(1/((PARAM(1)*LOG10(HRAD/D84))+PARAM(2)))**2
          ENSL= (UBAR**2)*FF/(8*G*HRAD)
      ELSE IF (EQUATION.EQ.2) THEN
          MANNINGN=PARAM(1)*(D84**PARAM(2))
          ENSL=(UBAR*MANNINGN/(HRAD**(0.667)))**2
C PATRICK
      ELSE IF (EQUATION.EQ.3) THEN
          MANNINGN=PARAM(1)
          ENSL=(UBAR*MANNINGN/(HRAD**(0.667)))**2
C END
      ENDIF
C
      FF=(ENSL*8*G*HRAD)/(UBAR**2)
C
      END
C
C     ******************************************************************
C   Routine to perform the standard step-backwater computations. Uses
C   various traps to deal with shallow depth problems and to promote
C   rapid convergence. If flow is super-critical, water depth is set
C   to critical flow depth (Fr=1).
C
      SUBROUTINE BACKWATER (NMAX,N,XSN,Q,HDS,SURV,RECORD,
     +EQUATION,PARAM)
C
      REAL AWET,BEDMIN,CALC(2),CALCDOWN,CALCUP,CRITWS(250),
     +D165084ACT(4,250),DIFF(2),DIFFMIN,DISTANCE(250),
     +ENSL,ESLOPE(250),EST(2),ESTDOWN,ESTMIN,ESTUP,
     +FF,FFACTOR(250),FR(250),G,HBAR,HRAD,
     +MANNING(250),MAX,MEANDEP(250),PARAM(5),Q(250),R(250),
     +SCRIT(250),SFDOWN,SURV(100,500),
     +TEMPINFO(2,15),TOL,UBAR,UDOWN,UUP,
     +VELOCITY(250),WATSURF(250),WSCALC,WSEST,WSWIDTH(250)
C
      INTEGER BRACKET,CH,CODE(250),EQUATION,ITER,K,L,N,NMAX,OFF,
     +RECORD,SET,XSN
C
      CHARACTER TYPE*7
C
      COMMON /INFO/ CODE,CRITWS,D165084ACT,DISTANCE,ESLOPE,FFACTOR,FR,
     +MANNING,MEANDEP,R,SCRIT,TOL,VELOCITY,WATSURF,WSWIDTH
C
      PARAMETER (OFF=0,SET=1)
      G=9.81
      ITER=OFF
C PATRICK DEBUG FOR VARIABLE DISCHARGE OPTION
C       IF (QT.GT.1) THEN
C       WRITE (*,9999) XSN,QT,Q(XSN)
C9999   FORMAT (I2,1X,I2,1X,F6.2)
C       PAUSE
C       ENDIF
C END
      DO 10,L=1,2
          EST(L)=0
          CALC(L)=0
          DIFF(L)=0
10    CONTINUE
C
      ESTUP=0
      ESTDOWN=0
      BRACKET=OFF
      DIFFMIN=0
      ESTMIN=0
      K=0
      TYPE='NONE'
C
      IF ((XSN+1).EQ.NMAX) THEN
          CALL AREA(SURV,HDS,NMAX,AWET,WSB,WP)
          HRAD=AWET/WP
          HBAR=AWET/WSB
          CALL SFRICT(Q,NMAX,HRAD,AWET,D165084ACT,
     +    ENSL,UBAR,FF,EQUATION,PARAM)
          VELOCITY (NMAX)=UBAR
          ESLOPE (NMAX)=ENSL
          WATSURF (NMAX)=HDS
          MEANDEP (NMAX)=HBAR
          R (NMAX)=HRAD
          FFACTOR (NMAX)=FF
```

```
            FR (NMAX)=UBAR/((G*HBAR)**0.5)
            WSWIDTH (NMAX)=WSB
            MANNING (NMAX)=(HRAD**(0.667))*(ENSL**0.5)/UBAR
            IF (FR(NMAX).GT.0.95) THEN
               CALL LOWBED (SURV,NMAX,BEDMIN)
               TEMPINFO(1,13)=0
               CALL CRITFLOW (BEDMIN,TEMPINFO,NMAX,Q,SURV,TYPE,
     +         (XSN+1),RECORD,EQUATION,PARAM)
            ENDIF
            UDOWN=UBAR
            SFDOWN=ENSL
            WSEST= HDS+(ENSL*(DISTANCE(XSN+1)-DISTANCE(XSN)))
         ELSE
            WSEST=WATSURF(XSN+1)+((ESLOPE(XSN+2)*ESLOPE(XSN+1))**0.5)*
     +      (DISTANCE(XSN+1)-DISTANCE(XSN))
         ENDIF
C
         IF (ITER.EQ.SET .AND. RECORD.EQ.SET) THEN
            WRITE (8,1900)
            WRITE (8,1910)
            WRITE (7,1930)
            WRITE (7,1935)
         ENDIF
C
         CALL LOWBED (SURV,XSN,BEDMIN)
         IF ((WSEST-BEDMIN).LT.0.05) WSEST=BEDMIN+MEANDEP(XSN+1)
         IF ((2*(WSEST-BEDMIN)).LT.MEANDEP(XSN+1))
     +WSEST=BEDMIN+MEANDEP(XSN+1)/2
C
         DO 60,K=1,50
            TEMPINFO(1,13)=0
            CALL WSURFACE (SURV,WSEST,XSN,Q,TEMPINFO,WSCALC,AWET,WSB,
     +      UUP,HBAR,EQUATION,PARAM)
            IF (RECORD.EQ.SET .AND. XSN.LE.N .AND. ITER.EQ.SET)
     +      WRITE (7,1940) CODE(XSN),K,VELOCITY(XSN),ESLOPE(XSN),
     +      WATSURF(XSN),WSEST,FR(XSN)
C             TOL=0.005
            MAX=BEDMIN+(2*MEANDEP(XSN))
            CALL ESTIMATE(K,WSEST,WSCALC,EST,CALC,CALCUP,CALCDOWN,
     +      ESTUP,ESTDOWN,TYPE,BRACKET,BEDMIN,HBAR,DIFFMIN,ESTMIN,TOL,
     +      MAX,DIFF)
            IF (TYPE.EQ.'NOINT') THEN
               CALL APPROX (SURV,ESTMIN,DIFFMIN,XSN,Q,MEANDEP,
     +         APPROOT,AWET,WSB,EQUATION,PARAM)
               IF (RECORD.EQ.SET .AND. ITER.EQ.SET) THEN
                  IF (XSN.LE.N) THEN
                     WRITE (7,1940) CODE(XSN),K,VELOCITY(XSN),
     +               ESLOPE(XSN),WATSURF(XSN),WSEST,FR(XSN)
                     WRITE (7,1980) DIFFMIN,ESTMIN
                  ENDIF
               ENDIF
               GOTO 65
            ENDIF
            IF (K.EQ.50) TYPE='MAXITS'
            IF (K.EQ.51) PRINT *,'BACKWATER CALC FAILS TO CONVERGE!!!'
            IF(TYPE.EQ.'SUBCRIT') GOTO 65
60       CONTINUE
C
65       TEMPINFO(1,13)=0
         CALL CRITFLOW(BEDMIN,TEMPINFO,NMAX,Q,SURV,TYPE,XSN,RECORD,
     +EQUATION,PARAM)
         CH=0
         IF (TYPE .EQ. 'HCRIT') CH=1
         IF (TYPE .EQ. 'HISLOPE') CH=1
         IF (CH .EQ. 1) THEN
C        Now to check if there is a sub-critical root as well
C        as a super-critical one.
            DO 80,M=XSN,XSN+1
               IF (M.EQ.XSN) THEN
                  J=1
               ELSE
                  J=2
               ENDIF
               TEMPINFO(J,1)=D165084ACT(3,M)
               TEMPINFO(J,2)=VELOCITY(M)
               TEMPINFO(J,3)=ESLOPE(M)
               TEMPINFO(J,4)=WATSURF(M)
               TEMPINFO(J,5)=MEANDEP(M)
               TEMPINFO(J,6)=R(M)
               TEMPINFO(J,7)=FFACTOR(M)
               TEMPINFO(J,8)=FR(M)
               TEMPINFO(J,9)=SCRIT(M)
               TEMPINFO(J,10)=CRITWS(M)
               TEMPINFO(J,11)=WSWIDTH(M)
               TEMPINFO(J,12)=MANNING(M)
               TEMPINFO(J,13)=1
               TEMPINFO(J,14)=REAL(CODE(M))
               TEMPINFO(J,15)=DISTANCE(M)
80          CONTINUE
            ESTDOWN=WATSURF(XSN)
            ESTUP=WATSURF(XSN) + (2*MEANDEP(XSN))
            CALL WSURFACE (SURV,ESTUP,XSN,Q,TEMPINFO,CALCUP,AWET,WSB,
     +      UUP,HBAR,EQUATION,PARAM)
            DIFF(2)=CALCUP-ESTUP
            CALL WSURFACE (SURV,ESTDOWN,XSN,Q,TEMPINFO,CALCDOWN,
     +      AWET,WSB,UUP,HBAR,EQUATION,PARAM)
            DIFF(1)= CALCDOWN-ESTDOWN
            IF (DIFF(1)*DIFF(2).LT.0.00) THEN
               DO 100,K=1,20
                  WSEST=((ESTDOWN*CALCUP)-(CALCDOWN*ESTUP))/
     +            (ESTDOWN-ESTUP+CALCUP-CALCDOWN)
                  CALL WSURFACE (SURV,WSEST,XSN,Q,TEMPINFO,WSCALC,AWET,
     +            WSB,UUP,HBAR,EQUATION,PARAM)
                  IF (ABS(WSCALC-WSEST).LT.0.005) GOTO 101
                  IF (WSCALC.GT.WSEST) THEN
                     IF (DIFF(2).GT.0.00) THEN
                        ESTUP=WSEST
                        CALCUP=WSCALC
                     ELSE
                        ESTDOWN=WSEST
                        CALCDOWN=WSCALC
                     ENDIF
                  ELSE
                     IF (DIFF(2).GT.0.00) THEN
                        ESTDOWN=WSEST
                        CALCDOWN=WSCALC
                     ELSE
                        ESTUP=WSEST
                        CALCUP=WSCALC
                     ENDIF
                  ENDIF
100            CONTINUE
101            IF (K.LE.20) CALL CRITFLOW (BEDMIN,TEMPINFO,NMAX,Q,SURV,
     +         TYPE,XSN,RECORD,EQUATION,PARAM)
```

```
            IF (TYPE.EQ.'SUBCRIT') THEN
               WATSURF(XSN)=(WSEST+WSCALC)/2
               CALL AREA (SURV,WATSURF(XSN),XSN,AWET,WSB,WP)
               HRAD=AWET/WP
               HBAR=AWET/WSB
               CALL SFRICT(Q,XSN,HRAD,AWET,D165084ACT,
     +            ENSL,UBAR,FF,EQUATION,PARAM)
               VELOCITY(XSN)=UBAR
               ESLOPE(XSN)=ENSL
               MEANDEP(XSN)=HBAR
               R(XSN)=HRAD
               FFACTOR(XSN)=FF
               FR(XSN)=(UBAR/(G*HBAR)**0.5)
               WSWIDTH(XSN)=WSB
               MANNING(XSN)=(HRAD**(0.667))*(ENSL**0.5)/UBAR
            ENDIF
         ENDIF
      ENDIF
C
      IF (TYPE .EQ. 'NOINT') THEN
         CALL AREA (SURV,WATSURF(XSN),XSN,AWET,WSB,WP)
         HRAD=AWET/WP
         HBAR=AWET/WSB
         CALL SFRICT(Q,XSN,HRAD,AWET,D165084ACT,
     +   ENSL,UBAR,FF,EQUATION,PARAM)
         VELOCITY(XSN)=UBAR
         ESLOPE(XSN)=ENSL
         MEANDEP(XSN)=HBAR
         R(XSN)=HRAD
         FFACTOR(XSN)=FF
         FR(XSN)=(UBAR/(G*HBAR)**0.5)
         WSWIDTH(XSN)=WSB
         MANNING(XSN)=(HRAD**(0.667))*(ENSL**0.5)/UBAR
      ENDIF
C
      IF (RECORD.EQ.SET .AND. XSN.LE.N .AND. ITER.EQ.SET) THEN
         WRITE (7,1990)
         WRITE (8,1920) CODE(XSN),SCRIT(XSN),CRITWS(XSN),K,TYPE
      ENDIF
C
 1900 FORMAT(' CROSS   CRITICAL   CRITICAL   NUMBER   SOLUTION')
 1910 FORMAT(' SECT      SLOPE       DEPTH      ITERS        TYPE')
 1920 FORMAT(1X,F5.0,3X,F6.4,3X,F7.4,4X,I2,6X,A7)
 1930 FORMAT(' CROSS   ITERATION   MEAN    ENERGY   WSCALC    WSEST     Fr')
 1935 FORMAT(' SECT      NUMBER     VEL      SLOPE')
 1940 FORMAT(1X,I3,4X,I2,5X,F6.3,2X,F6.4,1X,F8.4,1X,F8.4,2X,F4.2)
 1980 FORMAT ('No intersection of the iteration was found.',/
     +,'The smallest absolute difference between estimated and',/
     +,'calculated values was',2X,F6.3,'.  This occurred with an',/
     +,'estimated water surface of',2X,F6.3,'.  This estimate is',/
     +,'used as the water surface for subsequent calculations,',/
     +,'unless the flow was critical [indicated by Cr in the',/
     +,'next line].')
 1990 FORMAT ('________________________________________________________')
C
      END
C
C     ********************************************************************
      SUBROUTINE CRITFLOW (BEDMIN,TEMPINFO,NMAX,Q,SURV,TYPE,XSN,RECORD,
     +EQUATION,PARAM)
C
C     This subroutine checks whether the flow is sub- or super
C     critical.  Checks are made for energy slope < critical slope,
C     and flow depth > critical depth.  If either indicates
C     super-critical flow, flow parameters for critical flow
C     (Fr=1) are computed and used in subsequent calculations.
C
      REAL AWET,BEDMIN,CRITSL,CRITWS(250),
     +D165084ACT(4,250),DISTANCE(250),ESLOPE(250),
     +FF,FFACTOR(250),FR(250),G,
     +HCRIT,HEAD1,HEAD2,HEAD3,HEADMIN,HRAD,
     +MANNING(250),MEANDEP(250),PARAM(5),Q(250),R(250),
     +SCRIT(250),SURV(100,500),TEMPINFO(2,15),
     +U1,U2,U3,UMIN,UPHEAD,VELOCITY(250),
     +WATSURF(250),WP,WS1,WS2,WS3,WSB,WSMIN,WSS,WSWIDTH(250)
C
      INTEGER CODE(250),CRITICAL,DONE,EQUATION,FLOW,I,ITER,LOOP,NMAX,
     +PROFILE,RECORD,SLOPE,SUBCRIT,STATE,XSN
C
      CHARACTER TYPE*7
C
      COMMON /INFO/ CODE,CRITWS,D165084ACT,DISTANCE,ESLOPE,FFACTOR,FR,
     +MANNING,MEANDEP,R,SCRIT,TOL,VELOCITY,WATSURF,WSWIDTH
C
      PARAMETER (DONE=0,LOOP=1)
      PARAMETER (SUBCRIT=0,CRITICAL=1)
      PROFILE=SUBCRIT
      FLOW=SUBCRIT
      SLOPE=SUBCRIT
      TYPE='SUBCRIT'
      ITER=0
      G=9.81
C
      CALL AREA (SURV,WATSURF(XSN),XSN,AWET,WSB,WP)
      HRAD=AWET/WP
      CALL SFRICT (Q,XSN,HRAD,AWET,D165084ACT,
     +ENSL,UBAR,FF,EQUATION,PARAM)
C
      IF (XSN.LT.NMAX) THEN
         CRITSL=(AWET*FF)/(8*WSB*HRAD)
         IF (INT(TEMPINFO(1,13)).EQ.1) THEN
            TEMPINFO (1,9)=CRITSL
            WSS=(TEMPINFO(1,4)-TEMPINFO(2,4))+
     +         ((TEMPINFO(1,2)**2-TEMPINFO(2,2)**2)/(2*G))/
     +         (TEMPINFO(2,15)-TEMPINFO(1,15))
         ELSE
            SCRIT (XSN)=CRITSL
            WSS=(WATSURF(XSN)-WATSURF(XSN+1))+
     +         ((VELOCITY(XSN)**2-VELOCITY(XSN+1)**2)/(2*G))/
     +         (DISTANCE(XSN+1)-DISTANCE(XSN))
         ENDIF
         IF (CRITSL.LT.WSS) SLOPE=CRITICAL
      ENDIF
C
      HCRIT=AWET/(2*WSB)
C
      IF (INT(TEMPINFO(1,13)).EQ.1) THEN
         UPHEAD=(TEMPINFO(1,2)**2)/(2*G)
         WS2=TEMPINFO(1,4)
      ELSE
         UPHEAD=(VELOCITY(XSN)**2)/(2*G)
         WS2=WATSURF(XSN)
      ENDIF
C
```

```
      IF ((UPHEAD/HCRIT).GT.0.94) PROFILE=CRITICAL
      IF(SLOPE.EQ.CRITICAL) PROFILE=CRITICAL
C
      IF (PROFILE.EQ.CRITICAL) THEN
         DO 80,I=1,50
            IF (INT(TEMPINFO(1,13)).EQ.1) THEN
               WS1=WS2 + (TEMPINFO(1,5)/4)
               WS3=WS2 - (TEMPINFO(1,5)/4)
            ELSE
               WS1=WS2 + (MEANDEP(XSN)/4)
               WS3=WS2 - (MEANDEP(XSN)/4)
            ENDIF
            IF (WS3.LT.(BEDMIN+0.1)) THEN
               WS3=BEDMIN+0.1
               IF (INT(TEMPINFO(1,13)).EQ.1) THEN
                  WS1=WS3+TEMPINFO(1,5)/2
                  WS2=WS3+TEMPINFO(1,5)/4
               ELSE
                  WS1=WS3+MEANDEP(XSN)/2
                  WS2=WS3+MEANDEP(XSN)/4
               ENDIF
            ENDIF
            CALL AREA(SURV,WS1,XSN,AWET,WSB,WP)
            U1=Q(XSN)/AWET
            HEAD1= WS1 + (U1**2)/(2*G)
            CALL AREA (SURV,WS2,XSN,AWET,WSB,WP)
            U2=Q(XSN)/AWET
            HEAD2=WS2 + (U2**2)/(2*G)
            CALL AREA(SURV,WS3,XSN,AWET,WSB,WP)
            U3=Q(XSN)/AWET
            HEAD3= WS3 + (U3**2)/(2*G)
            WSMIN= (((WS3**2-WS2**2)*(HEAD1-HEAD2))-
     +      ((WS1**2-WS2**2)*(HEAD3-HEAD2)))/
     +      (2*((WS3-WS2)*(HEAD1-HEAD2)-(WS1-WS2)*(HEAD3-HEAD2)))
            IF (ABS((WS2-WSMIN)/(WS2-BEDMIN)).GT.0.02) THEN
               STATE=LOOP
            ELSE
               CALL AREA(SURV,WSMIN,XSN,AWET,WSB,WP)
               UMIN=Q(XSN)/AWET
               HEADMIN= WSMIN + (UMIN**2)/(2*G)
               IF ((HEAD2-HEADMIN).GT.0.005) THEN
                  STATE=LOOP
               ELSE
                  STATE=DONE
               ENDIF
            ENDIF
            IF (STATE.EQ.DONE) THEN
               WSCRIT=WSMIN
               IF (INT(TEMPINFO(1,13)).EQ.1) THEN
                  TEMPINFO (1,10)=WSCRIT
                  CHECK=TEMPINFO(1,4)
               ELSE
                  CRITWS (XSN)=WSCRIT
                  CHECK=WATSURF(XSN)
               ENDIF
               IF (WSCRIT.GT.CHECK) THEN
                  HRAD=AWET/WP
                  CALL SFRICT (Q,XSN,HRAD,AWET,D165084ACT,ENSL,UBAR,
     +            FF,EQUATION,PARAM)
                  IF (TYPE.EQ.'CDEPTH') THEN
                     VELOCITY (XSN)=UMIN
                     ESLOPE (XSN)=ENSL
                     WATSURF (XSN)=WSCRIT
                     MEANDEP (XSN)=AWET/WSB
                     R (XSN)=HRAD
                     FFACTOR (XSN)=FF
                     FR (XSN)=UMIN/((G*MEANDEP(XSN))**0.5)
                     WSWIDTH (XSN)=WSB
                     MANNING (XSN)=(HRAD**(0.667))*(ENSL**0.5)/UBAR
                     IF (FR(XSN).GT.1) FR(XSN)=1.00
                  ENDIF
                  TYPE='HCRIT'
                  FLOW=CRITICAL
               ELSE IF (SLOPE.EQ.CRITICAL) THEN
                  HRAD=AWET/WP
                  CALL SFRICT (Q,XSN,HRAD,AWET,D165084ACT,ENSL,UBAR,
     +            FF,EQUATION,PARAM)
                  IF (TYPE.EQ.'CDEPTH') THEN
                     VELOCITY (XSN)=UMIN
                     ESLOPE (XSN)=ENSL
                     WATSURF (XSN)=WSCRIT
                     MEANDEP (XSN)=AWET/WSB
                     R (XSN)=HRAD
                     FFACTOR (XSN)=FF
                     FR (XSN)=UMIN/((G*MEANDEP(XSN))**0.5)
                     WSWIDTH (XSN)=WSB
                     MANNING (XSN)=(HRAD**(0.667))*(ENSL**0.5)/UBAR
                     IF (FR(XSN).GT.1) FR(XSN)=1.00
                  ENDIF
                  TYPE='HISLOPE'
                  FLOW=CRITICAL
               ELSE
                  FLOW=SUBCRIT
               ENDIF
               GOTO 90
            ELSE
               WS2=0.5*(WSMIN+WS2)
               IF (WS2.LT.(BEDMIN+0.01)) WS2=BEDMIN+(0.1*I)
               IF (I.EQ.50) THEN
                  FR (XSN)=9.99
                  FLOW=CRITICAL
               ENDIF
            ENDIF
90          IF (FLOW.EQ.CRITICAL) THEN
c              IF (ITER.EQ.SET .AND. RECORD.EQ.SET) THEN
c           ENDIF
            ENDIF
C            IF (XSN.EQ.3) THEN
C           WRITE (90,1000) I,CODE(XSN),VELOCITY(XSN),ESLOPE(XSN),
C    +      WATSURF(XSN),WSCRIT,FR(XSN)
C           WRITE (90,1000) I,CODE(XSN),UMIN,ENSL,WATSURF(XSN),
C    +      WSCRIT,(UMIN/(G*HRAD)**0.5),WS1,WS2,WS3
C           ENDIF
80       CONTINUE
      ENDIF
C
C1000  FORMAT(I2,1X,I4,1X,F6.4,1X,F8.6,1X,F7.4,1X,F10.4,1X,F5.2,
C     +3(1X,F6.3))
C1000  FORMAT(I2,1X,I4,1X,F6.4,1X,F8.6,1X,F7.4,1X,F10.4,1X,F5.2)
C
      END
C
C     ****************************************************************
      SUBROUTINE LOWBED (SURV,XSN,BEDMIN)
```

```
      REAL SURV (100,500),BEDMIN
      INTEGER I,XSN
C
      BEDMIN=SURV(1,2*XSN)
C
      DO 10,I=2,100
         IF (SURV(I,2*XSN).GT.9000) THEN
            GOTO 20
         ELSE IF (SURV(I,2*XSN).LT.BEDMIN) THEN
            BEDMIN=SURV(I,2*XSN)
         ENDIF
10    CONTINUE
C
20    END
C
C     ******************************************************************
      SUBROUTINE WSURFACE (SURV,WSEST,XSN,Q,TEMPINFO,WSCALC,AWET,WSB,
     +UUP,HBAR,EQUATION,PARAM)
C
      INTEGER CODE(250),EQUATION,XSN
C
      REAL AWET,CRITWS(250),D165084ACT(4,250),DISTANCE(250),
     +ENSL,ESLOPE(250),FFACTOR(250),FR(250),G,
     +HDOWN,HEAD,HRAD,MANNING(250),MEANDEP(250),PARAM(5),Q(250),
     +R(250),SCRIT(250),SFDOWN,SFBAR,SFUP,SURV(100,500),
     +TEMPINFO(2,15),UDOWN,UUP,VELOCITY(250),
     +WATSURF(250),WSCALC,WSEST,WSWIDTH(250)
C
      COMMON /INFO/ CODE,CRITWS,D165084ACT,DISTANCE,ESLOPE,FFACTOR,FR,
     +MANNING,MEANDEP,R,SCRIT,TOL,VELOCITY,WATSURF,WSWIDTH
C
      G=9.81
C
      CALL AREA (SURV,WSEST,XSN,AWET,WSB,WP)
      HRAD=AWET/WP
      CALL SFRICT (Q,XSN,HRAD,AWET,D165084ACT,
     +ENSL,UBAR,FF,EQUATION,PARAM)
      SFUP=ENSL
      SFDOWN=ESLOPE(XSN+1)
C
      IF (SFUP.LT.SFDOWN .AND. (SFUP+SFDOWN).LT.0.2) THEN
         SFBAR=(SFUP+SFDOWN)/2
      ELSE
         SFBAR=(2*SFUP*SFDOWN)/(SFUP+SFDOWN)
      ENDIF
C
      HEAD=SFBAR*(DISTANCE(XSN+1)-DISTANCE(XSN))
      UUP=Q(XSN)/AWET
      UDOWN=VELOCITY(XSN+1)
      HDOWN=WATSURF(XSN+1)
      WSCALC=HEAD+HDOWN+((UDOWN**2)/(G*2))-((UUP**2)/(2*G))
      VELOCITY (XSN)=UUP
      ESLOPE (XSN)=SFUP
      WATSURF (XSN)=WSCALC
      MEANDEP (XSN)=AWET/WSB
      R (XSN)=HRAD
      FFACTOR (XSN)=FF
      FR (XSN)=UUP/((G*(AWET/WSB))**0.5)
      WSWIDTH (XSN)=WSB
      MANNING (XSN)=(HRAD**(0.667))*(ENSL**0.5)/UBAR
C
      END
C
C     ******************************************************************
      SUBROUTINE APPROX (SURV,ESTMIN,DIFFMIN,XSN,Q,MEANDEP,
     +APPROOT,AWET,WSB,EQUATION,PARAM)
C
      REAL APPROACH,APPROOT,AWET,DIFF,DIFFMIN,ESTMIN,G,MEANDEP(250),
     +PARAM(5),Q(250),
     +SURV(100,500),TEMPINFO(2,15),WATSURF(250),WSB,WSCALC,WSEST
C
      INTEGER EQUATION,I,XSN
C
      APPROACH=1
      BEDMIN=0
      G=9.81
      WSEST=ESTMIN+0.01
C
      DO 50,I=1,20
         CALL LOWBED (SURV,XSN,BEDMIN)
         IF (WSEST.LT.BEDMIN) GOTO 51
         TEMPINFO(1,13)=0
         CALL WSURFACE (SURV,WSEST,XSN,Q,TEMPINFO,WSCALC,AWET,WSB,UUP,
     +   HBAR,EQUATION,PARAM)
         DIFF=WSCALC-WSEST
         IF (ABS(DIFF).LT.ABS(DIFFMIN)) THEN
            DIFFMIN=ABS(DIFF)
            ESTMIN=WSEST
            WSEST=ESTMIN+(0.01*APPROACH)
         ELSE
            IF (I.EQ.1) THEN
               WSEST=ESTMIN-0.01
               APPROACH=-1
            ELSE
               GOTO 51
            ENDIF
         ENDIF
50    CONTINUE
C
51    TEMPINFO(1,13)=0
      CALL WSURFACE(SURV,ESTMIN,XSN,Q,TEMPINFO,WSCALC,AWET,WSB,UUP,
     +HBAR,EQUATION,PARAM)
C
      IF (ESTMIN.GT.BEDMIN) THEN
         IF (WSCALC.GT.BEDMIN) THEN
            APPROOT=(WSCALC+ESTMIN)/2
         ELSE
            APPROOT=(ESTMIN+BEDMIN)/2
         ENDIF
      ELSE
         IF (WSCALC.GT.BEDMIN) THEN
            APPROOT=(BEDMIN+WSCALC)/2
         ELSE
            APPROOT=BEDMIN+MEANDEP(XSN+1)
         ENDIF
      ENDIF
C
      IF (ESTMIN.GT.WSCALC) WATSURF(XSN)=ESTMIN
      IF (ESTMIN.LT.WSCALC) WATSURF(XSN)=WSCALC
C
      END
C
C     ******************************************************************
      SUBROUTINE EXTEND (SURV,Q,HDS,N,D165084ACT,DISTANCE,MEANDEP,
```

```
     +WATSURF,CODE,EXTMETHOD,EXTSLOPE,NMAX,HLOW,EQUATION,PARAM)
C
C Routine to extend the reach downstream in order to achieve
C   convergence of slope/discharge at the downstream limit.
C
      REAL AWET,D165084ACT(4,250),DELTAX,DISTANCE(250),
     +EXTSLOPE,
     +G,HDS,HDIFF(2),HEND(2),HEST(3),HLOW,HRAD,
     +MEANDEP(250),MIN1,MIN2,MIN3,PARAM(5),Q(250),SADD,
     +SURV(100,500),SBAR1,WATSURF(250)
C
      INTEGER CODE(250),EQUATION,EXTRA,M,N,NMAX,NO,OFF,RECORD,YES
C
C PATRICK DS water level definition
      CHARACTER EXTMETHOD*5
C
      PARAMETER(YES=1,NO=0)
      PARAMETER(OFF=0)
      RECORD=OFF
      G=9.81
      DELTAX= DISTANCE(N)-DISTANCE(N-1)
      CALL LOWBED(SURV,N,MIN1)
      CALL LOWBED(SURV,N-1,MIN2)
      CALL LOWBED(SURV,N-2,MIN3)
      CALL AREA(SURV,HDS,N,AWET,WSB,WP)
      HRAD=AWET/WP
      CALL SFRICT(Q,N,HRAD,AWET,D165084ACT,ENSL,UBAR,FF,
     +EQUATION,PARAM)
      SBAR1=(MIN2-MIN1)/DELTAX
C PATRICK add option to use a specific ds water level
      IF (EXTMETHOD.EQ. 'FIXED') THEN
         SADD=EXTSLOPE
      ELSE
         IF (SBAR1.GT.0) THEN
            SADD=SBAR1
         ELSE
            IF (N.GT.10) THEN
               M=N-10
            ELSE
               M=1
            ENDIF
            CALL LOWBED (SURV,M,MIN2)
            SADD=(MIN2-MIN1)/(DISTANCE(M)-DISTANCE(N))
         ENDIF
      ENDIF
C
      DO 500,K=5,100,5
         EXTRA=NO
         DO 100,M=(N+1),(N+K)
            DO 50,I=1,100
               IF (SURV(I,2*(M-1)).LT.9000) THEN
                  SURV(I,2*M)=SURV(I,2*(M-1))-(SADD*DELTAX)
                  SURV(I,(2*M-1))= SURV(I,(2*M-3))
               ELSE
                  SURV(I,2*M)=99999
                  SURV(I,(2*M-1))=99999
                  GOTO 80
               ENDIF
50          CONTINUE
80          CODE (M)= CODE(M-1) +1
            Q(M)=Q(M-1)
            D165084ACT(3,M)= D165084ACT (3,M-1)
               DISTANCE (M)= DISTANCE(M-1) +DELTAX
100      CONTINUE
         HLOW=HDS-(K*SADD*DELTAX)
         DO 300,M=(N+K-1),N,-1
            CALL BACKWATER ((N+K),N,M,Q,HLOW,SURV,RECORD,EQUATION,
     +      PARAM)
300      CONTINUE
         HEST(2)=WATSURF(N)
         HEND(1)=HLOW+MEANDEP(N+K)/20
         HEND(2)=HLOW+MEANDEP(N+K)/10
         DO 310,M=(N+K-1),N,-1
            CALL BACKWATER((N+K),N,M,Q,HEND(1),SURV,RECORD,EQUATION,
     +      PARAM)
310      CONTINUE
         HEST(3)=WATSURF(N)
         DO 320,M=(N+K-1),N,-1
            CALL BACKWATER((N+K),N,M,Q,HEND(2),SURV,RECORD,EQUATION,
     +      PARAM)
320      CONTINUE
         HEST(1)=WATSURF(N)
         HDIFF(1)=(HEST(1)-HEST(2))/MEANDEP(N)
         HDIFF(2)=(HEST(3)-HEST(2))/MEANDEP(N)
         IF (HDIFF(1).GT.0.05) EXTRA=YES
         IF (HDIFF(2).GT.0.05) EXTRA=YES
         IF (EXTRA.EQ.NO) GOTO 600
C END
500   CONTINUE
C
600   IF (EXTRA.EQ.YES) WRITE (11,1000) HEST(3)-HEST(2),HEST(1)-
     +HEST(2)
      NMAX=N+K
C
1000  FORMAT ('After extending the reach by 100 cross-sections',/
     +,'a backwater effect persisted.  With changes in the',/
     +,'downstream water surface of +0.005 and +0.01 of the flow',/
     +,'depth water surface differences at the end of the reach',/
     +,'were ',F6.4,' and ',F6.4,'m.')
C
      END
C
C     ******************************************************************
      SUBROUTINE ESTIMATE(K,LEST,LCALC,EST,CALC,CALCUP,CALCDOWN,
     +ESTUP,ESTDOWN,TYPE,BRACKET,MIN,INCR,DIFFMIN,ESTMIN,TOL,MAX,DIFF)
C
      REAL CALC(2),CALCUP,CALCDOWN,DIFF(2),DIFFMIN,
     +ERROR,EST(2),ESTDOWN,ESTMIN,ESTUP,
     +INCR,LCALC,LEST,MAX,MIN,SUM,TOL
C
      INTEGER BISECT,BRACKET,K,METHOD,OFF,SECANT,SET,SUCCSUB
C
      CHARACTER TYPE*7
C
      PARAMETER (SECANT=1,SUCCSUB=0,BISECT=2)
      PARAMETER (OFF=0,SET=1)
C
      IF (TYPE.EQ.'APPROX') THEN
         IF (DIFFMIN*(LEST-LCALC).LT.0.0) THEN
            ESTUP=ESTDOWN
            CALCUP=CALCDOWN
            ESTDOWN=LEST
            CALCDOWN=LCALC
            METHOD=BISECT
```

```
          ELSE
            TYPE='NOINT'
            GOTO 200
          ENDIF
        ENDIF
C
        IF (K.GE.3) THEN
          IF (METHOD.EQ.SECANT) THEN
            IF (BRACKET.EQ.SET) THEN
              IF (LCALC.GT.LEST) THEN
                IF (ABS(LEST-EST(2)).LT.
     +          ABS(0.05*(LCALC-CALCUP))) METHOD=BISECT
              ELSE
                IF (ABS(LEST-EST(2)).LT.
     +          ABS(0.05*(LCALC-CALCDOWN))) METHOD=BISECT
              ENDIF
            ENDIF
          ENDIF
        ENDIF
C
        IF (K.EQ.1) THEN
          CALC(1)=LCALC
          EST(1)=LEST
          DIFF(1)=CALC(1)-EST(1)
          DIFFMIN=ABS(DIFF(1))
          ESTMIN=EST(1)
          IF (DIFF(1).GT.0.00) THEN
            ESTDOWN=EST(1)
            CALCDOWN=CALC(1)
          ELSE
            ESTUP=EST(1)
            CALCUP=CALC(1)
          ENDIF
        ELSE IF (K.EQ.2) THEN
          IF (ABS(LCALC-LEST).GT.ABS(DIFF(1))) THEN
            CALC(2)=CALC(1)
            EST(2)=EST(1)
            DIFF(2)=DIFF(1)
            CALC(1)=LCALC
            EST(1)=LEST
            DIFF(1)=CALC(1)-EST(1)
            IF (DIFF(1).GT.0.00) THEN
              IF (ESTDOWN.LT.EST(1)) THEN
                ESTDOWN=EST(1)
                CALCDOWN=CALC(1)
              ENDIF
            ELSE
              IF (ESTUP.GT.0.00) THEN
                IF (ESTUP.GT.EST(1)) THEN
                  ESTUP=EST(1)
                  CALCUP=CALC(1)
                ENDIF
              ELSE
                ESTUP=EST(1)
                CALCUP=CALC(1)
              ENDIF
            ENDIF
          ELSE
            CALC(2)=LCALC
            EST(2)=LEST
            DIFF(2)=CALC(2)-EST(2)
          ENDIF
        ELSE
          CALC(1)=CALC(2)
          EST(1)=EST(2)
          DIFF(1)=DIFF(2)
          CALC(2)=LCALC
          EST(2)=LEST
          DIFF(2)=CALC(2)-EST(2)
        ENDIF
C
        IF(K.EQ.2) THEN
          IF (DIFF(1).GT.0.00) THEN
            IF (DIFF(2).GT.0.00) THEN
              IF(ABS(CALC(1)-CALC(2)).LT.(0.1*DIFF(1))) THEN
                METHOD=SUCCSUB
              ELSE
                METHOD=SECANT
              ENDIF
            ELSE
              METHOD=SECANT
            ENDIF
          ELSE
            METHOD=SECANT
          ENDIF
        ENDIF
C
        IF (METHOD.EQ.SECANT .AND. K.GE.3 .AND. BRACKET.EQ.OFF) THEN
          IF ((DIFF(2)*DIFF(1)).GT.0.00) THEN
            IF (ABS(DIFF(2)).GT.ABS(DIFF(1))) THEN
              TYPE='NOINT'
              GOTO 200
            ENDIF
          ENDIF
        ENDIF
C
        IF (K.GE.2) THEN
          IF (ESTUP.GT.ESTDOWN) THEN
            IF (DIFF(2).GT.0.00) THEN
              IF (ESTDOWN.LT.EST(2)) THEN
                ESTDOWN=EST(2)
                CALCDOWN=CALC(2)
              ENDIF
            ELSE
              IF (ESTUP.GT.0.00) THEN
                IF (ESTUP.GT.EST(2)) THEN
                  ESTUP=EST(2)
                  CALCUP=CALC(2)
                ENDIF
              ELSE
                ESTUP=EST(2)
                CALCUP=CALC(2)
              ENDIF
            ENDIF
          ELSE
            IF (DIFF(2).GT.0.00) THEN
              IF (ESTDOWN.GT.EST(2)) THEN
                ESTDOWN=EST(2)
                CALCDOWN=CALC(2)
              ENDIF
            ELSE
              IF (ESTUP.GT.0.00) THEN
                IF (ESTUP.LT.EST(2)) THEN
                  ESTUP=EST(2)
```

```
                        CALCUP=CALC(2)
                     ENDIF
                  ELSE
                     ESTUP=EST(2)
                     CALCUP=CALC(2)
                  ENDIF
               ENDIF
            ENDIF
         ENDIF
C
         IF (BRACKET.EQ.OFF) THEN
            IF (ESTUP.GT.0.00  .AND.  ESTDOWN.GT.0.00) BRACKET=SET
         ENDIF
C
         IF (ABS(LCALC-LEST).LT.DIFFMIN) THEN
            DIFFMIN=ABS(LCALC-LEST)
            ESTMIN=LEST
         ENDIF
C
         ERROR=ABS(LCALC-LEST)
C
         IF (ERROR.GT.TOL) THEN
            IF (K.EQ.1) THEN
               IF ((CALC(1)-EST(1)).GT.(2*INCR)) THEN
                  LEST=CALC(1)-(0.9*(CALC(1)-EST(1)))
               ELSE
                  LEST=(CALC(1)+EST(1))/2
               ENDIF
            ELSE
               SUM=0
               DO 30,L=1,2
                  IF (L.EQ.1) THEN
                     IF (BRACKET.EQ.SET) SUM=10000*
     +                  (ESTDOWN-ESTUP+CALCUP-CALCDOWN)
                  ELSE
                     SUM=10000*(EST(2)+CALC(1)-EST(1)-CALC(2))
                  ENDIF
                  IF (ABS(SUM).LT.1.0) METHOD=BISECT
 30            CONTINUE
               IF (METHOD.EQ.SUCCSUB) THEN
                  LEST=LCALC
               ELSE IF (METHOD.EQ.BISECT) THEN
                  IF (BRACKET.EQ.SET) THEN
                     LEST=(ESTUP+ESTDOWN)/2
                  ELSE
                     LEST=(LEST+LCALC)/2
                  ENDIF
               ELSE
                  IF (BRACKET.EQ.SET) THEN
                     LEST=((ESTDOWN*CALCUP)-(CALCDOWN*ESTUP))/
     +                  (ESTDOWN-ESTUP+CALCUP-CALCDOWN)
                  ELSE
                     LEST=((EST(2)*CALC(1))-(EST(1)*CALC(2)))/
     +                  (EST(2)+CALC(1)-EST(1)-CALC(2))
                  ENDIF
               ENDIF
            ENDIF
            IF (LEST.LT.(MIN+0.05)) THEN
               IF (K.LE.10) THEN
                  LEST=MIN+0.1
               ELSE
                  TYPE='NOINT'
                  GOTO 200
               ENDIF
               IF (ABS(LEST-EST(2)).LT.0.02) LEST=LEST+0.01
            ENDIF
            IF (K.GE.5  .AND.  METHOD.EQ.SECANT  .AND.  LEST.GT.MAX) THEN
               LEST=MIN+INCR
               TYPE='APPROX'
            ENDIF
         ELSE
            TYPE='SUBCRIT'
         ENDIF
C
 200     END
C
C        ******************************************************************
         SUBROUTINE SLOPEST(N,Y,X,GRAD)
C
         INTEGER N
         REAL Y(5),X(5),GRAD,SIGXY,SIGXSIGY,SIGXX,SIGX2,SIGX,SIGY
C
         SIGXX=0
         SIGX2=0
         SIGXSIGY=0
         SIGXY=0
         SIGX=0
         SIGY=0
C
         DO 50,I=1,N
            SIGXX=X(I)**2 + SIGXX
            SIGXY=SIGXY + X(I)*Y(I)
            SIGX=SIGX + X(I)
            SIGY=SIGY + Y(I)
 50      CONTINUE
C
         SIGXSIGY = SIGX*SIGY
         SIGX2 = SIGX**2
         GRAD=((N*SIGXY)-SIGX*SIGY)/((N*SIGXX)-SIGX**2)
C
         END
C
C        ******************************************************************
         SUBROUTINE SEDROUT (ACTSTART,SIZESTART,SIZELAYER,THICKLAYER,
        +DELTAT,N,SURV,TTOT,M,PARKER,MAXALTDEP,BEDFRACT,QBIN,QBFRACTIN,
        +DXTEST,DXINT,INF,JKJK,DEFINT,DEFREAL,SIZEFINE,INSED,KVISC,SS,
        +RHOSED,NCLASS,EXPROP,TRIBLOC,TCODE,SUBTHICK,Q,CH,SCXS,NSECT)
C
C This subroutine deals with 1 node at a time: it is called from within
C a loop that calls cross-sections sequentially.
C
         INTEGER ACTMETHOD,AGGEX,AGGRADING,CALC,CASE,CHANGE,CODE(250),CH,
        +DEFINT(10),DEGRADING,DXDIFF,DXTEST,DZ0,EQUCODE,INF(20),KXQB1,
        +LAYER,M,N,NCLASS,NOCALC,QBCGSDV,QBCONST,SELECT(10),TCODE,USBDY,
        +SCXS(25,5,2),XS(6),NSECT
C
C Variables used in calculations, including common variables.
C
         REAL ACTSTART(125),AREA,AREAEST,
        +BEDCH(2,125),BEDDATA(25),BEDFRACT(125,25),
        +COMP(2),CRITWS(250),
        +D165084ACT(4,250),D165084SUB(4,250),D165084BLD(4,250),
        +D84EST,DEFREAL(20),DELEV,DELTAT,DELTAX,DIFF(2),DISTANCE(250),
        +DXINT,D50SURF,DGMACT(250),
```

```
      +ERROR, ESLOPE(250), EST(2), EXCHSIZE(25), EXPROP(25),
      +FFACTOR(250), FR(250), G, HIDINGG, HIDINGS, INSED(26),
      +KVISC, LAMBDA, LAYEREST, LCALC, LOAD,
      +MANNING(250), MAXALTDEP(125), MEANDEP(250), MEANWIDTH,
      +NEWACTIVE, NEWCUMPC, NEWDEP, NEWSURF(25),
      +PARKER(36,3),
      +Q(250), QBEDLOAD(125), QBED(6), QBFRACT(25,6), QBFRACTIN(25),
      +QBIN, QBSIZE(25,2),
      +R(250), RHOSED,
      +SCRIT(250), SEDTOTAL(10), SIZEDATA(25), SIZEFINE(25),
      +SIZELAYER(5,125,25), SIZES(11), SIZESTART(2,125,25), SS, STORE(25),
      +STRAINC, SURV(100,500), SUBTHICK(125),
      +TAUREF, THICKLAYER(125), TOTSTORE, TOTVOL,
      +TQB, TRIBFRACT(25,5), TRIBK(5), TRIBLOC(5), TRIBPROP, TRIBQB(5),
      +TTOT,
      +VELOCITY(250), VOLCH(2,125), WATSURF(250), WIDTH(2), WSWIDTH(250)
C
       CHARACTER TINPUT(5)*10, TRIBGSD(5)*5, TRIBHERE*4
C
       COMMON /SEDINFO/ D165084SUB, D165084BLD, DGMACT, QBEDLOAD, BEDCH,
      +VOLCH, SEDTOTAL, STRAINC, TRIBFRACT, TRIBK, TRIBQB, TRIBGSD, TRIBHERE,
      +TINPUT
C
       COMMON /INFO/ CODE, CRITWS, D165084ACT, DISTANCE, ESLOPE, FFACTOR, FR,
      +MANNING, MEANDEP, R, SCRIT, TOL, VELOCITY, WATSURF, WSWIDTH
C
       PARAMETER(DEGRADING=-1,AGGRADING=1)
       PARAMETER(CALC=1,NOCALC=0)
       PARAMETER (DXDIFF=0)
       PARAMETER (KXQB1=3,DZ0=1,QBCONST=2,KXS1FIX=4,QBCGSDV=5)
       INF(7)=0
       LAMBDA=DEFREAL(3)
       G=9.81
       USBDY=DEFINT(3)
       AGGEX=DEFINT(4)
       KACTIVE=DEFREAL(5)
       HIDINGG=DEFREAL(6)
       HIDINGS=DEFREAL(8)
       LOAD=DEFREAL(4)
       TAUREF=DEFREAL(9)
       EQUCODE=DEFINT(9)
       STRAINC=DEFREAL(10)
C
       DO 1,L=1,2
          EST(L)=0
          COMP(L)=0
1      CONTINUE
C
       DO 5,K=1,10
          SELECT(K)=NOCALC
5      CONTINUE
C
       IF (M.NE.1) THEN
C PATRICK extra statements for multiple channel option
          IF (NSECT.GE.2) THEN
             XS(1)=SCXS(CH,1,1)
             XS(2)=SCXS(CH,1,2)
             XS(3)=SCXS(CH,3,1)
             XS(4)=SCXS(CH,3,2)
             XS(5)=SCXS(CH,4,1)
             XS(6)=SCXS(CH,4,2)
             IF (M.EQ.XS(1) .AND. SCXS(CH,2,2).NE.0) THEN
                DELTAX=
      +         ((DISTANCE(XS(3))-DISTANCE(XS(3)-1))*WSWIDTH(XS(3)-1)
      +         +(DISTANCE(XS(4))-DISTANCE(XS(4)-1))*WSWIDTH(XS(4)-1))/
      +         (WSWIDTH(XS(3)-1)+WSWIDTH(XS(4)-1))
                WIDTH(1)=WSWIDTH(XS(3)-1)+WSWIDTH(XS(4)-1)
                WIDTH(2)=WSWIDTH(M)
             ELSE IF (M.EQ.XS(1)+1 .AND. SCXS(CH,2,2).EQ.0 .AND.
      +      CH.NE.1) THEN
                DELTAX=DISTANCE(M)-DISTANCE(M-1)
                WIDTH(1)=WSWIDTH(XS(3))*WSWIDTH(M)/(
      +         WSWIDTH(SCXS(SCXS(CH,2,1),5,1)+1)+
      +         WSWIDTH(SCXS(SCXS(CH,2,1),5,2)+1))
                WIDTH(2)=WSWIDTH(M)
             ELSE
                DELTAX=DISTANCE(M)-DISTANCE(M-1)
                WIDTH(1)=WIDTH(2)
                WIDTH(2)=WSWIDTH(M)
             ENDIF
          ELSE
             DELTAX=DISTANCE(M)-DISTANCE(M-1)
             WIDTH(1)=WIDTH(2)
             WIDTH(2)=WSWIDTH(M)
          ENDIF
       ELSE
          DELTAX=DISTANCE(2)-DISTANCE(1)
          WIDTH(2)=WSWIDTH(M)
          WIDTH(1)=WIDTH(2)
       ENDIF
C END
       MEANWIDTH=0.5*(WIDTH(1)+WIDTH(2))
C
       DO 10,I=1,NCLASS
          BEDDATA(I)=SIZELAYER(1,M,I)
10     CONTINUE
C
C      *  *  *  *  *  *  *  *  *  *  *  *  *  *  *
C      Calculate the u/s sediment supply rate
       IF (M.EQ.1) THEN
          CASE=2
          IF (EQUCODE.EQ.1) THEN
             CALL BEDLOAD(HIDINGG,HIDINGS,TAUREF,BEDDATA,M,PARKER,CASE
      +      ,SIZEFINE,NCLASS,STRAINC,QBED,QBFRACT,ESLOPE,R,WSWIDTH)
          ELSE IF (EQUCODE.EQ.2) THEN
             CALL EINSTEIN (BEDDATA,M,CASE,SIZEFINE,QBED,
      +      QBFRACT,RHOSED,SS,KVISC,NCLASS,ESLOPE,WSWIDTH,R)
          ELSE IF (EQUCODE.EQ.3) THEN
             D50SURF=D165084ACT(2,M)
             CALL WILCOCK (BEDDATA,CASE,D50SURF,M,SIZEFINE,
      +      NCLASS,QBED,QBFRACT,ESLOPE,R,WSWIDTH)
C PATRICK added Ackers and White option
          ELSE IF (EQUCODE.GE.4 .AND. EQUCODE.LE.6) THEN
             CALL ACKERS(BEDDATA,CASE,D165084SUB,ESLOPE,EQUCODE,M,
      +      MEANDEP,NCLASS,SIZEFINE,Q,QBED,QBFRACT,R,WSWIDTH)
          ENDIF
          IF (USBDY.EQ.KXQB1) THEN
             IF (QBED(2).GT.0) THEN
                QBED(1)=QBED(2)*LOAD
                DO 20,I=1,NCLASS
                   QBFRACT(I,1)=QBFRACT(I,2)*LOAD
                   QBSIZE(I,1)=100*QBFRACT(I,1)/QBED(1)
20              CONTINUE
C PATRICK when there is no tranport at the upstream boundary
```

```
                  ELSE
                                                  QBED(1)=0
                     DO 22,I=1,NCLASS
                        QBFRACT(I,1)=0
                        QBSIZE(I,1)=0
 22                  CONTINUE
                  ENDIF
               ELSE IF (USBDY.EQ.DZ0) THEN
                  QBED(1)=QBED(2)
                  DO 25,I=1,NCLASS
                     QBFRACT(I,1)=QBFRACT(I,2)
                     IF (QBED(1).GT.0.00000001) THEN
                        QBSIZE(I,1)=100*QBFRACT(I,1)/QBED(1)
C PATRICK when there is no tranport at the upstream boundary
                     ELSE
                        QBSIZE(I,1)=SIZELAYER(2,M,I)
                     ENDIF
 25               CONTINUE
               ELSE IF (USBDY.EQ.QBCONST) THEN
                  QBED(1)=INSED(1)*WSWIDTH(1)
                  DO 35,I=1,NCLASS
                     QBSIZE(I,1)=INSED(I+1)
                     QBFRACT(I,1)=0.01*QBSIZE(I,1)*QBED(1)
 35               CONTINUE
               ELSE IF (USBDY.EQ.KXS1FIX) THEN
                  QBED(1)=QBED(2)*LOAD
                  DO 32,I=1,NCLASS
                     QBSIZE(I,1)=INSED(I+1)
                     QBFRACT(I,1)=0.01*QBSIZE(I,1)*QBED(1)
 32               CONTINUE
               ELSE IF (USBDY.EQ.QBCGSDV) THEN
                  QBED(1)=INSED(1)*WSWIDTH(1)
                  DO 36,I=1,NCLASS
                     QBFRACT(I,1)=QBFRACT(I,2)
                     IF (QBED(1).GT.0.00000001) QBSIZE(I,1)=
     +               100*QBFRACT(I,1)/QBED(1)
 36               CONTINUE
               ENDIF
               QBIN=QBED(1)
               DO 26,I=1,NCLASS
                  QBFRACTIN(I)=QBFRACT(I,1)
 26            CONTINUE
               SEDTOTAL(1)=SEDTOTAL(1)+QBIN*DELTAT
            ELSE IF (M.LE.N) THEN
C PATRICK added statments for mulitple channel option
               IF (M.EQ.XS(1)) THEN
                  QBED(1)=QBEDLOAD(M)
                  IF (QBED(1).GT.0.00) THEN
                     DO,I=1,NCLASS
                        QBFRACT(I,1)=BEDFRACT(M,I)/1000
                        QBSIZE(I,1)=QBFRACT(I,1)*100/QBED(1)
                     ENDDO
                  ELSE
                     DO,I=1,NCLASS
                        QBFRACT(I,1)=BEDFRACT(M,I)/1000
                        QBSIZE(I,1)=SIZELAYER(2,M,I)
                     ENDDO
                  ENDIF
C              ELSE IF (M.EQ.XS(1)+1 .AND. SCXS(CH,2,2).EQ.0) THEN
               ELSE IF (M.EQ.XS(1)+1 .AND. SCXS(CH,2,2).EQ.0 .AND.
     +         CH.NE.1) THEN
                  QBED(1)=QBEDLOAD(M-1)
                  IF (QBED(1).GT.0.00) THEN
                     DO,I=1,NCLASS
                        QBFRACT(I,1)=BEDFRACT(M-1,I)/1000
                        QBSIZE(I,1)=QBFRACT(I,1)*100/QBED(1)
                     ENDDO
                  ELSE
                     DO,I=1,NCLASS
                        QBFRACT(I,1)=BEDFRACT(M-1,I)/1000
                        QBSIZE(I,1)=SIZELAYER(2,M-1,I)
                     ENDDO
                  ENDIF
               ELSE
                  QBED(1)=QBED(2)
                  DO 40,I=1,NCLASS
                     QBSIZE(I,1)=QBSIZE(I,2)
                     QBFRACT(I,1)=QBFRACT(I,2)
 40               CONTINUE
               ENDIF
C END
               CASE=2
               IF (EQUCODE.EQ.1) THEN
                  CALL BEDLOAD(HIDINGG,HIDINGS,TAUREF,BEDDATA,M,
     +            PARKER,CASE,SIZEFINE,NCLASS,STRAINC,QBED,QBFRACT,
     +            ESLOPE,R,WSWIDTH)
               ELSE IF(EQUCODE.EQ.2) THEN
                  CALL EINSTEIN (BEDDATA,M,CASE,SIZEFINE,QBED,
     +            QBFRACT,RHOSED,SS,KVISC,NCLASS,ESLOPE,WSWIDTH,R)
               ELSE IF(EQUCODE.EQ.3) THEN
                  D50SURF=D165084ACT(2,M)
                  CALL WILCOCK (BEDDATA,CASE,D50SURF,M,SIZEFINE,
     +            NCLASS,QBED,QBFRACT,ESLOPE,R,WSWIDTH)
C PATRICK added Ackers and White option
               ELSE IF(EQUCODE.GE.4 .AND. EQUCODE.LE.6) THEN
                  CALL ACKERS(BEDDATA,CASE,D165084SUB,ESLOPE,EQUCODE,M,
     +            MEANDEP,NCLASS,SIZEFINE,Q,QBED,QBFRACT,R,WSWIDTH)
               ENDIF
            ENDIF
C
C  Is there a tributary entering?
            TQB=0
            TRIBPROP=0
C
            IF (TRIBHERE.EQ.'TRIB') THEN
               TRIBPROP=(TRIBLOC(TCODE)-DISTANCE(M-1))/
     +         (DISTANCE(M)-DISTANCE(M-1))
               IF (TINPUT(TCODE).EQ.'KXMAIN') THEN
                  TQB=TRIBK(TCODE)*(QBED(1)+(QBED(2)-QBED(1))*TRIBPROP)
                  TRIBQB(TCODE)=TQB
               ELSE IF (TINPUT(TCODE).EQ.'CONST') THEN
                  TQB=TRIBQB(TCODE)
               ELSE IF (TINPUT(TCODE).EQ.'KXUSMAIN') THEN
                  TQB=TRIBK(TCODE)*QBIN
                  TRIBQB(TCODE)=TQB
               ENDIF
               SEDTOTAL(5+TCODE)=SEDTOTAL(5+TCODE)+TQB*DELTAT
C  If TINPUT='CONST' then TRIBQB has already been set; Similarly if
C  TRIBGSD='FIXED' the tributary gsd has already been specified.
               IF (TRIBGSD(TCODE).NE.'FIXED') THEN
                  DO 90,I=1,NCLASS
                     IF (QBED(1) .GT. 0.00 .AND. QBED(2) .GT. 0.00) THEN
                        TRIBFRACT(I,TCODE)=(QBFRACT(I,1)/QBED(1))+
     +                  ((QBFRACT(I,2)/QBED(2))-(QBFRACT(I,1)/QBED(1)))
```

```
     +                 *TRIBPROP
                    TRIBFRACT(I,TCODE)=TRIBFRACT(I,TCODE)*100
                 ELSE
                    TRIBFRACT(I,TCODE)=QBSIZE(I,1)
                 ENDIF
 90           CONTINUE
           ENDIF
C  Update the gsd of the material coming into the section being
C  calculated, according to the ratio of bedload (main vs. trib).
C  tpt. rates.
           DO 95,I=1,NCLASS
              IF (QBED(1).GT.0.00) THEN
                 QBSIZE(I,1)=(QBSIZE(I,1)*QBED(1)/(QBED(1)+TQB))+
     +           (TRIBFRACT(I,TCODE)*TQB/(QBED(1)+TQB))
              ENDIF
 95        CONTINUE
        ENDIF
C
C     Solve the continuity equation for bed elevation change.
        IF (M.EQ.N) SEDTOTAL(2)=SEDTOTAL(2)+QBED(2)*DELTAT
        DELEV=DELTAT*(TQB+QBED(1)-QBED(2))/((1-LAMBDA)*DELTAX*MEANWIDTH)
C
C  The bedload gsd at the receiving section is not varied due to
C  tributary input. At this time, the tributary influences the bed
C  elevation and gsd of the sediment being input to the section.
        IF (QBED(2).GT.0.00) THEN
           DO 110,I=1,NCLASS
              QBSIZE(I,2)=QBFRACT(I,2)*100/QBED(2)
 110       CONTINUE
        ELSE
           DO 115,I=1,NCLASS
              QBSIZE(I,2)=SIZELAYER(2,M,I)
 115       CONTINUE
        ENDIF
C
        EXPMIN=1.0
C
        DO 117,I=1,NCLASS
           IF (EXPROP(I).LT.EXPMIN) EXPMIN=EXPROP(I)
 117    CONTINUE
C
        IF (DELEV.LT.0.00) THEN
           CHANGE=DEGRADING
C PATRICK extra statement for fixed layer option
           IF (ABS(DELEV).GT.SUBTHICK(M) .AND. DEFINT(5).EQ.2) THEN
              DO 131,I=1,NCLASS
                 EXCHSIZE(I)=(SIZELAYER(2,M,I)*SUBTHICK(M)+
     +           SIZELAYER(3,M,I)*(ABS(DELEV)-SUBTHICK(M)))/ABS(DELEV)
 131          CONTINUE
           ELSE
              DO 130,I=1,NCLASS
                 EXCHSIZE(I)=SIZELAYER(2,M,I)
 130          CONTINUE
           ENDIF
C END
        ELSE
           CHANGE=AGGRADING
           DO 122,I=1,NCLASS
              EXCHSIZE(I)=(QBSIZE(I,2)*(1-EXPROP(I)))+(SIZELAYER(1,M,I)
     +        *EXPROP(I))
 122       CONTINUE
        ENDIF
C
cccccccccccccccccccccccccccccccccccccccccccccccccccccccccccccccccc
C       Now solve sediment continuity equation for each size fraction.
C
        LAYEREST=THICKLAYER(M)
        AREAEST=LAYEREST*MEANWIDTH
        AREA=AREAEST
C
        DO 150,K=1,20
           NEWCUMPC=0.0
           DO 300,I=1,NCLASS
C             IF (EXCHSIZE(I)-QBSIZE(I,2).LT.0) THEN
C                WRITE (7,789) M,I,TTOT,EXCHSIZE(I),QBSIZE(I,2),DELTAT
C             ENDIF
C789          FORMAT (2(I3,1X),4(F20.9,1X))
              NEWSURF(I)=SIZELAYER(1,M,I)-
     +        ((SIZELAYER(1,M,I)-EXCHSIZE(I))*(AREAEST-AREA)/AREA)+
     +        ((DELTAT/((1-LAMBDA)*DELTAX*AREA))*(((QBED(2)-QBED(1)-TQB)
     +        *(EXCHSIZE(I)-QBSIZE(I,2)))-
     +        (QBED(2)*(QBSIZE(I,2)-QBSIZE(I,1)))))
              NEWCUMPC=NEWCUMPC+NEWSURF(I)
C  DEBUGGING BLOCK
C             IF (TTOT.EQ.1) THEN
C                IF (I.EQ.1 .AND.M.EQ.29) THEN
C                   WRITE (7,781) M,AREAEST,AREA,QBED(1),QBED(2),DELEV,
C    +              DELTAT
C                ENDIF
C                WRITE (7,777) NEWSURF(I),SIZELAYER(1,M,I),EXCHSIZE(I),
C    +           QBSIZE(I,1),QBSIZE(I,2)
C             ENDIF
C781    FORMAT (I2,2X,5(F12.5,1X),F10.2)
C  END OF BLOCK
 300       CONTINUE
           DO 301,I=1,NCLASS
              NEWSURF(I)=NEWSURF(I)*100/NEWCUMPC
 301       CONTINUE
           SELECT(8)=CALC
C       WRITE(*,4321) M,(QBSIZE(J,2),J=1,5),(QBED(J),J=1,2)
C4321   FORMAT (I3,1X,5(F7.3,1X),2(F10.8,1X))
C       IF (M.EQ.2) THEN
C       WRITE(*,4322) (QBSIZE(J,1),J=1,5)
C       ENDIF
C4322   FORMAT (5(F10.3,1X))
           CALL SIZEPARM(NEWSURF,SELECT,SIZEFINE,NCLASS,SIZES)
C PATRICK LAYEREST is already equal to KACTIVE, so ERROR=0
           IF (DEFINT(5).EQ.2) THEN
              GOTO 152
           ELSE
              D84EST=SIZES(8)
              ERROR=(LAYEREST-(KACTIVE*D84EST))/
     +        (LAYEREST+(KACTIVE*D84EST))
           ENDIF
C END
           IF (ABS(ERROR).LT.0.001) GOTO 152
           IF (EXPMIN.GT.0.99) GOTO 152
           LCALC=KACTIVE*D84EST*MEANWIDTH
           CALL ACTESTIMATE(K,ACTMETHOD,AREAEST,LCALC,EST,COMP,DIFF)
           IF (ACTMETHOD.EQ.2) GOTO 151
           LAYEREST=AREAEST/MEANWIDTH
 150    CONTINUE
C
 151    KCHECK=0
```

```
      IF (K.EQ.21) KCHECK=1
      IF (ACTMETHOD.EQ.2) KCHECK=1
C
      IF (KCHECK.EQ.1) THEN
         IF (DELTAT.GT.0.001) THEN
            DXTEST=DXDIFF
C PATRICK keep time in whole seconds when over 2sec
            IF (DELTAT.GE.2) THEN
               DXINT=AINT(DELTAT/2)
            ELSE
               DXINT=DELTAT/2
            ENDIF
            GOTO 500
         ENDIF
         PRINT *,'MAX # ITERATIONS REACHED IN SURFACE LAYER CALC!!'
         WRITE (7,776) M,AREAEST,LCALC,QBED(1),QBED(2),DELTAT,AREA,
     +   DELEV
         DO 778,I=1,NCLASS
            WRITE (7,777) NEWSURF(I),SIZELAYER(1,M,I),EXCHSIZE(I),
     +      QBSIZE(I,1),QBSIZE(I,2)
 778     CONTINUE
 776     FORMAT (I2,1X,4(F10.7,1X),F6.1,1X,F10.7,3(1X,F8.5))
 777     FORMAT (F20.5,1X,4(F10.7,1X))
C
         DO 170,I=1,NCLASS
            NEWSURF(I)=SIZELAYER(1,M,I)
 170     CONTINUE
         D84EST=D165084ACT(3,M)
         LAYEREST=THICKLAYER(M)
      ENDIF
C
C     NEWSURF(I) <0 should be impossible.  If NEWSURF(I)<-0.001
C     a warning is printed.
C
 152  DO 135,I=1,NCLASS
         IF (NEWSURF(I).LT.0.00) THEN
            IF (SIZELAYER(1,M,I).GT.0.01) THEN
               IF (DELTAT.LT.0.001) THEN
                  PRINT *,'NEWSURF(I)<0.00'
                  WRITE (7,776) M,AREAEST,LCALC,QBED(1),QBED(2),
     +            DELTAT,AREA
                  DO 779,II=1,NCLASS
                     WRITE (7,777) NEWSURF(II),SIZELAYER(1,M,II),
     +               EXCHSIZE(II),QBSIZE(II,1),QBSIZE(II,2)
 779              CONTINUE
                  GOTO 136
               ELSE
                  DXTEST=DXDIFF
C PATRICK keep time in whole seconds when over 2sec
            IF (DELTAT.GE.2) THEN
               DXINT=AINT(DELTAT/2)
            ELSE
               DXINT=DELTAT/2
            ENDIF
                  GOTO 500
               ENDIF
            ELSE
               NEWSURF(I)=0.0
            ENDIF
         ENDIF
 135  CONTINUE
C
      TOTVOL=0.0
C
      DO 140,I=1,NCLASS
         TOTVOL=TOTVOL+NEWSURF(I)
 140  CONTINUE
C
      DO 145,I=1,NCLASS
         NEWSURF(I)=NEWSURF(I)*100/TOTVOL
 145  CONTINUE
C
      CALL SIZEPARM(NEWSURF,SELECT,SIZEFINE,NCLASS,SIZES)
      D84EST=SIZES(8)
C PATRICK for fixed transport layer thickness
 136  IF (DEFINT(5).EQ.2) THEN
         NEWACTIVE=LAYEREST
      ELSE
         LAYEREST=(LAYEREST+KACTIVE*D84EST)/2
         NEWACTIVE=KACTIVE*D84EST
      ENDIF
C END
C     Now to update the sediment info. for each bed layer.
C
      IF (NEWACTIVE.GT.MAXALTDEP(M)) THEN
         NEWDEP=NEWACTIVE
      ELSE
         NEWDEP=MAXALTDEP(M)
      ENDIF
C
      TOTSTORE=0.0
      IF (CHANGE.EQ.AGGRADING) THEN
         DO 210,I=1,NCLASS
            STORE(I)=((DELEV-(NEWACTIVE-THICKLAYER(M)))*EXCHSIZE(I))+
     +      (SUBTHICK(M)*SIZELAYER(2,M,I))
            TOTSTORE=TOTSTORE+STORE(I)
 210     CONTINUE
         DO 230,I=1,NCLASS
            SIZELAYER(2,M,I)=100*STORE(I)/TOTSTORE
 230     CONTINUE
      ENDIF
C PATRICK routine to update layer when using fixed transport layer
c thickness
      SUBTHICK(M)=SUBTHICK(M)+DELEV-(NEWACTIVE-THICKLAYER(M))
C
      IF (SUBTHICK(M).GT.(1.5*ACTSTART(M))) THEN
         DO 260,LAYER=5,3,-1
            DO 262,I=1,NCLASS
               SIZELAYER(LAYER,M,I)=SIZELAYER(LAYER-1,M,I)
 262        CONTINUE
 260     CONTINUE
         SUBTHICK(M)=SUBTHICK(M)-ACTSTART(M)
      ELSE IF (SUBTHICK(M).LT.0) THEN
         DO 270,LAYER=2,4
            DO 272,I=1,NCLASS
               SIZELAYER(LAYER,M,I)=SIZELAYER(LAYER+1,M,I)
 272        CONTINUE
 270     CONTINUE
         SUBTHICK(M)=SUBTHICK(M)+ACTSTART(M)
      ENDIF
C END
      DO 250,I=1,NCLASS
         SIZELAYER(1,M,I)=NEWSURF(I)
 250  CONTINUE
```

```
C
      SELECT(3)=CALC
      SELECT(6)=CALC
      SELECT(9)=CALC
      CALL SIZEPARM (NEWSURF,SELECT,SIZEFINE,NCLASS,SIZES)
      D165084ACT(2,M)=SIZES(6)
      D165084ACT(3,M)=SIZES(8)
      D165084ACT(1,M)=SIZES(3)
      D165084ACT(4,M)=SIZES(9)
      DGMACT(M)=SIZES(11)
C
      DO 350,I=1,NCLASS
         SIZEDATA(I)=SIZELAYER(2,M,I)
 350  CONTINUE
C
      CALL SIZEPARM (SIZEDATA,SELECT,SIZEFINE,NCLASS,SIZES)
      D165084SUB(2,M)=SIZES(6)
      D165084SUB(3,M)=SIZES(8)
      D165084SUB(1,M)=SIZES(3)
      D165084SUB(4,M)=SIZES(9)
C
      DO 360,I=1,NCLASS
         SIZEDATA(I)= QBSIZE(I,2)
 360  CONTINUE
C
      CALL SIZEPARM (SIZEDATA,SELECT,SIZEFINE,NCLASS,SIZES)
C
      D165084BLD(2,M)=SIZES(6)
      D165084BLD(3,M)=SIZES(8)
      D165084BLD(1,M)=SIZES(3)
      D165084BLD(4,M)=SIZES(9)
C
      DO 370,I=1,NCLASS
         BEDFRACT (M,I)=1000*QBFRACT(I,2)
 370  CONTINUE
C
      THICKLAYER(M)=NEWACTIVE
      MAXALTDEP(M)=NEWDEP
      QBEDLOAD(M)=QBED(2)
      VOLCH(1,M)=DELEV*WIDTH(2)
      BEDCH(1,M)=DELEV
      VOLCH(2,M)=VOLCH(2,M)+VOLCH(1,M)
      BEDCH(2,M)=BEDCH(2,M)+BEDCH(1,M)
C
 500  IF (INF(7).EQ.1  .AND.  DXTEST.EQ.DXDIFF) THEN
         WRITE (7,1111) M,INT(TTOT),DELTAT
         WRITE (8,776) M,AREAEST,LCALC,QBED(1),QBED(2),DELTAT,AREA
         DO 521,II=1,NCLASS
            WRITE (8,777) NEWSURF(II),SIZELAYER(1,M,II),EXCHSIZE(II),
     +         QBSIZE(II,1),QBSIZE(II,2)
 521     CONTINUE
         WRITE (8,776) M,DELEV,(DELEV+LAYEREST-THICKLAYER(M)),
     +   QBED(1),QBED(2),DELTAT,AREA
         JKJK=JKJK+1
      ENDIF
C
 1111 FORMAT (I2,2X,I6,2X,F7.2)
C
      END
C
C     *******************************************************************
      SUBROUTINE SIZEPARM(SIZEDATA,SELECT,SIZEFINE,NCLASS,SIZES)
C
      REAL SIZEDATA(25),SIZES(11),PCS(10),CUMPC,LOW,PHI,SIZEFINE(25),
     +LOWPHI,DMG,LDMG,DMED,PHIMED
C
      INTEGER SELECT(10),CALC
      PARAMETER (CALC=1)
C
      PCS(1)=5
      PCS(2)=10
      PCS(3)=16
      PCS(4)=25
      PCS(5)=35
      PCS(6)=50
      PCS(7)=65
      PCS(8)=84
      PCS(9)=90
      PCS(10)=95
C
      DO 100,I=1,10
         IF (SELECT(I).EQ.CALC) THEN
            CUMPC=0
            DO 20,J=1,NCLASS
               CUMPC=CUMPC+SIZEDATA(J)
               IF(CUMPC.GT.PCS(I)) THEN
                  LOW=CUMPC-SIZEDATA(J)
                  IF (J.EQ.1) THEN
                     LOWPHI=2*SIZEFINE(1)-SIZEFINE(2)
                  ELSE
                     LOWPHI=SIZEFINE(J-1)
                  ENDIF
                  PHI=LOWPHI+(PCS(I)-LOW)*(SIZEFINE(J)-LOWPHI)/
     +            (CUMPC-LOW)
                  SIZES(I)=2**PHI/1000
                  GOTO 100
               ENDIF
               IF (J.EQ.1  .AND.  CUMPC.GT.PCS(I))  SIZES(I)=0.0
 20         CONTINUE
         ENDIF
 100  CONTINUE
C
      LDMG=0
      PHIMED=(3*SIZEFINE(1)-SIZEFINE(2))/2
C
      DO 30,I=1,NCLASS
         DMED=2**PHIMED
         LDMG=LDMG+(SIZEDATA(I)*LOG(DMED))/100
         IF (I.LT.NCLASS) PHIMED=(SIZEFINE(I)+SIZEFINE(I+1))/2
 30   CONTINUE
C
      DMG=(EXP(LDMG))/1000
      SIZES(11)=DMG
C
      END
C
C     *******************************************************************
      SUBROUTINE BEDLOAD (HIDINGG,HIDINGS,TAUREF,BEDDATA,NUM,
     +PARKER,CASE,SIZEFINE,NCLASS,STRAINC,QBED,QBFRACT,ESLOPE,R,
     +WSWIDTH)
C
      REAL BEDDATA(25),DMED,DMG,DUMMY(25),ENSL,ESLOPE(250),
     +G,GG(25),GODI(25),HIDINGG,HIDINGS,HRAD,
     +LDMG,OMEGA,PARKER(36,3),PHIMED,PHISGO,QBED(6),QBFRACT(25,6),
```

```
     + R(250) ,RHO, SIZEFINE(25) , SSI ,STRAINC ,TAUREF ,UNITQB ,USTAR,
     +WIDTH, WISTAR(25) ,WSWIDTH(250)
C
      INTEGER CASE,NUM
C
      RHO=2.65
      G=9.81
      SSI=RHO-1
      WIDTH=WSWIDTH(NUM)
      HRAD=R (NUM)
      ENSL=ESLOPE (NUM)
      LDMG=0
      PHIMED=(3*SIZEFINE(1)-SIZEFINE(2))/2
C
      DO 20 ,I=1 ,NCLASS
         DMED=2**PHIMED
         LDMG=LDMG+(BEDDATA(I)*LOG(DMED))/100
         IF (I.LT.NCLASS) PHIMED=(SIZEFINE(I)+SIZEFINE(I+1))/2
 20   CONTINUE
C
      DMG=(EXP(LDMG))/1000
      USTAR=(G*ESLOPE(NUM)*R(NUM))**0.5
      PHISGO=(USTAR**2)/(SSI*G*DMG*TAUREF)
      CALL OMEGAEST(BEDDATA,DMG,NUM, PHISGO ,PARKER, SIZEFINE ,NCLASS,
     +OMEGA,STRAINC)
C
C THIS LINE KEEPS OMEGA>1 AT ALL TIMES
      IF (OMEGA.LT.0.00000001) OMEGA=0.00000001
C *************************************
      PHIMED=(3*SIZEFINE(1)-SIZEFINE(2))/2
      UNITQB=0.0
C
      DO 40 ,I=1 ,NCLASS
         DMED=2**PHIMED/1000
         IF (DMED.LT.0.002) THEN
            GODI(I)=((0.002/DMG)**(HIDINGG-HIDINGS))*
     +      ((DMED/DMG)**HIDINGS)
         ELSE
            GODI(I)=(DMED/DMG)**HIDINGG
         ENDIF
         DUMMY(I)=OMEGA*PHISGO*GODI(I)
         IF (DUMMY(I).LT.1.00) THEN
            GG(I)=DUMMY(I)**14.2
         ELSE IF (DUMMY(I).GT.1.59) THEN
            GG(I)=5474*((1-(0.853/DUMMY(I)))**4.5)
         ELSE
            GG(I)=EXP(14.2*(DUMMY(I)-1)-9.28*((DUMMY(I)-1)**2))
         ENDIF
         WISTAR(I)=0.00218*GG(I)
         QBFRACT(I,CASE)=WISTAR(I)*(USTAR**3)*0.01*BEDDATA(I)/(SSI*G)
         IF (I.LT.NCLASS) PHIMED=(SIZEFINE(I)+SIZEFINE(I+1))/2
         UNITQB=UNITQB+QBFRACT(I,CASE)
 40   CONTINUE
C
      QBED(CASE)=UNITQB*WIDTH
C
      DO 50 ,J=1 ,NCLASS
         QBFRACT(J,CASE)=QBFRACT(J,CASE)*WIDTH
 50   CONTINUE
C
      END
C
C     ******************************************************************
      SUBROUTINE OMEGAEST(BEDDATA,DMG,NUM,PHISGO,PARKER,SIZEFINE ,
     +NCLASS,OMEGA,STRAINC)
C
      REAL BEDDATA(25) ,COEFF(3,3) ,COEFF2(3,3) ,
     +DMED,DET,DET2,DETPRIME(3) ,DETPRIME2(3) ,INHOM(3) ,INHOM2(3) ,
     +OMEGA,OMEGAOAK,PARKER(36,3) ,PHIMED,
     +SIGOAK, SIGPHI, SIGPHI2, SIZEFINE(25) ,
     +SOLN(3) ,SOLN2(3) ,STORE(3) ,STORE2(3) ,STRAINC ,Z
C
      INTEGER NCLASS,NUM
C
      SIGPHI2=0.0
      PHIMED=(3*SIZEFINE(1)-SIZEFINE(2))/2
C
      DO 20 ,I=1 ,NCLASS
         DMED=2**PHIMED/1000
         Z=2
         SIGPHI2=SIGPHI2 + BEDDATA(I)*0.01*((LOG(DMED/DMG)/LOG(Z))**2)
         IF (I.LT.NCLASS) PHIMED=(SIZEFINE(I)+SIZEFINE(I+1))/2
 20   CONTINUE
C
      SIGPHI=SIGPHI2**0.5
C
      IF (PHISGO.LT.0.6684) THEN
         SIGOAK=0.8157
         OMEGAOAK=1.011
      ELSE
         DO 40 ,J=2 ,36
            IF (PHISGO.LT.PARKER(J,1)) THEN
               DO 50 ,K=1 ,3
                  DO 60 ,L=3 ,1 ,-1
                     COEFF(K,(4-L))=PARKER((J+K-2),1)**L
                     COEFF2(K,(4-L))=PARKER((J+K-2),1)**L
 60               CONTINUE
 50            CONTINUE
               DO 70 ,K=1 ,3
                  INHOM(K)=PARKER((J+K-2),2)
                  INHOM2(K)=PARKER((J+K-2),3)
 70            CONTINUE
               CALL DETERMINANT (COEFF,DET)
               CALL DETERMINANT (COEFF2,DET2)
               DO 80 ,K=1 ,3
                  DO 90 ,L=1 ,3
                     IF (K.GE.2) THEN
                        COEFF(L,(K-1))=STORE(L)
                        COEFF2(L,(K-1))=STORE2(L)
                     ENDIF
                     STORE(L)=COEFF(L,K)
                     COEFF(L,K)=INHOM(L)
                     STORE2(L)=COEFF2(L,K)
                     COEFF2(L,K)=INHOM2(L)
 90               CONTINUE
                  CALL DETERMINANT (COEFF,DETPRIME(K))
                  CALL DETERMINANT (COEFF2,DETPRIME2(K))
 80            CONTINUE
               GOTO 45
            ENDIF
 40      CONTINUE
 45      DO 100 ,L=1 ,3
            SOLN(L)=DETPRIME(L)/DET
            SOLN2(L)=DETPRIME2(L)/DET2
```

```
 100     CONTINUE
         OMEGAOAK=SOLN(1)*(PHISGO**3)+SOLN(2)*(PHISGO**2)+SOLN(3)*
     +   PHISGO
         SIGOAK=SOLN2(1)*(PHISGO**3)+SOLN2(2)*(PHISGO**2)+SOLN2(3)*
     +   PHISGO
       ENDIF
C
C   THIS IS MODIFIED STRAINING FUNCTION
       OMEGA=1+((SIGPHI/SIGOAK)**STRAINC)*(OMEGAOAK-1)
C
       END
C
C      ******************************************************************
       SUBROUTINE WILCOCK (BEDDATA,CASE,D50SURF,NUM,SIZEFINE,
      +NCLASS,QBED,QBFRACT,ESLOPE,R,WSWIDTH)
C
       REAL BEDDATA(25),D50SURF,DMED,DMG,ENSL,ESLOPE(250),FS,
      +G,HRAD,LDMG,PHI(25),PHIMED,QBED(6),QBFRACT(25,6),R(250),
      +RHO,SIZEFINE(25),SSI,TAURM,UNITQB,USTAR,WIDTH,WISTAR(25),
      +WSWIDTH(250)
C
       INTEGER CASE,NUM,NCLASS
C
       RHO=2.65
       G=9.81
       SSI=RHO-1
       WIDTH=WSWIDTH(NUM)
       HRAD=R(NUM)
       ENSL=ESLOPE(NUM)
       LDMG=0
       FS=0
C
       DO 10,I=1,NCLASS
         IF (SIZEFINE(I).LT.1.01) FS=FS+BEDDATA(I)
 10    CONTINUE
C
       PHIMED=(3*SIZEFINE(1)-SIZEFINE(2))/2
C
       DO 20,I=1,NCLASS
         DMED=2**PHIMED
         LDMG=LDMG+(BEDDATA(I)*LOG(DMED))/100
         IF (I.LT.NCLASS) PHIMED=(SIZEFINE(I)+SIZEFINE(I+1))/2
 20    CONTINUE
C
       DMG=(EXP(LDMG))/1000
       USTAR=(G*ENSL*HRAD)**0.5
       TAURM=0.021+0.015*EXP(-0.2*FS)
       PHIMED=(3*SIZEFINE(1)-SIZEFINE(2))/2
       UNITQB=0.0
C
       DO 40,I=1,NCLASS
         DMED=2**PHIMED/1000
C        PHI(I)=(USTAR**2)/(TAURM*SSI*G*D50SURF)/
C       +(DMED/D50SURF)**(0.67/(1+EXP(1.5-DMED/DMG)))
C This version matches TRIB; DMG not D50SURF used x2
         PHI(I)=(USTAR**2)/(TAURM*SSI*G*DMG)/
      +  (DMED/DMG)**(0.67/(1+EXP(1.5-DMED/DMG)))
         IF (PHI(I).LT.1.35) THEN
           WISTAR(I)=0.002*PHI(I)**7.5
         ELSE
           WISTAR(I)=14*(1-(0.894/(PHI(I)**0.5)))**4.5
         ENDIF
         QBFRACT(I,CASE)=WISTAR(I)*(USTAR**3)*0.01*BEDDATA(I)/(SSI*G)
         IF (I.LT.NCLASS) PHIMED=(SIZEFINE(I)+SIZEFINE(I+1))/2
         UNITQB=UNITQB+QBFRACT(I,CASE)
 40    CONTINUE
C
       QBED(CASE)=UNITQB*WIDTH
C
       DO 50,J=1,NCLASS
         QBFRACT(J,CASE)=QBFRACT(J,CASE)*WIDTH
 50    CONTINUE
C
       END
C
C      ******************************************************************
       SUBROUTINE DETERMINANT(M,DET)
C
       REAL M(3,3),DET
C
       DET=M(1,1)*M(2,2)*M(3,3) - M(1,1)*M(2,3)*M(3,2) +
      +M(1,2)*M(2,3)*M(3,1) - M(1,2)*M(2,1)*M(3,3) +
      +M(1,3)*M(2,1)*M(3,2) - M(1,3)*M(2,2)*M(3,1)
C
       END
C
C      ******************************************************************
       SUBROUTINE EINSTEIN(BEDDATA,NUM,CASE,SIZEFINE,QBED,
      +QBFRACT,RHOSED,SS,KVISC,NCLASS,ESLOPE,WSWIDTH,R)
C
C      VARIABLE DEFINITIONS
C
C    BEDDATA   Array of % in each size class
C    BBX2      Array of (beta/betax)^2 values
C    BETAX     Array of betax values
C    DI        Median size of size class [m]
C    DRATIO    Dummy variable (=Di/XL)
C    Dxx       (xx=65,35) size parameter value [m]
C    ENSL      Energy slope [m/m]
C    GBED      Bedload transport rate [kg/m/s]
C    GBFRACT   Fractional rates in i size classes [kg/m/s]
C    HF        Hiding factor for size class i
C    HRAD      Hydraulic radius based on selected roughness equ.
C    KSAPP     Apparent roughness diameter [m]
C    KSSUB     =D65/SUB
C    KVSIC     Kinematic viscosity [m2/s]
C    PHIS      Array of phi* values for each size fraction
C    PSI       Psi(i), for each size fraction
C    PSIS      Psi*(i) for each size fraction
C    QBED      volume transport rates [m3/s]
C    QBFRACT   Fractional volume transport rates in each class [m3/s]
C    R1        R' (grain component of hyd. radius) [m]
C    RATIO     Dummy variable
C    RHOSED    Sediment density [kg/m3]
C    RHOW      Water density [kg/m3]
C    SELECT    Control variable for Size parameter calculation
C    SIZES     Size parameter values [m]
C    SIZEFINE  Upper end of each size class for gsd, in -phi
C              units
C    SS        Specific gravity (rhosed/rho)
C    SUB       Laminar sub-layer thickness [m]
C    US1       Grain component of shear velocity [m/s]
C    WIDTH     flow width [m]
C    XCORR     correction for smooth flow (from Fig. 4)
```

```
C     XL          array of ref. grain sizes (smallest affected
C                 by turbulent flow) [m]
C     Y           array of values from Fig. 8, for class i
C
      REAL BBX2(25),BEDDATA(25),BETAX(25),
     +DI,DRATIO,D65,D35,ENSL,ESLOPE(250),GBED,GBFRACT(25),
     +HF(25),HRAD,KSAPP,KSSUB,KVISC,
     +PHIS(25),PSIS(25),PSI(25),QBED(6),QBFRACT(25,6),
     +R(250),RATIO,RHOSED,RHOW,R1,SIZEFINE(25),SIZES(11),SS,SUB,US1,
     +WIDTH,WSWIDTH(250),XCORR,XL(25),Y(25)
C
      INTEGER  CASE,NCLASS,NUM,SELECT(10)
C
      G=9.81
      HRAD=R(NUM)
      WIDTH=WSWIDTH(NUM)
      ENSL=ESLOPE(NUM)
C  Assume that hydraulic radius using roughness equation covers
C  grain roughness only
      R1=HRAD
C  CALCULATE D35, D65
C
      DO 20,I=1,10
         SELECT(I)=0
 20   CONTINUE
C
      SELECT(5)=1
      SELECT(7)=1
      CALL SIZEPARM(BEDDATA,SELECT,SIZEFINE,NCLASS,SIZES)
      D65=SIZES(7)
      D35=SIZES(5)
      GBED=0
      US1=(ENSL*G*R1)**0.5
      SUB=11.6*KVISC/US1
      KSSUB=D65/SUB
C   DETERMINE WHAT (IF ANY) CORRECTION IS NEEDED FOR NON-ROUGH
C   FLOW
      CALL FIG4(KSSUB,XCORR)
      KSAPP=D65/XCORR
C
      DO 50,I=1,NCLASS
         IF (I.EQ.1) THEN
            DI=0.001*2**((3*SIZEFINE(1)-SIZEFINE(2))/2)
         ELSE
            DI=0.001*2**((SIZEFINE(I)+SIZEFINE(I-1))/2)
         ENDIF
         PSI(I)=(SS-1)*DI/(R1*ENSL)
         RATIO=KSAPP/SUB
         IF (RATIO.GT.1.80) THEN
            XL(I)=0.77*KSAPP
         ELSE
            XL(I)=1.39*SUB
         ENDIF
         DRATIO=DI/XL(I)
C  Determine hiding factor and Y value
         CALL FIG7 (DRATIO,HF(I))
         CALL FIG8 (KSSUB,Y(I))
         BETAX(I)=LOG10(10.6*XL(I)/KSAPP)
         BBX2(I)=(1.025/BETAX(I))**2.0
C  THIS LINE TO SUPPRESS HIDING
         HF(I)=1
C
C ******************************************
            PSIS(I)=HF(I)*Y(I)*BBX2(I)*PSI(I)
C  Interpolate phi* from Figure 10
            CALL FIG10(PSIS(I),PHIS(I))
            RHOW=1000
            GBFRACT(I)=PHIS(I)*BEDDATA(I)*0.01*RHOW*SS*(G**0.5)*
     +      (DI**1.5)*(SS-1)**0.5
            GBED=GBED+GBFRACT(I)
 50   CONTINUE
C
      QBED(CASE)=GBED*WIDTH/RHOSED
C
      DO 60,I=1,NCLASS
         QBFRACT(I,CASE)=GBFRACT(I)*WIDTH/RHOSED
 60   CONTINUE
C
      END
C
C     *****************************************************************
      SUBROUTINE FIG4(X,XCORR)
C
      REAL X,XCORR
C
      IF (X.LE.0.40) XCORR=1.769*LOG10(X/0.8)
      IF (X.GT.0.40.AND.X.LE.0.56)XCORR=1.495*LOG10(X/0.059)
      IF (X.GT.0.56.AND.X.LE.0.76)XCORR=0.920*LOG10(X/0.0145)
      IF (X.GT.0.76.AND.X.LE.0.96)XCORR=0.292*LOG10(X/0.0000029)
      IF (X.GT.0.96.AND.X.LE.1.35)XCORR=0.277*LOG10(632000/X)
      IF (X.GT.1.35.AND.X.LE.3.00)XCORR=1.115*LOG10(34.4/X)
      IF (X.GT.3.00.AND.X.LE.4.00)XCORR=0.725*LOG10(128/X)
      IF (X.GT.4.00.AND.X.LE.6.70)XCORR=0.399*LOG10(2160/X)
      IF (X.GT.6.70) XCORR=1.0
C
      END
C
C     *****************************************************************
      SUBROUTINE FIG5 (PSI1,UUS11)
C
      REAL PSI1,UUS11
C
      IF (PSI1.LE.1.0) UUS11=40.0*PSI1**(-1.288)
      IF (PSI1.GT.1.0 .AND. PSI1.LE.2.0) UUS11=40.0*PSI1**(-0.982)
      IF (PSI1.GT.2.0 .AND. PSI1.LE.4.0) UUS11=31.1*PSI1**(-0.618)
      IF (PSI1.GT.4.0 .AND. PSI1.LE.8.0) UUS11=26.0*PSI1**(-0.486)
      IF (PSI1.GT.8.0) UUS11=21.4*PSI1**(-0.394)
C
      END
C
C     *****************************************************************
      SUBROUTINE FIG7 (DR,HF)
C
      REAL DR,HF
C
      IF (DR.LE.0.20) HF=(DR/1.09)**(-2.088)
      IF (DR.GT.0.20.AND.DR.LE.0.40) HF=(DR/0.877)**(-2.402)
      IF (DR.GT.0.40.AND.DR.LE.0.65) HF=(DR/0.832)**(-2.582)
      IF (DR.GT.0.65.AND.DR.LE.0.80) HF=(DR/0.990)**(-1.515)
      IF (DR.GT.0.80.AND.DR.LE.1.00) HF=(DR/1.185)**(-0.826)
      IF (DR.GT.1.00.AND.DR.LE.1.45) HF=(DR/1.450)**(-0.375)
      IF (DR.GT.1.45) HF=1.0
C
      END
```

```
C
C     ******************************************************************
      SUBROUTINE FIG8 (KSSUB,Y)
C
      REAL KSSUB,Y
C
      IF (KSSUB.LE.0.66) Y=(KSSUB/1.005)**1.178
      IF (KSSUB.GT.0.66.AND.KSSUB.LE.0.84) Y=(KSSUB/1.104)**(0.957)
      IF (KSSUB.GT.0.84.AND.KSSUB.LE.1.10) Y=(KSSUB/1.94)**(0.31)
      IF (KSSUB.GT.1.10.AND.KSSUB.LE.1.30) Y=(KSSUB/0.475)**(-0.208)
      IF (KSSUB.GT.1.30.AND.KSSUB.LE.2.20) Y=(KSSUB/0.93)**(-0.633)
      IF (KSSUB.GT.2.20.AND.KSSUB.LE.3.10) Y=(KSSUB/0.278)**(-0.266)
      IF (KSSUB.GT.3.10) Y=0.53
C
      END
C
C     ******************************************************************
      SUBROUTINE FIG10 (PS,PH)
C
      REAL PS,PH
C
      IF (PS.LE.0.77) PH=(7.56/PS)**1.01
C
      IF (PS.GT.0.77.AND.PS.LE.2.12) PH=(5.35/PS)**1.19
      IF (PS.GT.2.12.AND.PS.LE.4.1) PH=(4.1/PS)**1.67
      IF (PS.GT.4.1.AND.PS.LE.6.1) PH=(4.1/PS)**2.3
      IF (PS.GT.6.1.AND.PS.LE.11.) PH=(4.6/PS)**3.23
      IF (PS.GT.11.AND.PS.LE.16.7) PH=(5.66/PS)**4.26
      IF (PS.GT.16.7.AND.PS.LE.22.5) PH=(9.28/PS)**7.81
      IF (PS.GT.22.5) PH=(13.04/PS)**12.66
C
      END
C
C PATRICK***************************************************************
      SUBROUTINE ACKERS (BEDDATA,CASE,D165084SUB,ESLOPE,EQUCODE,NUM,
     +MEANDEP,NCLASS,SIZEFINE,Q,QBED,QBFRACT,R,WSWIDTH)
C      calculate sediment transport with the Ackers and White's formula
C
      REAL A,ALFA,BEDDATA(25),C,
     +D165084SUB(4,250),DEPTH,DGR,DISCHARGE,DMED,
     +ENSL,ESLOPE(250),FGR,
     +G,GGR,HRAD,KVISC,MEANDEP(250),MM,PHIMED,R(250),RHO,
     +Q(250),QBED(6),QBFRACT(25,6),SIZEFINE(25),SSI,TEXP,
     +UBAR,UNITQB,USTAR,WIDTH,WSWIDTH(250)
C
      INTEGER CASE,EQUCODE,NCLASS,NUM
C
      ALFA=10
      DEPTH=MEANDEP(NUM)
      DISCHARGE=Q(NUM)
      ENSL=ESLOPE(NUM)
      HRAD=R(NUM)
      G=9.81
      KVISC=0.0000013
      RHO=2.65
      UNITQB=0
      WIDTH=WSWIDTH(NUM)
      PHIMED=(3*SIZEFINE(1)-SIZEFINE(2))/2
      SSI=RHO-1
      UBAR=DISCHARGE/(DEPTH*WIDTH)
      USTAR=(G*ENSL*HRAD)**0.5
C
      DO 20,I=1,NCLASS
        DMED=2**PHIMED/1000
C determine value of dimensionless grain diameter (DGR)
        DGR=DMED*(G*SSI/(KVISC**2))**(0.333)
C determine values of n(TEXP),A,m,C from dgr
        IF (DGR.LT.60) THEN
          TEXP=1-0.56*LOG10(DGR)
          A=0.23/DGR**0.5+0.14
          IF (EQUCODE.EQ.4 .OR. EQUCODE.EQ.6) THEN
            MM=9.66/DGR+1.34
            C=10**(2.86*LOG10(DGR)-(LOG10(DGR))**2-3.53)
            IF (EQUCODE.EQ.6) THEN
              DA=D165084SUB(2,NUM)*(1.62*((D165084SUB(3,NUM)
     +           /D165084SUB(1,NUM))**0.5)**(-0.55))
              A=(0.4*((DA/DMED)**0.5)+0.6)*A
            ENDIF
          ELSE IF (EQUCODE.EQ.5) THEN
            MM=6.83/DGR+1.67
            C=10**(2.79*LOG10(DGR)-(0.98*LOG10(DGR))**2-3.46)
          ENDIF
        ELSE
          TEXP=0
          A=0.17
          C=0.025
          IF (EQUCODE.EQ.4 .OR. EQUCODE.EQ.6) THEN
            MM=1.5
            IF (EQUCODE.EQ.6) THEN
              DA=D165084SUB(2,NUM)*(1.62*(D165084SUB(3,NUM)
     +           /D165084SUB(1,NUM)**0.5)**(-0.55))
              A=(0.4*((DA/DMED)**0.5)+0.6)*A
            ENDIF
          ELSE IF (EQUCODE.EQ.5) THEN
            MM=1.78
          ENDIF
        ENDIF
C compute the value of particle mobility (FGR)
        FGR=(USTAR**TEXP)*((G*DMED*SSI)**(-0.5))*
     +  ((UBAR/((32**0.5)*LOG10(ALFA*DEPTH/DMED)))**(1-TEXP))
C determine the value of GGR
        IF (FGR.GT.A) THEN
          GGR=C*((FGR/A-1)**MM)
        ELSE
          GGR=0
        ENDIF
C convert Ggr into sediment concentration
        QBFRACT(I,CASE)=(GGR*DMED*RHO*0.01*BEDDATA(I))/
     +  DEPTH*((UBAR/USTAR)**TEXP)
        UNITQB=UNITQB+QBFRACT(I,CASE)
        IF (I.LT.NCLASS) PHIMED=(SIZEFINE(I)+SIZEFINE(I+1))/2
C     WRITE (*,995) I,QBFRACT(I,CASE)
20    CONTINUE
C convert concentration into volume metric transport
      QBED(CASE)=UNITQB*DISCHARGE/RHO
C
      DO 30,J=1,NCLASS
        QBFRACT(J,CASE)=QBFRACT(J,CASE)*DISCHARGE/RHO
C     WRITE (59,995) J,QBFRACT(J,CASE)
30    CONTINUE
C
C     WRITE (*,999) NUM,QBED(CASE)
C995  FORMAT ('QBFRACT(',I2,'): ',F10.6)
C999  FORMAT ('XSN',I3,/,'QBED(CASE): ',F10.6)
```

```
C       PAUSE
      END
C
C     ******************************************************************
      SUBROUTINE DISTRIB (N,NEWSURV,SURV,TREAL,BEDCH,WATSURF)
C
      INTEGER I,N,XSN
C
      REAL BEDCH(2,125),NEWSURV(100,500),SURV(100,500),TREAL,
     +WATSURF(250)
C
      DO 100,XSN=1,N
         DO 50,I=1,100
            IF (SURV(I,(2*XSN)).GT.9000) THEN
               GOTO 90
            ELSE
               IF (TREAL.LT.1.1) THEN
                  NEWSURV(I,((2*XSN)-1))=SURV(I,((2*XSN)-1))
                  IF (SURV(I,(2*XSN)).LT.WATSURF(XSN)) THEN
                     NEWSURV(I,(2*XSN))=SURV(I,(2*XSN))+BEDCH(1,XSN)
                  ELSE
                     NEWSURV(I,(2*XSN))=SURV(I,(2*XSN))
                  ENDIF
               ELSE
                  IF (NEWSURV(I,(2*XSN)).LT.WATSURF(XSN)) THEN
                     NEWSURV(I,(2*XSN))= NEWSURV(I,(2*XSN))+BEDCH(1,XSN)
                  ELSE
                     NEWSURV (I,(2*XSN))= NEWSURV (I,(2*XSN))
                  ENDIF
               ENDIF
            ENDIF
50       CONTINUE
90       NEWSURV (I,((2*XSN)-1))=9999
         NEWSURV (I,(2*XSN))=9999
100   CONTINUE
C
      END
C
C     ******************************************************************
      SUBROUTINE COURANT (N,DELTAT,DISTANCE,BEDCH,D165084ACT,
     +ESLOPE,QBEDLOAD,WSWIDTH,DELTATC,THICKLAYER,DEFINT,SCXS)
C
C PATRICK THICKLAYER added at real and DEFINT at integer
      REAL ALPHA,BEDCH(2,125),
     +DELTAT,DELTATC,DISTANCE(250),DTHAT,DTNEW,DT1,DT2,DZTOL,
     +D165084ACT(4,250),ESLOPE(250),
     +LAMBDA,QBEDLOAD(125),SAFETY,THICKLAYER(125),UNITQB,WSWIDTH(250)
C
      INTEGER CH,DEFINT(10),N,SCXS(25,5,2),XSN
C
      LAMBDA=0.3
      ALPHA=5.5
      SAFETY=1.1
      CH=1
C
      DO 100,XSN=1,N
         UNITQB=QBEDLOAD(XSN)/WSWIDTH(XSN)
         IF (UNITQB.LT.0.0000000001) UNITQB=0.0000000001
C PATRICK no clac of COURANT condition for first XS of section
         IF (XSN.EQ.SCXS(CH,1,2)) THEN
            CH=CH+1
            GOTO 100
         ENDIF
C END
C     Park and Jain (1986) equation
         IF (XSN.LT.N) DX=(DISTANCE(XSN+1)-DISTANCE(XSN))
         DT1=((1-LAMBDA)*3*ESLOPE(XSN)*(DX**2)/(2*ALPHA*UNITQB))
     +   /SAFETY
         IF (XSN.EQ.1) DTNEW=DT1
         IF (DT1.LT.DTNEW) DTNEW=DT1
C     Parker equation
         DT2=(D165084ACT(3,XSN)*(1-LAMBDA)*DX/UNITQB)/SAFETY
         IF (DT2.LT.DTNEW) DTNEW=DT2
C PATRICK vertical restriction based on layer thickness for constant
C  layer thickness option
         IF (DEFINT(5).NE.2) THEN
            DZTOL=D165084ACT(3,XSN)/100
         ELSE
            DZTOL=THICKLAYER(XSN)/100
         ENDIF
C END
         IF (ABS(BEDCH(1,XSN)).GT.0.0000001) THEN
            DTHAT=(DZTOL*DELTAT)/(ABS(BEDCH(1,XSN))*SAFETY)
         ELSE
            DTHAT=DELTAT*100
         ENDIF
         IF (DTHAT.LT.DTNEW) DTNEW=DTHAT
100   CONTINUE
C
      DELTATC=5*(AINT(DTNEW/5))
      IF (DELTATC.LT.5) DELTATC=1
C
      END
C
C     ******************************************************************
      SUBROUTINE ACTESTIMATE(K,ACTMETHOD,LEST,LCALC,EST,CALC,DIFF)
C
      INTEGER ACTMETHOD,ADD,K,NOROOT,SUBTRACT,SUCCSUB
C
      REAL CALC(2),DIFF(2),EST(2),LCALC,LEST
C
      PARAMETER (SUBTRACT=-1,ADD=1,SUCCSUB=0,NOROOT=2)
C
      IF (K.EQ.1) THEN
         EST(1)=LEST
         CALC(1)=LCALC
         DIFF(1)=LCALC-LEST
         LEST=(LCALC+LEST)/2
      ELSE IF(K.EQ.2) THEN
         EST(2)=LEST
         CALC(2)=LCALC
         DIFF(2)=LCALC-LEST
         IF(DIFF(1).GT.0.0) THEN
            IF (DIFF(2).GT.DIFF(1)) THEN
               ACTMETHOD=SUBTRACT
            ELSE
               ACTMETHOD=SUCCSUB
            ENDIF
         ELSE
            IF (ABS(DIFF(2)).GT.ABS(DIFF(1))) THEN
               ACTMETHOD=ADD
            ELSE
               ACTMETHOD=SUCCSUB
            ENDIF
```

```
            ENDIF
         ENDIF
C
      IF  (K.GE.2)  THEN
         EST(2)=EST(1)
         CALC(2)=CALC(1)
         EST(1)=LEST
         CALC(1)=LCALC
         DIFF(1)=CALC(1)-EST(1)
         DIFF(2)=CALC(2)-EST(2)
         IF  (ACTMETHOD.EQ.SUCCSUB)  THEN
            LEST=LCALC
         ELSE IF  (ACTMETHOD.EQ.ADD)  THEN
            IF  (LCALC.GT.LEST)  THEN
               LEST=(EST(2)*LCALC-CALC(2)*LEST)/
     +         (LCALC-CALC(2)+EST(2)-LEST)
            ELSE
               LEST=LEST+ABS(LEST-LCALC)
            ENDIF
         ELSE
            IF  (LCALC.LT.LEST)  THEN
               LEST=(LEST*CALC(2)-LCALC*EST(2))/
     +         (CALC(2)-LCALC-EST(2)+LEST)
            ELSE
               LEST=LEST-ABS(LEST-LCALC)
            ENDIF
         ENDIF
      ENDIF
C
      IF  (K.GE.3)  THEN
         IF  (DIFF(2)*DIFF(1).GT.0.0  .AND.  ABS(DIFF(1)).GT.
     +   ABS(DIFF(2)))  ACTMETHOD=NOROOT
      ENDIF
C
      END
C
C     ******************************************************************
      SUBROUTINE  TRACINIT  (TRACERS,TPOS,NTRAC,TSTART,TREC,THROPUT)
C
      REAL   SIZE,THROPUT,TPOS,TRACERS  (500,5),TREC,TSTART
C
      INTEGER  LONUMBER,NFRACT,NTRAC,NUMBER,TOTNUMBER
C
      TOTNUMBER=1
      NTRAC=0
      READ  (5,*)  TPOS,NFRACT,TSTART
      READ  (5,*)  TREC,THROPUT
      TREC=TREC*60
C
      DO  100,I=1,NFRACT
         READ  (5,*)  SIZE,CODE,LONUMBER,NUMBER
         DO  110,J=1,NUMBER
            TRACERS  (TOTNUMBER,1)=CODE
            TRACERS  (TOTNUMBER,2)=J
            TRACERS  (TOTNUMBER,3)=SIZE
            TRACERS  (TOTNUMBER,4)=TPOS
            TRACERS  (TOTNUMBER,5)=0
            TOTNUMBER=TOTNUMBER+1
 110     CONTINUE
         NTRAC=NTRAC+NUMBER
 100  CONTINUE
C
      OPEN  (16,FILE='TRSTART.TXT')
C
      DO  555,JJ=1,NTRAC
         WRITE  (16,560)  (TRACERS(JJ,K),K=1,5)
 555  CONTINUE
C
 560  FORMAT  (5(1X,F9.3))
      CLOSE(16)
C
      END
C
C     ******************************************************************
      SUBROUTINE  TRACING(TRACERS,TPOS,NTRAC,THROPUT,DELTAT,BEDFRACT,
     +SIZELAYER,THICKLAYER,DISTANCE,WSWIDTH,QBEDLOAD)
C
      REAL  BEDFRACT(125,25),DELTAT,DISTANCE(250),FI,LA,
     +PHITRAC,PI,PRMOVE,PROPDIST,PRSTOP,QBED,QBEDLOAD(125),QBFI1,QBFI2,
     +SIZELAYER(5,125,25),THICKLAYER(125),THROPUT,TPOS,TRACERS  (500,5),
     +TWO,WIDTH,WIDTH1,WIDTH2,WSWIDTH(250),XDIST
C
      INTEGER  ISTOP,ITRAC,IXS,UXS(500)
C
      DOUBLE  PRECISION  RANDOM,RNUM(5)
C
      TWO=2
C
      DO  100,I=1,NTRAC
         DO  110,IXS=1,125
            IF  (TRACERS(I,4).LT.DISTANCE(IXS))  THEN
               UXS(I)=IXS-1
               GOTO  100
            ENDIF
 110     CONTINUE
 100  CONTINUE
C
      CALL  DATE_TIME_SEED@
C
      DO  200,I=1,NTRAC
         PHITRAC=LOG10(TRACERS(I,3))/LOG10(TWO)
         ITRAC=INT(2*PHITRAC)-1
         XDIST=DISTANCE(UXS(I)+1)-DISTANCE(UXS(I))
         PROPDIST=(TRACERS(I,4)-DISTANCE(UXS(I)))/XDIST
         QBED=QBEDLOAD(UXS(I))+
     +   PROPDIST*(QBEDLOAD(UXS(I)+1)-QBEDLOAD(UXS(I)))
         WIDTH1=WSWIDTH(UXS(I))
         WIDTH2=WSWIDTH(UXS(I)+1)
         WIDTH=WIDTH1+PROPDIST*(WIDTH2-WIDTH1)
         QBED=QBED/WIDTH
         PI=BEDFRACT(UXS(I),ITRAC)+
     +   PROPDIST*(BEDFRACT(UXS(I)+1,ITRAC)-BEDFRACT(UXS(I),ITRAC))
         PI=100*(0.001*PI/WIDTH)/QBED
         FI=SIZELAYER(1,UXS(I),ITRAC)+PROPDIST*
     +   (SIZELAYER(1,UXS(I)+1,ITRAC)-SIZELAYER(1,UXS(I),ITRAC))
         LA=THICKLAYER(UXS(I))+PROPDIST*
     +   (THICKLAYER(UXS(I)+1)-THICKLAYER(UXS(I)))
         PRMOVE=(PI/FI)*(QBED*DELTAT*(1-THROPUT))/LA
         RNUM(1)=(RANDOM()**2)**0.5
         IF  (PRMOVE.GT.RNUM(1))  THEN
            DO  210,ISTOP=1,100
               TRACERS(I,4)=TRACERS(I,4)+1
               RNUM(1)=(RANDOM()**2)**0.5
               QBFI1=BEDFRACT(UXS(I)+1,ITRAC)
```

```
                  QBFI2=BEDFRACT(UXS(I),ITRAC)
                  IF (QBFI1.LT.QBFI2) THEN
                     PRSTOP=THROPUT+((QBFI2-QBFI1)/QBFI2)*(1-THROPUT)
                  ELSE
                     PRSTOP=THROPUT
                  ENDIF
                  IF (RNUM(1).LT.PRSTOP) GOTO 200
210            CONTINUE
            ENDIF
200   CONTINUE
C
      END
C
C     ******************************************************************
      SUBROUTINE INITIALISE (RIVER,OPERATOR,RUNCODE,INFILE,QHFILE,
     +QTYPE,DATE,ENDDATE,N,NSECT,NTOT,SCXS,HTYPE,HCHANGE,HYEAR,
     +WLDFILE,TIDE)
C This routine accesses the basic initialisation file, and
c allows the operator to confirm names for all input files.
      CHARACTER RIVER*20,OPERATOR*20,RUNCODE*8,INFILE(3)*12,QHFILE*62,
     +WLDFILE*62
C
      INTEGER CHOICE,DATE(7),ENDDATE(3),I,N,NSECT,NTOT,QTYPE,
     +SCXS(25,5,2),HTYPE,HYEAR
C
      REAL HCHANGE,TIDE
C
      OPEN (99,FILE='SEDFILES.INI')
C PATRICK read (path)names of *.wld and *.qdt files
      READ (99,'(A)') (INFILE(J),J=1,3),WLDFILE,QHFILE
      CLOSE (99)
      OPEN (5,FILE=INFILE(1))
      READ (5,'(A)') RIVER,OPERATOR,RUNCODE
      CALL CLEAR_SCREEN@
      WRITE (*,800)
      WRITE (*,805) RIVER,OPERATOR
      WRITE (*,810) INFILE(1)
      WRITE (*,820) INFILE(2)
      WRITE (*,825) INFILE(3)
C PATRICK Read start date of simulation (time=0s)
      DO J=1,7
         DATE(J)=0
      END DO
      READ (5,*) (DATE(J),J=1,3)
      READ (5,*) (ENDDATE(J),J=1,3)
C END
c Read nature of Q vs. time, and input file name if relevant.
C PATRICK added options for ds water level change read from ini file
C and the number of sections to include bifurcations and islands
      READ (5,*) QTYPE,HTYPE,HYEAR,HCHANGE,TIDE
      IF (QTYPE.EQ.2) WRITE (*,1010) WLDFILE,QHFILE
      READ (5,*) N,NSECT
      NTOT=N
      IF (NSECT.GE.2) THEN
         DO I=1,7
            DO J=1,5
               DO K=1,2
                  SCXS(I,J,K)=0
               END DO
            END DO
         END DO
         SCXS(1,1,1)=1
         SCXS(NSECT,1,2)=N
         DO 10,I=1,NSECT-1
            READ (5,*) SCXS(I,1,2),SCXS(I,4,1),SCXS(I,4,2)
            DO J=1,2
               IF (SCXS(I,4,J).NE.0) THEN
                  IF (SCXS(SCXS(I,4,J),2,1).EQ.0) THEN
                     SCXS(SCXS(I,4,J),2,1)=I
                  ELSE
                     SCXS(SCXS(I,4,J),2,2)=I
                  ENDIF
               ENDIF
            END DO
10       CONTINUE
         DO,I=2,NSECT
            SCXS(I,1,1)=SCXS(I-1,1,2)+1
         END DO
         DO I=1,NSECT
            DO J=1,2
               IF (SCXS(I,2,J).NE.0)
     +         SCXS(I,3,J)=SCXS(SCXS(I,2,J),1,2)
               IF (SCXS(I,4,J).NE.0)
     +         SCXS(I,5,J)=SCXS(SCXS(I,4,J),1,1)
            END DO
         END DO
      ENDIF
      WRITE (*,830)
C END
      WRITE (*,860) RUNCODE,RUNCODE
C     READ *,CHOICE
      CHOICE=0
      IF (CHOICE.EQ.0) CALL CLEAR_SCREEN@
800   FORMAT ('   ***  PROGRAM  SEDROUT 4-M   ***',/,'  ',/,
     +'This program performs step-backwater hydraulic calculations'
     +,/,'and sediment routing.',/,'  ')
805   FORMAT ('River:      ',A20,'    Operator:      ',A20,/,'  ')
810   FORMAT ('  1. Input control file                    ',A12)
820   FORMAT ('  2. Input cross-section file              ',A12)
825   FORMAT ('  3. Input grain size data file            ',A12,/,'  ')
830   FORMAT
     +('To continue program execution enter 0 and press ENTER',/
     +,'If any of the input file names are wrong interrupt the run',/
     +,'by CTRL-C.',/,'  ')
860   FORMAT ('The default output files from this run are:'
     +,/,A8,'.res      Key hydraulic, transport and grain size data',/
     +,A8,'.inf      Information on run options and parameters',/
     +,'Other files will be written according to the list at the end'
     +,/,'of the .ini file')
1010  FORMAT ('The option selected is for d/s condition to vary as',/
     +,'a function of time. Data read from:',/,'Waterlevels: ',A62,/
     +,'Discharges:  ',A62,'  ')
C
      END
C
C     ******************************************************************
      SUBROUTINE INDATA (N,SIZESTART,SURV,INFILE,TYPE,QTYPE,
     +SIZEFINE,RMETHOD,EQUATION,PARAM,SECTCODE,NCLASS,EXPROP,
     +CODE,DISTANCE,D165084ACT,D165084SUB,DGMACT,TRIBLOC,TRIBQ,
     +TRIBQB,TRIBK,TRIBFRACT,TINPUT,TRIBGSD,TRIBSED,NTRIB,
     +EXTMETHOD,EXTSLOPE)
C
      INTEGER CALC,CODE(250),EQUATION,L,M,
     +N,NCLASS,NOCALC,NTRIB,QTYPE,RMETHOD,SELECT(10),TYPE
```

```
C
      REAL DISTANCE(250),D165084ACT(4,250),D165084SUB(4,250),
     +DGMACT(250),EXPROP(25),EXTSLOPE,PARAM(5),
     +SIZEDATA(25),SIZEFINE(25),SIZES(11),SIZESTART(5,125,25),
     +SIZESUMM(10),SURV(100,500),
     +TRIBFRACT(25,5),TRIBK(5),TRIBLOC(5),TRIBQ(5),TRIBQB(5),TVAR
C
      PARAMETER (CALC=1,NOCALC=0)
C
      CHARACTER EXTMETHOD*5,INFILE(3)*12,SECTCODE(125)*6,TYPEC*9,
     +TINPUT(5)*10,TRIBGSD(5)*5,TRIBSED(5)*5
C
c Read number of sections and check nature of grain size data.
      READ (5,'(A)') TYPEC
      READ (5,*) NCLASS
C
      IF (TYPEC.EQ.'FRACTIONS') THEN
         TYPE=1
         DO 10,I=1,NCLASS
            READ (5,*) SIZEFINE(I),EXPROP(I)
10       CONTINUE
      ENDIF
C
      IF (TYPEC.EQ.'D84') TYPE=2
c Select which grain size parameters to calculate routinely. (6)
c  and (8) are for D50 and D84
C
      DO 20,K=1,10
         SELECT(K)=NOCALC
20    CONTINUE
C PATRICK added for Ackers and White's formula
      SELECT(3)=CALC
      SELECT(6)=CALC
      SELECT(8)=CALC
      CALL CLEAR_SCREEN@
C
      DO 200,M=1,N
         READ (3,'(A)') SECTCODE(M)
         READ (3,*) DISTANCE(M)
         CODE(M)=M
c  Read survey data
         DO 100,I=1,100
            READ (3,*) SURV (I,(2*M-1)),SURV(I,2*M)
            IF (SURV(I,2*M).GT.9000) GOTO 101
100      CONTINUE
c  Read grain size data
101      IF (TYPE.EQ.1) THEN
            DO 45,K=1,5
               SIZESUMM(K)=0
45          CONTINUE
            READ (4,'(A)') SECTCODE(M)
            DO 50,I=1,NCLASS
               READ (4,*) (SIZESTART(L,M,I),L=1,5)
               DO 55,K=1,5
                  SIZESUMM(K)=SIZESUMM(K)+SIZESTART(K,M,I)
55             CONTINUE
50          CONTINUE
            DO 60,I=1,NCLASS
               DO 65,K=1,5
                  IF (SIZESUMM(K).GT.1.00) THEN
                     SIZESTART(K,M,I)=SIZESTART(K,M,I)*100/SIZESUMM(K)
                  ELSE
                     SIZESTART(K,M,I)=SIZESTART(K-1,M,I)
                  ENDIF
65             CONTINUE
60          CONTINUE
         ELSE
            READ (4,'(A)') SECTCODE(M)
            READ (4,*) D165084ACT(3,M)
            CODE(M)=M
         ENDIF
         IF (TYPE.EQ.1) THEN
            DO 150,I=1,NCLASS
               SIZEDATA(I)=SIZESTART(1,M,I)
150         CONTINUE
            CALL SIZEPARM(SIZEDATA,SELECT,SIZEFINE,NCLASS,SIZES)
            D165084ACT(3,M)=SIZES(8)
            D165084ACT(2,M)=SIZES(6)
            DGMACT(M)=SIZES(11)
            DO 160,I=1,NCLASS
               SIZEDATA(I)=SIZESTART(2,M,I)
160         CONTINUE
            CALL SIZEPARM(SIZEDATA,SELECT,SIZEFINE,NCLASS,SIZES)
            D165084SUB(3,M)=SIZES(8)
            D165084SUB(2,M)=SIZES(6)
C PATRICK
            D165084SUB(1,M)=SIZES(3)
         ENDIF
200   CONTINUE
C
c Read the method for calculating the reach-extension slope. Options
c are CALC (use survey data to project at same slope as lower end of
c the measured reach) or FIXED (user-specified slope; fixed throughout
c the run)
C
      READ (5,*) EXTMETHOD
      IF (EXTMETHOD.EQ. 'FIXED') READ (5,*) EXTSLOPE
C
c  Read in the nature of the d/s boundary condition.
C  Method 1=Roughness law-Q specified; 2=Roughness law-depth specified
C  3=Rating curve Q=a+b.h^c; 4= depth, Q specified directly;
C  5= waterlevel, Q specified directly, EXTEND not used;
C  6= Q specified directly, waterlevel with rating curve
C  Hds=((Q-a)/b)^(1/c).
C  Equation 1= Keulegan type 1/f^.5=alog(R/D84)+b; 2= Manning-Strickler
C  with n=a.D84^b; 3= Manning type constant value n=a
C
      READ (5,*) RMETHOD,EQUATION
C PATRICK reading param values. If RMETHOD=3 then what to use for
C roughness?? Make param array of 5 values??
      IF (EQUATION.LE.2) THEN
         READ (5,*) (PARAM(L),L=1,2)
      ELSE IF (EQUATION.EQ.3) THEN
         READ (5,*) PARAM(1)
      ENDIF
      IF (RMETHOD.EQ.3  .OR. RMETHOD.EQ.6) THEN
        READ (5,*) (PARAM(L),L=3,5)
      ENDIF
C
      READ (5,*) NTRIB
C
      IF (NTRIB.EQ.0) THEN
         READ (5,'(A)') TRIBSED(1)
      ELSE
```

```
          READ (5,'(A)') (TRIBSED(L),L=1,NTRIB)
        ENDIF
C
        IF (NTRIB.EQ.0) THEN
          READ (5,*) TRIBLOC(1),TRIBQ(1)
          READ (5,'(A)') TINPUT(1)
          READ (5,*) TVAR
          READ (5,'(A)') TRIBGSD(1)
        ELSE
          DO 250,L=1,NTRIB
            READ (5,*) TRIBLOC(L),TRIBQ(L)
250       CONTINUE
          DO 130,IT=1,NTRIB
            READ (5,'(A)') TINPUT(IT)
            READ (5,*) TVAR
            IF (TINPUT(IT).EQ.'CONST') TRIBQB(IT)=TVAR
            IF (TINPUT(IT).EQ.'KXMAIN') TRIBK(IT)=TVAR
            IF (TINPUT(IT).EQ.'KXUSMAIN') TRIBK(IT)=TVAR
            READ (5,'(A)') TRIBGSD(IT)
            IF (TRIBSED(IT).EQ.'SED') THEN
              IF (TRIBGSD(IT).EQ.'FIXED') THEN
                DO 240,I=1,NCLASS
                  READ (5,*) TRIBFRACT(I,IT)
240             CONTINUE
              ENDIF
            ENDIF
130       CONTINUE
        ENDIF
C
        END
C
C       ******************************************************************
        SUBROUTINE SEDDEF (DEFREAL,DEFINT,NFRACT,INSED)
C
        REAL DEFREAL(20),DELTAT,HIDINGG,HIDINGS,INSED(26),
       +KACTIVE,LAMBDA,LOAD,STRAINC,TAUC,TINT,TINTYR,TLENGYR,TLENGTH
C
        INTEGER ACT,DEFINT(10),EQUCODE,EXC,IVAL,NFRACT,
       +USB,WINT,WT
C
        CHARACTER INTERVAL*8,WTYPE*5,USBDY*10,ACTIVE*8,TRACER*7,
       +EQUATION*12
C
C  Initialise LOAD (upstream bdy condition) and
C  EXC (4=mixture of bedload and surface in exchange)
        WINT=1
        LOAD=1
        EXC=4
C  Read run length, and interval between writing to output files
        READ (5,*) TLENGYR,TINTYR
        TINT=TINTYR*60*60*24*365.25
        TLENGTH=TLENGYR*60*60*24*365.25
        READ (5,'(A)') INTERVAL,WTYPE
C
        IF (INTERVAL.EQ.'CONSTANT') THEN
          READ (5,*) DELTAT
          IVAL=1
        ELSE
          IVAL=2
          DELTAT=1
        ENDIF
C
        IF (WTYPE.EQ.'TIME') WT=1
C
        IF (WTYPE.EQ.'ITERS') THEN
          WT=2
          WINT=INT(TINTYR)
        ENDIF
C PATRICK interval to write output
        IF (WTYPE.EQ.'YEAR') WT=3
        IF (WTYPE.EQ.'DAILY') WT=4
C END
C  Read sediment routing info.
        READ (5,*) LAMBDA
        READ (5,'(A)') ACTIVE
C
        IF (ACTIVE.EQ.'K.D84') THEN
          READ (5,*) KACTIVE
          ACT=1
        ELSE IF (ACTIVE.EQ.'CONSTANT') THEN
          READ (5,*) KACTIVE
          ACT=2
        ELSE IF (ACTIVE.EQ.'K.DGM') THEN
          READ (5,*) KACTIVE
          ACT=3
        ENDIF
C
        READ (5,'(A)') EQUATION
C
        IF (EQUATION.EQ.'PARKER1990') THEN
          READ (5,*) HIDINGG,HIDINGS,TAUC,STRAINC
          EQUCODE=1
C PATRICK options for other sediment transport equeations
        ELSE
c Read next 4 lines of info, although not used at all.
          READ (5,*) HIDINGG,HIDINGS,TAUC,STRAINC
          IF (EQUATION.EQ.'EINSTEIN') THEN
            EQUCODE=2
          ELSE IF (EQUATION.EQ.'WILCOCK') THEN
            EQUCODE=3
          ELSE IF (EQUATION.EQ.'ACKERS1973') THEN
            EQUCODE=4
          ELSE IF (EQUATION.EQ.'ACKERS1990') THEN
            EQUCODE=5
          ELSE IF (EQUATION.EQ.'ACKERSDAY') THEN
            EQUCODE=6
          ENDIF
        ENDIF
C END
C
        READ (5,'(A)') USBDY
C
        IF (USBDY.EQ.'QBCONST') THEN
          USB=2
          READ (5,*) INSED(1)
          READ (5,*) (INSED(J),J=2,NFRACT+1)
        ELSE IF (USBDY.EQ.'KXQB1') THEN
          READ (5,*) LOAD
          USB=3
        ELSE IF (USBDY.EQ.'KXS1FIX') THEN
          READ (5,*) LOAD
          READ (5,*) (INSED(J),J=2,NFRACT+1)
          USB=4
        ELSE IF (USBDY.EQ.'QBCGSDV') THEN
```

```
        READ (5,*) INSED(1)
        USB=5
      ELSE
        USB=1
      ENDIF
C
      READ (5,'(A)') TRACER
      IF (TRACER.EQ.'TRACERS') DEFINT(8)=2
      IF (TRACER.EQ.'NO') DEFINT(8)=1
C
      DEFREAL(1)=TLENGTH
      DEFREAL(2)=DELTAT
      DEFREAL(3)=LAMBDA
      DEFREAL(4)=LOAD
      DEFREAL(5)=KACTIVE
      DEFREAL(6)=HIDINGG
      DEFREAL(7)=TINT
      DEFREAL(8)=HIDINGS
      DEFREAL(9)=TAUC
      DEFREAL(10)=STRAINC
C
      DEFINT(1)=IVAL
      DEFINT(2)=WT
      DEFINT(3)=USB
      DEFINT(4)=EXC
      DEFINT(5)=ACT
      DEFINT(6)=WINT
      DEFINT(9)=EQUCODE
C
      END
C
C     ********************************************************************
      SUBROUTINE DRAW (DISTANCE,MEANDEP,WATSURF,N,TRIBLOC,TRIBQ,NTRIB)
C
      INTEGER AX1,AX2,AY1,AY2,B1,B2,COL,D1,D2,I,N,NTRIB,TD1,XSN,WS1,WS2
C
      REAL DEPTH,DISTANCE(250),DMAX,DMIN,DDIFF,HMAX,HMIN,HDIFF,
     +MEANDEP(250),TRIBLOC(5),TRIBQ(5),WATSURF(250)
C
      CALL CLEAR_SCREEN@
      CALL VGA@
      COL=7
      AX1=40
      AX2=640
      AY1=430
      AY2=430
      CALL VGA@
      CALL DRAW_LINE@(AX1,AY1,AX2,AY2,COL)
      AX2=40
      AY2=30
      CALL DRAW_LINE@(AX1,AY1,AX2,AY2,COL)
      DMAX=DISTANCE(N)
      DMIN=DISTANCE(1)
      DDIFF=DMAX-DMIN
      HMAX=WATSURF(1)
      HMIN=WATSURF(N)-MEANDEP(N)
C
      DO 50,I=1,N
        DEPTH=WATSURF(I)-MEANDEP(I)
        IF (DEPTH.LT.HMIN) THEN
          HMIN=DEPTH
        ENDIF
 50   CONTINUE
C
      HDIFF=HMAX-HMIN
      XSN=N
C
      DO 100,I=1,(N-1)
        WS1=INT(430-(400*((WATSURF(XSN)-HMIN)/HDIFF)))
        WS2=INT(430-(400*((WATSURF(XSN-1)-HMIN)/HDIFF)))
        D1=INT(600*((DISTANCE(XSN)-DMIN)/DDIFF)+60)
        D2=INT(600*((DISTANCE(XSN-1)-DMIN)/DDIFF)+60)
        B1=INT(430-(400*((WATSURF(XSN)-MEANDEP(XSN)-HMIN)/HDIFF)))
        B2=INT(430-(400*((WATSURF(XSN-1)-MEANDEP(XSN-1)-HMIN)
     +  /HDIFF)))
        COL=9
        CALL DRAW_LINE@(D1,WS1,D2,WS2,COL)
        COL=4
        CALL DRAW_LINE@(D1,B1,D2,B2,COL)
        XSN=XSN-1
 100  CONTINUE
C
      DO 120,I=1,NTRIB
        IF (TRIBQ(I).GT.0) THEN
          TD1=INT(600*((TRIBLOC(I)-DMIN)/DDIFF)+60)
          CALL DRAW_LINE@(TD1,30,TD1,430,7)
        ENDIF
 120  CONTINUE
C
      END
C
C PATRICK*****************************************************************
C     This subroutine updates the discharges as specified in the
C     .qdt-file and calls READQ to read new data.
C
      SUBROUTINE QDATA (DATE,DISTANCE,DSDEPTH,DSWATER,HDS,LENGTH,
     +MSECT,N,NTRIB,NSECT,PARAM,Q,QDATE,QDS,QHFILE,QT,RMETHOD,
     +TCODE,TMAX,TRIBLOC,TRIBQ,XSN,QSECT,SCXS)
C
      INTEGER DATE(7),LENGTH,N,NTRIB,QDATE(500,3),QT,RMETHOD,
     +TCODE,XSN,SCXS(25,5,2)
C
      REAL DISTANCE(250),DSDEPTH(500),DSWATER(500),MSECT,PARAM(5),
     +Q(250),QDS(500),QOLD,QSECT(25),
     +TMAX,TRIBLOC(5),TRIBQ(5)
C
      CHARACTER QHFILE*62
C
      QOLD=QDS(QT)
      IF (QDATE(QT,1).LT.QDATE(QT+1,1)) THEN
        IF (DATE(1).GE.QDATE(QT+1,1)) THEN
          QT=1
          GOTO 100
        ENDIF
      ELSE IF (QDATE(QT,2).LT.QDATE(QT+1,2)) THEN
        IF (DATE(2).GE.QDATE(QT+1,2)) THEN
          IF (DATE(3).GE.QDATE(QT+1,3)) THEN
            QT=QT+1
            GOTO 110
          ENDIF
        ENDIF
      ELSE IF (DATE(3).GE.QDATE(QT+1,3)) THEN
        QT=QT+1
        GOTO 110
```

```
      ENDIF
C
      GOTO 120
C
100   DO 10 J=LENGTH,LENGTH-3,-1
         NAME=ICHAR(QHFILE(J:J))+1
         IF (NAME.GT.57) THEN
            NAME=NAME-10
            QHFILE(J:J)=CHAR(NAME)
         ELSE
            QHFILE(J:J)=CHAR(NAME)
            GOTO 11
         ENDIF
10    CONTINUE
11    CALL READQDATA (DATE,DSDEPTH,DSWATER,I,LENGTH,
     +QHFILE,QDS,QDATE,RMETHOD)
C
110   IF (NSECT.GT.1) THEN
          DO I=1,NSECT
             QSECT(I)=QSECT(I)*QDS(QT)/QOLD
          END DO
          CALL QDISTRIB(N,NSECT,Q,QSECT,SCXS)
          GOTO 120
       ENDIF
       TCODE=NTRIB
       DO 20,XSN=N,1,-1
         IF (NTRIB.NE.0) THEN
            IF (TCODE.EQ.0) THEN
               Q(XSN)=Q(XSN+1)
            ELSE IF (TRIBLOC(TCODE).LT.DISTANCE(XSN)) THEN
               IF (XSN.EQ.N) THEN
                  Q(XSN)=QDS(QT)
C                  Q(XSN)=QDS(QT+1)-QTLEFT/86400*(QDS(QT+1)-QDS(QT))
               ELSE
                  Q(XSN)=Q(XSN+1)
               ENDIF
            ELSE
               Q(XSN)=Q(XSN+1)-TRIBQ(TCODE)
               TCODE=TCODE-1
            ENDIF
         ELSE
            IF (XSN.EQ.N) THEN
                Q(XSN)=QDS(QT)
C               Q(XSN)=QDS(QT+1)-QTLEFT/86400*(QDS(QT+1)-QDS(QT))
            ELSE
               Q(XSN)=Q(XSN+1)
            ENDIF
         ENDIF
20    CONTINUE
C
C      IF (RMETHOD.EQ.5) THEN
C         HDS=DSWATER(QT)
C      ENDIF
       IF (RMETHOD.EQ.6) THEN
          HDS=((QDS(QT)-PARAM(3))/PARAM(4))**(1/PARAM(5))
       ENDIF
C Calculate TMAX to avoid program from stepping over flood data or big
C jump in specified discharge and/or waterlevel.
120   TMAX=(23-DATE(4))*3600+(59-DATE(5))*60+60-DATE(6)-MSECT
C
      END
C
C PATRICK***************************************************************
C      This subroutine transforms the elapsed time in seconds to a
C      date from the starting date.
      SUBROUTINE NEWDATE (DATE,DELTAT,MSECT)
C
      REAL COR,DELTAT,TREST,RLIMIT(6),YEAR,MSEC,MSECT
C
      INTEGER MDAYS,LEAPYR,CHECK,LIMITS(6),DATE(7)
C
      MDAYS=31
      YEAR=DATE(1)
      LEAPYR=4*(AINT(YEAR/4))
      IF (DATE(1).EQ.LEAPYR .AND. DATE(2).EQ.2) THEN
         MDAYS=29
      ELSE
         IF (DATE(2).EQ.2) MDAYS=28
         IF (DATE(2).EQ.4 .OR. DATE(2).EQ.6 .OR. DATE(2).EQ.9
     +    .OR. DATE(2).EQ.11) MDAYS=30
      ENDIF
C
      LIMITS(6)=60
      LIMITS(5)=60
      LIMITS(4)=24
      LIMITS(3)=MDAYS
      LIMITS(2)=12
      LIMITS(1)=9999
      RLIMIT(1)=LIMITS(1)
      RLIMIT(2)=LIMITS(2)
      RLIMIT(3)=LIMITS(3)
      RLIMIT(4)=LIMITS(4)
      RLIMIT(5)=LIMITS(5)
      RLIMIT(6)=LIMITS(6)
      TREST=DELTAT
      MSEC=(DELTAT-AINT(DELTAT))
C
      IF (MSEC.GT.0) THEN
         MSECT=MSECT+MSEC
         DATE(7)=1000*MSECT
         IF (DATE(7).GE.1000) THEN
            MSECT=MSECT-1
            DATE(7)=DATE(7)-1000
            TREST=TREST+1
         ENDIF
      ENDIF
C
      DO 10,N=6,2,-1
         COR=TREST-(AINT(TREST/RLIMIT(N))*RLIMIT(N))
         TREST=AINT(TREST/RLIMIT(N))
         DATE(N)=DATE(N)+COR
         IF (N.GT.3)THEN
            IF (DATE(N).GE.LIMITS(N)) THEN
               DATE(N)=DATE(N)-LIMITS(N)
               TREST=TREST+1
            ENDIF
         ELSE IF (N.LE.3) THEN
            IF (DATE(N).GT.LIMITS(N)) THEN
               DATE(N)=DATE(N)-LIMITS(N)
               TREST=TREST+1
            ENDIF
         ENDIF
10    CONTINUE
C
```

```
      CHECK=TREST
      IF (CHECK.GT.0) DATE(1)=DATE(1)+TREST
C
      END
C
C PATRICK****************************************************************
      SUBROUTINE READQDATA (DATE,DSDEPTH,DSWATER,I,LENGTH,
     +QHFILE,QDS,QDATE,RMETHOD)
C
      REAL DSDEPTH(500),DSWATER(500),QDS(500),QRDATE(3)
C
      INTEGER DATE(7),LENGTH,QDATE(500,3),RMETHOD,I
C
      CHARACTER QHFILE*62
C
      OPEN(6,FILE=QHFILE)
      DO 10,I=1,500
         IF (RMETHOD.EQ.1) THEN
            READ (6,*) (QRDATE(J),J=1,3),QDS(I)
         ELSE IF (RMETHOD.EQ.2) THEN
            READ (6,*) (QRDATE(J),J=1,3),DSDEPTH(I)
         ELSE IF (RMETHOD.EQ.3) THEN
            READ (6,*) (QRDATE(J),J=1,3),DSDEPTH(I)
         ELSE IF (RMETHOD.EQ.4) THEN
            READ (6,*) (QRDATE(J),J=1,3),QDS(I),DSDEPTH(I)
         ELSE IF (RMETHOD.EQ.5) THEN
            READ (6,*) (QRDATE(J),J=1,3),QDS(I)
C,DSWATER(I)
         ELSE IF (RMETHOD.EQ.6) THEN
            READ (6,*) (QRDATE(J),J=1,3),QDS(I)
         ENDIF
         DO 15,J=1,3
            QDATE(I,J)=QRDATE(J)
15       CONTINUE
         IF (I.GT.1) THEN
            IF (QDATE(I,1).GT.QDATE(I-1,1)) GOTO 90
         ENDIF
10    CONTINUE
90    CLOSE(6)
C
      END
C PATRICK****************************************************************
      SUBROUTINE QDISTRIB (N,NSECT,Q,QSECT,SCXS)
C
      REAL Q(250),QSECT(25)
C
      INTEGER I,N,XSN,SCXS(25,5,2),NSECT
C
      DO I=1,NSECT
         DO XSN=SCXS(I,1,1),SCXS(I,1,2)
            Q(XSN)=QSECT(I)
         END DO
      END DO
      DO I=1,NSECT
         IF (SCXS(I,4,2).NE.0) THEN
            Q(SCXS(I,5,1))=QSECT(I)
            Q(SCXS(I,5,2))=QSECT(I)
         ENDIF
         IF(SCXS(I,2,2).NE.0) THEN
            Q(SCXS(I,3,1))=QSECT(I)
            Q(SCXS(I,3,2))=QSECT(I)
         ENDIF
      END DO
C
      END
C PATRICK****************************************************************
      SUBROUTINE WATERLEVEL(DSWATER,HDATE,HDS,HT,DATE,HTYPE,HCHANGE,
     +HYEAR,TMAX,MSECT,TIDE)
C
      REAL DSWATER(500),HDS,HCHANGE,TMAX,MSECT,TIDE
C
      INTEGER DATE(7),HDATE(500,2),HT,HTYPE,HYEAR,HOUR,SIGN
C
      IF (HDATE(HT,1).LT.HDATE(HT+1,1)) THEN
         IF (DATE(2).GE.HDATE(HT+1,1)) THEN
            IF (DATE(3).GE.HDATE(HT+1,2)) THEN
               HT=HT+1
            ENDIF
         ENDIF
      ELSE IF (DATE(3).GE.HDATE(HT+1,2)) THEN
         HT=HT+1
      ENDIF
C
      IF (HDATE(HT+1,1).GE.99) THEN
         IF (DATE(2).EQ.HDATE(1,1) .AND. DATE(3).EQ.HDATE(1,2)) THEN
            IF (HTYPE.EQ.1) THEN
               DO I=1,HT
                  DSWATER(I)=DSWATER(I)+HCHANGE
               END DO
            ELSE IF (HTYPE.EQ.2 .AND. DATE(1).EQ.HYEAR) THEN
               DO I=1,HT
                  DSWATER(I)=DSWATER(I)+HCHANGE
               END DO
            ENDIF
            HT=1
         ENDIF
      ENDIF
C
      IF (TIDE.LE.0) THEN
         HDS=DSWATER(HT)
      ELSE
         SIGN=1
         HOUR=DATE(4)
         IF (HOUR.GE.12) HOUR=HOUR-12
         IF (HOUR.GE.6) THEN
            HOUR=HOUR-6
            SIGN=-1
         ENDIF
         IF (HOUR.LT.1) THEN
            HDS=DSWATER(HT)
         ELSE IF (HOUR.LT.2 .OR. HOUR.GT.5) THEN
            HDS=DSWATER(HT)+0.5*TIDE*SIGN
         ELSE IF (HOUR.LT.3 .OR. HOUR.GT.4) THEN
            HDS=DSWATER(HT)+0.866*TIDE*SIGN
         ELSE
            HDS=DSWATER(HT)+TIDE*SIGN
         ENDIF
         TMAX=(59-DATE(5))*60+60-DATE(6)-MSECT
      ENDIF
C
      END
C PATRICK****************************************************************
      SUBROUTINE READWLD (DATE,DSWATER,HI,WLDFILE,HDATE)
C
```

```
      REAL DSWATER(500),HRDATE(2)
C
      INTEGER DATE(7),HDATE(500,2),I
C
      CHARACTER WLDFILE*62
C
      OPEN(6,FILE=WLDFILE)
      DO 10,I=1,500
         READ (6,*) (HRDATE(J),J=1,2),DSWATER(I)
         DO 15,J=1,2
            HDATE(I,J)=HRDATE(J)
15       CONTINUE
         IF (I.GT.1) THEN
            HI=I
            IF (HDATE(I,1).GE.99) GOTO 90
         ENDIF
10    CONTINUE
90    CLOSE(6)
C
      END
C     *****************************************************************
```

Appendix IV

Example input-files for Saint-François River

An example of the required input files can be found in Appendix IV where the required input files for SEDROUT4-M are presented for the simulation of ECHAM4 discharge scenario with the gradual base level fall, in the Saint-François River starting from the beginning of 2010. In Appendix IV.1 the `Fran2010.ini`-file is shown with a brief description of the changes. The `sedfile.ini`-file (Appendix IV.2) requires two extra lines to specify the location of the `.wld`-file (Appendix IV.3) and `.qdt`-file (Appendix IV.4) that contain respectively the yearly hydrograph at the downstream end and the daily discharges of the first year at the upstream boundary. Appendices IV.5 and IV.6 respectively show the topography input per cross section (`.sds`-file) and the grain size distribution per cross section (`.gss`-file) in the same way as before.

IV.1 Francois.ini

Lines 4 and 5 contain respectively the start and end date of the simulation in the `YYYY MM DD` format. On line 6 four new input variables need to be specified after the discharge option. The first is a switch for downstream water level scenario (0=no change, 1=change). On line 7 a second input variable is required to incorporate the island configuration. The next number of lines depends on the number of sections and is the number of sections minus 1, that contain the number of the downstream cross section followed by the section number(s) downstream of the section. The second variable specifies if there is a change in downstream water level (0=no;1=yes) and the third new input variable specifies the type of change (0=gradual, `YYYY` is sudden change, followed by the amplitude and direction (negative values for a decrease) of the fourth variable. The last new input variable gives the half amplitude of the tide at the downstream end independently from the others. Line 27 is the bed slope for downstream channel extension if equilibrium depth is assumed while using real cross section shapes, because the channel is extended based on the slope of the deepest points, which can increase due to change in cross-sectional shape. The value entered forces SEDROUT to extend the channel in the right direction. Line 37 is added for the discharge distribution option, the iteration is repeated until the specified tolerance is satisfied. Line 42 has two new options `YEAR` and `DAILY` to write output to the selected files at the beginning of each year or every day. Line 46 has three options for the Ackers and White sediment transport formula, `ACKERS1973`, `ACKERS1990` and `ACKERSDAY`. Finally the lines 89–92 are added for the four extra output files.

```
Francois                  River/site name
PMV                       Operator
Fran2100          Name of output files
2010 01 01        start date of siumlation (yyyy mm dd)
2100 01 01        end date of simulation (yyyy mm dd)
2 1 0 -0.01 0     Discharge fixed (=1), or variable (=2) followed by 3 values (see code
                  ...for details)
100      4        Number of cross-sections, Number of sections (1 section use 0)
27       2        3
37       4        0
55       4        0
FRACTIONS         Input of grain-size data as FRACTIONS or D84 (hydraulics only)
13                Number grain-size classes (<=25)
-2.5     1        psi-class upper limits on classes, followed by c parameter
-2       1
-1.5     1
-1       1
-0.5     1
0        1
0.5      1
1        1
2        1
3        1
4        1
4.3      1
4.5      1
FIXED             How to determine reach extension slope; CALC (from .sds data) or FIXED (
                  ...read from 2nd column here)
0.001             REACH EXTENSION SLOPE (IF NEEDED)
5        3        Roughness methode (1-5) and equation (1-3): see code for detials
0.03              Parameters for roughness equetion or roughness value n
0                 Number of Tributaries (NT; 0 to 5 maximum)
SED               SED or NOSED; if 0 tribs. then anything can go here; if NT>1 put SED or
                  ...NOSED NT times on NT lines
0        0        Location at which trib. enters and Q; if 0 tribs any values can go here;
                  ... otherwise NT rows of location ,Q; MUST be ordered from u/s to d/s.
NOTRIB            Trib. bedload input rate type; KXUSMAIN, KXMAIN or CONST (ALL IN CAPS
                  ...PLEASE); if no tribs. then anything in these next 3 lines; if >1 then
                  ...repeat these 3 lines NT times in the same order; if NOSED then these 3
                  ... still needed for each trib, although info. not used
0                 K or bedload input rate (m3/s) according to prev. line
NOTRIB            Trib. input gsd (FIXED = specified on next N lines, where N is number of
                  ... gs classes; or main = main channel)
5.5      250      For Q method, this is a first estimation of the depth Q at d/s end of
                  ...reach (so includes tributary conditions)
0.0001            Tolerance for hydraulic computation
CALC              Slope calculation methode at d/s end
SED               Sediment routing?
1        1        Run length (yrs) and frequency of data recording (yrs or iterations as
                  ...specified below)
VARIABLE          Timestep (VARIABLE or CONSTANT; if CONSTANT line after next is timestep
                  ...dt)
DAILY             Data output written after TIME or ITERS (fixed # iterations) or YEAR
                  ...every first of January
0.3               Bed prorsity
CONSTANT          Active layer thickness (K.D84, K.DGM, or CONSTANT)
0.1               K or active layer thickness (m)
ACKERSDAY         Bedload equation (PARKER1990 followed by 4 lines; gravel hiding, sand
                  ...hiding, tauref, straining exponent; if WILCOCK or EINSTEIN then keep
                  ...the next4 lines)
-0.0951
-0.0951
0.0386
0.3
FIXED ELEV        u/s boundary condition (FIXED ELEV; QBCONST; KXS1FIX; KXQB1 ;QBCGSDV)
NO                Tracers? if YES then furthe info. required
Y        sed      sediment summary data *** LISTING OF OUTPUT FILE EXTENSIONS WITH Y OR N
                  ...***
```

```
Y    tpt    bedload transport data
Y    sur    surface % in each size class
Y    sub    sub-surface % in each size class
Y    bld    bedload % in each size class
Y    hyd    hydraulic data
Y    50a    active layer D50
Y    84a    active layer D84
Y    qb     unit bedload tpt. rate
Y    50b    bedload D50
Y    S      energy slope
Y    tau    dimensionless stress based on active layer D50
Y    zz     bed elevation
Y    R      hydraulic radius
Y    FR     Froude number
Y    ff     friction factor
Y    16a    active layer D16
Y    16s    sub-surface D16
Y    50s    sub-surface D50
Y    84s    sub-surface D84
Y    16b    bedload D16
Y    84b    bedload D84
Y    n      Manning n
Y    h      mean flow depth
Y    dz     bed elevation change per timestep
Y    Sdz    cumulative bed elevation change
Y    dA     bed area change per timestep
Y    SdA    cumulative bed area change
Y    pcs    % sand in active layer
Y    u      mean flow velocity
Y    wws    water surface elevation
Y    lat    tributary (lateral) sediment input
Y    dgm    geometric mean size of surface layer
Y    90a    surface D90
Y    90s    sub-surface D90
Y    90b    bedload D90
Y    DT     time step (time elapse; time step used; critical time step)
Y    LA     active layer thickness
Y    LP     Long profile based on deepest points
Y    YQS    Cumulative sediment transport at boundaries
```

IV.2 sedfiles.ini

Lines 4 and 5 are added with the pathname of the `.wld` and `.qdt` files. The length available is 64 characters the description needs to start after these, this number can be increased if necessary by specifying a longer vector in the SEDROUT4-M code.

```
1 Francois.INI          Name of control file (.ini)
2 Fran2010.sds          Name of input cross-section data file (.sds)
3 Fran2010.gss          Name of input grain size data file  (.gss)
4 D:\patrick\Waterlevel\LacStPie.wld                                   (Path)Name of
      ...waterlevel data file (.wld)
5 D:\patrick\Hydrodat\Francois\FrEA2010.QDT                            (Path)Name of
      ...discharge data files (.qdt)
```

IV.3 LacStPie.wld

```
 1    1    4.15
 1    2    4.20
 1    7    4.10
 1    8    4.05
 1   14    4.10
 1   15    4.15
 1   16    4.20
 1   17    4.25
 1   19    4.30
 1   20    4.40
 1   21    4.45
 1   25    4.40
 1   26    4.35
 1   27    4.30
 1   28    4.25
 1   30    4.30
 1   31    4.35
 2    3    4.30
 2    5    4.25
 2   10    4.30
 2   13    4.25
 2   15    4.30
 2   18    4.35
 2   20    4.40
 2   21    4.45
 2   22    4.50
 2   23    4.45
 2   27    4.40
 3    4    4.35
 ⋮    ⋮     ⋮
10   12    3.80
10   13    3.85
10   16    3.90
10   17    3.95
10   23    4.00
10   26    4.05
10   28    4.10
10   30    4.05
11    1    4.00
11    8    4.05
11    9    4.10
11   13    4.15
11   24    4.10
11   26    4.15
11   28    4.20
11   29    4.25
12    1    4.30
12    3    4.25
12    5    4.20
12    8    4.15
12   10    4.20
12   11    4.25
12   13    4.20
12   18    4.15
12   20    4.10
12   24    4.15
12   26    4.20
12   27    4.15
99   99    9999
```

IV.4 FrEA2010.qdt

1	2010	1	1	32.89
2	2010	1	2	32.25
3	2010	1	3	31.67
4	2010	1	4	31.13
5	2010	1	5	30.63
6	2010	1	6	30.17
7	2010	1	7	29.75
8	2010	1	8	29.36
9	2010	1	9	28.99
10	2010	1	10	28.65
11	2010	1	11	28.33
12	2010	1	12	28.03
13	2010	1	13	27.74
14	2010	1	14	27.48
15	2010	1	15	27.26
16	2010	1	16	27.18
17	2010	1	17	27.16
18	2010	1	18	27.07
19	2010	1	19	26.89
20	2010	1	20	26.66
21	2010	1	21	26.40
22	2010	1	22	26.14
23	2010	1	23	25.88
24	2010	1	24	25.63
25	2010	1	25	25.38
26	2010	1	26	25.13
27	2010	1	27	24.88
28	2010	1	28	24.63
29	2010	1	29	24.39
30	2010	1	30	24.16
31	2010	1	31	23.92
	⋮	⋮	⋮	⋮
338	2010	12	4	157.91
339	2010	12	5	577.69
340	2010	12	6	778.81
341	2010	12	7	628.14
342	2010	12	8	436.92
343	2010	12	9	324.43
344	2010	12	10	270.29
345	2010	12	11	242.44
346	2010	12	12	232.78
347	2010	12	13	226.17
348	2010	12	14	215.82
349	2010	12	15	203.90
350	2010	12	16	190.89
351	2010	12	17	177.27
352	2010	12	18	163.92
353	2010	12	19	154.31
354	2010	12	20	162.81
355	2010	12	21	174.64
356	2010	12	22	174.57
357	2010	12	23	167.76
358	2010	12	24	158.57
359	2010	12	25	148.49
360	2010	12	26	138.32
361	2010	12	27	128.75
362	2010	12	28	125.12
363	2010	12	29	146.46
364	2010	12	30	157.50
365	2010	12	31	150.06
366	2011	1	1	137.99

IV.5 Fran2010.sds

```
27054
      0.00
  0.000000    20.000000
  0.000000     5.670000
  5.020000     4.300000
 10.070000     3.440000
 15.200000     3.020000
 20.219999     3.040000
 25.070000     3.000000
 30.160000     3.170000
     ⋮             ⋮
175.080002     1.130000
180.130005     0.880000
185.110001     1.130000
189.839996     1.340000
194.570007     2.760000
194.570007    20.000000
9999.000000  9999.000000
27053
    240.88
  0.000000    20.000000
  0.000000     2.612827
  4.860000     2.102827
  9.970000     1.953402
 15.240000     1.873402
 19.459999     1.993402
 25.180000     2.212827
     ⋮             ⋮
305.109985     3.561420
310.179993     3.771420
314.880005     4.021909
320.239990     5.185267
320.720001     4.699570
320.720001    20.000000
9999.000000  9999.000000
26035
  15017.41
  0.000000    20.000000
  0.000000     4.130629
  8.210000     3.929002
 15.960000     3.949024
 23.910000     4.007958
 31.790001     3.819097
 40.189999     4.007958
     ⋮             ⋮
735.909973     4.453962
743.940002     4.335372
752.090027     4.443962
768.440002     4.591931
776.309998     4.777431
780.510010     5.185570
780.510010    20.000000
9999.000000  9999.000000
```

IV.6 Fran2010.gss

```
27054
  1.9541    1.9541    1.9541    1.9541    1.9541
  4.0905    4.0905    4.0905    4.0905    4.0905
  4.3354    4.3354    4.3354    4.3354    4.3354
  3.2533    3.2533    3.2533    3.2533    3.2533
  2.8278    2.8278    2.8278    2.8278    2.8278
  1.9714    1.9714    1.9714    1.9714    1.9714
  2.1695    2.1695    2.1695    2.1695    2.1695
  2.1208    2.1208    2.1208    2.1208    2.1208
  8.1116    8.1116    8.1116    8.1116    8.1116
 18.9867   18.9867   18.9867   18.9867   18.9867
 27.8399   27.8399   27.8399   27.8399   27.8399
 14.1006   14.1006   14.1006   14.1006   14.1006
  8.2384    8.2384    8.2384    8.2384    8.2384
27053
  1.9822    1.9541    1.9541    1.9541    1.9541
  3.9059    4.0905    4.0905    4.0905    4.0905
  3.8107    4.3354    4.3354    4.3354    4.3354
  2.6268    3.2533    3.2533    3.2533    3.2533
  2.1277    2.8278    2.8278    2.8278    2.8278
  1.4229    1.9714    1.9714    1.9714    1.9714
  1.5390    2.1695    2.1695    2.1695    2.1695
  1.5705    2.1208    2.1208    2.1208    2.1208
  7.2297    8.1116    8.1116    8.1116    8.1116
 20.2550   18.9867   18.9867   18.9867   18.9867
 29.6977   27.8399   27.8399   27.8399   27.8399
 15.0428   14.1006   14.1006   14.1006   14.1006
  8.7891    8.2384    8.2384    8.2384    8.2384
27052
  2.3154    1.9624    1.9541    1.9541    1.9541
  4.9500    4.1274    4.0905    4.0905    4.0905
     ⋮         ⋮         ⋮         ⋮         ⋮
  0.0000    0.0000    0.0000    0.0000    0.0000
  0.0000    0.0000    0.0000    0.0000    0.0000
26034
  2.2519    6.8578    9.5157    9.5157    9.5157
  3.0699    5.2823    6.1928    6.1928    6.1928
 28.1053   51.7351   64.8970   64.8970   64.8970
 21.7644   18.4749   14.1888   14.1888   14.1888
 20.8659   10.1493    3.8185    3.8185    3.8185
 13.0532    4.4205    0.7751    0.7751    0.7751
  6.9789    1.8863    0.3498    0.3498    0.3498
  2.1121    0.7368    0.1431    0.1431    0.1431
  1.7984    0.4570    0.1192    0.1192    0.1192
  0.0000    0.0000    0.0000    0.0000    0.0000
  0.0000    0.0000    0.0000    0.0000    0.0000
  0.0000    0.0000    0.0000    0.0000    0.0000
  0.0000    0.0000    0.0000    0.0000    0.0000
26035
  2.1819    3.1987    9.7109    9.5157    9.5157
  3.2942    4.1745    6.4105    6.1928    6.1928
 32.6313   43.1120   64.6385   64.8970   64.8970
 23.5386   26.3629   14.1172   14.1888   14.1888
 19.4997   14.4227    3.7908    3.8185    3.8185
 11.0234    5.7742    0.7607    0.7751    0.7751
  5.2219    2.0075    0.3331    0.3498    0.3498
  1.6022    0.6715    0.1321    0.1431    0.1431
  1.0068    0.2761    0.1063    0.1192    0.1192
  0.0000    0.0000    0.0000    0.0000    0.0000
  0.0000    0.0000    0.0000    0.0000    0.0000
  0.0000    0.0000    0.0000    0.0000    0.0000
  0.0000    0.0000    0.0000    0.0000    0.0000
```